The Ages of the Old Open Clusters NGC 188, NGC 6791, Melotte 66, and NGC 2204

by

Anne-Marie Monteith

Honours B.Sc., University of Ottawa, 1988

A THESIS SUBMITTED IN PARTIAL FULFILLMENT
OF THE REQUIREMENTS FOR THE DEGREE OF
MASTER OF SCIENCE

in the Department

of

Physics and Astronomy

We accept this thesis as conforming

to the required standard

[redacted]

Supervisor: Dr. D. A. VandenBerg — Supervisor: Dr. R. D. McClure

[redacted]

Dr. A. C. Gower — Dr. J. B. Tatum

[redacted]

Dr. T. W. Dingle — Dr. J. E. Hesser

Abstract

CCD photometry is presented for the three oldest known open clusters: NGC 188, NGC 6791, and Melotte 66. The CCD frames were reduced using DAOPHOT, and the resultant colour-magnitude diagrams were compared with theoretical isochrones in order to determine the ages of the clusters. The age of NGC 188 has been estimated to be near 8 Gyr; this is a compromise between the best fits for $Z = 0.010$ and $Z = 0.017$, the mean of which corresponds to the observed metallicity, [Fe/H] $= -0.11$. The age of NGC 6791 was found to be 8-8.5 Gyr (for $Z = 0.024$). Although the uncertainties are large, NGC 6791 seems to be slightly older than NGC 188. Melotte 66 is shown to have an age of 5-6 Gyr (for $Z = 0.006$). The colour-magnitude diagram of NGC 2204 was also obtained from new CCD data: an age of 3 Gyr was estimated for it (assuming $Z = 0.006$).

[redacted]

Supervisor: Dr. D. A. VandenBerg

[redacted]

Supervisor: Dr. R. D. McClure

[redacted]

Dr. A. C. Gower

[redacted]

Dr. J. B. Tatum

[redacted]

Dr. T. W. Dingle

[redacted]

Dr. J. E. Hesser

With equal passion I have sought knowledge. I have wished to understand the hearts of men, I have wished to know why the stars shine. And I have tried to apprehend the Pythagorean power by which number holds sway above the flux. A little of this, but not much, I have achieved.

– Bertrand Russell, Autobiography, Prologue.

Acknowlegements

I would like to thank Dr. D. A. VandenBerg and Dr. R. D. McClure for the topic of this research project, and for the help they provided throughout its duration. I would also like to thank the staff of the DAO/NRC for their support and advice, especially P. Stetson, M. Bolte, and E. Friel. And thank you to the graduate students, especially P. Bergbusch, who introduced me to world of clusters. I aknowledge the financial help provided by NSERC in the form of a post-graduate scholarship extending over the two years of this project.

Contents

List of Figures

List of Tables

Chapter 1

Introduction and Overview

Stellar clusters are amongst the most intriguing objects in the sky, easily identified by the distinct appearance of their "vast sun-clusters' gathered blaze" (Tennyson, *Epilogue*). There are three types of star clusters: stellar associations, globular clusters, and open clusters (also known as Galactic clusters). Stellar associations are loose, irregular groups of unbound stars which generally dissolve on timescales of a few million years. Globular clusters, on the other hand, are dynamically bound, are believed to have formed roughly at the same time as the Galaxy, if not before (Sandage 1986), and are therefore amongst the oldest objects in the universe. They have a very dense core, an overall spherical shape, and contain of the order of 10^6 stars. Open clusters, as their name suggests, are more irregular and more sparsely populated groups of gravitationally bound stars, with ages varying from about 10^3 to 10^{10} yr. Unlike the globular clusters, which tend to populate the halo of the Galaxy, open clusters are mostly localized to the Galactic disk. Further differentiating the two types is the fact that in globular clusters the abundances of elements heavier than helium range from slightly less than solar to less than 1% of the solar abundances, whereas open clusters rarely have a metal content less than 10% of the Sun and may range to 2-3 times that of the Sun.

Just as the ages of globular clusters set the timescale for the formation of the halo, those for the open clusters assist in our understanding of the evolution of the disk. The oldest of the open clusers are of particular interest since they set a lower bound to the age of the disk. This is not to say, however, that the oldest open cluster is coeval with the formation of the disk: open clusters are readily disrupted through tidal interactions, so that unless they were unusually massive when they formed, the oldest open clusters will have dissolved (e.g., King 1966, King 1968). It is the main purpose of the present investigation to present new CCD data for three of the oldest known open clusters and to reassess their ages using the best available isochrones. In the following few pages, the properties of open clusters in general, and of those clusters considered in this thesis, will be reviewed. First, the method of determining ages will be described.

1.1 Method of Analysis: Isochrones

Theoretical evolutionary models can be most readily compared with observational data when they are in the form of isochrones, which offer a snapshot of the colour-magnitude diagram (hereafter CMD) of a cluster at a specific time in its evolution.

To a good approximation, a stellar cluster is a self-gravitating group of stars which all formed at about the same time, though with different initial masses. Because the distance to every cluster member is essentially the same, a plot of the apparent magnitude versus colour will show a fairly tight locus of stars with (if there are sufficient numbers of stars) a main sequence, subgiant branch, giant branch and red-giant clump (or horizontal branch) – i.e., a Hertzprung-Russell diagram. The location of the stars in the CMD will depend upon the time elapsed since their initial formation. As a cluster ages, the more massive stars will have progressively evolved off the main sequence: the most massive remaining stars, still burning hydrogen in their core, will be located at the so-called "turnoff" (a turn-around point between the main sequence and the red-giant branch), where the stellar structure begins to change dramatically. In populous clusters, stars will be found along the subgiant branch; they are supported by a hydrogen burning shell around an inert helium core; as the shell moves outward and becomes ever thinner, the star's radius grows dramatically. At the red-giant tip, the helium core is ignited – the "helium flash" – and the star evolves quickly to the horizontal-branch, a fairly long-lived phase where the star is supported by both hydrogen and helium burning. Its further evolution depends on the mass of the star at this point – which may have been altered from its initial value as a consequence of mass loss during its giant-branch evolution.

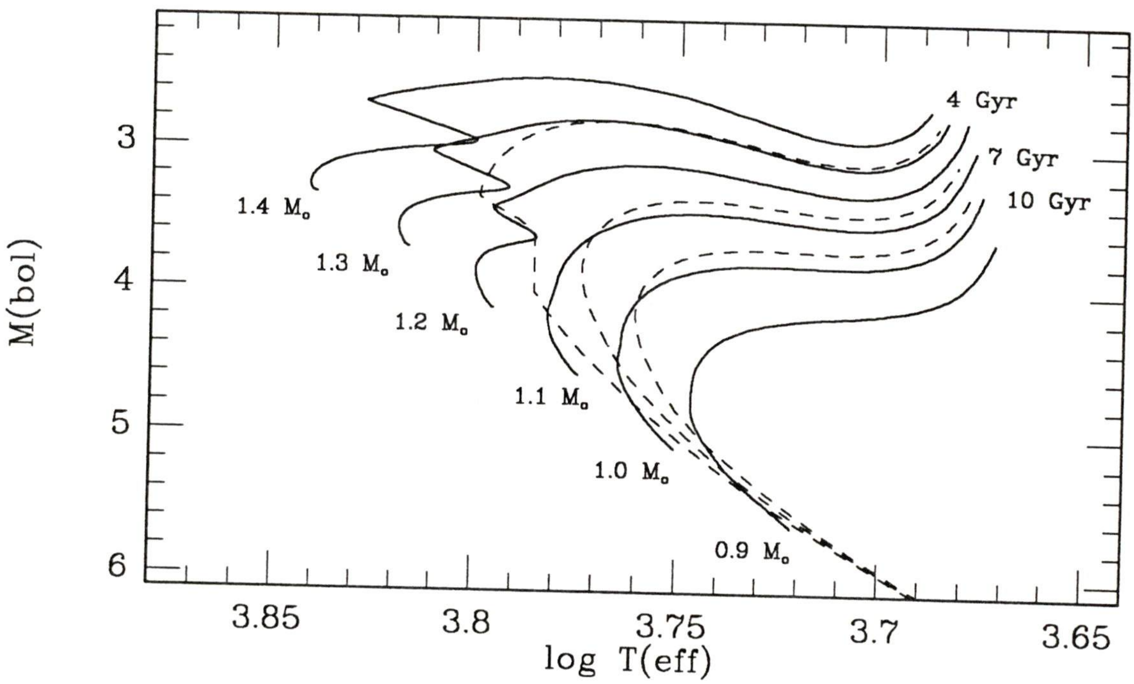

Fig. 1. Evolutionary tracks (solid curves) for stars of masses $0.9M_\odot$ to $1.4M_\odot$, of solar abundance, and isochrones (dashed curves) obtained by interpolation of the tracks at ages 4, 7, and 10 Gyr. (Data provided by Dr. D. A. VandenBerg.)

A plot of the points connecting the star's surface luminosity and temperature values as a function of time is its evolutionary track (see Figure 1). The observed CMD represent the loci of the ends of the evolutionary tracks for member stars to that particular time since their formation. These loci are called *isochrones*, or constant-time lines.

Theoretical isochrones are the result of stellar evolution modeling, a boundary-value problem in which the history of the star depends mainly on four parameters: the initial mass M, the composition, by mass fraction, of helium (Y) and metals (Z), and the mixing-length parameter α. Fig. 1 shows evolutionary tracks for stars of masses ranging from $0.9M_\odot$ to $1.4M_\odot$, and the solar chemical abundance $Z = 0.017$, or [Fe/H] = 0. The dashed curves give isochrones of 4, 7, and 10 Gyr, in the order of decreasing ages.

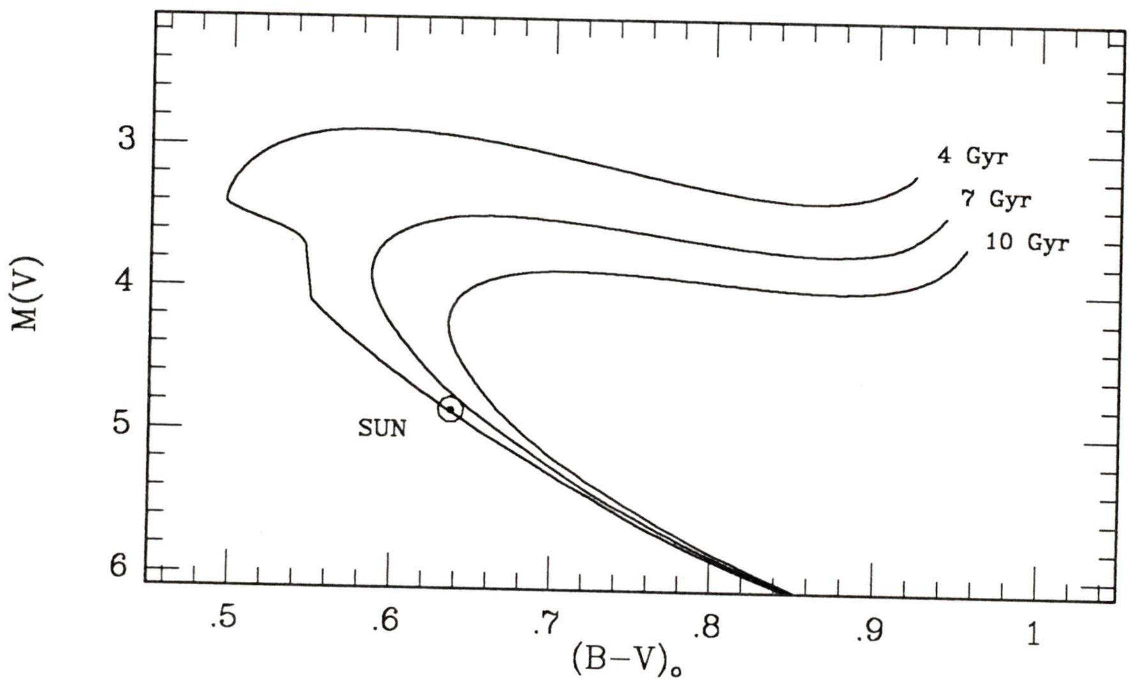

Fig. 2. The isochrones from Fig. 1 are plotted on the observational plane. The location of the Sun is indicated to show that the calculations have been well normalized to solar values. (Data provided by Dr. D. A. VandenBerg.)

A theoretical isochrone can be obtained by interpolating in the evolutionary tracks for stars of different masses at a particular time after formation. Both Fig. 1 and Fig. 2 show three isochrones, for ages 4, 7, and 10 Gyr. In order to compare the theoretical predictions of luminosity and temperature of Fig. 1 with observational measurements of apparent fluxes (usually done in the UBV system), as in Fig. 2, a transformation between the two planes is needed. Generally model atmosphere-derived relations are used: the atmospheric flux distribution depends only on the effective temperature, the gravity, and the chemical composition; these are all known from the evolutionary model. Magnitudes in any bandpass are calculated from the filter response functions and relative zero points of the colour system. One can convert relative to absolute magnitudes if the distance to the stars is known.

The classic way of fitting isochrones is to try to match the luminosities or effective temperatures of the stars near the turnoff point on the CMD to the turnoff region of the theoretical isochrones. Indeed, the turnoff point is the principal indicator of age, where the stars begin rapid migration from the main sequence to the giant branch. However there can be serious discrepancies: while an isochrone might pass directly through the turnoff point, it may deviate systematically away from the cluster locus on either side of the turnoff. This could be due to a poorly determined set of parameters (e.g., value of α) and/or to weaknesses in the theoretical models. Flannery and Johnson (1982) made a critical review of the method, including a determination of the age and other parameters, the statistical uncertainty and covariance among the parameters, and the goodness of the fit of the model. The statistics they used measured the overall coincidence between an isochrone and stars in the CMD; they analysed only the main sequence and lower subgiant branch and thus avoided using the less reliable theoretical results for advanced stages of evolution. They concluded that the major causes of uncertainty are two uncalibratable sources of systematic error, namely the uncertainty in the stellar temperatures induced by the choice of mixing-length parameter and the unknown errors in the stellar atmospheres. The formal errors in the fit were considered to be minor.

In summary, to generate an isochrone and to transform it to the observational plane requires the specification of the ratio of mixing-length to pressure scale height

α (see VandenBerg 1983 for a full discussion of this uncertainty), the helium abundance Y, the metallicity [Fe/H] or Z, the distance to the cluster $(m - M)_0$, and the interstellar reddening $E(B - V)$. The oxygen abundance is sometimes taken into consideration separately. Other parameters such as rotation and composition diffusion are usually not included in the models, though some recent work (e.g. Proffitt and Michaud 1990, Deliyannis *et al.* 1990) is investigating the effects of these processes.

1.2 Open Clusters

Over 1200 open clusters have been identified in our Galaxy (Janes and Adler 1982). They usually contain a few hundred to a few thousand stars, and have masses of 100 to 3000 $M_{\odot}$. Most of them are concentrated in the Galactic disk, and have heavy element abundances characteristic of Population I stars. Their radii tend to be of order 10 pc, the central densities can vary from 0.25 to 100 stars/pc^3, and the velocity dispersions are typically less than 1 km/s. Most of the open clusters are young (much less than 1 Gyr), but the oldest ones may be as old as 10-12 Gyr. Some useful catalogues containing information on individual clusters are: Hagen's (1970) "Catalogue of Open Cluster Colour-Magnitude Diagrams", and Lyngå's (1987) "Catalogue of Open Cluster Data" . The two primary sources of information on the properties of open clusters are: Janes and Adler (1982), which contains useful tables of cluster properties; and Janes, Tilley, and Lyngå (1988), which updates the previous article using the data from Lyngå (1987). The latter study discusses in detail the properties of the open cluster system.

How long a cluster survives depends essentially on its dynamical evolution, which is, to a certain extent, related to its linear size (Wielen 1971, 1975): a large cluster would be readily disrupted by tidal interactions with the Galactic field, while a small cluster of the same mass would tend to dissolve because of encounters among its member stars. The age-diameter relation was studied by Janes, Tilley, and Lyngå (1988), and led to the following results. First, there is a high number of large clusters with ages less than 5×10^7 yr (some of which may be unbound OB associations). Second, there is no correlation between age and linear size for systems with ages between 5×10^7 yr and 10^9 yr. Third, there are only a few old clusters with large diameters. It was found that these old clusters were distributed by age and location very differently from the other clusters, and that the average cluster age increased outwards in the Galaxy. Also studied were an inconclusive relation between metal abundance and age, which was found not to be clearly independent of the galactocentric metallicity gradient, and a relation between richness and age (very few old clusters have fewer than 50 members – something which is common to younger clusters), supporting the theory that small clusters will be disrupted more easily than clusters with a higher mass. Their analysis led them to distinguish between three types of objects: unbound clusters, bound clusters in the thin disk, and older bound clusters.

The properties of the open cluster system can be a guide to a better understanding the structure of the Galaxy. Janes, Tilley, and Lyngå (1988), reviewed variations in cluster properties such as metallicity, longevity, and linear diameter, as a function of galactocentric radius and as a function of position perpendicular to the galactic disk. The metallicity gradient, for example, was found to be -0.07 dex in [Fe/H] per kpc, based on clusters younger than 0.2 Gyr, or -0.14 dex per kpc, based on the few clusters older than 0.2 Gyr.

Star clusters are also ideal objects to test models of stellar evolution: being gravitationally bound systems, the stars are roughly at the same distance and were formed at about the same time, though with a range of initial masses. Confirmation of this is provided by the tight colour-magnitude diagrams being obtained using CCDs (e.g. see the recent study of NGC 2420 by Anthony-Twarog *et al.* 1990). Stars with $M/M_{\odot} \leq 2$ (or so) evolve in much the same way as stars in globular clusters, in that they develop an electronically-degenerate He core during the red-giant branch phase and ignite central helium in the helium flash. Stars with $M/M_\odot \geq 1.15$ have convective hydrogen-burning cores during their entire main sequence evolution, while lower mass stars have radiative interiors. These differences appear in the evolutionary tracks of Fig. 1: the tracks of the more massive stars show a "blueward hook" near the turnoff point; this hook corresponds to a rapid contraction of the star while it shifts its energy source from a hydrogen-burning core to a shell source. In the case of the less massive star, the core hydrogen-burning phase merges smoothly with the phase of hydrogen-burning in a thick shell, and there is no clear-cut distinction between the two phases. The less massive stars will undergo fewer structural changes and subsequent contractions than the more massive stars, and their evolutionary tracks are generally simpler, and considerably smoother.

1.3 NGC 188

NGC 188 ($\alpha(1950.0) = 00^h39^m.4$, $\delta(1950.0) = +85^o04'$) has a high profile in the field of open clusters: it is the nearest, best-studied old open cluster and, hence, its basic characteristics are well known in comparison with most other clusters.

Demarque and Larson (1964), and later Iben (1967), were the first to compare the photometry of the cluster with modern theoretical models of stellar evolution, and independently derived age estimates for NGC 188. Demarque and Larson found an age of 12 Gyr. Iben's attempt was essentially designed as a test for the ability of his evolutionary models to reproduce the morphology of the observed CMD. In particular, his estimate of the age rests on the observation that the stars evolve very rapidly along the subgiant and giant branches; these features on the CMD of the cluster will look very similar to the subgiant and giant portions of the evolutionary tracks for a particular mass. A rough value for the age may be found by estimating the time required for the appropriate star to attain the base of the giant branch.

He obtained an age of 11±2 Gyr for NGC 188.

A decade later, Demarque and McClure (1977) used then-new theoretical models – the Yale isochrones (Ciardullo and Demarque 1977) – to determine the age of the cluster. Demarque and McClure adopted a distance of $(m-M)_0 = 11.13$ (taken from Eggen and Sandage 1969, corrected for a Hyades distance modulus of $(m-M)_0 = 3.30$), and a reddening of $E(B-V) = 0.08$. A comparison of the CMD with the appropriate isochrones gave an age of 5-6 Gyr, sharply lower than previous estimates. VandenBerg (1985) attributed this low age estimate in part to the isochrones (much cooler than his) and to the distance assumed for the cluster by Demarque and McClure.

Twarog (1978) tried to determine the age of the cluster by making a comparative study of NGC 188 and M67. He adopted a reddening of $E(B-V) = 0.09$ for NGC 188 (the maximum value that had been found for the reddening, in Eggen and Sandage 1969) and $E(B-V) = 0.04$ for M67; these are upper and lower estimates. Adopting a lower reddening increases the age of a cluster, and so the ages for NGC 188 and M67 will be be lower and upper estimates, respectively. The metallicities were assumed to be identical ([Fe/H] = 0.06) although NGC 188 was acknowledged to be slightly more metal-poor than M67. With distance moduli of $(m-M)_0 = 9.69$ for M67 (average of the values of Eggen and Sandage 1962, and Racine 1971, similarly corrected to a Hyades distance modulus of $(m-M)_0 = 3.30$) and $(m-M)_0 = 11.13$ for NGC 188 (taken from Eggen and Sandage 1969, corrected for the same Hyades distance modulus), a comparison with the Yale isochrones led to ages of 3.5 ± 0.5 Gyr and 4.3 ± 1.0 Gyr for M67 and NGC 188 respectively. However, the isochrones used for the comparison with NGC 188 do not convincingly reproduce the morphology of its CMD. VandenBerg (1985) also observed that the 5 Gyr isochrone for near solar abundances was displaced from the position of the Sun at $(B-V)_\odot \simeq 0.63$, and that an appropriate horizontal adjustement would lead to an increase in the age estimates of both M67 and NGC 188.

Barbaro and Pigatto (1984) analyzed open clusters in two ways: they compared their CMDs with Yale isochrones, and they compared the observed luminosity functions of the red giants with theoretical predictions. They adopted the distance modulus $(m-M)_0 = 10.85$ from Eggen and Sandage (1969); the metal abundance was derived from the position of the red giant branch and from the temperature of red stars; for [Fe/H] $= -0.23$, the morphology of NGC 188's CMD was found to correspond to an age of 6-7 Gyr. The distribution of the red giants (number versus magnitude) led to an age greater than 9 Gyr, due essentially to the low luminosity of the base of the red giant branch. NGC 188 was one of the few clusters for which the two approaches did not yield consistent results, and they concluded that NGC 188's red-giant branch was anomalous. McClure and Twarog (1977) also discussed this anomalous giant branch.

VandenBerg (1985) computed a range of stellar models which were fitted to a number of clusters, including NGC 188. For a reddening of $E(B-V) = 0.08$, the [Fe/H] $= 0$ isochrone for an age of 10 Gyr was found to reproduce the observed CMD in a satisfactory way, implying a distance modulus of $(m-M)_V = 11.10$.

Twarog and Anthony-Twarog (1989) compared the apparent magnitude of NGC 188's red giant clump ($V = 12.35$) with that of M67 ($V = 10.55$). Assuming a distance modulus of $(m-M)_V = 9.7$ for M67 (implying an absolute magnitude of $M_V = 0.85$ mag for the clump) would lead to a distance modulus for NGC 188 of $(m-M)_V = 11.5$. This analysis relies on the theoretical prediction that the luminosity of the red giant clump should grow fainter as a young cluster ages, but should remain constant for clusters older than 2 Gyr (Cannon 1970). Using a reddening of $E(B-V) = 0.03$ and $E(B-V) = 0.12$ for M67 and NGC 188, respectively, they compared the CMDs of the two clusters to VandenBerg's (1985) isochrones for solar metallicities (normalized to their choice of solar colour $(B-V)_\odot = 0.65$), and found ages of 4.5-5 Gyr and 6.5 Gyr for M67 and NGC 188, respectively. However, their choices of reddening are again lower and upper estimates for M67 and NGC 188, respectively, thereby minimizing the age difference between the clusters. The difference in reddening of $E(B-V)_{Twarog\ et\ al.} - E(B-V)_{VandenBerg\ 1985} = 0.04$, and the different solar colours to which the isochrones were normalized (VandenBerg 1985 used $(B-V)_{\odot} = 0.63$), account for most of the 4 Gyr difference in the age of NGC 188, as reported in the two studies.

The age derived by Caputo et *al.* (1990) is the result of comparing the CMD with isochrones computed by Chieffi and Straniero (1989), using the Yale transformations (Green, Demarque, and King 1987) from the theoretical to the observational plane, and with the Vandenberg (1985) isochrones. Assuming a solar metallicity, and adopting a reddening of $E(B-V) = 0.12$ and a distance modulus of $(m-M)_V = 11.5$ (these values were taken from Twarog and Anthony-Twarog 1989), they found that both sets of isochrones gave a satisfactory fit for the upper portion of the main sequence, the turnoff and the subgiant regions for the 6 Gyr isochrone. However, they found that the VandenBerg isochrones had a discrepancy in colour for the main sequence stars (being too blue for the best fit with the data) which grew more important toward lower luminosities.

Another recent CCD photometry study of NGC 188 was made by Kaluzny (1990); the study was conducted primarily to identify variable stars in the cluster, and no attempt was made to determine its age. His photometry will be of use in comparisons with our own CCD photometry.

Hobbs et *al.* (1990) derived, from a spectroscopic study of seven stars in the turnoff region, an average effective temperature of $< T_e >_{turnoff} = 5885 \pm 120$ K. They used this temperature to estimate the age from evolutionary tracks, and found 7.7 ± 1.4 Gyr. They measured up to six weak Fe II lines in each of the spectra and using model atmospheres by Kurucz (1979), they derived [Fe/H] $= -0.12 \pm 0.16$. This method has the advantage of being independent of both reddening and distance estimates.

1.4 NGC 6791

NGC 6791 ($\alpha(1950.0) = 19^h1^m.0$, $\delta(1950.0) = +37^o45'$) is a very populous, distant, compact object in a fairly crowded star field. It was the subject of a classic study by Kinman (1965), but attracted little attention until the mid 1980's. Recent studies have shown it to be one of the oldest known open clusters (Anthony-Twarog and Twarog 1985), perhaps even the oldest (Harris and Canterna 1981, Janes 1984).

The colour-magnitude diagram of the cluster has a very well-defined red-giant branch and red-giant clump; however the main-sequence below the turnoff seems to have considerable intrinsic scatter, making its delineation more difficult. The striking feature of NGC 6791's colour-magnitude diagram is its close similarity with that of NGC 188. However, its basic parameters are still very uncertain:

1. The metallicity: because of the similarity of the morphology of the CMDs of NGC 6791 and NGC 188, one could infer that the two clusters are also similar in metallicity. However, independent measurements of NGC 6791's metallicity seem to argue against such a conclusion: the most recent estimates (Friel and Janes 1990) found $[Fe/H] = 0.23 \pm 0.15$, making NGC 6791 one of the most metal-rich open clusters in the Galaxy. A high abundance, together with the height of 1 kpc of the cluster above the Galactic plane, would have interesting consequences for the metallicity gradient at right angles to the Galactic disk.

2. The reddening of the cluster has been measured to be around 0.10 mag (Harris and Canterna 1981, Janes 1984) or around 0.20 mag (Kinman 1965). If the higher value of the reddening is adopted, the age of the cluster is (as we will show) about the same as the age of NGC 188. A lower reddening would tend to increase the inferred age of the cluster significantly.

3. The distance modulus of the cluster can be obtained either by main-sequence fitting (although the cluster fiducial is not clearly defined nor photometered to very faint magnitudes) or by assuming something about the absolute magnitude of the

red-giant clump. If, for instance, it is independent of age, one could first align the clump of NGC 6791 with that of another cluster of similar metallicity whose distance is well-known (e.g. M67), and then make an appropriate adjustment for the difference in [Fe/H].

Kinman (1965) was the first to estimate the basic parameters of the cluster: he found a reddening of $E(B-V) = 0.22$, a slight metal deficiency with respect to NGC 188, a distance modulus of $(m-M)_0 = 13.55$, and a rough estimate of its age, 10-12 Gyr, from a fit to theoretical evolutionary curves derived by Sandage (1962).

The next study occurred two decades later when Harris and Canterna (1981) obtained UBV photometry for the cluster. They obtained a reddening of $E(B-V) = 0.13$ (explaining the difference with Kinman's value as being the result of systematic differences in the photometry, the calibration, and by the intrinsic scatter among the stars), a metallicity of $[Fe/H] = -0.2 \pm 0.3$ (from the ultra violet excess on the colour-colour diagram), and, by a fit to Yale isochrones (Ciardullo and Demarque 1977) with $Z = 0.02$ and an interpolated helium abundance of $Y = 0.25$, found a distance modulus of $(m-M)_V = 14.0 \pm 0.2$ and an age of 6-7 Gyr.

Janes (1984) carried out DDO photometry of the cluster. He obtained a reddening of $E(B-V) = 0.10 \pm 0.03$ and a metallicity of $[Fe/H] = -0.08 \pm 0.07$.

Anthony-Twarog and Twarog (1985) obtained CCD photometry of the cluster. They pointed out that, according to the reddening maps of Burstein and Heiles (1982), the position of NGC 6791 corresponds to $E(B-V) = 0.17 \pm 0.02$, and for various reasons they disputed previous results for a lower value of the reddening. They chose to adopt a value of $E(B-V) = 0.20$ in their analysis. The metallicity was assumed to be solar. The distance and the age were obtained from a fit to theoretical isochrones. The Yale isochones gave $(m-M)_V = 13.5$ and an age of 6.0 ± 0.7 Gyr; the VandenBerg isochrones gave $(m-M)_V = 13.2$ and and age of

12 ± 1 Gyr. The difference of 0.3 in the distance moduli is not enough to account for the factor of two difference in the age; it also comes from differences in the computation of the evolutionary tracks and isochrones, and from the normalization to different solar values. For a discussion of the status of stellar evolution models, see VandenBerg (1990).

Kaluzny (1989) obtained his results by fitting VandenBerg isochrones for $Z = 0.0169$ (solar metallicity) to his CCD photometry. His final values are a compromise between two satisfactory fits: $E(B-V) = 0.24$, $(m-M)_V = 13.6$, age of 10 Gyr, and $E(B-V) = 0.21$, $(m-M)_V = 13.35$, age of 12.5 Gyr.

1.5 Melotte 66

Melotte 66 ($\alpha(1950.0) = 07^h24^m.9$, $\delta(1950.0) = -47^\circ 38'$) is a faint, metal-poor open cluster, whose colour-magnitude diagram shows no apparent subgiant branch, though the giant branch is well-developed and there exists a number of stars in the red-giant clump region. The colour-magnitude diagram shows significant scatter amongst the brighter giants, which could be due to field star contamination, abundance variations, or the presence of both a red-giant branch and an asymptotic giant branch (Geisler and Smith 1984).

Hawarden (1976a) was the first to make a thorough analysis of the cluster's properties: he derived a reddening of $E(B-V) = 0.14$ (although later in the analysis he preferred the value of $E(B-V) = 0.17$), a metallicity of [Fe/H] $= -0.4$, and a distance modulus of $(m-M)_0 = 12.4$. He used the morphology of the CMD, the difference in colour between the main-sequence turnoff and the subgiant branch at a point one magnitude brighter in V, to estimate the age of the cluster to be about 6-7 Gyr. This method is sensitive to both the age and the chemical composition of the cluster.

Anthony-Twarog *et al.* (1979) obtained new photometry, and used the Yale isochrones (Ciardullo and Demarque 1977) with $Z = 0.007$ and $Y = 0.30$, to estimate simultaneously the distance and the age of the cluster. Using $E(B-V) = 0.14$ and [Fe/H] = −0.6, they obtained a distance modulus of $(m-M)_V = 12.2$ and an age 6-7 Gyr, in good agreement with Hawarden's values. However, although the fit to the main-sequence was satisfactory, the giant branch clump was approximately 1 mag fainter than those in other clusters, at $M_V = 2$ mag.

Gratton (1982) focused his work on determining the chemical composition of Melotte 66. Using high dispersion spectra of two red giants and a model atmosphere analysis, he derived a metallicity of [Fe/H] = -0.7 ± 0.1. The Yale isochrones (Ciardullo and Demarque 1979) were used, with $Z = 0.004$ (assuming a solar value of $Z = 0.020$) and a helium abundance of $Y = 0.30$. A fit to the observational CMD gave a distance modulus of $(m-M)_0 = 12.98$ and an age of 6 Gyr. Gratton remarked that the distance modulus was extremely sensitive to the choice of Z (for NGC 2243, an increase of +0.003 in Z decreased the distance modulus by 0.25 mag). With this distance modulus, the magnitude of the clump agrees better with those of other clusters.

CCD photometry was obtained by Kaluzny and Shara (1988) for the purpose of finding contact binaries in the cluster, but no attempt was made to derive an age.

1.6 NGC 2204

NGC 2204 ($\alpha(1950.0) = 06^h13m.5$, $\delta(1950.0) = -18°38'$) is a moderately metal-poor, diffuse open cluster, much younger than the other three clusters with an age of about 3 Gyr (Hawarden 1976b). It has a prominent giant branch clump which can be used to determine its distance.

Hawarden (1976b) was the first to obtain photometry of the system. He obtained a reddening of $E(B-V) = 0.08$, and a metallicity of [Fe/H] = −0.2. In order to determine the age of the cluster, he made a differential comparison with M67 and

NGC 188, based on the main sequence turnoff colour; an age of 5.5 Gyr for M67, on the one hand, and 9 Gyr for NGC 188, on the other, would imply an age of 2.8 Gyr and 3.1 Gyr, respectively, for NGC 2204. He then compared his fiducial for the main-sequence with an "evolutionary deviation curve" (derived from an isochrone computed by Hartwick and VandenBerg 1973) corresponding to an age of 5 Gyr, and a distance modulus of $(m - M)_0 = 13.25$.

Since then, Dawson (1978) and Cameron (1985) measured its reddening to be $E(B - V) = 0.08 \pm 0.01$ and $E(B - V) = 0.11 \pm 0.01$, respectively. Its metallicity has also been re-evaluated: Dawson (1978) found [Fe/H] $= -0.41 \pm 0.19$, Cameron (1985) found [Fe/H] $= -0.62$, and Geisler (1987) found [Fe/H] $= -0.47 \pm 0.10$.

1.7 Objectives of study

In view of the diversity of results that have been obtained in the past for NGC 188, NGC 6791, and Mel 66, it is clearly worthwhile to re-examine each of these old clusters more closely.

The main objective of this study is to present and discuss new CCD photometry for these three old open clusters. The data was reduced using the software package DAOPHOT (Stetson 1987), designed for simultaneous-multiple-fitting photometry reduction in crowded fields. The observational colour-magnitude diagrams were then be compared with appropriate theoretical isochrones, provided by D. A. VandenBerg, in order to estimate the absolute ages of these clusters.

A secondary objective is to determine the age of a younger open cluster, NGC 2204, for which no CCD photometry has yet been published.

Chapter 2

Observations and Data Reduction

2.1 NGC 188 and NGC 6791

2.1.1 Observations

The data were obtained at Kitt Peak National Observatory by R. D. McClure and D. A. VandenBerg on the nights of 1986, September 7/8 to 11/12. Images of the clusters NGC 188 and NGC 6791 as well as other fields were taken with the RCA CCD #1 at the f/7.5 focus of the #1 0.9m telescope. The detector chip has a gain of 9.75 electrons/ADU and a readout noise of 7.0 electrons/pixel. Each frame contains 320 x 512 pixels, at a scale of 0.86 arcsec/pixel, yielding an image size of 4.6 arcmin N/S by 7.3 arcmin E/W. Flat-fielding and defringing were done on site using dome flats and standard Kitt Peak fringe frames, respectively. Each frame is the result of averaging three exposures for NGC 6791, and five exposures for NGC 188. Details of the CCD frames obtained for NGC 6791 and NGC 188 are shown in Tables 2.1 and 2.2 respectively.

For NGC 6791 the unique field is centered roughly 4″ W and 73″ S of the cluster center, with the long axis of the CCD oriented in the E-W direction. The seeing was variable; the stellar image cores have a full-width at half-maximum (FWHM) varying from 1″.9 to 2″.1. NGC 188 has five different fields, centered roughly around the cluster center as follows: field NW is centered 103″ N and 73″ W, field NE is

Table 2.1: Journal of Observations for NGC 6791

UT	Region	Filter	Exp.	Airmass	FWHM
10/09/86					
04:07	center	V	180 s	1.016	1″.88
04:21	center	V	360 s	1.025	1″.86
04:50	center	B	180 s	1.053	2″.06
05:01	center	B	420 s	1.065	2″.04

109″ N and 268″ E, field SW is 85″ S and 61″ W, field SE is 91″ S and 268″ E, field SS is 298″ S and 61″ E.

2.1.2 Data Reduction

Instrumental Magnitudes

The photometric reductions were carried out at the Dominion Astrophysical Observatory with codes written by P. B. Stetson: DAOPHOT (Stetson 1987) and ALLSTAR (Stetson, private communication), along with smaller pieces of software.

The first part of the reduction deals with profile-fitting photometry. The reduction procedure has been well documented (see Stetson 1987 sec. IV. and DAOPHOT User's Manual sec. B). DAOPHOT begins by identifying all objects which have a roughly star-like intensity profile. The user then chooses "typical" bright stars in order to derive a point-spread function (hereafter PSF). This PSF is in turn applied to all stars on the frame, and the scaling which is required to fit the intensity profiles of the stars to the PSF profile determines the magnitudes. Simultaneous profile-fitting photometry was done using ALLSTAR (Stetson, private communication): the stars identified by DAOPHOT were subtracted from the frame, the remaining stars were identified and added to the list. DAOPHOT was then used once more to obtain photometry for the stars in the updated list.

Table 2.2: Journal of Observations for NGC 188

UT	Field	Filter	Exp.	Airmass	FWHM
10/09/86					
06:12	NW	B	60 s	1.718	2″.03
06:25	NW	V	60 s	1.710	1″.95
06:32	NW	V	500 s	1.706	1″.96
07:24	NW	B	600 s	1.685	2″.06
08:22	SW	B	60 s	1.669	2″.26
08:30	SW	V	60 s	1.668	2″.06
08:38	SW	V	500 s	1.668	2″.17
09:22	SW	B	600 s	1.669	2″.41
10:19	SE	B	600 s	1.681	2″.28
11:18	SE	V	500 s	1.706	2″.15
12:02	SE	V	60 s	1.733	1″.83
12:09	SE	B	60 s	1.738	2″.13
11/09/86					
03:47	NE	B	60 s	1.836	2″.33
03:54	NE	V	60 s	1.829	2″.24
04:02	NE	V	500 s	1.821	2″.46
04:52	NE	R	40 s	1.775	2″.27
04:57	NE	R	360 s	1.771	2″.11
05:53	SE	R	40 s	1.728	2″.05
05:59	SE	R	360 s	1.724	1″.91
06:39	NE	B	600 s	1.703	1″.84
08:00	NW	R	40 s	1.674	1″.73
08:06	NW	R	360 s	1.673	1″.81
08:45	SW	R	40 s	1.667	1″.82
08:51	SW	R	360 s	1.667	1″.96
10:05	SS	B	60 s	1.677	1″.87
10:12	SS	B	600 s	1.679	1″.72
11:05	SS	V	500 s	1.701	1″.94
11:56	SS	R	40 s	1.732	1″.52

DAOPHOT/ALLSTAR
subtract photometered stars from original frame
locate remaining stars using FIND
add to list of objtars using FIND

↓

DAOPHOT/ALLSTAR
subtract photometered stars from original frame
identify remaining stars by hand
add to list of objects

↓

DAOPHOT/ALLSTAR
create master-list of objects
recreate list of objects for each frame

↓

DAOPHOT/ALLSTAR
final list for profile-fitting magnitudes.

Fig. 3. Steps in Profile-Fitting Photometry.

The following is a more detailed description of the subroutines of DAOPHOT.

(1) FIND: this routine searches the frame for starlike objects. The user has to specify two quantities: the "lowest good data-value" (any pixel whose brightness is below this value will be considered a bad pixel) and the "star detection threshold" (the minimum central height of a star image above the local sky background). Following the suggestion in the DAOPHOT User's Manual, the lowest good data-value was taken five sigma below the mean sky value of the frame; in a 300 x 500 image, this means that there is only one chance in twenty that a real datum would be mistaken for noise. Rather than following the suggested procedure for determining the star detection threshold (DAOPHOT User's Manual Appendix II), a plot of the number of stars detected versus the detection threshold was made. As the threshold approaches zero, the number of would-be stars that are detected increases in an exponential-like way. A reasonable value for the threshold is read

directly from the plot, just above the bend marking the start of the exponential growth. This method enables the user to visualize how the number of stars detected varies with the threshold parameter, and allows for a very consistent choice of the star detection threshold in each frame.

The "maximum good value-data" is an optional parameter corresponding to the maximum brightness of a pixel operating within the linear-response range of the CCD chip. For the RCA #1 chips that were used, this limit was set at 18000 ADU. The brightest stars on the images were therefore saturated and could not be included in further analysis.

(2) PHOTOMETRY: for each detected object, this routine computes an approximate synthetic-aperture magnitude and a local sky value. It uses an "aperture photometry parameter table" in which twelve different apertures are listed, along with the photons per ADU (9.75) and the readout noise (7.00), both parameters obtained from the Kitt Peak National Observatory. The magnitudes which are listed correspond to an aperture radius of 3 pixels, slightly larger than the full-width at half-maximum of the stellar core images. These magnitudes will be used as starting guesses for the profile-fitting photometry.

(3) PSF: the Point-Spread Function is a numerical model of how the actual brightness of a star varies as a function of x and y. It is not an analytical profile, but rather an empirical one obtained by averaging the profiles of a number of "typical" bright stars in one particular frame. It iteratively fits the star profile and subtracts any nearby neighbor which may contaminate the profile. Appendix III of the DAOPHOT User's Manual gives a detailed procedure for deriving PSFs.

(4) NSTAR: this is the multiple-simultaneous-profile-fitting photometry routine. It works with the routine GROUP, which divides the stars in the frame into natural groups, each group to be reduced as a unit, so that two stars which are close enough to influence each other's profile-fit will be reduced simultaneously. This iterative non-linear least-squares algorithm gives more precise positions and magnitudes for the stars on the frame.

(5) SUBSTAR: by subtracting the fitted model profiles of the stars from the original image, we can go back to step (1) and use FIND to identify any left-over stars. We can append the list to the previous one, and repeat the reduction procedure using PHOTOMETRY, NSTAR, and SUBSTAR. The remaining stars (if any) can then be identified by eye and appended to the FIND list. A final run through PHOTOMETRY and NSTAR will give the latest estimates positions and magnitudes.

(6) ALLSTAR: this combines the routines GROUP, NSTAR, SUBSTAR, and will give us the final best estimates of the positions and magnitudes. However, before applying ALLSTAR, we can improve the background noise of the images. In deep CCD images (especially those of NGC 188) the brightest stars saturate the detector, producing charge-overflow columns. The columns were removed using a power law model for trailing columns, and cubic polynomials for preceding columns (see Stetson and Harris 1988 Sec. IIIa for a complete discussion of the problem). The remaining effect of charge leakage was an increase in background noise in the columns above and below each bright star. A second problem which can arise is a varying sky background due to a large number of unresolved faint cluster stars. However NGC 6791 is only a moderately crowded cluster and NGC 188 is a rather sparse cluster, so that the approximation done by DAOPHOT to account for this effect should be sufficient (it uses a separate sky estimate for each group of mutually overlapping stars - see Stetson 1987, Sec. III.D.2.a). Before submitting the final list of objects, the faint objects that were identified on at least two frames (within 2 pixels) were considered to be "real" and were added to the list of objects to be reduced on the third frame. The list was submitted to ALLSTAR which then performed the final reduction.

Aperture Corrections

The magnitudes derived from the profile-fitting procedure are the result of scaling the model point-spread function to the intensity profiles of the stars on the frame. These are referenced to a zero-point which varies from frame to frame. The next step will reduce these magnitudes to a single, absolute zero-point by finding the corrections required to place the profile-fitting photometry on the system of the aperture photometry, using the so-called "aperture corrections" . This will place the cluster stars on the same absolute instrumental scale as the standard stars. All but the ten brightest unsaturated stars were subtracted from the frame, and DAOPHOT performed photometry on these stars at different apertures. Using PSFAP, a code written by R. D. McClure (private communication), the stars were corrected to the photometry corresponding to an aperture of 4.5 pixels; the correction factor was obtained by reading the difference in the photometry at 4.5 pixels, and the photometry at large apertures (typically 15 pixels). This correction factor usually converged rapidly for apertures greater than 10 pixels.

Calibration

The instrumental magnitudes can now be calibrated to a standard system using CCDCAL (Stetson, private communication). Frames of standard stars (Landolt 1983) were taken throughout the course of the observing run with B, V, and R filters (the V−R colour will not be studied in this project but will be available for future studies). To these Landolt standards were added some of Eggen and Sandage's (1969) photoelectric standards. The transformation equations which were used in order to obtain Johnson magnitudes are:

$$v = V + A_0 + A_1(B - V) + A_2X + A_3\,t + A_4\,t^2 + A_5\,t^3,$$
$$b = B + B_0 + B_1(B - V) + B_2X + B_3\,t + B_4\,t^2 + B_5\,t^3.$$

where b and v are the instrumental magnitudes, B and V are the standard Johnson magnitudes, X is the airmass and t is the time (UT) of the observations. The standard stars span 8.38≤V≤17.50 and −0.04≤B−V≤1.39. The range in airmass was 1.17≤X≤2.33. We used the CCDSTD software package (Stetson 1988, private communication) to obtain least-squares solution for the coefficients (with the exception of the extinction coefficient, which was set to the value obtained for a first-order time dependence). For the night of 1986, Sept. 10/11, 131 standard stars were used, and the values of the coefficients are:

$$
\begin{array}{ll}
A_0 = 4.779 \pm 0.045, & B_0 = 4.524 \pm 0.042, \\
A_1 = -0.006 \pm 0.008, & B_1 = -0.230 \pm 0.008, \\
A_2 = 0.115, & B_2 = 0.220, \\
A_3 = -0.125 \pm 0.021, & B_3 = -0.142 \pm 0.018, \\
A_4 = 0.022 \pm 0.003, & B_4 = 0.021 \pm 0.002, \\
A_5 = -0.001 \pm 0.000, & B_5 = -0.001 \pm 0.000.
\end{array}
$$

The average standard error per observation is 0.027 mag and 0.025 mag, for the V and B magnitudes respectively. For the night of 1986, Sept. 11/12, a second order time dependence was used, with 44 standard stars. The coefficients are:

$$
\begin{array}{ll}
A_0 = 4.562 \pm 0.012, & B_0 = 4.211 \pm 0.013, \\
A_1 = 0.005 \pm 0.004, & B_1 = -0.208 \pm 0.005, \\
A_2 = 0.181, & B_2 = 0.226, \\
A_3 = 0.005 \pm 0.005, & B_3 = 0.008 \pm 0.004, \\
A_4 = -0.000 \pm 0.000, & B_4 = -0.000 \pm 0.000.
\end{array}
$$

The average standard error per observation is 0.012 mag and 0.014 mag, for the V and B magnitudes respectively. The fitting of the residuals for the standards is shown in Figures 4 and 5.

Once the calibration to the standard system has been done, stars which are detected on more than one frame (overlapping regions) can be compared in order to detect any differences in the derived magnitudes (only stars within 2.5σ of the

Table 2.3: Photometry Comparison for NGC 188

Frames	ΔV	σ	N	Δ(B-V)	σ	N
NE_L-SW_L	0.03	0.04	21	−0.06	0.03	19
NW_L-SW_L	0.01	0.03	51	−0.02	0.03	50
SE_L-SW_L	−0.03	0.03	43	−0.01	0.02	42
NE_S-SW_L	0.03	0.04	17	−0.02	0.05	18
NW_S-SW_L	0.04	0.04	48	−0.02	0.02	33
SE_S-SW_L	0.03	0.02	35	−0.04	0.02	30
SW_S-SW_L	0.02	0.02	160	0.02	0.02	150

average were included in this comparison). Table 2.3 displays these differences. Column 1 indicates which frames were compared, where the "L" refers to long-exposure frames and the "S" to short-exposure frames. Column 2, 3, and 4 list the average ΔV, the sigma associated with the mean, and the number of stars which were compared, respectively. Columns 5, 6, and 7 list the average $\Delta(B-V)$, the sigma, and the number of stars, respectively. The differences are typically a few hundredths of a magnitude. In order to minimize the internal scatter, we will take the average (weighted by $1/\sigma^2$) of these differences and determine an "absolute" zero-point, to which we adjusted the photometry of the different frames.

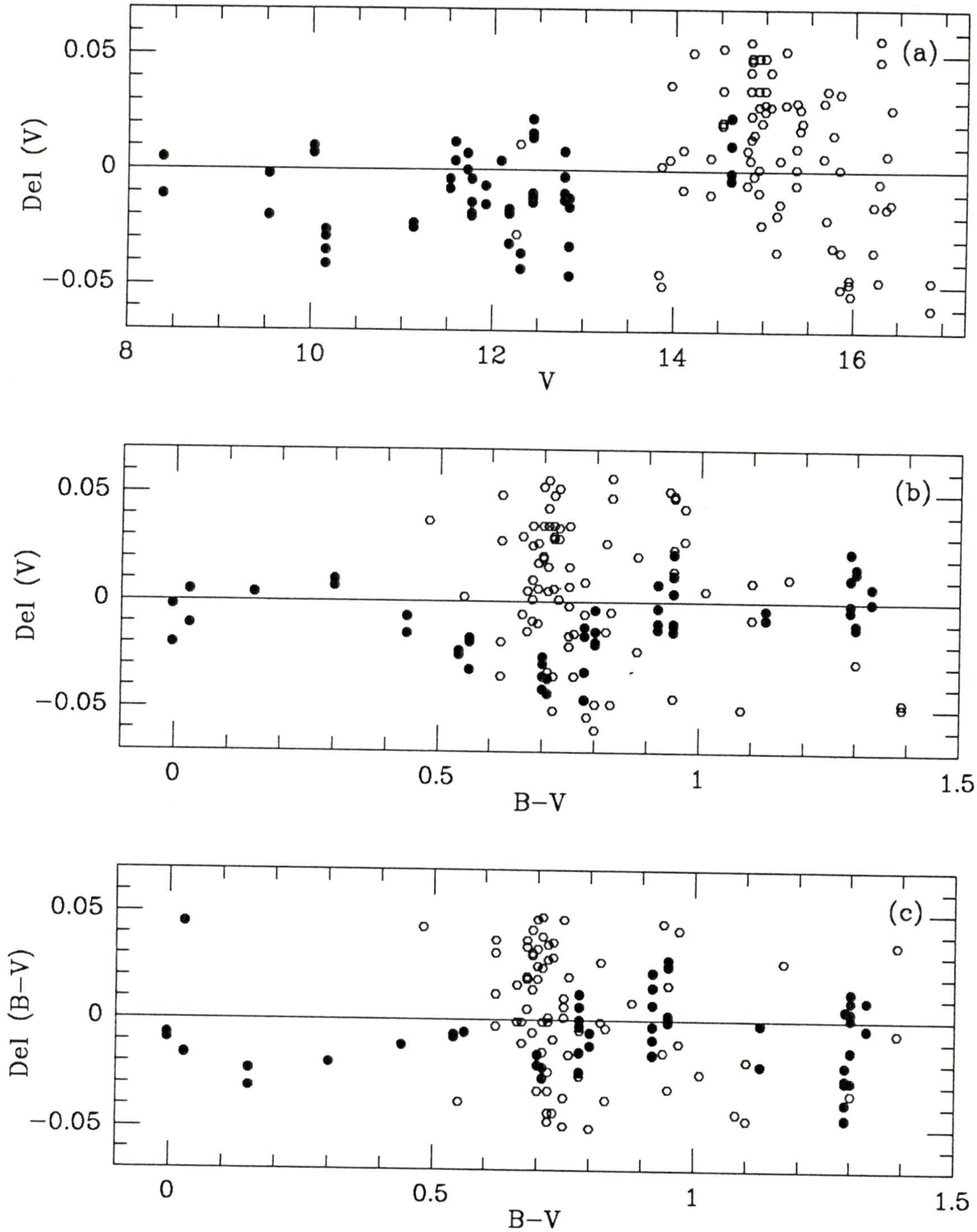

Fig. 4. Fitting residuals (present−published): (a), (b) in V and (c) in $B-V$ for the standards of night of Sept. 10/11, 1986. The filled circles are the Landolt standards (1983), and the open circles are Eggen and Sandage's (1969) photoelectric standards.

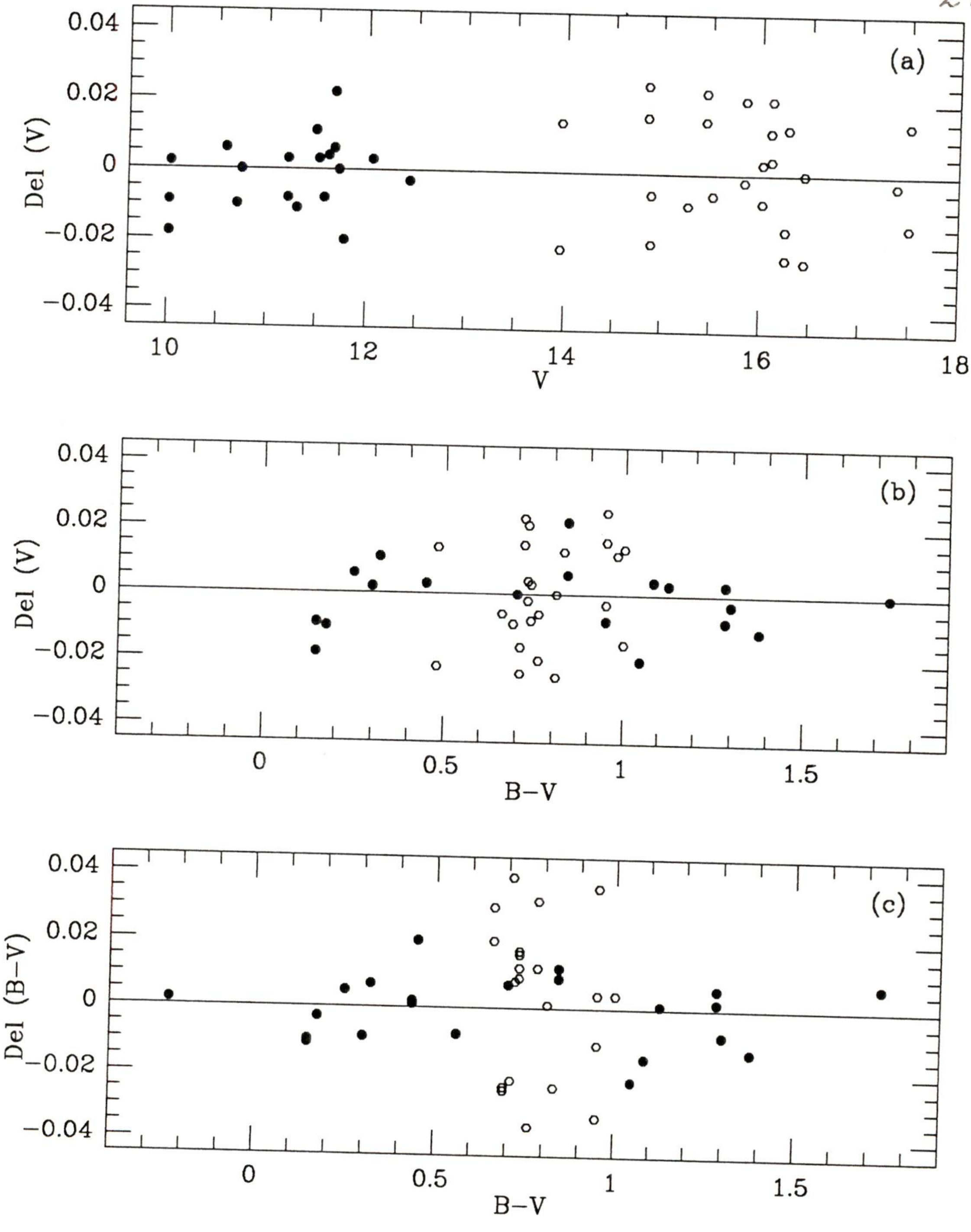

Fig. 5. Fitting residuals (present−published): (a), (b) in V and (c) in $B - V$ for the standards of night of Sept. 11/12, 1986. The filled circles are the Landolt standards (1983), and the open circles are Eggen and Sandage's (1969) photoelectric standards.

2.1.3 The Colour-Magnitude Diagrams (CMDs)

Final Photometry

Before one can obtain the final list of the calibrated magnitudes and colours, two more steps remain: first, the average is determined of the photometry for stars appearing on more than one frame (overlapping regions); then the photometry of the short exposure and long exposure frames is combined for every field. In order to combine the different exposure frames, the CMDs for the short exposures and long exposures were plotted separately. The magnitude at which the scatter of the short exposures outweighed the scatter of the long exposures was determined, and the average was taken of the photometry of brightest stars of the short exposures with the photometry of the corresponding stars of the long exposure frames.

The photometry tables in the appendix show the the final, calibrated photometry for the clusters NGC 6791 and NGC 188, respectively. Column 1 gives positional coordinates for the stars in the images: they are expressed in units of pixels at the scale of the 1.09m telescope ($0''.86$ pixel^{-1}), with x increasing to the west and y increasing toward the north. Columns 2 to 7 list the V magnitude and the B-V colour, with their respective sigma.

Comparison with other published results

We compared our CCD photometry for NGC 188 to the results of Eggen and Sandage (1969). The residuals between Eggen and Sandage's photoelectric values and our values are shown as filled dots in Fig. 6. Comparing 29 stars randomly chosen in ring I gave a mean residual of $V_{present} - V_{Eggen\ and\ Sandage} = 0.005 \pm 0.030$ mag in V. For the B$-$V colour, the mean residual is -0.012 ± 0.020 compared to Eggen and Sandage's photometry. McClure and Twarog (1977) also published photographic photometry of the cluster and observed a systematic difference from Eggen and Sandage's work: $V_{MT} - V_{Eggen\ and\ Sandage} = 0.015 \pm 0.010$.

The photometry for NGC 6791 was compared with Kinman (1965)'s photographic photometry. The residuals $\Delta V = V_{present} - V_{Kinman}$ are shown in Fig. 7. The 22 stars were chosen randomly, and are all situated within $2'$ of the center of the cluster. Colour-magnitude diagrams based on CCD photometry have been obtained by Kaluzny (preprints 1989) for both NGC 6791 and NGC 188. The photometry was reduced using the DAOPHOT package. Although the photometry for individual stars is not available, a rough comparison shows his main-sequence about 0.02 mag to the red of our main-sequence for NGC 188, and his main sequence for NGC 6791 roughly coinciding with ours (the scatter makes the latter comparison difficult).

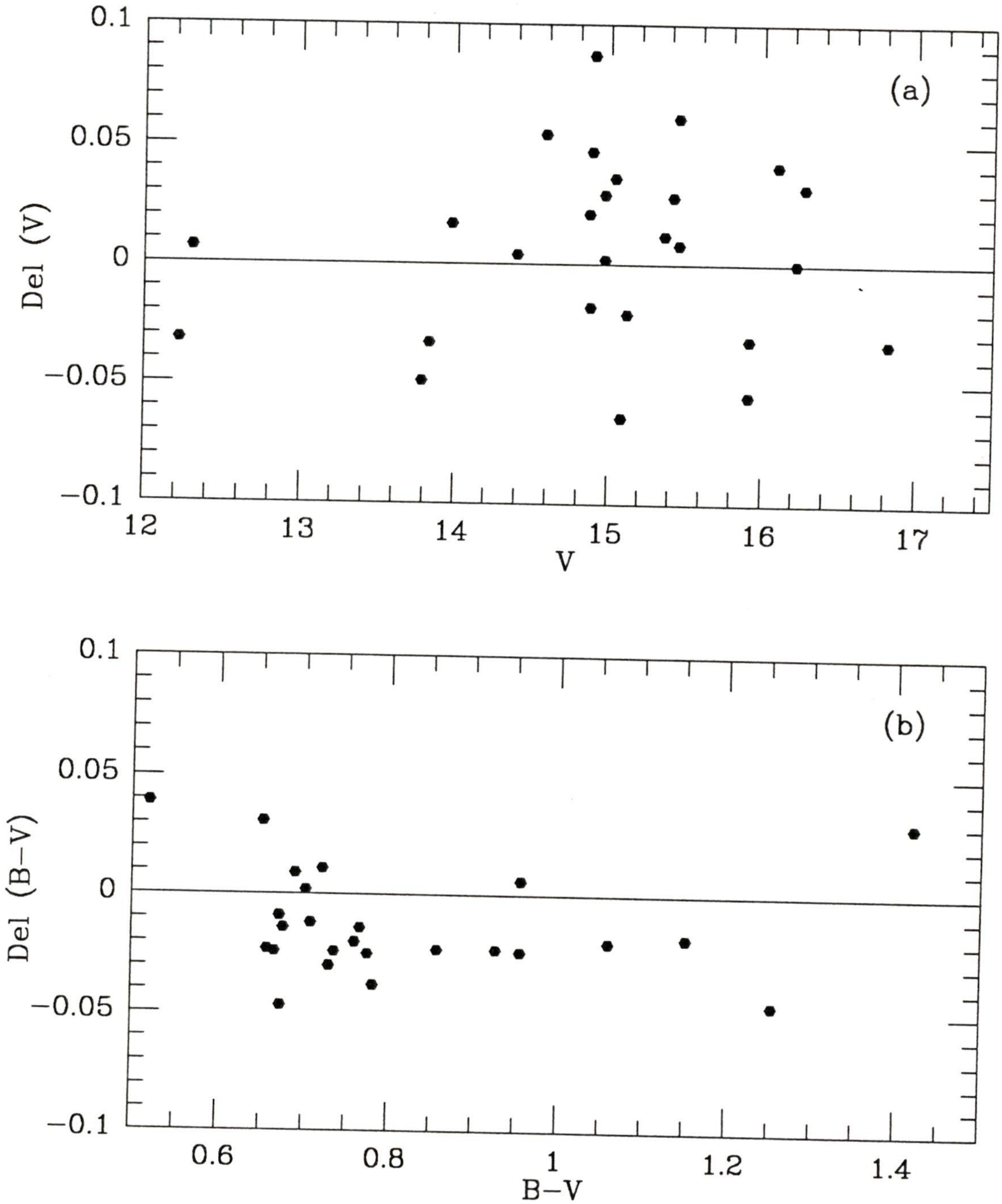

Fig. 6. Comparison of photometry of NGC 188 between present work and Eggen and Sandage's (1969), residuals appearing as filled dots. The residuals are in the sense (present)-(published).

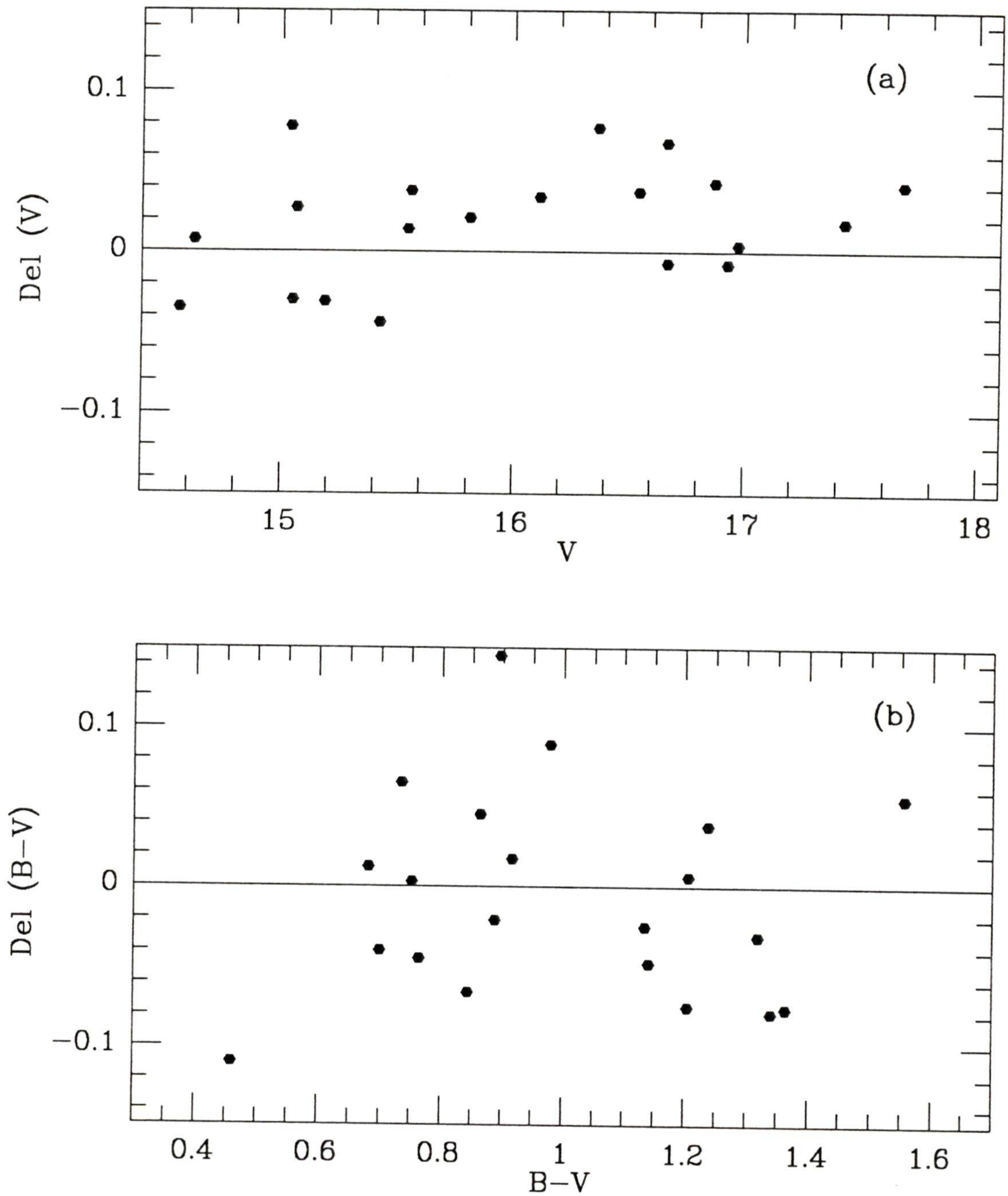

Fig. 7. Comparison of photometry of NGC 6791 between present work and Kinman (1965)'s. All residuals are in the sense (present)-(Kinman).

The CMDs

The CMD of NGC 188 is shown in Fig. 8. The main sequence is well-defined above the 19th magnitude, and there seems to be what may be a binary sequence about 0.75 magnitude above the main sequence. The gap near $V = 15.55$ mag which appears in Eggen and Sandage (1969)'s photometry is not apparent in our photometry. However, there is a slight deficiency of main sequence stars around $V = 15.55$ mag; these few main-sequence stars could include field stars. This gap would be in qualitative agreement with stellar evolution theory, corresponding to the phase of hydrogen exhaustion of the core. However, McClure and Twarog (1977) pointed out that this gap is only marginally expected for clusters as old as NGC 188. The subgiant and giant branches are well defined up to $V = 13.5$ mag. The scatter of the giant branch, much greater than the scatter of the main sequence, has been attributed to possible mass loss (see the discussion in McClure and Twarog 1977).

The CMD of NGC 6791, shown in Fig. 9., shows a striking similarity to the CMD of NGC 188. It is very well-populated, both in its main sequence and in its subgiant and giant branches. The main sequence is defined above the 19.8 magnitude, but seems to have intrinsic scatter associated with it. It shows no apparent gap below the turnoff point, as may be present in the CMD of NGC 188. However, there is a clear gap in the giant branch, centered on $V = 16.3$ mag. A red-giant clump is present, centered on $V = 14.6$ mag.

Future work that will be done on these CMDs will include identifying gaps from cumulative luminosity functions, binary sequences, blue stragglers, and field star contamination.

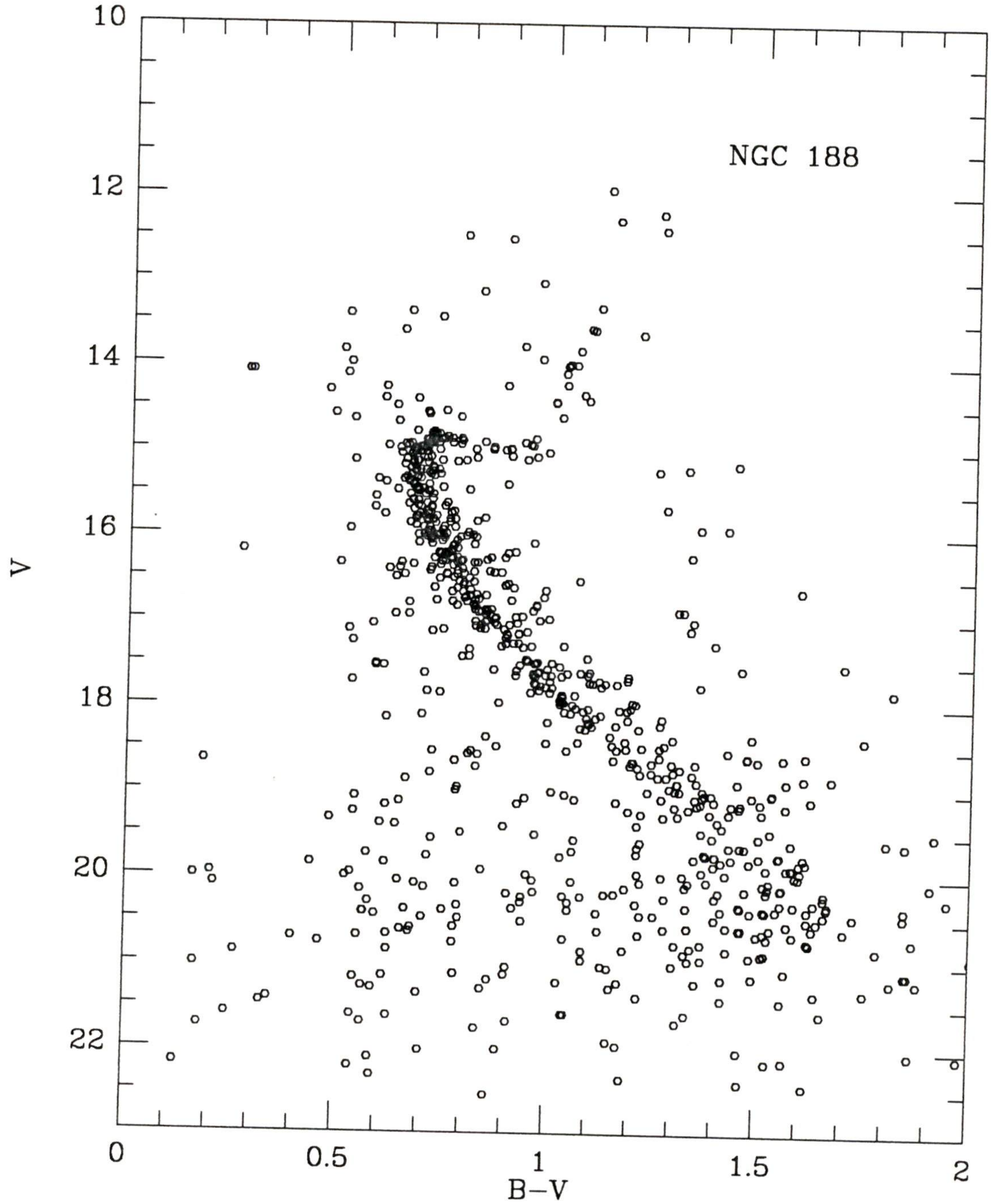

Fig. 8. Colour-magnitude diagram for 840 stars of NGC 188, including field stars. The photometry is listed in the appendix.

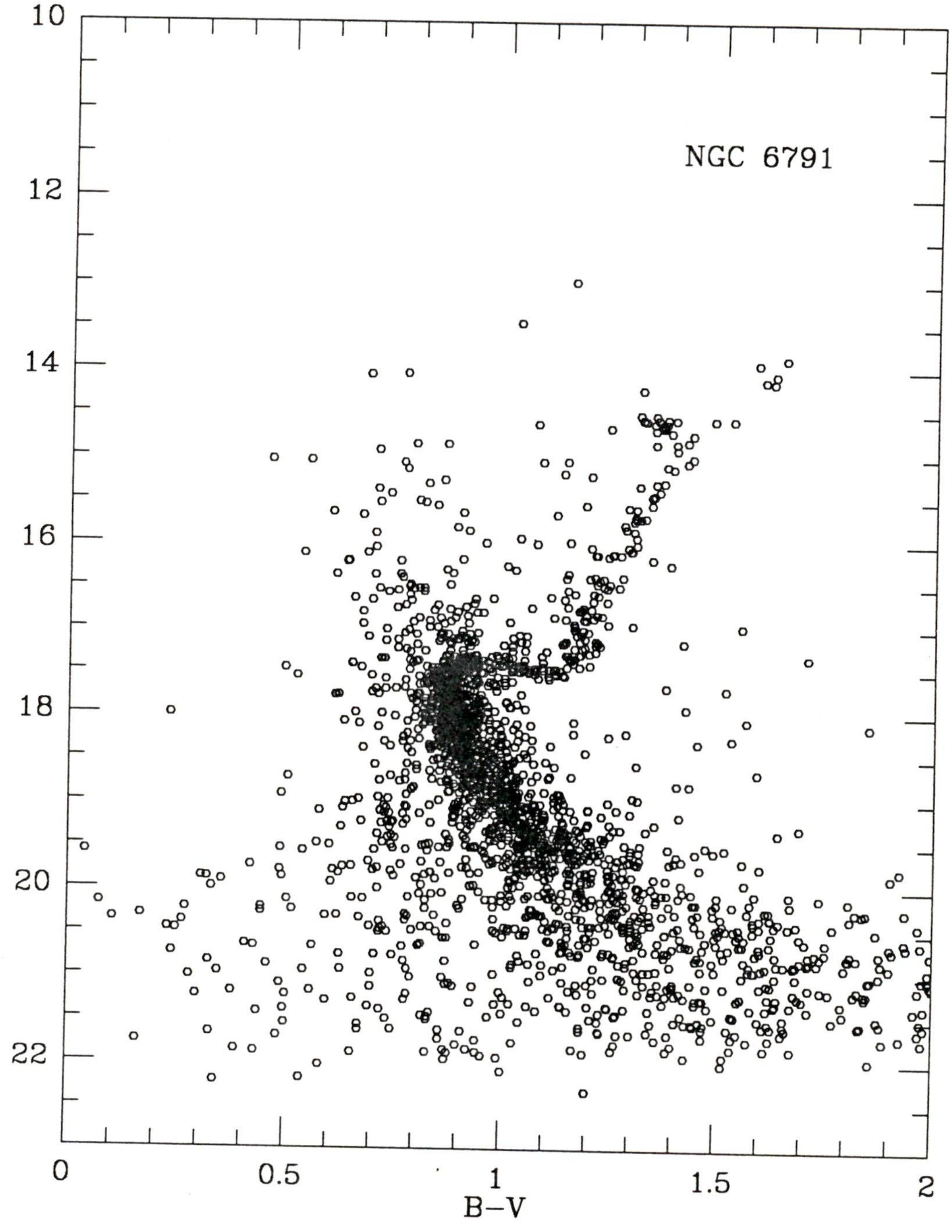

Fig. 9. Colour-magnitude diagram for 2370 stars of NGC 6791, including field stars. The photometry is listed in the appendix.

Table 2.4: Journal of Observations for Melotte 66

UT	Region	Filter	Exp.	Airmass	FWHM
09/02/86					
01:58	Center(SB)	B	30 s	1.060	$1''.28$
02:04	Center(LB)	B	150 s	1.060	$1''.38$
02:32	Center(LV)	V	100 s	1.050	$1''.47$
02:46	Center(SV)	V	30 s	1.040	$1''.26$

2.2 Melotte 66

2.2.1 Observations

The data were obtained at the Cerro Tololo Inter-American Observatory by R. D. McClure on the night of 1986, Feb. 9/10. Images of the cluster Melotte 66 and other fields were taken with a RCA CCD chip at the PF1 focus of the 4 m telescope. For the frames LV and LB (long exposures in V and B, respectively), the CCD chip had a gain of 70.0 photons/ADU and a readout noise of 3.0 electrons/pixel; for the fields SV and SB, the gain was 10.0 photons/ADU and the readout noise 8.0 electrons/pixel. Each frame contains 320 x 512 pixels, at a scale of 0.60 arcsec/pixel yielding an image size of 3.0 arcmin N/S by 5.1 arcmin E/W. The B and V filters that were used were from the CTIO filter set # 2. Flat fielding and defringing were done on site. Only one field was studied, centered $50''$ S and $13''$ E of the cluster center. Details of the observations are shown in Table 2.4 (each long exposure frame is an average of seven exposures).

2.2.2 Data Reduction

The same reduction procedure was followed as for NGC 188 and NGC 6791, using DAOPHOT. The transformation equations are:

$$v = V + A_0 + A_1(B - V) + A_2X + A_3t + A_4t^2,$$
$$b = B + B_0 + B_1(B - V) + B_2X + B_3t + B_4t^2$$

where b and v are the instrumental magnitudes, B and V are the standard Johnson magnitudes, X is the airmass and t is the time (UT) of the observations. The 32 standard stars have a span of $10.59 < V < 16.76$ mag, and $-0.23 < B - V < 1.32$ mag. The range in airmass is 1.053 to 1.397.

For Melotte 66 observations on the night of 1986, Feb. 10, the values of the coefficients in the transformation equations are:

$$A_0 = 1.951 \pm 0.006, \quad B_0 = 1.942 \pm 0.007,$$
$$A_1 = 0.020 \pm 0.008, \quad B_1 = -0.075 \pm 0.010,$$
$$A_2 = 0.158, \quad B_2 = 0.300,$$
$$A_3 = -0.026, \quad B_3 = -0.026,$$
$$A_4 = 0.002, \quad B_4 = 0.002.$$

The average standard error per observation is 0.020 mag in V, and 0.026 mag in B. The fitting of the residuals of the standard stars is shown in Figure 10.

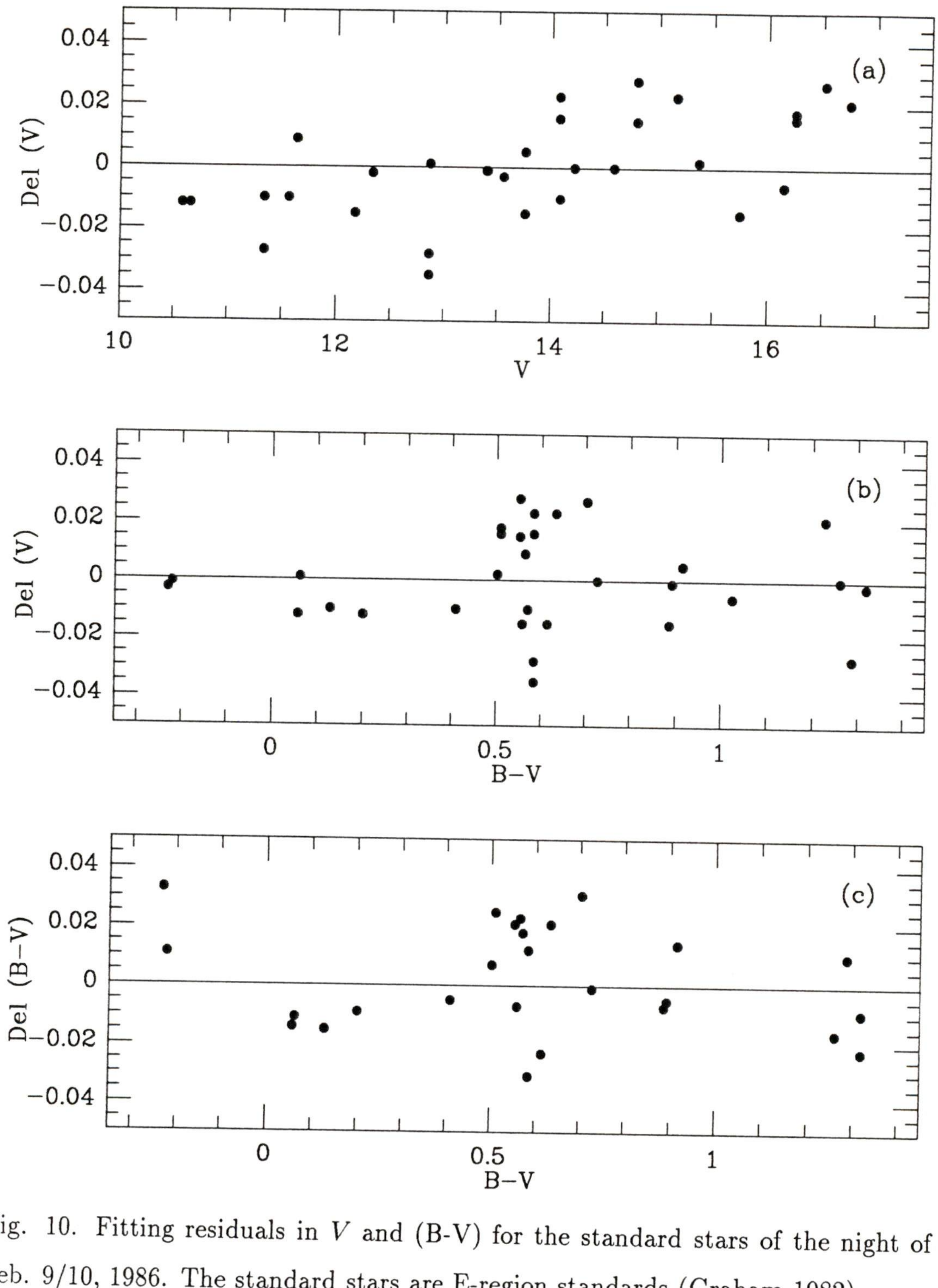

Fig. 10. Fitting residuals in V and (B-V) for the standard stars of the night of Feb. 9/10, 1986. The standard stars are E-region standards (Graham 1982).

2.2.3 The CMD

The final photometry is the result of taking the average of the photometry of the brightest stars ($V < 18.5$ mag) of the short exposures with the photometry of the corresponding stars in the long exposure frames. It is listed in Table 3 of the appendix.

Comparison with previously published photographic and photoelectric photometry (Hawarden 1976a, and Anthony-Twarog *et al.* 1979, respectively) for Melotte 66 is shown in Figure 11. The residuals $V_{present} - V_{AT\,et\,al.}$ are shown as filled dots and $V_{present} - V_{Hawarden}$ are shown as crosses, for the same stars, chosen randomly. The scatter is large, but the different sets of photometry are in reasonable agreement.

The CMD of Melotte 66 is plotted in Figure 12. The main sequence is well-populated, from $V = 20.5$ mag to $V = 16.5$ mag. There is a distinct gap centered around $V = 16.75$ mag, which was also noticed by Hawarden (1976a) and Anthony-Twarog *et al.* (1979) in their studies of the cluster. This gap could correspond to the hydrogen exhaustion phase in the evolution of the cluster. There is a possible binary sequence which follows closely the shape of the main sequence, but about 0.75 magnitude above it. Judging from the scatter of stars to the blue of the main sequence turn-off, there is a number of blue stragglers. These are indeed expected to be concentrated near the center of the cluster (Hawarden 1976a), and have been suggested to be the result of close binaries having undergone mass exchange (Anthony-Twarog *et al.*). There are few stars in the area of the horizontal subgiant branch and on the rising subgiant branch (the brightest stars were saturated on the CCD frames). Hawarden pointed out that the members of the giant clump at $V \simeq 14.5$ were not very concentrated: he found their density in ring 2 (stars within $3'$ to $5'$ of the center) to be higher than in ring 1 (stars within $3'$ of the center); the only field we have of Melotte 66 is contained in his ring 1, and this may partly explain the paucity of giants in our CMD.

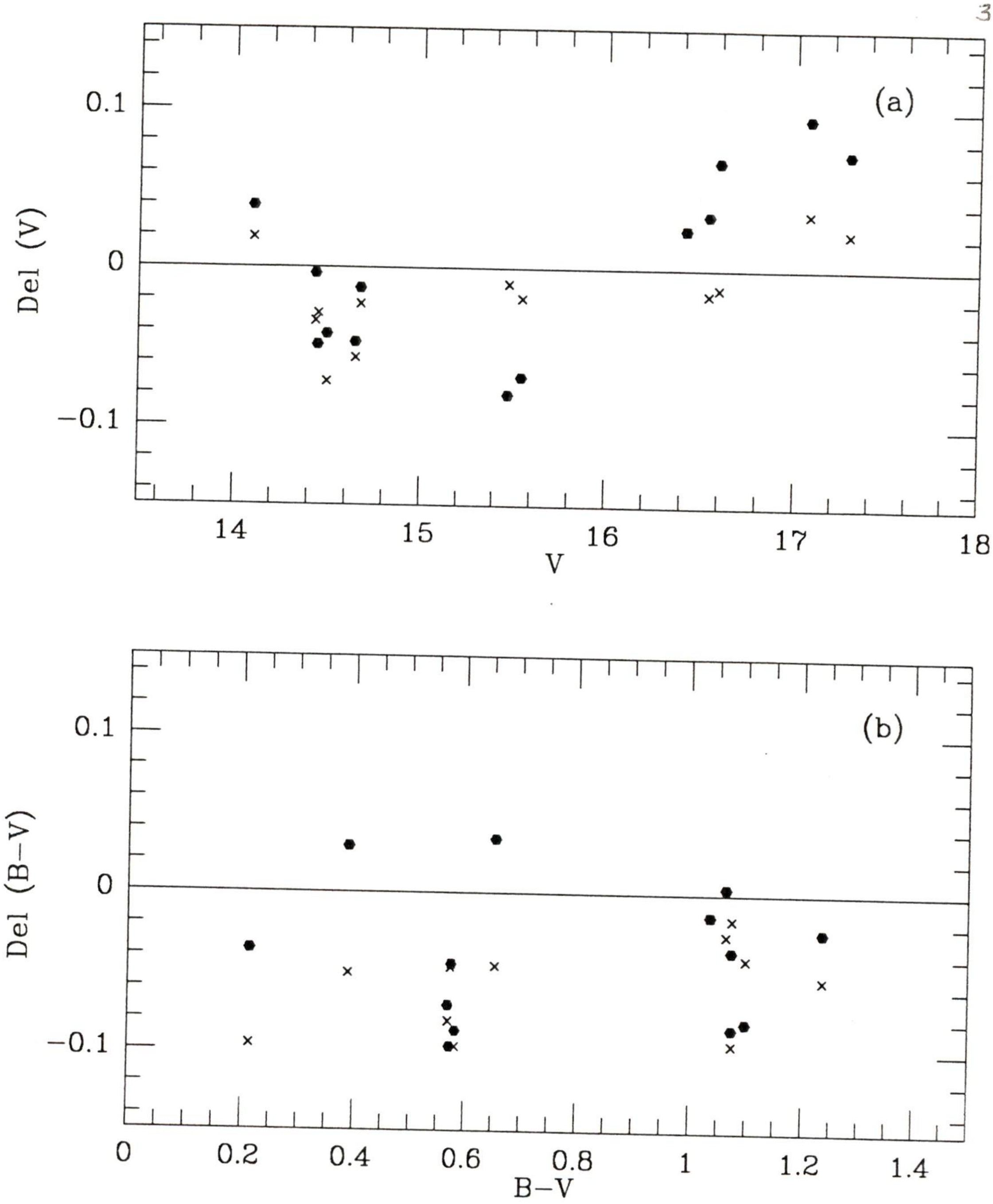

Fig. 11. Comparison of present photometry with published photometry. All residuals are in the sense (present)-(published), and the x-axis corresponds to (present) data. Filled dots are for comparison with Hawarden (1976a)'s photographic photometry (based on a photoelectric sequence), and crosses for Anthony-Twarog *et al.*'s (1979) photoelectric photometry.

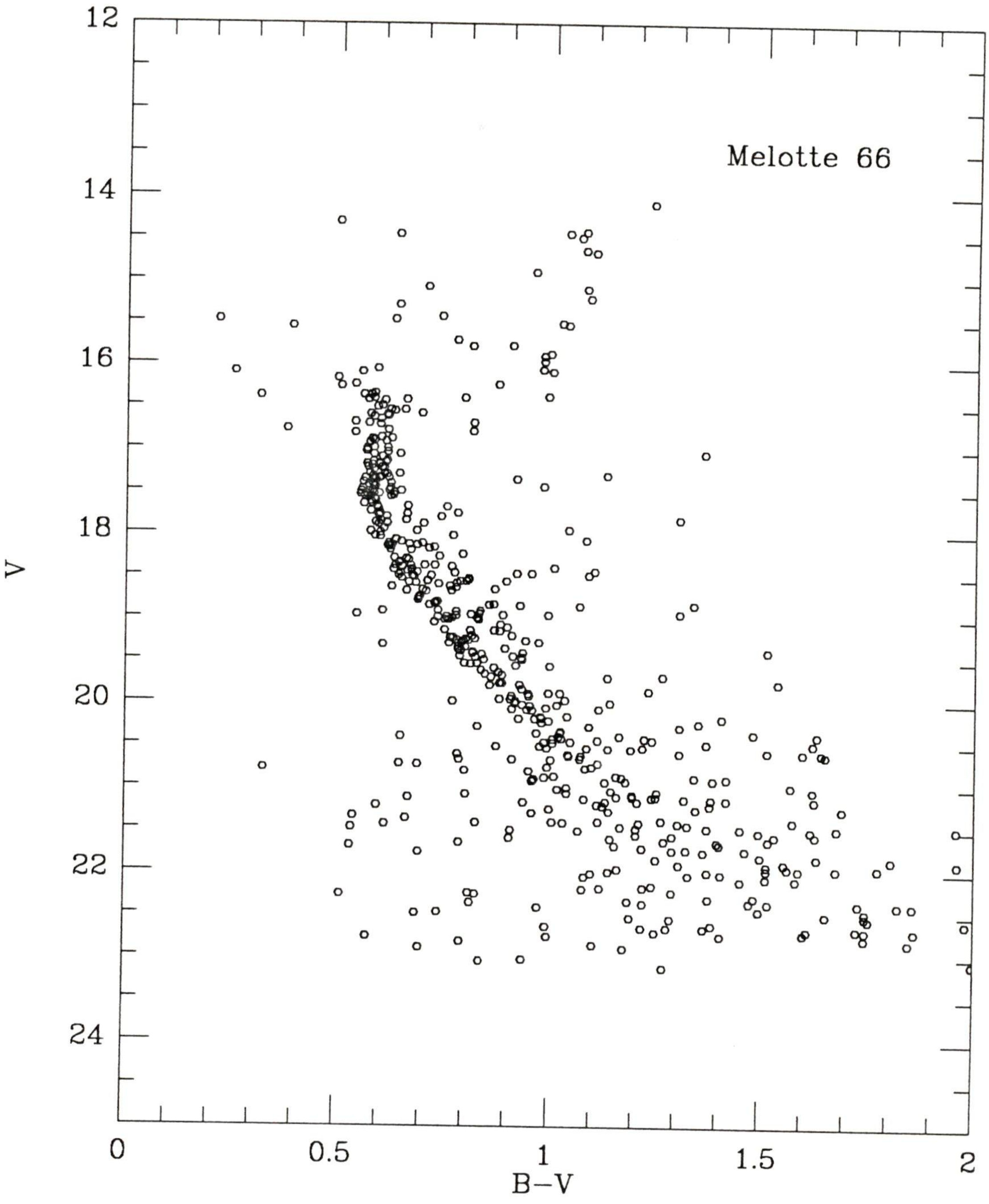

Fig. 12. Colour-magnitude diagram for 564 stars in Melotte 66, including field stars. The photometry is listed in the appendix.

Table 2.5: Journal of Observations for NGC 2204

UT	Region	Filter	Exp.	Airmass	FWHM
23/01/87					
04:14	NE	B	250 s	1.080	$1''.78$
04:25	NE	V	150 s	1.100	$1''.56$
04:30	SE	B	250 s	1.110	$1''.72$
04:38	SE	V	150 s	1.130	$1''.64$
05:03	NW	B	300 s	1.190	$1''.65$
05:09	NW	V	180 s	1.210	$1''.59$

2.3 NGC 2204

2.3.1 Observations

The data were obtained at CTIO by D. A. VandenBerg on the night of 1987, Jan. 23/24. Images of the cluster NGC 2204 and other cluster and fields, were taken with the RCA CCD # 5 at the f/13.5 Cassegrain (direct) focus of the 0.9 m telescope. This chip has a gain of 2.16 electrons/ADU and a readout noise of 22.0 electrons/pixel. Each CCD chip contains 320 x 512 pixels, at a scale of 0.50 arcsec/pixel yielding an image size of 2.6 arcmin N/S by 4.2 arcmin E/W. The filters used were standard CTIO glass filters for the B and V passbands. Flat-fielding and defringing were done on site using dome flats and the CTIO library fringe frames. Details of the CCD frames obtained for NGC 2204 are shown in Table 2.5, where each frame is the result of a single exposure. NGC 2204 has three different fields, centered roughly around the cluster center as follows: field NE is $19''$ N and $45''$ E , field SE is $103''$ S and $45''$ E, field NW is $90''$ N and $135''$ W.

2.3.2 Data Reduction

The calibration to the standard system was done by P. Bergbusch, who used to following transformation equations in order to obtain Johnson magnitudes:

$$v = V + A_0 + A_1(B - V) + A_2X + A_3\,t,$$
$$b = B + B_0 + B_1(B - V) + B_2X + B_3X\,(B - V) + B_4\,t$$

where b and v are the instrumental magnitudes, B and V are the standard Johnson magnitudes, X is the airmass, and t is the time (UT) of the observations. The 23 standards span 9.24 $<$V$<$ 13.10 mag, and $-0.25 < B - V < 1.91$ mag. The range in airmass is 1.030 to 1.440.

For the night of 1987, Jan.24 (NGC 2204), the values of the coefficients are:

$$A_0 = 3.118 \pm 0.002, \quad B_0 = 3.255 \pm 0.003,$$
$$A_1 = 0.007, \quad B_1 = -0.141,$$
$$A_2 = 0.204 \pm 0.023, \quad B_2 = 0.399 \pm 0.023,$$
$$A_3 = -0.002, \quad B_3 = -0.039,$$
$$B_4 = -0.002.$$

The average standard error is 0.010 mag in V, and 0.013 mag in B. The fitting of the residuals is shown in Figure 13.

Table 2.6 displays the differences between the photometry of the stars in the overlapping regions of the fields of NGC 2204 (including only the stars within 2.5σ of the mean). As for NGC 188, we will take the average (weighted by $1/\sigma^2$) of these differences to determine an absolute zero-point, to which we will adjust the photometry of the different frames.

Table 2.6: Photometry Comparison for NGC 2204

Frames	$<\Delta V>$	σ	N	$<\Delta(B-V)>$	σ	N
SE-NE	−0.04	0.02	15	0.05	0.14	20
NW-NE	−0.06	0.05	26	0.01	0.08	25

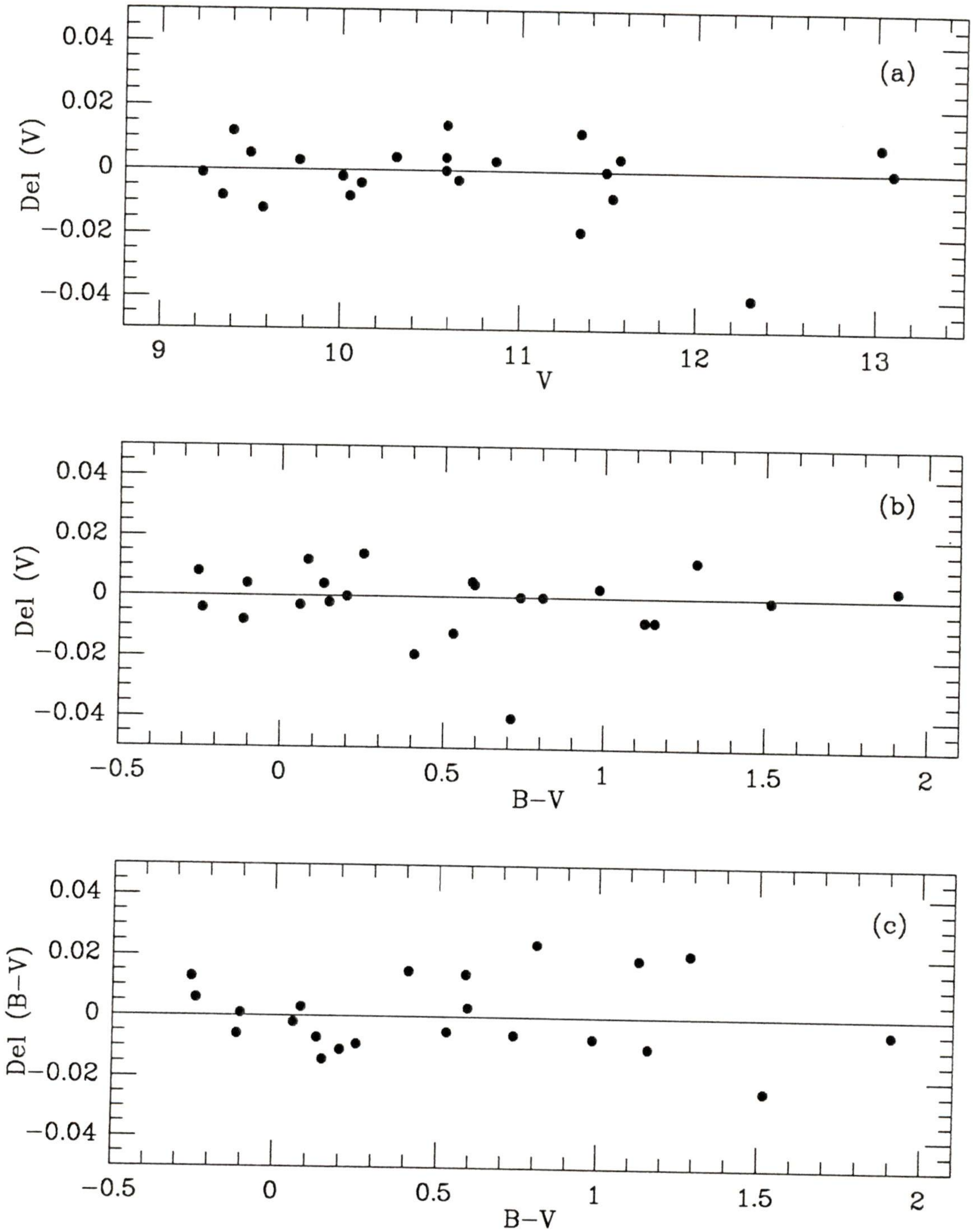

Fig. 13. Fitting residuals in V and (B-V) for the standard stars of night Jan. 23/24, 1987. The standards are E-region standards (Graham 1982).

2.3.3 The CMD

In order to obtain the final photometry list, we took the average photometry of stars appearing on different frames (stars which were within 2.5σ of the average), and combined it with the single photometry of all remaining stars. The final list appears in the appendix.

The photometry was compared to the only previous photometric study of this cluster, by Hawarden (1976b). The residuals show reasonable agreement (see Fig.14), but systematic trends are present.

The CMD of NGC 2204 appears in Figure 15. It is immediately apparent that this cluster is much younger than the other three. The main sequence is well-populated, but the scatter blurs its outline. There is a gap near $V = 15.8$ mag, as in the other CMDs. Few blue stragglers are present. There is a no apparent subgiant branch or giant branch, but there is a giant clump centered around $V = 13.8$ mag.

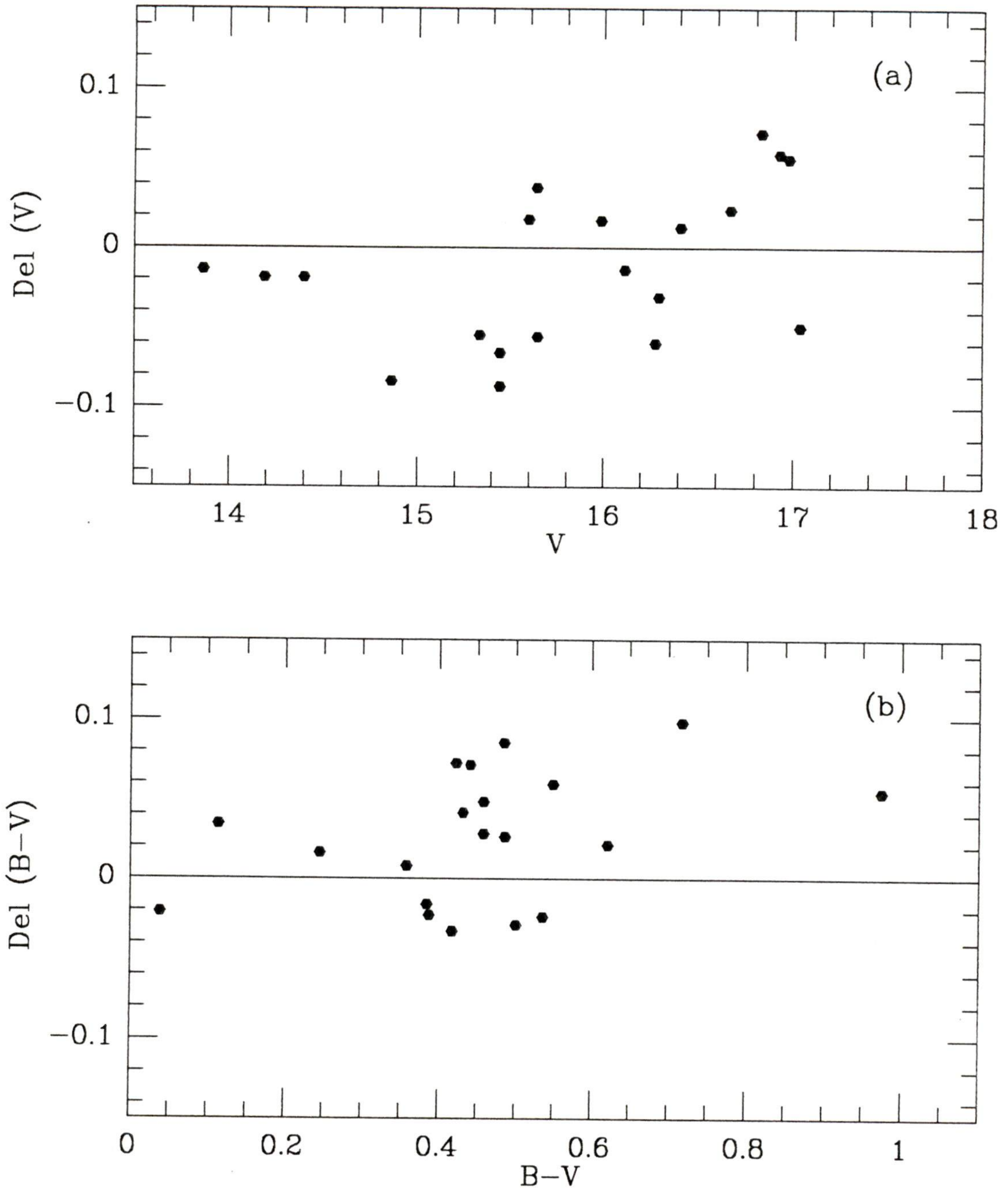

Fig. 14. Comparison of present photometry with that of Hawarden (1976b). Residuals are in the sense (present)-(Hawarden), and the x-axis corrsponds to (present) data.

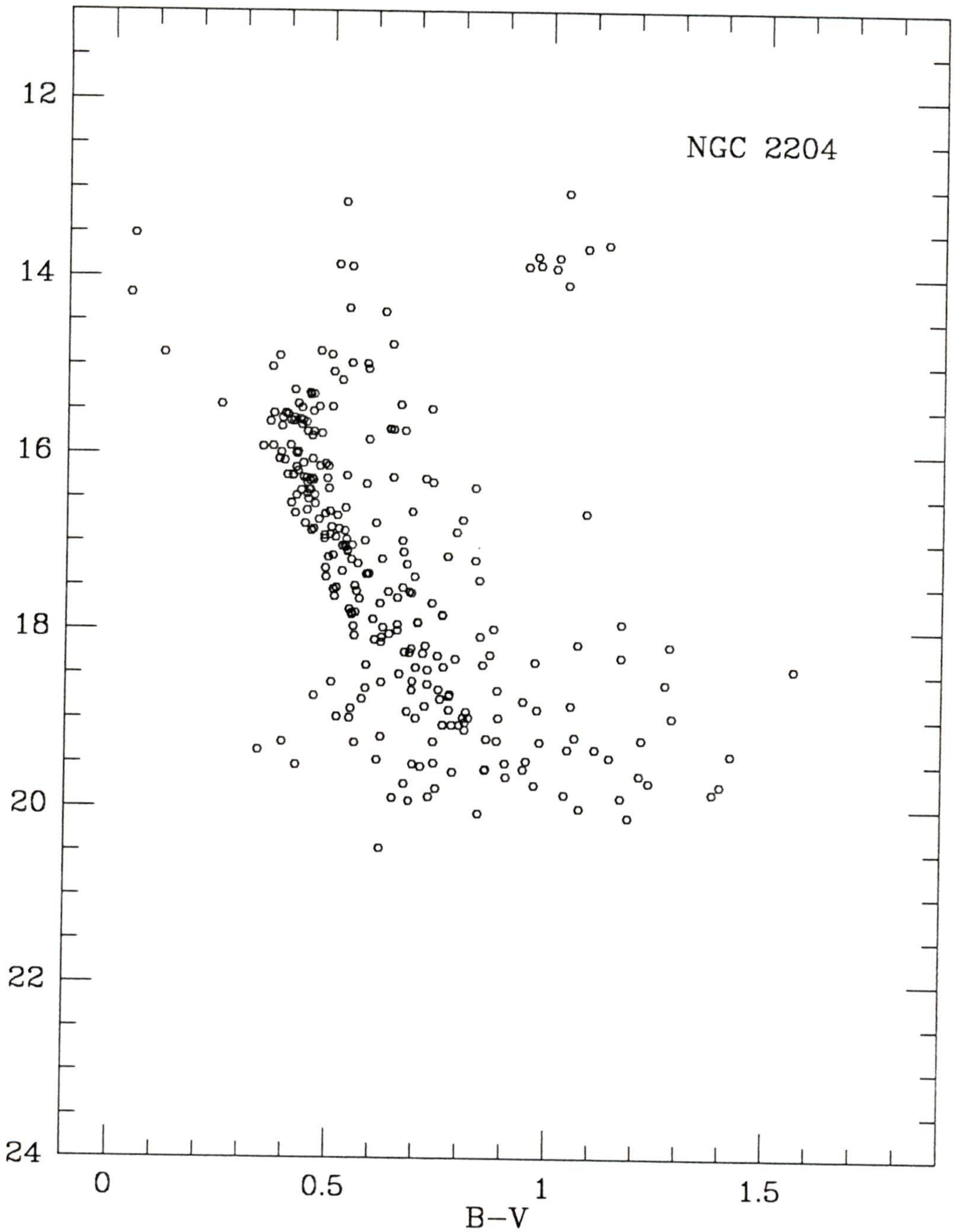

Fig. 15. Colour-magnitude diagram for 279 stars of NGC 2204, including field stars. The photometry for individual stars is listed in the appendix.

Chapter 3

Analysis of the CMDs

The CMDs of the clusters NGC 188, NGC 6791, Mel 66, and NGC 2204 were obtained in chapter 2 (see Figs. 8, 9, 12, and 15, respectively). They will now be compared with theoretical isochrones. First, the fitting procedure, based on the morphology of the CMD and its dependence on various parameters, will be reviewed.

Some of the parameters that must be defined (in this thesis) in the theoretical models are the mixing-length parameter α, the helium abundance Y (fraction by mass of He) and the metal abundance Z. $\alpha = 1.58$, $Y = 0.268$, and $Z = 0.0169$, have been chosen to be the solar parameters, so that a 1.0 $M_{\odot}$ model with the values of Y, Z, and α match the properties of the Sun ($(B-V)_{\odot} = 0.637$, $V = 4.85$, $T_{eff} = 5780$ K, and $L = 3.846\ 10^{26}$ J/sec) when evolved to an age of 4.6 Gyr. α was held constant in the computation of the different models; Y was varied only in one set of isochrones (of solar abundance) by changing the opacities corresponding to the $Z = 0.0169$ element mix. The CNO abundance was held constant at [O/Fe] = 0, corresponding to no oxygen enhancement relative to iron, with respect to the Sun.

metal abundance determines the choice of the set of isochrones to be used. The available models are for abundances $Z = 0.004$, $Z = 0.006$, $Z = 0.010$, $Z = 0.017$, $Z = 0.024$ (VandenBerg 1990, Bergbusch and VandenBerg 1990). The reddening and the distance modulus determine the magnitudes of the horizontal and vertical shifts, respectively, which are needed to align the main sequence of the observational CMD on the $(B-V, V)$ scale, to the main sequence of the isochrones on the unreddened and absolute magnitude scale $((B-V)_0, M_V)$. In order to minimize errors, external contraints are used – i.e., the values of the metal abundance and the reddening are estimated according to the results of photometric or spectroscopic studies. Once the reddening and the metallicity are known, a reliable distance modulus can be derived by main sequence fitting to other clusters of known distance, and/or to theoretical isochrones that have been appropriately normalized. An indirect verification of this result can be made by using the red-giant clump of the CMD – if it is present – since its absolute magnitude has been shown to be effectively constant for clusters of age greater than 2 Gyr (Cannon 1970). The main results of the intercomparison of observations and isochrones are the distance and the age of the cluster.

The next section will present a review of the values obtained for these parameters, as they have been reported in the literature. The distance and the age will then be obtained simultaneously by fitting the main sequence and the turnoff region of the CMD to the isochrones.

3.1 Metallicity and Reddening

Metallicity and reddening estimates were found from a literature survey for previous, independent determinations of these parameters for all four clusters. The results are presented in tabular form (Tables 3.1 to 3.4), and include the method by which the metallicity was obtained.

Metallicity

The metal abundance will determine the choice of isochrones to be used. It will usually be an intermediate value between those available in the theoretical models, in which case fits with the most appropriate model will be used. The metal abundance can obtained using a wide range of methods, which will be very briefly described.

Photometric methods measure general line blanketing in stellar spectra to estimate the metal abundance. UBV photometry uses the correlation of the ultra-violet excess in the $(U-B, B-V)$ diagram with the overall metallicity (Wildey *et al.* 1962). DDO photometry can be used to determine the CN strength of mostly metal-rich stars, which is in turn correlated with metallicity (Janes 1975). Washington photometry also uses late-type giants to determine indices $\Delta(C-M)$ and $\Delta(M-T_1)$, which are found to be correlated with metallicity. These methods provide internally consistent relative measures of metallicity, but they must all be tied to an absolute scale of [Fe/H] established by other means, usually high-dispersion spectroscopy.

More direct methods can be used, involving spectroscopic measurements and model atmospheres; see for example the papers by Cohen (1978, 1979) or Suntzeff (1981), Carbon *et al.* (1982). High resolution spectra can be used to match the line strengths and shapes in observed and theoretical spectra in order to determine stellar and atomic parameters, thus the number of absorbers of each element and the individual elemental abundances in the star. Alternative methods are spectrum synthesis of low resolution spectra, or curve of growth analysis to predict the integrated line strengths of individual lines as a function of elemental abundance. All these methods depend on models which are subject to the uncertainties on stellar temperatures and surface gravities. Systematic differences of ± 0.2 dex are common from study to study.

Reddening

The reddening will determine the magnitude of the horizontal shift of the CMD. The reddening is important, because it affects the age determination in two ways: it distorts the metallicity estimate when the latter is determined photometrically, and it shifts the colour of the turnoff point in the CMD.

Reddening estimates are often obtained from spectral type-colour relations applied to foreground stars. The reddening maps of Burstein and Heiles (1982) are also used to find the reddening at the particular location of the clusters. The best reddening estimates have an uncertainty of ± 0.02 dex.

Tables with Reddening and Metallicity estimates

The following tables list the sources, the reddening, the metallicity estimate and the technique used for determining the metallicity (columns 1 to 4, respectively). A reddening indicated in parentheses means that it has been assumed by the authors in their derivation of the metallicity.

Table 3.1: Reddening and Metallicity for NGC 188

Source	$E(B-V)$	$[Fe/H]$	Technique
1	0.09	+0.07	UBV photometry
2		+0.04	CN blocking fraction
3	0.07	0.00	DDO photometry (δCN)
4	0.04	−0.49	UBV photometry
5	0.13±0.01	0.055	UBV photometry
6	(0.08)	−0.05±0.1	Washington photometry (6 stars)
7	0.12	($\simeq$ 0)	differential comp. with M67
8	0.10±0.03	−0.12±0.16	Synthetic spectra (7 stars)

Sources: (1) Eggen and Sandage, 1969; (2) Pagel, 1974; (3) McClure, 1977; (4) Jennens and Helfer, 1975; (5) Cameron, 1985; (6) Canterna *et al.*, 1986; (7) Twarog and Anthony-Twarog, 1989; (8) Hobbs, Thorburn, and Rodriguez-Bell, 1990.

Table 3.2: Reddening and Metallicity for NGC 6791

Source	$E(B-V)$	$[Fe/H]$	Technique
1	0.22±0.02	≤ 0	slope of subgiant branch
2	(0.22)	+0.75±0.2	scanner abundances (Na D-line ratios)
3	0.13±0.03	−0.2±0.3	UBV photometry
4	0.10±0.03	−0.08±0.07	DDO photometry (7 stars), UBV analysis
5	(0.15)	+0.05	Washington photometry (14 stars)
6	(0.12)	+0.23	Spectroscopy (9 stars)

Sources: (1) Kinman, 1965; (2) Spinrad and Taylor, 1971; (3) Harris and Canterna, 1981; (4) Janes, 1984; (5) Canterna *et al.*, 1986; (6) Friel and Janes, 1990.

Table 3.3: Reddening and Metallicity for Melotte 66

Source	$E(B-V)$	$[Fe/H]$	Technique
1	0.13		UBV photometry
2	0.14	−0.4	UBV photometry
3	0.137±0.017	−0.39±0.18	DDO photometry (8 stars)
4	(0.14)	−0.7±0.1	echelle spectroscopy (2 stars)
5	(0.14)	−0.49±0.2	Washington photometry (4 stars)
6		−0.35	reanalysis of (5)

Sources: (1) Eggen and Stoy, 1963; (2) Hawarden, 1976a; (3) Dawson, 1978; (4) Gratton, 1982; (5) Geisler and Smith, 1984; (6) Canterna *et al.*, 1986.

Table 3.4: Reddening and Metallicity for NGC 2204

Source	$E(B-V)$	$[Fe/H]$	Technique
1	0.08	−0.20	UBV photometry
2	0.08±0.01	−0.41±0.19	DDO photometry (13 stars)
3	0.11±0.01	−0.618	UBV photometry
4	(0.10±0.03)	−0.47±0.10	Washington photometry (8 stars)

Sources: (1) Hawarden, 1976b; (2) Dawson, 1978; (3) Cameron, 1985; (4) Geisler, 1987.

3.2 NGC 188

In order to facilitate the comparison of the CMD with theoretical isochrones, a fiducial of the CMD's principal sequences was derived (see Fig. 16). It was drawn by hand through the data when plotted on a larger scale than that shown in Fig. 16, and the coordinates of the points were determined using a ruler. Granted, this is a subjective procedure, and becomes particularly uncertain when there is scatter along the main sequence, or when there is a deficiency of stars, most often in the subgiant branch region. However, a more objective approach is not really possible when the scatter in the photometry is so large. Once the parameters for the "best fit " have been determined, the isochrones will be compared to the data rather than to the fiducial (Fig. 21).

Recent studies seem to suggest that NGC 188 has a slightly more metal-poor composition than the Sun. The fiducial of the CMD was fitted to both the $Z = 0.017$ (solar abundance) and the $Z = 0.010$ ([Fe/H] $= -0.22$) isochrones in Figures 17 and 18, respectively. The fits were obtained by assuming a reddening consistent with the findings of Table 3.1, and determining the distance modulus by a sliding vertical fit of the main sequences. Each plot therefore represents a fit for a different set of parameters ([Fe/H], $E(B-V)$, $(m-M)_V$).

The solar isochrones (Fig. 17) offer the best fit for a reddening of $E(B-V) = 0.07$ and a distance modulus of $(m-M)_V = 11.28$. As the reddening increases, the slope of the subgiant branch of the isochrones becomes increasingly too steep for the fiducial, and there is an increasing discrepancy of theory and observation at the lower red giant branch. This reddening is consistent with previous determinations, since the average of the $E(B-V)$ determinations to date is $E(B-V) \simeq 0.08$ (see Table 3.1). If one recalls the comparison between the present photometry and Eggen and Sandage's (1969) photoelectric photometry (see Fig. 6), there is an offset of $(B-V)_{present} - (B-V)_{ES} = -0.01$ mag between the two studies. If this systematic difference were the result of the present photometry being too blue by a hundredth of a magnitude, the reddening would be accordingly too small. However, a reddening of $E(B-V) = 0.07$ cannot be ruled out.

If one looks at the overall fit of the data and the isochrone, the fiducial points fall right along the main sequence, and follow quite closely the isochrone of age 8 Gyr. In Fig. 19(a), the fiducial points follow the main sequence of the isochrone, and the shape of the turnoff and the subgiant branch correspond almost exactly to a single isochrone of age intermediate to 7 and 8 Gyr. The discrepancy between data and isochrones begins at the base of the red-giant branch, where the colour of the lower red-giant branch of the isochrones is too red by a few hundredths of a magnitude. This colour is extremely sensitive to the parameters assumed in the theoretical models, and is considered to be very uncertain; the discrepancy with the data is therefore not necessarily a compelling argument against the inferred age (see VandenBerg 1990).

The second set of isochrones (see Fig. 18) is metal-poor relative to the Sun, with $Z = 0.010$ ([Fe/H] $= -0.22$). The best match of the shape of the data and theory would correspond to Figs. 18(a) and 18(b). Here, although the fiducial sits just above the lower part of the main sequence, the upper main sequence, the turnoff region and the slope of the subgiant branch agree well with the 9 Gyr isochrone. The best fit was found to be for a reddening of $E(B-V) = 0.11$ and a distance modulus of $(m-M)_V = 11.23$. Such a discrepancy between the main sequences could arise if the assumed solar colour, $(B-V)_\odot = 0.635$ mag, to which both the isochrones and the main sequence fit are normalized, was somewhat too blue.

The best fit with the isochrone of solar abundance (see Fig. 20(a)) was then compared to a third set of isochrones, also for solar abundance, but with enhanced opacities – see Fig. 20(b). (Opacity tables for $Z = 0.024$ were assumed in the calculation but the heavy element mix was retained at $Z = 0.0169$.) There is no significant improvement between the two, except for making the fiducial correspond to 7 Gyr rather than 7.5 Gyr.

The best fit for a metallicity of [Fe/H] = −0.12 (Hobbs *et al.* 1990) for NGC 188 would be halfway between the [Fe/H] = 0 and [Fe/H] = −0.22 isochrones, shown in Fig. 19(a) and 19(b), respectively. It corresponds to a reddening of $E(B-V) = 0.09$, a distance modulus of $(m-M)_V = 11.25$, and an age of approximately 8 Gyr.

The data points of the CMD of NGC 188 (shown in Fig. 8) were superimposed on the solar abundance isochrones (see Fig. 21). A direct comparison such as this, although more difficult to assess, has the advantage of avoiding any errors that may have been introduced by working with the fiducial. The overall agreement is better than that reported in any previous published work.

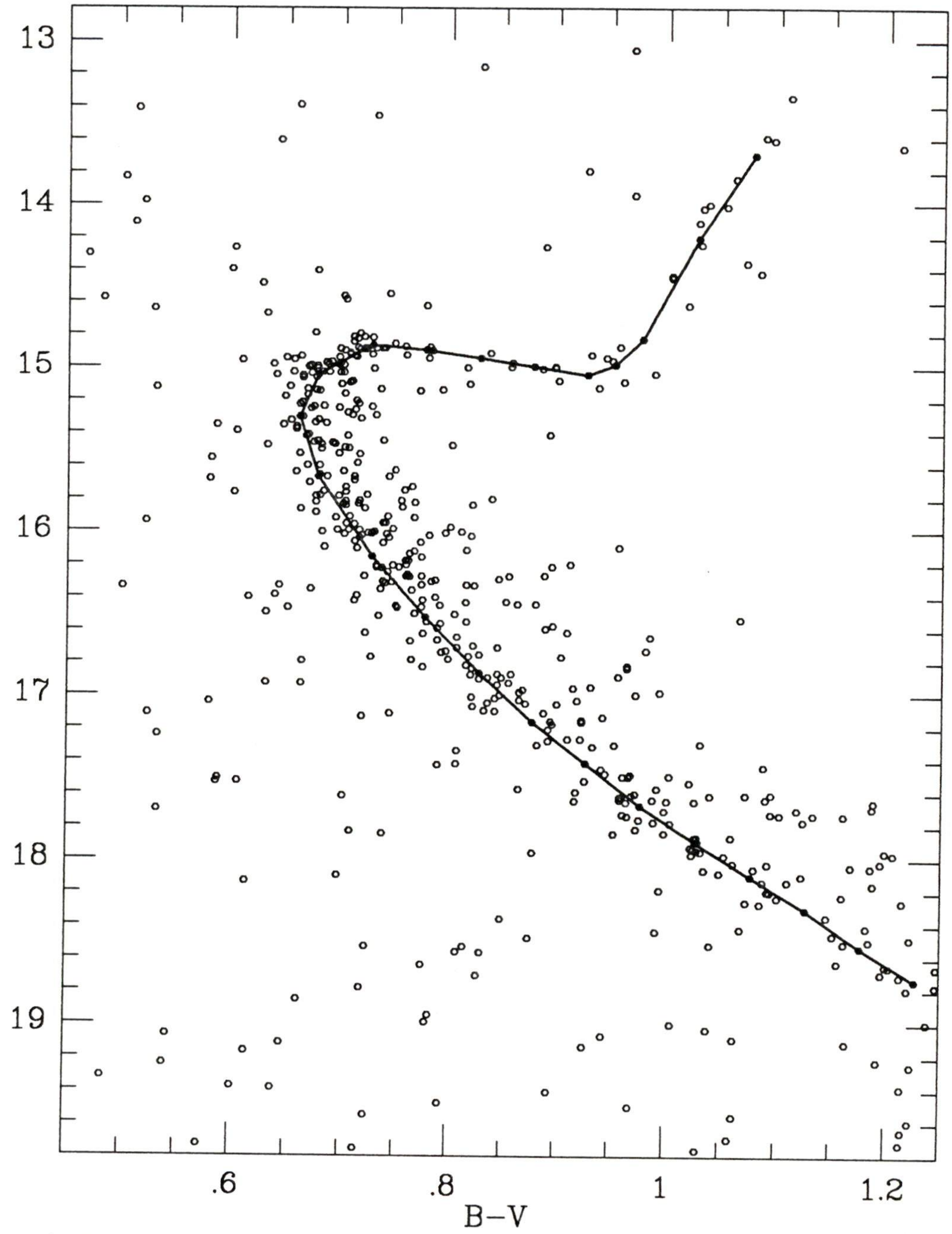

Fig. 16. CMD of NGC 188, with the fiducial superimposed on the data. This fiducial will be used in subsequent diagrams to estimate the goodness of the fit more easily.

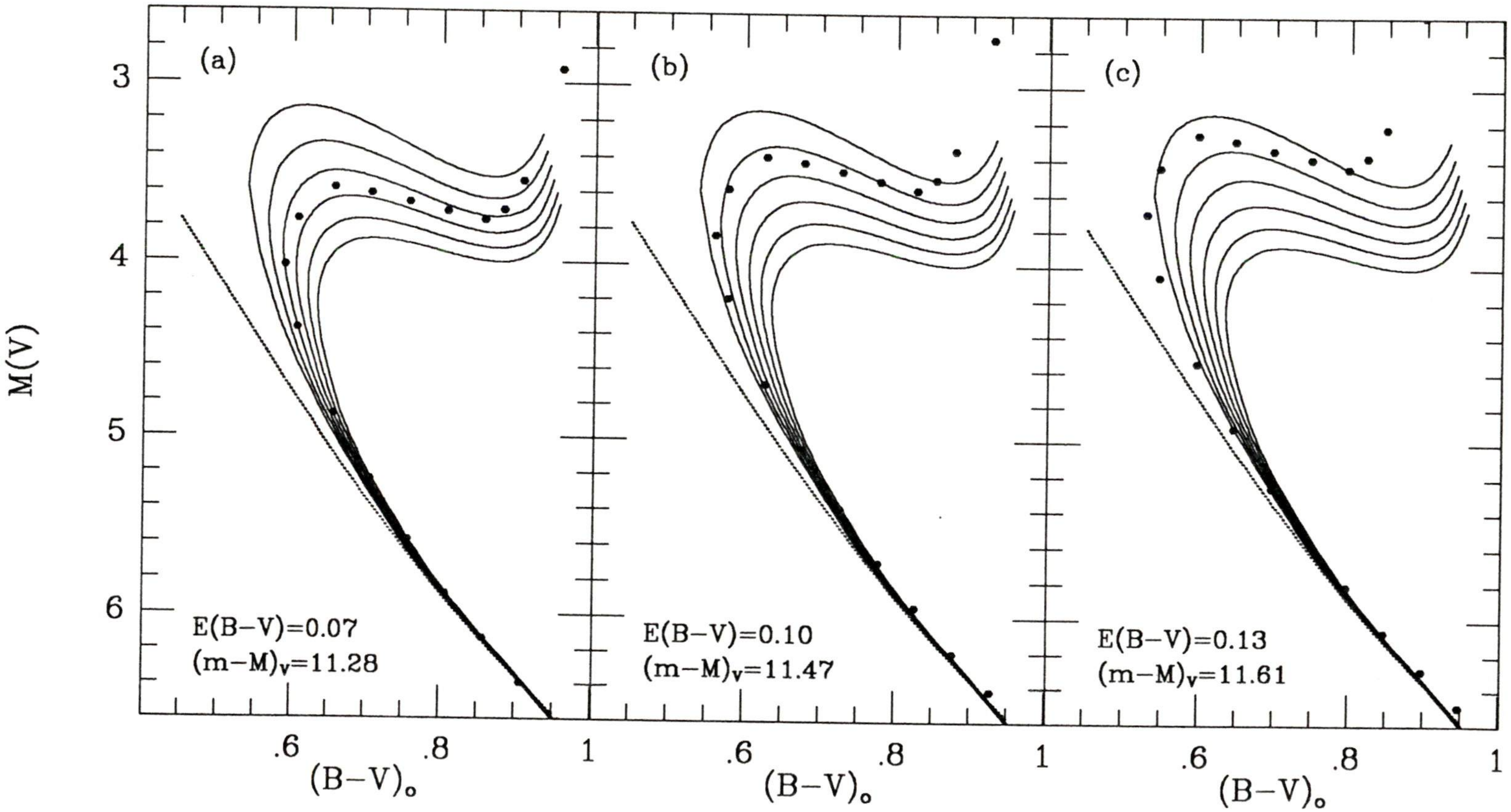

Fig. 17. Fiducial of NGC 188 superimposed on the isochrones for $Y = 0.27$, $Z = 0.017$ (solar abundance). (a), (b), and (c) show how the choice of the reddening $E(B-V)$ affects the distance modulus $(m-M)_V$, and the age. The isochrones are for ages of 5 to 10 Gyr, in steps of 1 Gyr.

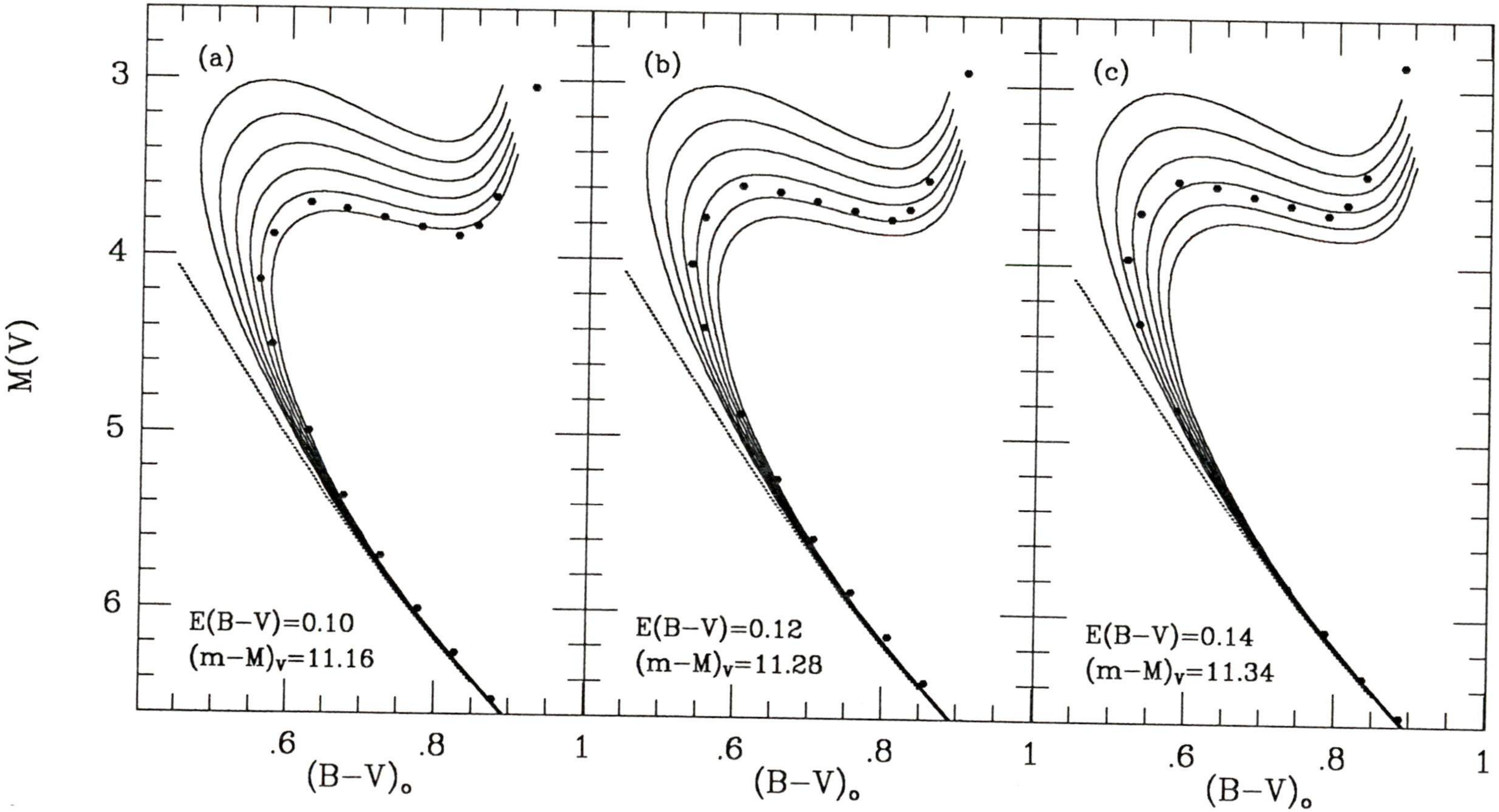

Fig. 18. Fiducial of NGC 188 superimposed on the isochrones for $Y = 0.27$, $Z = 0.010$ ([Fe/H] = −0.22). The isochrones are for ages of 5 to 10 Gyr, in steps of 1 Gyr.

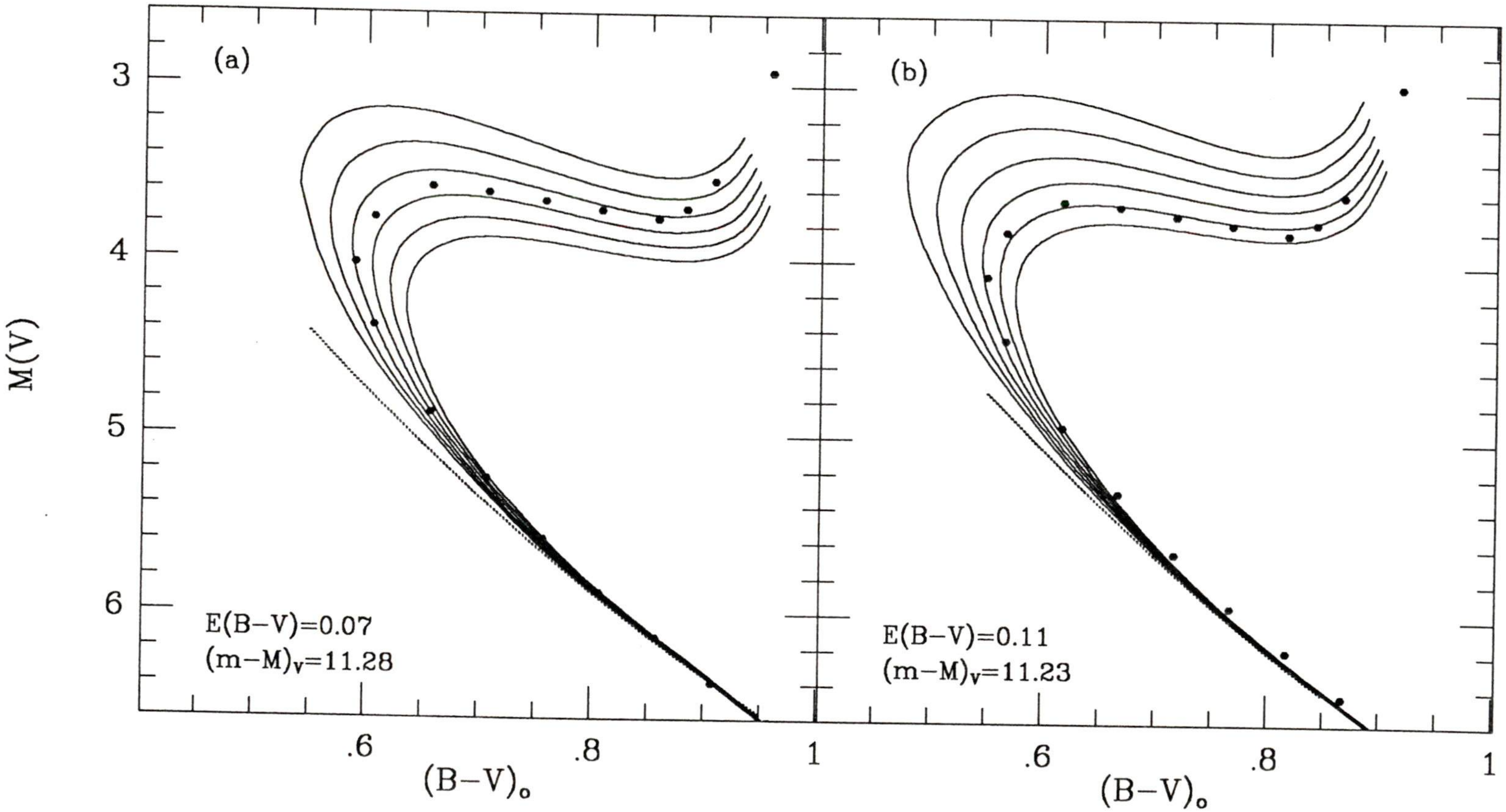

Fig. 19. Comparison of the fiducial of NGC 188 with (a) the $Z = 0.017$ (solar abundance) isochrones, and (b) the $Z = 0.010$ ([Fe/H] $= -0.22$) isochrones. The current best estimate of the cluster is [Fe/H] $\simeq -0.1$, approximately the mean of those of the two sets of models that have been plotted. In both cases the isochrone ages were from 5 to 10 Gyr, in steps of 1 Gyr.

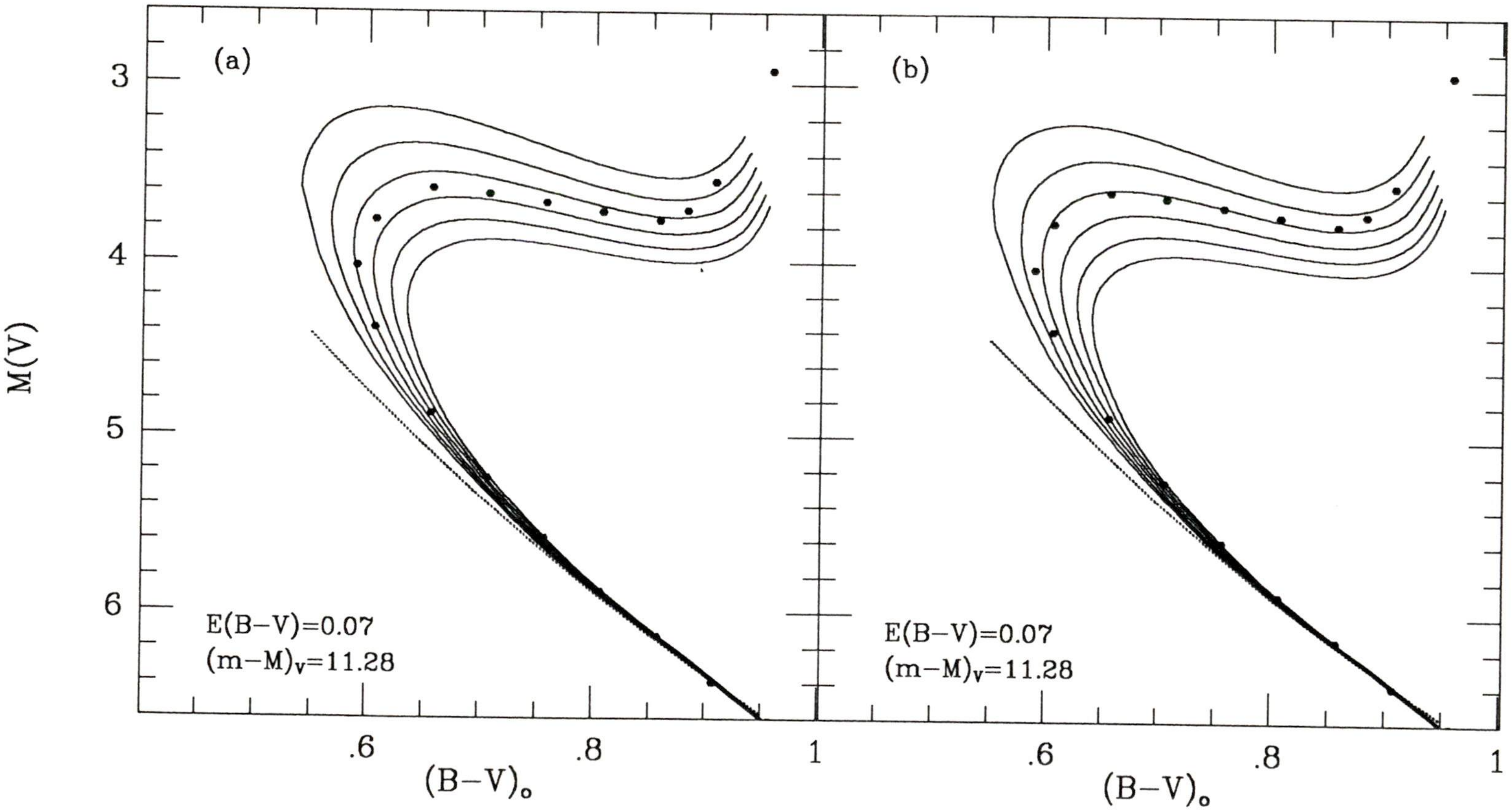

Fig. 20. Comparison of the fiducial of NGC 188 with (a) solar abundance isochrones and (b) solar abundance isochrones with enhanced opacities. The isochrones are for ages 5 to 10 Gyr, in steps of 1 Gyr.

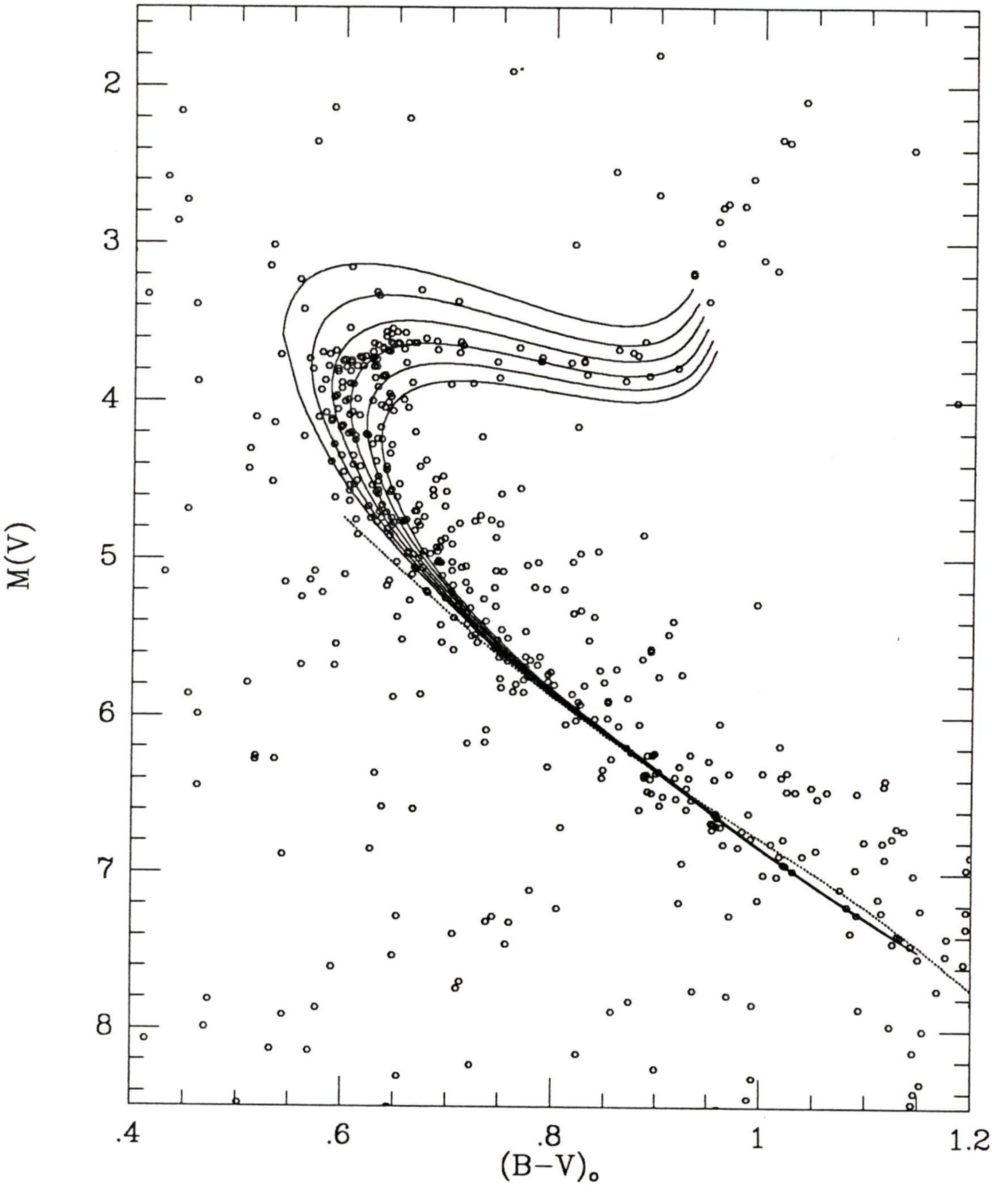

Fig. 21. Colour-Magnitude Diagram of NGC 188 superimposed on isochrones of ages 5 to 10 Gyr (in steps of 1 Gyr) for $Y = 0.27$, $Z = 0.017$ ([Fe/H] = 0), $E(B-V) = 0.07$, and $(m-M)_V = 11.28$.

3.3 NGC 6791

The only available spectroscopic study of NGC 6791 (Friel and Janes 1990) suggests that the cluster has a metal-rich composition with respect to the Sun. The fiducial, as defined in Fig. 22, was therefore compared to the set of isochrones with $Z = 0.024$ ([Fe/H] $= 0.15$), shown in Fig. 23.

The best fit was obtained for a reddening of $E(B-V) = 0.22$ to 0.24: the main sequence, the turnoff region and the subgiant branch follow a single isochrone, of 8 or 8.5 Gyr. There is still a discrepancy at the level of the red-giant branch, which was discussed in the previous section. The distance modulus $(m-M)_V \simeq 13.60$ is more subject to error, because the fit of the main sequence is not conclusive, for two reasons. First, the lowest fiducial point corresponds to an apparent magnitude of 18 mag, and cannot be reliably defined any fainter. Second, the scatter along the main sequence (see Fig. 22) makes the fiducial more difficult to define, and more at risk of being inaccurate.

However, the red-giant clump of NGC 6791 is very well defined (see Fig. 9), at an apparent magnitude of $V = 14.6$ mag. Recent theoretical work by Ben Dorman (private communication) has shown the clump's absolute magnitude to be $\simeq 1.0$ for solar metallicities and slightly fainter for more metal-rich clusters. This would agree with a distance modulus 13.6 (or a little less), which was found to correspond to the best fit to the data (see Fig. 23(c) and (d)).

The reddening of the cluster is still matter of controversy. The metallicity of [Fe/H] $= 0.23$ obtained by Friel and Janes (1990) was based on a reddening of $E(B-V) = 0.12$ (Janes, private communication). However, the isochrones for [Fe/H] $= 0.15$ (see Fig. 23) agree best with the fiducial for reddenings greater than $E(B-V) = 0.22$. If higher metallicity models were available, the reddening would be slightly lower, and the age even greater. The effect of a higher metallicity on the distance modulus can be estimated from a semi-empirical main sequence fit (described in detail in VandenBerg and Poll 1989). For a metallicity of [Fe/H] = 0.30, say, and a reddening of $E(B-V) = 0.23$, the best fit would be for a distance modulus of $(m - M)_V = 13.85 \pm 0.05$. This would imply an absolute magnitude of $M_V = 0.75 \pm 0.05$ for the red-giant clump, slightly brighter than for the solar abundance case, as expected from the theory.

Fig. 24 illustrates the effects of varying the distance modulus by 0.10 mag for an "optimum" reddening of $E(B-V) = 0.22$. Taking into account the uncertainty on the main sequence, and the possible errors introduced by the uncertainty on the solar colour to which the isochrones were normalized, all three fits are reasonable, and correspond to an age of about 8$\pm$0.5 Gyr. Fig. 25 shows a "best fit" with the CMD data points plotted rather than with the fiducial.

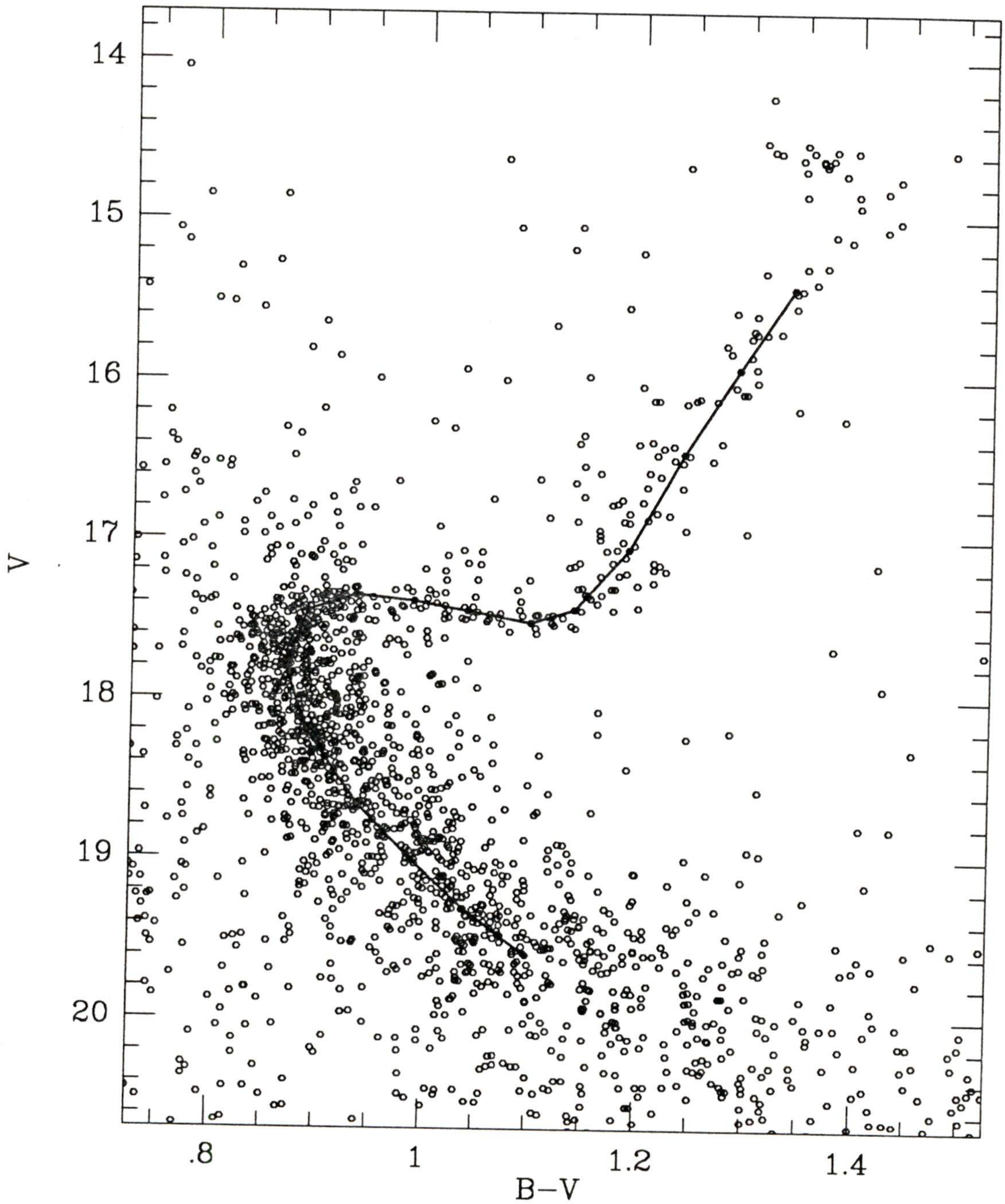

Fig. 22. Superposition of the CMD of NGC 6791 with the derived fiducial, which will be used in subsequent plots.

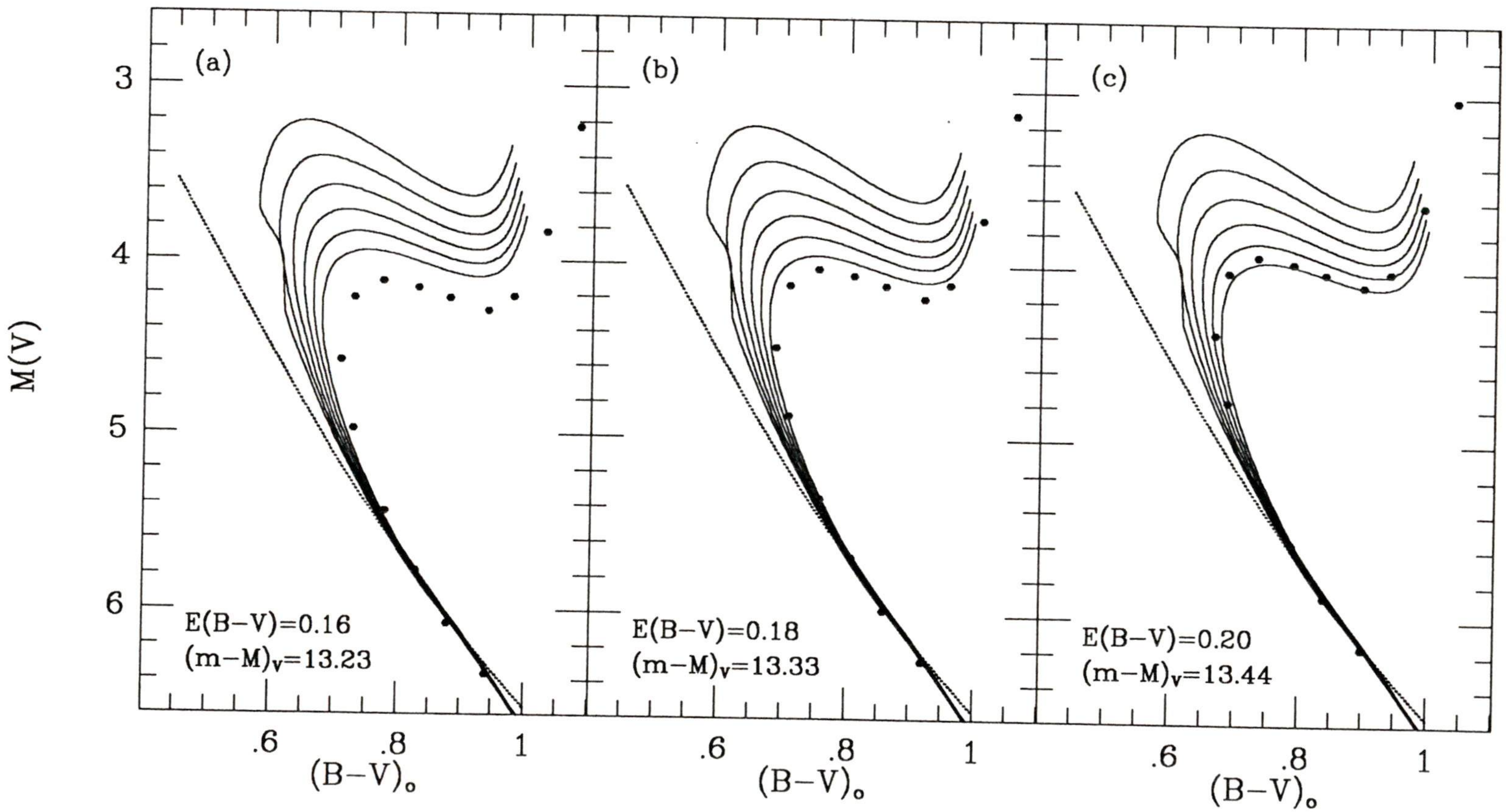

Fig. 23. Comparison of the fiducial of NGC 6791 with the $Z = 0.024$ ([Fe/H] = 0.15) isochrones, for ages of 5 to 10 Gyr, in steps of 1 Gyr.

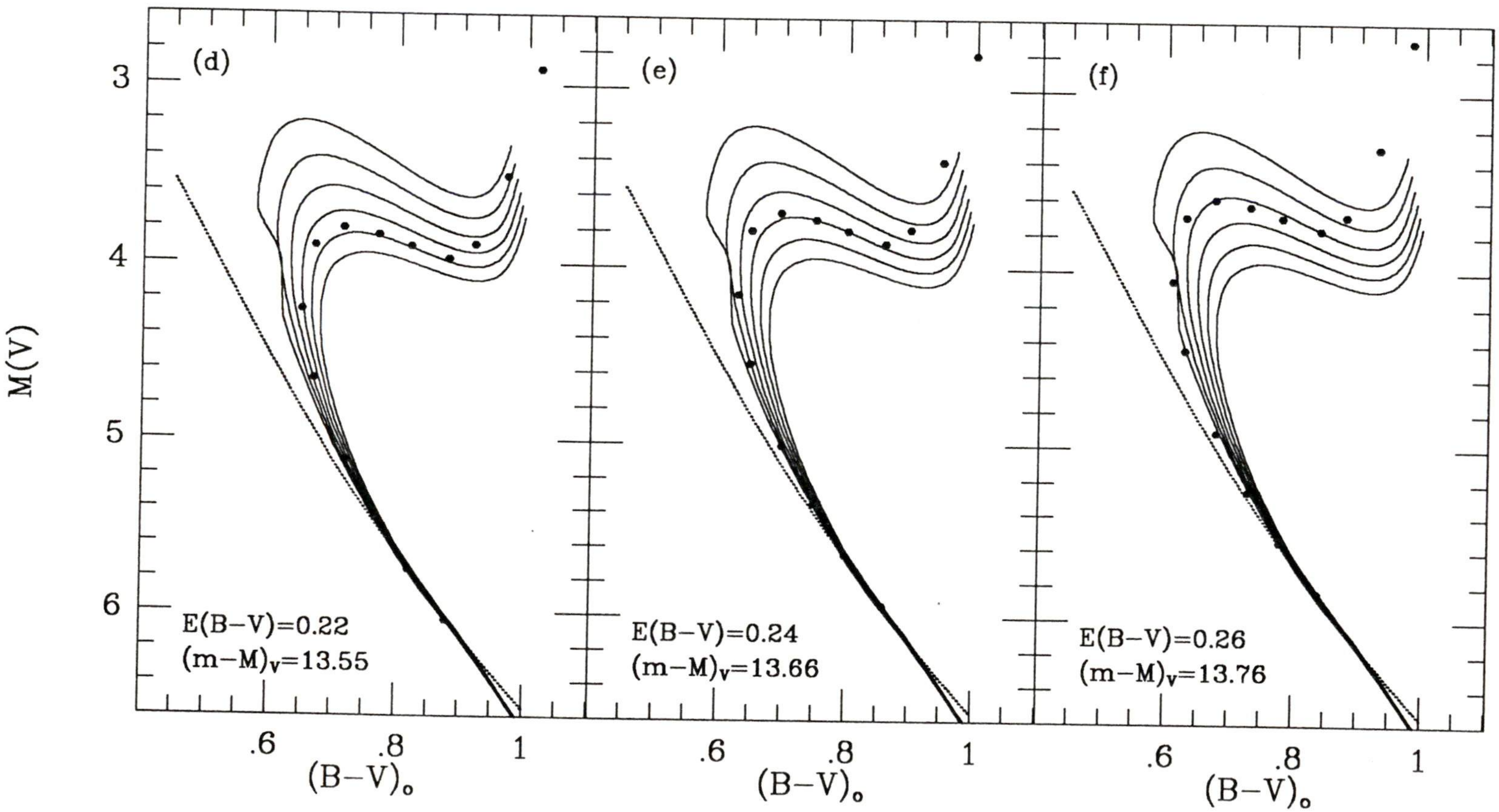
(d)
(e)
(f)
M(V)
3
4
5
6
E(B−V)=0.22
(m−M)v=13.55
E(B−V)=0.24
(m−M)v=13.66
E(B−V)=0.26
(m−M)v=13.76
.6
.8
1
(B−V)o

Fig. 23 (cont'd).

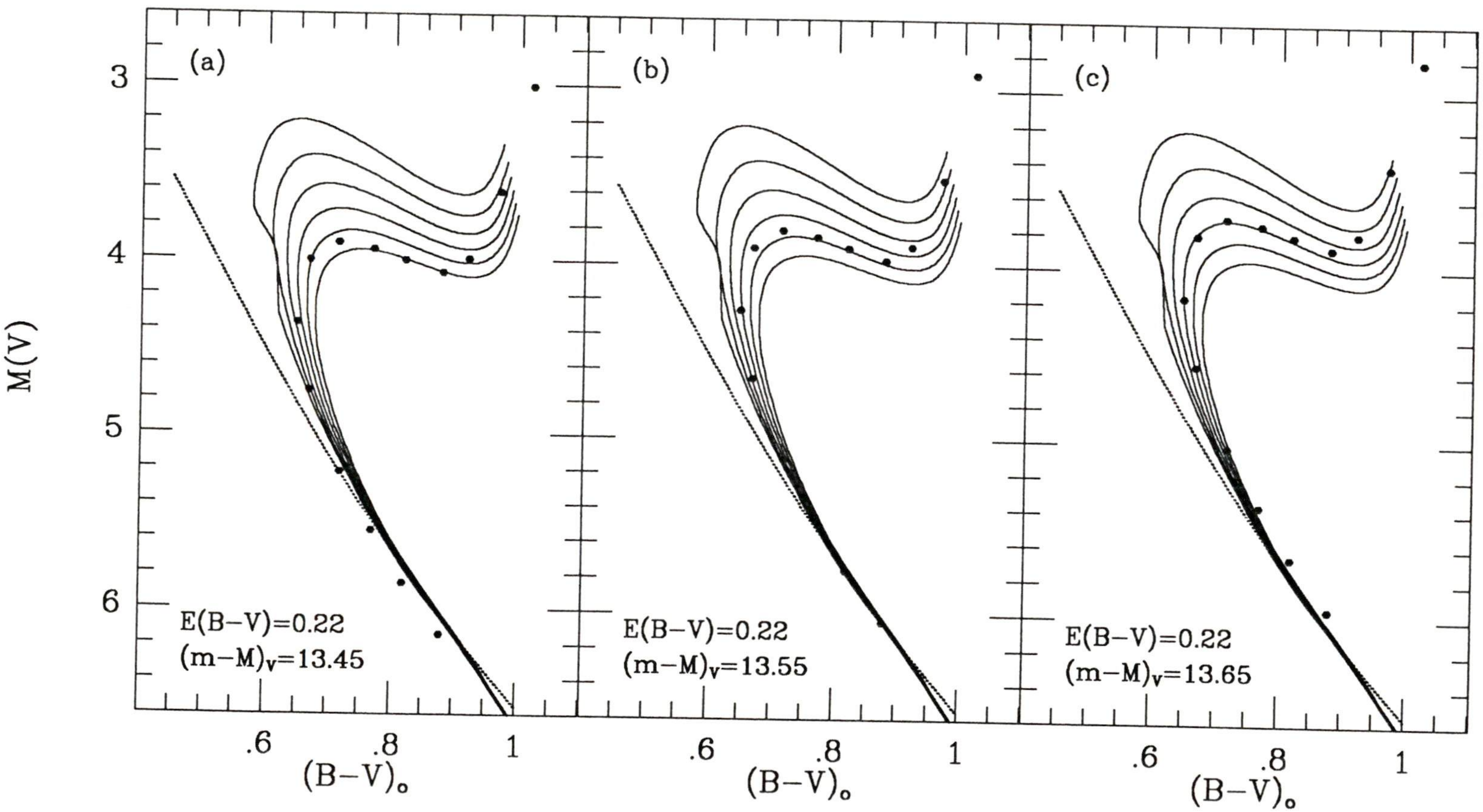

Fig. 24. Comparison of the fit with the $Z = 0.024$ isochrones for the best reddening, and different distance moduli. The isochrones are for ages 5 to 10 Gyr, in steps of 1 Gyr.

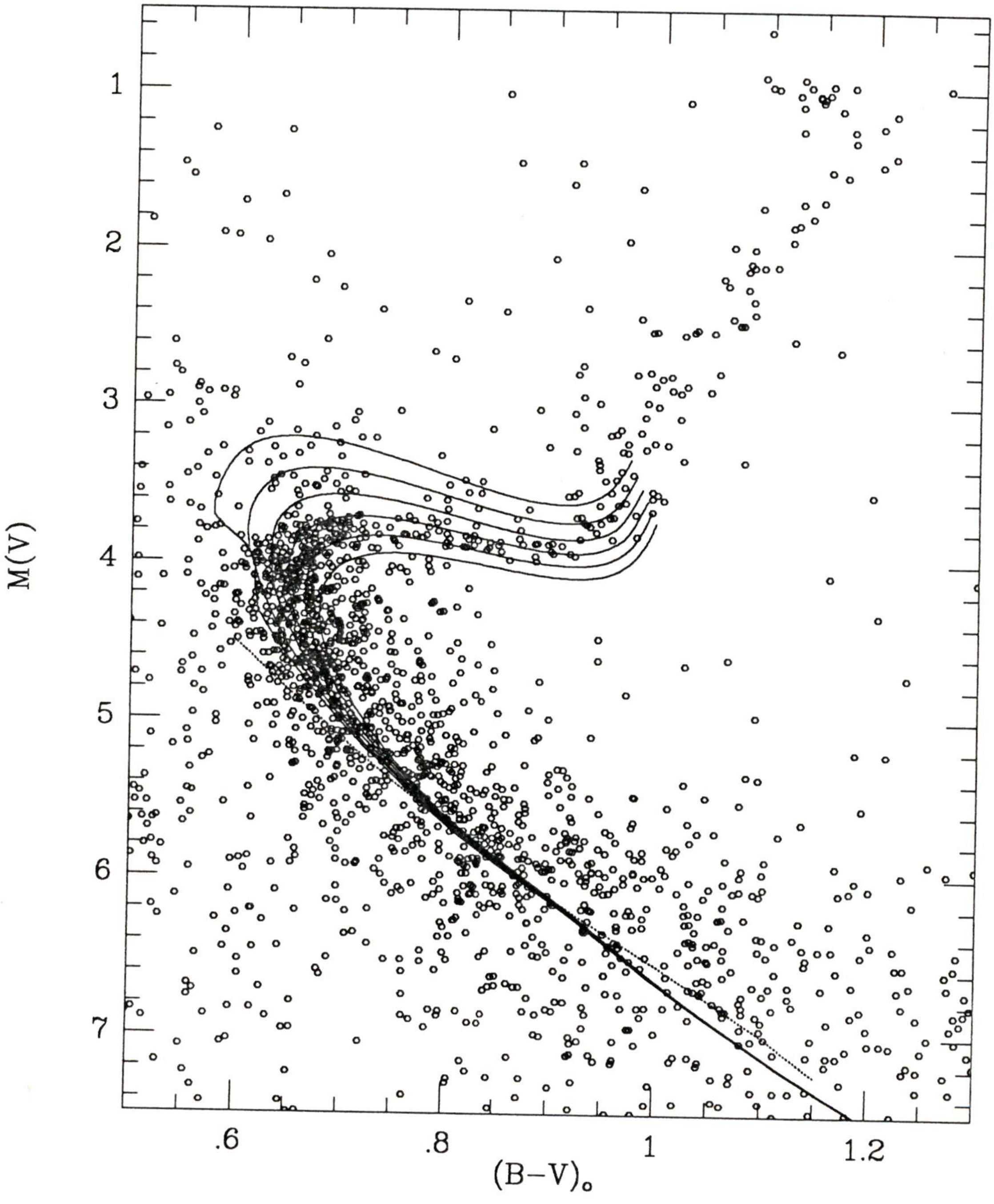

Fig. 25. Colour-Magnitude Diagram of NGC 6791 superimposed on isochrones of ages 5 to 10 Gyr (in steps of 1 Gyr) for $Y = 0.27$, $Z = 0.024$, $E(B - V) = 0.22$, and $(m - M)_V = 13.60$.

3.4 Mel 66

The reddening and the metallicity of Melotte 66 are relatively well determined: $E(B-V) = 0.14$, and $-0.35 < [Fe/H] < -0.49$. The fiducial (see Fig. 26) was fitted to the sets of isochrones for $Z = 0.006$ ([Fe/H] = −0.47), as shown in Fig. 27.

The main sequence of Melotte 66 is rather extensive, and fits the main sequence of the isochrones of ages 5 and 6 Gyr up to the turnoff region. In Fig. 27(b), the fiducial follows the 6 Gyr isochrone, then jumps to the 5 Gyr isochrone, and follows the shape of the subgiant branch. This discrepancy may be an indication that convective overshooting must be assumed in the theoretical models.

The discrepancy at the base of the giant branch, which was present in other models, is less obvious for this cluster. The colour discrepancy should be consistent from one cluster to another, i.e. the giant branch should be too red for the data. This is not the case for the more metal-poor composition: if the fiducial is fitted to the $Z = 0.004$ ([Fe/H] = −0.65) isochrones, the giant branch sits to the blue of the data. One would therefore expect the metal abundance not to be significantly more metal-poor than [Fe/H] = −0.47.

The best fit is shown in Fig. 28, for a reddening of $E(B-V) = 0.14$ and a distance modulus of $(m-M)_V = 13.66$ mag.

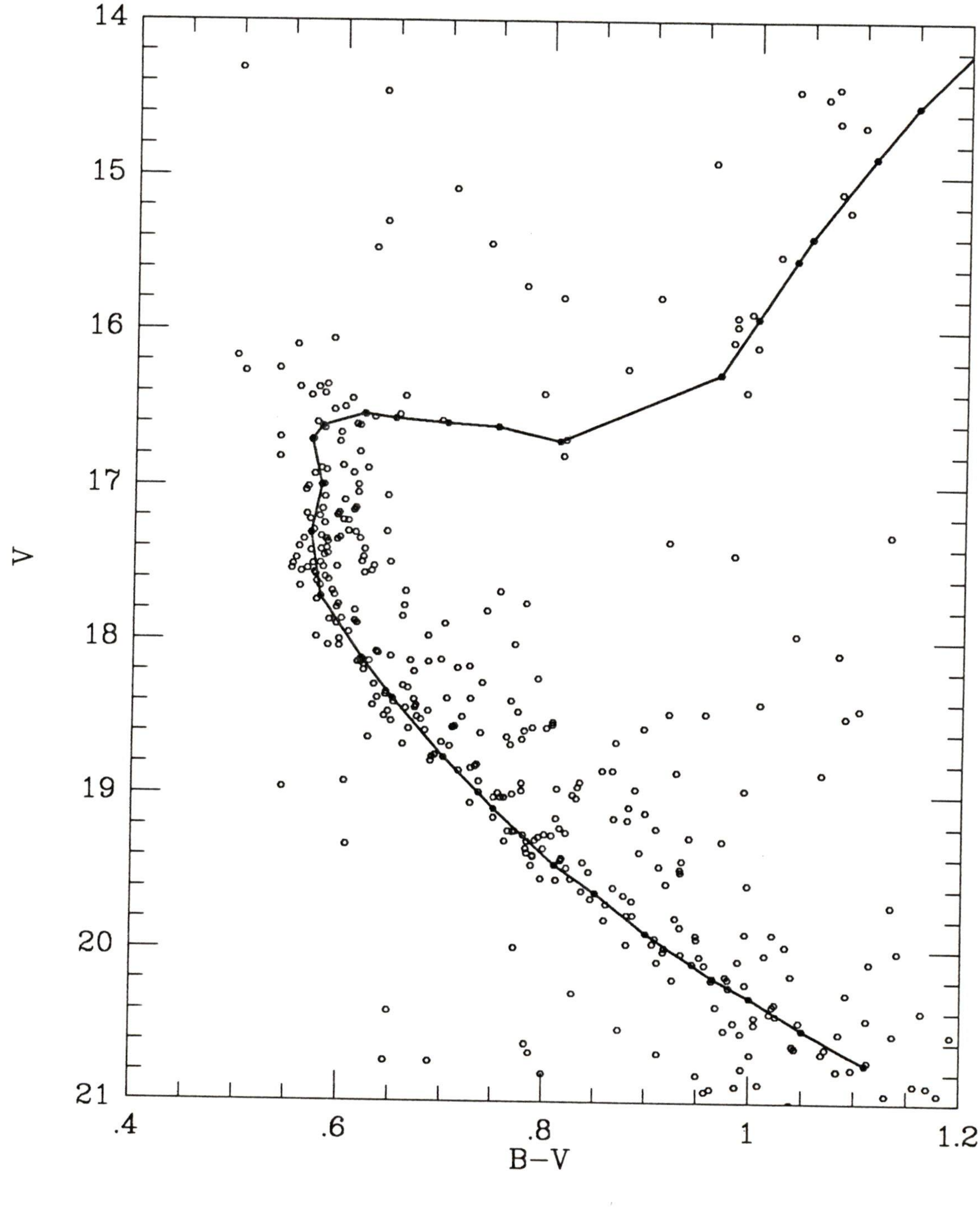

Fig. 26. Superposition of the CMD of Mel 66 with the derived fiducial used in subsequent plots.

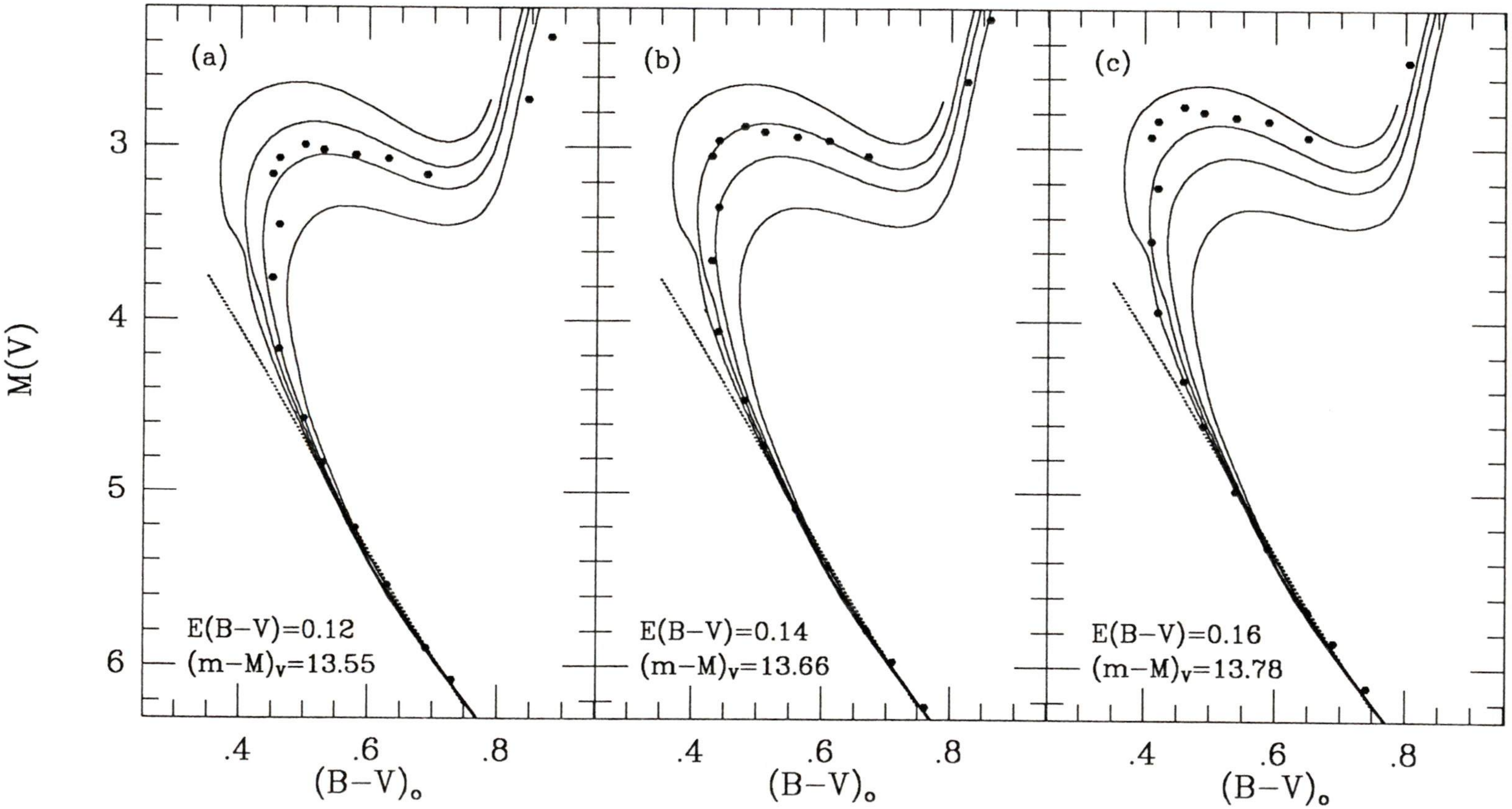

Fig. 27. Fiducial of Mel 66 compared with isochrones with $Z = 0.006$, of ages 4, 5, 6, and 8 Gyr.

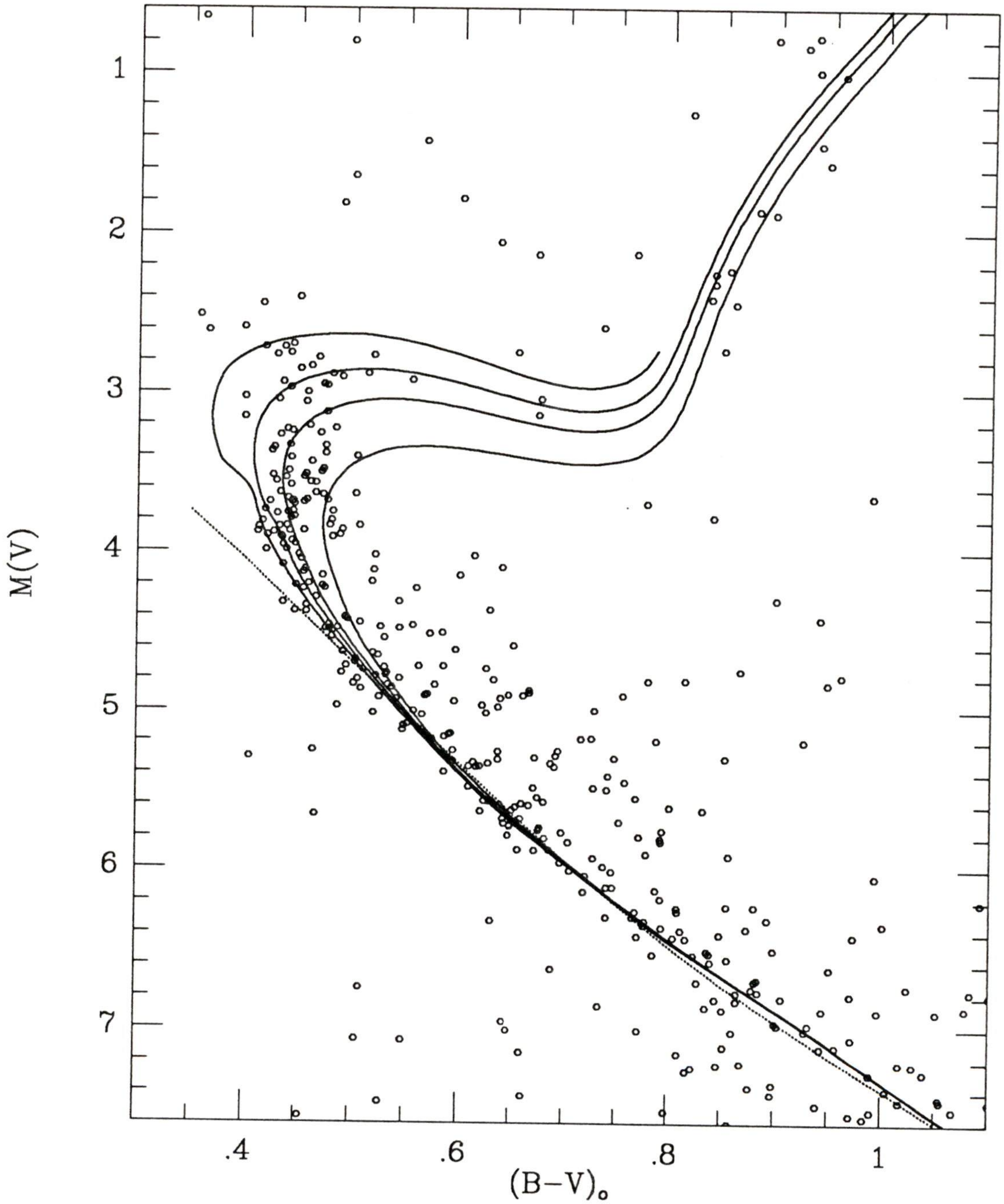

Fig. 28. Colour-Magnitude Diagram of Mel 66 superimposed on isochrones of ages 4, 5, 6 and 8 Gyr, for $Y = 0.27$, $Z = 0.006$, $E(B-V) = 0.14$, and $(m-M)_V = 13.66$.

3.5 NGC 2204

The fiducial of NGC 2204 is shown in Fig. 29. The scatter along the sequences makes the hand-drawn fiducial extremely vulnerable to errors.

NGC 2204 has a metal-poor composition, and is much younger than the other clusters. A different set of isochrones (VandenBerg 1985) had to be used, for a metallicity of $Z = 0.006$ and a range of ages from 2.5 Gyr to 5 Gyr (see Fig. 30). Fig. 30(b) offers the best fit: the data seem to agree with the 3 Gyr isochrone, except for two fiducial points, at $M_V = 2.8$ and $M_V = 2.2$. The discrepancy here suggests the need for overshooting in the models: the hook feature in those plotted is too faint compared with the observed location of the gap. The discrepancy for these points could be due in part to the statistical uncertainties of the fiducial itself. The distance modulus of $(m - M)_V = 13.15$ would imply an absolute magnitude of $M_V = 0.75$ mag for the red-giant clump. This is roughly what one would expect for the absolute magnitude of the clump of a metal-poor cluster.

Fig. 31 compares the fit of Fig. 30(b) with the data points of the CMD. The agreement is less obvious, but seems to correspond to an age intermediate to 2.5 Gyr and 3 Gyr.

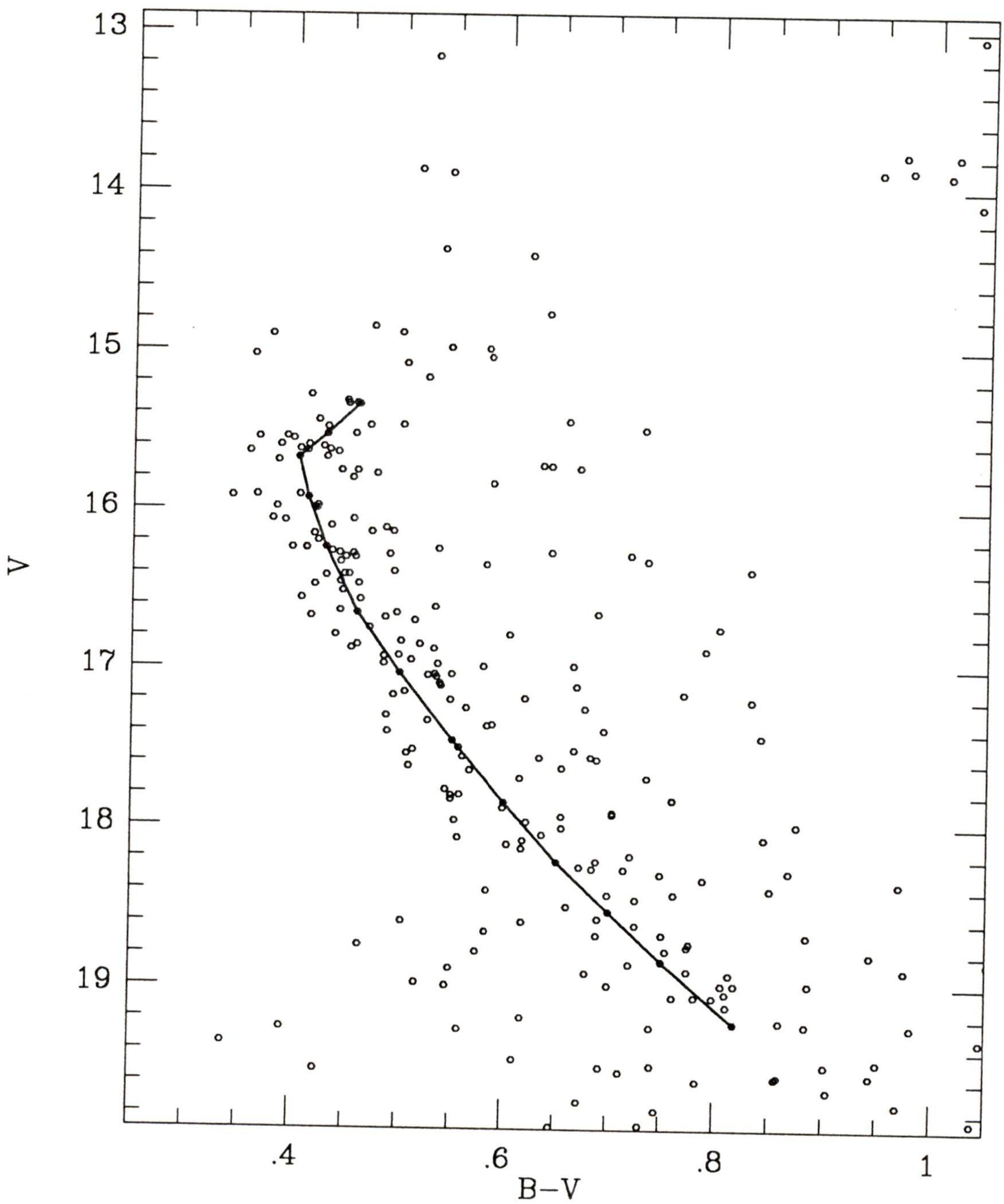

Fig. 29. Fiducial of NGC 2204 superimposed on the data.

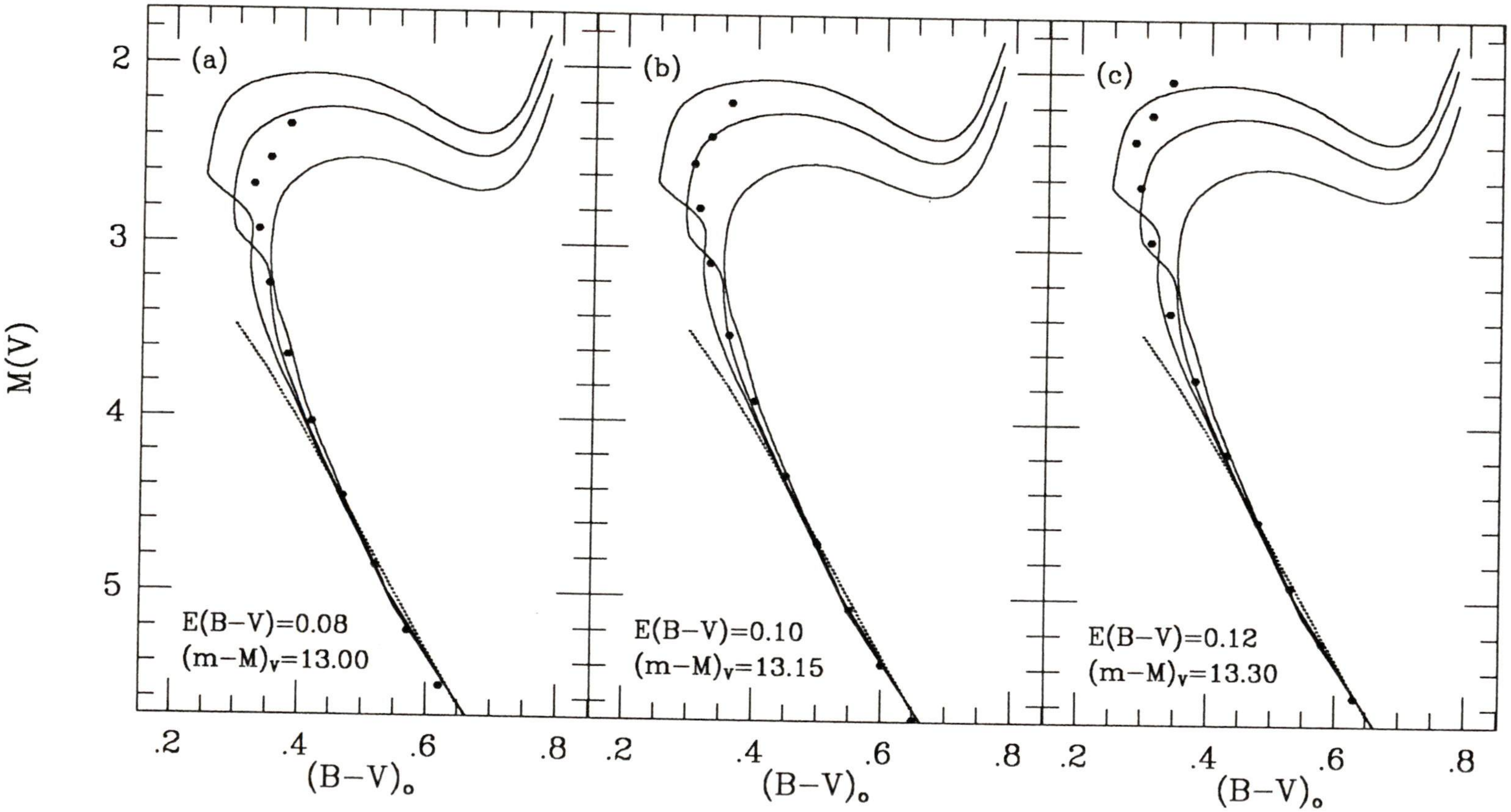

Fig. 30. Comparison of the fiducial of NGC 2204 with isochrones of $Z = 0.006$ ($[Fe/H] = -0.46$), of ages 2.5, 3, and 4 Gyr.

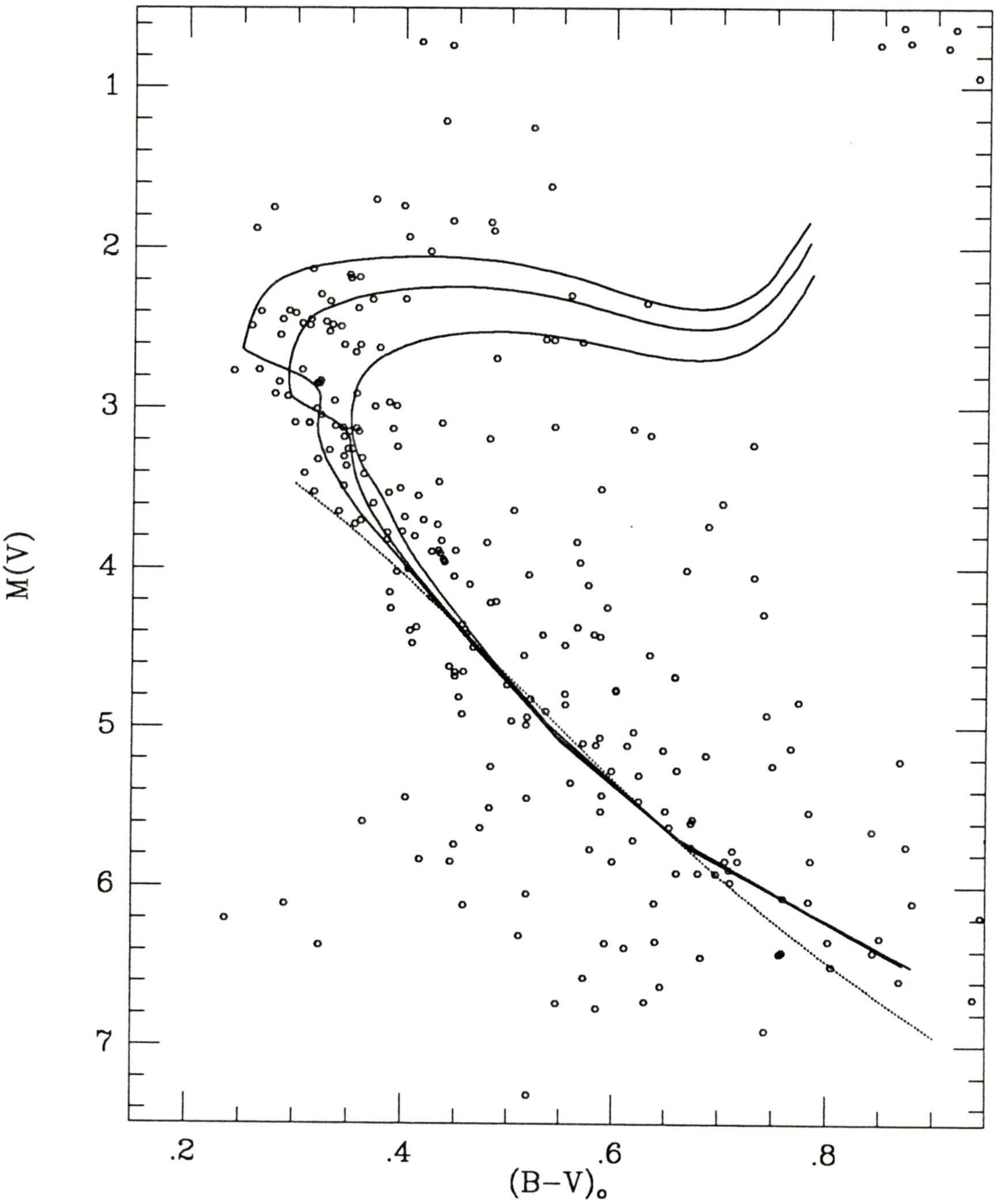

Fig. 31. Comparison of the CMD of NGC 2204 with isochrones of $Z = 0.006$ ([Fe/H] $= -0.46$), of ages 2.5, 3 and 4 Gyr, for $E(B-V) = 0.10$ and $(m-M)_V = 13.15$ mag.

3.6 Discussion of Errors

The previous sections compared the data with the isochrones. In each case, a set of parameters (metal abundance, reddening, distance modulus, and age) was determined from the "best fit". Because of the complexity of the problem and the intrinsic uncertainties associated with the procedure, no final uncertainty was mentioned on the resulting ages of the clusters. A quantitative assessment of the various sources of error will now be made.

3.6.1 Visual Effect of Typical Uncertainties

Fig. 32 shows two isochrones, identical except for their metallicities, which differ by ± 0.2 dex. This is a typical uncertainty on metal abundance estimates, and it translates itself primarily into a horizontal shift. In practice, if the isochrones for the wrong metallicity are used in a main sequence fit of an observed CMD, an incorrect reddening, distance, and age, will result. The determination of an accurate [Fe/H] is therefore of the utmost importance.

The best estimates for reddening are of the order of ± 0.02 dex. Fig. 33 illustrates the visual effect of such an uncertainty, by plotting two isochrones, identical except for the fact that one was shifted by ± 0.02 in the $B - V$ scale. Even such a minimal error would affect the distance moduli derived from main sequence fitting by ± 0.10 mag (scale factor of 5 between the $E(B - V)$ and the V axes), which would in turn affect the age determination.

Another source of concern is the colour calibration of the isochrones. Bell (1988) remarked that in order to obtain the best fit, a number of authors find it necessary to apply a colour shift to the isochrones (the isochrones being bluer than the data). As possible causes for this effect, he mentioned : differences in chemical composition between the stars and the models, including differences in the relative abundances of individual elements as well as differences in overall abundance; errors in evolutionary sequence calculations (e.g., due to errors in opacities); errors in colour-system transformations causing errors in the observations; errors in synthetic colour calculations. It is extremely difficult to assess quantitatively if any of these systematic errors are present in the fit.

It is therefore important, when fitting isochrones, not to emphasize the turnoff colour which is extremely sensitive to errors in the reddening, the model atmospheres, the transformation from T_{eff} to $(B-V)_0$, the mixing-length parameter, and the metallicity. It is preferable to stress the match of the main sequences (representing the unevolved part of the diagram) or the luminosity of the clump; the turnoff colour can then be used for a consistency check rather than as the primary fitting parameter.

Two isochrones, identical except for the fact that one was shifted by +0.2 mag in the absolute magnitude scale (in practice this would correspond to an uncertainty of ±0.2 mag in the distance moduli), are plotted in Fig. 34. This plot highlights the importance of fitting both the main sequence and the turnoff region in order to get accurate ages.

Finally, two isochrones of ages differing by 3 Gyr, but otherwise identical, are shown in Fig. 35. A difference of 3 Gyr gives a visual impression comparable to that coming from uncertainties of Δ[Fe/H] = 0.2 dex (Fig. 32), or $\Delta E(B-V) = 0.02$ dex (Fig. 33), or $\Delta(m-M)_V = 0.2$ mag (Fig. 34). Only a close inspection of the shape of the isochrones will minimize the errors enough to make an age determination possible to an accuracy of ±1 Gyr.

3.6.2 Quantitative Effects on Age Determination

The following is a rough "eye estimate" of the effect of the uncertainties mentioned above, on age determinations.

$\delta(m-M)_V = +0.3$ mag	$\Delta t \sim +20\%$ Gyr
$\delta E(B-V) = +0.02$ dex	$\Delta t \sim +15\%$ Gyr
δ[Fe/H] $= +0.25$ dex	$\Delta t \sim +15\%$ Gyr
$\delta Y = +0.05$	$\Delta t \sim -10\%$ Gyr

The fitting process itself is far from being an objective procedure – ultimately it has to be "pleasing to the eye". It could perhaps be improved by numerical techniques, such as the ones used by Flannery and Johnson (1982). This would have the advantage of providing errors on the parameters due to formal errors in the fit. Keeping in mind the "uncalibratable sources of error" , the overall uncertainty on the ages might be reduced to 1-2 Gyr.

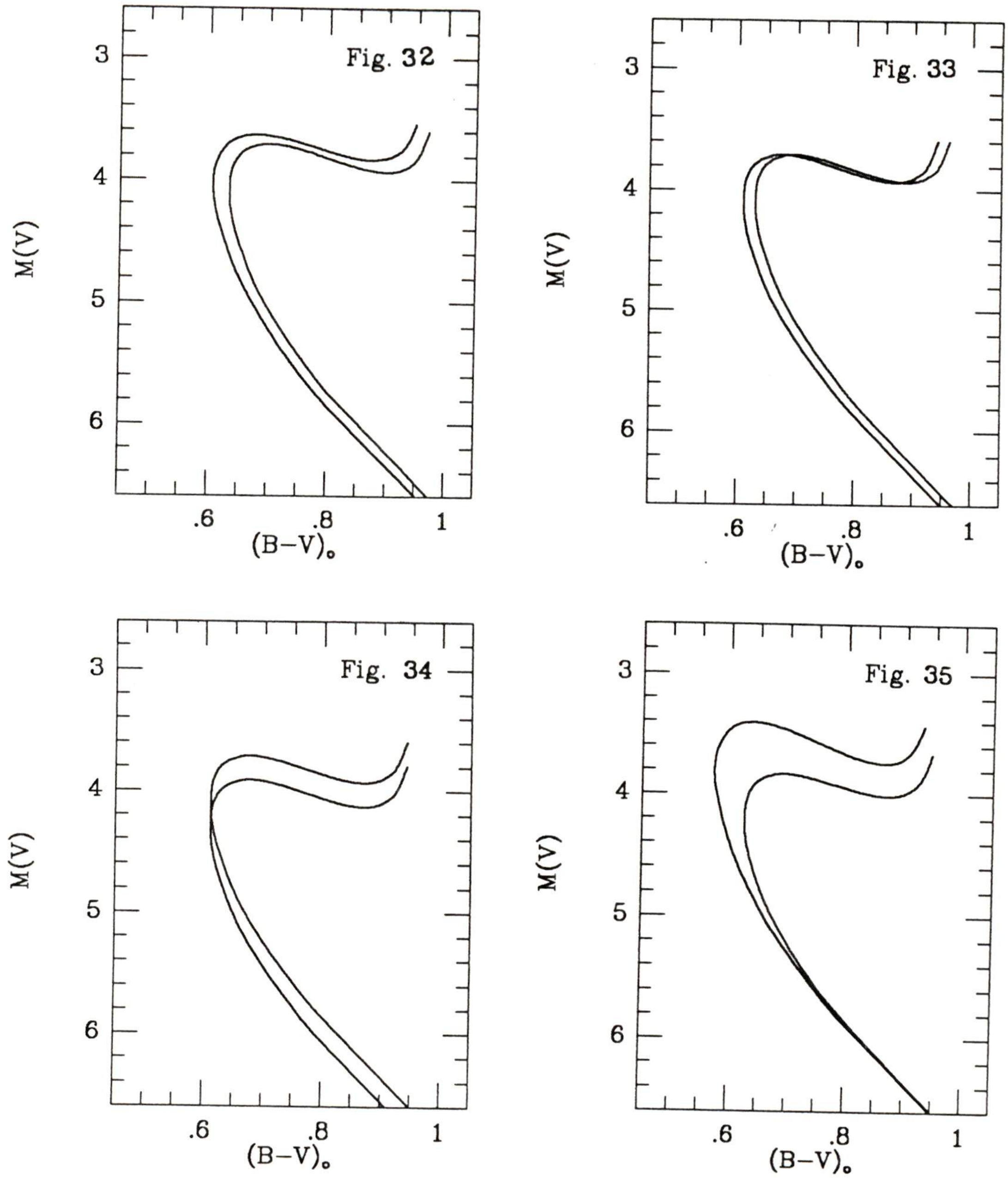

Identical isochrones are plotted in each panel, where they differ by typical uncertainties encountered, as follows: Fig.32. Δ[Fe/H] = 0.22 dex, Fig.33. $\Delta E(B-V) = 0.02$ dex, Fig.34. $\Delta(m-M)_V = 0.2$ mag, Fig.35. $\Delta age = 3$ Gyr.

Chapter 4

Conclusion

In conclusion, CCD photometry of the three old open clusters, namely NGC 188, NGC 6791 and Melotte 66, was reduced using the software DAOPHOT (Stetson 1987), and their CMDs were compared to theoretical isochrones (VandenBerg 1990).

NGC 188 was shown to have a tight sequence, corresponding to an isochrone of age 8 Gyr. This is a compromise between the isochrones of $Z = 0.010$ ([Fe/H] $= -0.22$) and of $Z = 0.017$ ([Fe/H] $= 0$), and gives a metallicity of [Fe/H] $= -0.11$, a reddening of $E(B-V) \simeq 0.09$, and a distance modulus of $(m-M)_V \simeq 11.25$. These parameters are consistent with previous findings (see Table 3.1).

NGC 6791 has a CMD very similar to that of NGC 188, but has a more metal-rich composition. This cluster was compared to isochrones of $Z = 0.024$ ([Fe/H] $= 0.15$), but the most recent estimate has found it to be even more metal-rich (Friel and Janes 1990, [Fe/H] $= 0.23$). The best fit was obtained for a reddening of $E(B-V) = 0.22$ and a distance modulus of $(m-M)_V = 13.60$, corresponding to an age of about 8 - 8.5 Gyr. Although the uncertainties are too important to be able to distinguish which one of NGC 188 or NGC 6791 is the older cluster, the fit to the isochrones seems to suggest that NGC 6791 may be slightly older.

Finally, Melotte 66 was found to be younger than the other two clusters. The CMD was fitted to isochrones of $Z = 0.006$ ([Fe/H] $= -0.46$); although there is an unexplained gap near the turnoff, the data correspond best to an age of 5 or 6 Gyr, for a reddening of $E(B-V) = 0.14$, and a distance modulus of $(m-M)_V = 13.66$. This is in good agreement with previous studies.

The last cluster which was studied is NGC 2204. Although there is still some scatter in the photometry, the results are surpisingly consistent with those of previous works. The data were fitted to an older isochrone (VandenBerg 1985), of $Z = 0.006$ ([Fe/H] $= -0.46$), and the age was found to be about 3 Gyr for a reddening of $E(B-V) = 0.10$ and a distance modulus of $(m-M)_V = 13.15$.

References

Ables, H.D., Hewitt, A.V., and Kron, G.E. 1969, *Publ. Astron. Soc. Pac.*, **81**, 530.

Anthony-Twarog, B.J., Kaluzny, J., Shara, M.M., and Twarog, B.A. 1990, *Astron. J.*, **99**, 1504.

Anthony-Twarog, B.J., and Twarog, B.A. 1985, *Astrophys. J.*, **291**, 595.

Anthony-Twarog, B.J., Twarog, B.A., and McClure R.D. 1979, *Astrophys. J.*, **233**, 188.

Barbaro, G., and Pigatto, L. 1984, *Astron. Astrophys.*, **136**, 355.

Bell, R.A. 1988, *Astron. J.*, **95**, 1491.

Bergbusch, P.A., and VandenBerg, D.A. 1990, in preperation.

Buonanno, R., Buscema, G., Corsi, C.E., Iannicola, G., and Fusi Pecci, F. 1983, *Astron. Astrophys. Suppl.*, **51**, 83.

Burstein, D., and Heiles, C. 1982, *Astron. J.*, **87**, 1165.

Cameron, L.M. 1985, *Astron. Astrophys.*, **147**, 39.

Cameron, A.C., and Reid, N. 1987, *Mon. Not. Roy. Astr. Soc.*, **224**, 821.

Cannon, R.D. 1970, *Mon. Not. Roy. Astr. Soc.*, **150**, 111.

Canterna, R., Geisler, D., Harris, H.C., Olszewski, E., and Schommer, R. 1986, *Astron. J.*, **92**, 79.

Caputo, F., Chieffi, A., Castellani, V., Collados, M., Roger, C.M., and Paez, E. 1990, *Astron. J.*, **99**, 261.

Carbon, D.F., Langer, G.E., Butler, D., Kraft, R.P., Suntzeff, N.B., Kemper, E., Trefzger, C.F. 1982, *Astrophys. J. Suppl.*, **49**, 207.

Chieffi, A., and Straniero, O. 1989, *Astrophys. J. Suppl.*, (submitted).

Ciardullo, R.B., and Demarque, P. 1977, *Transactions of the Yale Univ. Obs.*, **34**.

Cohen, J.G. 1978, *Astrophys. J.*, **223**, 487.

Cohen, J.G. 1979, *Astrophys. J.*, **231**, 751.

Dawson, D.W. 1978, *Astron. J.*, **83**, 1424.

Dawson, D.W. 1981, *Astron. J.*, **86**, 237.

Deliyannis, C.P., Demarque, P., and Kawaler, S.D. 1990, *Astrophys. J. Suppl.*, **73**, 21.

Demarque, P.R., and Larson R.B. 1964, *Astrophys. J.*, **140**, 544.

Demarque, P., and McClure, R.D. 1977, in *Evolution of Galaxies and Stellar Populations*, ed. B. M. Tinsley and R. B. Larson (New Haven: Yale Univsersity Observatory), p. 199.

Eggen, O.J., and Sandage, A. 1962, *Astrophys. J.*, **140**, 130.

Eggen, O.J., and Sandage, A. 1969, *Astrophys. J.*, **158**, 669.

Eggen, O.J., and Stoy, R.H. 1963, *Roy. Obs. Bull.*, No. **53**.

Flannery, B.P., and Johnson, B.C. 1982, *Astrophys. J.*, **263**, 166.

Friel, E. and Janes K.A. 1990, in preperation.

Geisler, D., and Smith, V.V. 1984, *Pub. Astronom. Soc. Pac.*, **96**, 871.

Geisler, D. 1987, *Astron. J.*, **94**, 84.

Geisler, D. 1988, *Publ. Astron. Soc. Pac.*, **100**, 338.

Graham, J. A. 1982, *Publ. Astron. Soc. Pac.*, **94**, 244.

Gratton, R.G. 1982, *Astrophys. J.*, **257**, 640.

Green, E.M., Demarque, P., and King, C.R. 1987, *The Revised Yale Isochrones and Luminosity Functions*, (Yale Univ. Obs., New Haven).

Hagen, G.L. 1970, *Catalogue of Open Cluster Color-Magnitude Diagrams*, Publications of the DDO, **4**, 1.

Harris, H.C., and Canterna, R. 1981, *Astron. J.*, **86**, 1332.

Hartwick, F.D.A., and VandenBerg, D.A. 1973, *Astrophys. J.*, **185**, 887.

Hawarden, T.G. (a) 1976, *Mon. Not. Roy. astr. Soc.*, **174**, 471.

Hawarden, T.G. (b) 1976, *Mon. Not. Roy. astr. Soc.*, **174**, 225.

Hobbs, L.M., Thorburn, J.A., and Rodriguez-Bell, T. 1990, *Astron. J.*, **100**, 710.

Iben, I., Jr. 1967, *Astrophys. J.*, **147**, 624.

Janes, K.A. 1975, *Astrophys. J. Suppl.*, **29**, 161.

Janes, K.A. 1984, *Publ. Astron. Soc. Pac.*, **96**, 977.

Janes, K.A., and Adler, D. 1982, *Astrophys. J. Suppl.*, **49**, 425.

Janes, K.A., Tilley C., and Lynga, G. 1988, *Astron. J.*, **95**, 771.

Jennens, P.A., and Helfer, H.L. 1975, *Mon. Not. Roy. Astron. Soc.*, **172**, 681.

Kaluzny, J. 1989, *preprint:* CCD BV Photometry of the Old Open Cluster NGC

6791.

Kaluzny, J. 1990, *preprint*: CCD Photometry of NGC 188.

Kaluzny, J., and Shara, M.M. 1987, *Astron. J.*, **95**, 785.

Kaluzny, J., and Shara, M.M. 1988, *Astrophys. J.*, **317**, 585.

King, I.R. 1966, *Astronom. J.*, **71**, 64.

King, I.R. 1968, *Astrophys. J. Lett.*, **151**, L59.

Kinman, T.D. 1965, *Astrophys. J.*, **142**, 655.

Kurucz, R.L. 1979, *Astrophys. J. Suppl.*, **40**, 1.

Landolt, A.U. 1973, *Astronom. J.*, **78**, 959.

Landolt, A.U. 1983, *Astronom. J.*, **88**, 439.

Lynga, G. 1987, *Astronom. Astrophys.*, **109**, 213.

McClure, R.D. 1974, *Astrophys. J.*, **194**, 355.

McClure, R.D. 1979, *Astrophys. J.*, **233**, 188.

McClure, R.D., and Twarog, B.A. 1977, *Astrophys. J.*, **214**, 111.

McClure, R.D., and Twarog, B.A. 1979, *Astrophys. J.*, **233**, 188.

Pagel, B.E.J. 1974, *Mon. Not. Roy. Astron. Soc.*, **167**, 413.

Proffitt, C.R., Michaud, G. 1990, *Astrophys. J.*, in press.

Racine, R. 1971, *Astrophys. J.*, **168**, 393.

Sandage, A. 1962, *Astrophys. J.*, **135**, 333.

Sandage, A. 1986, *Ann. Rev. Astronom. Astrophys.*, v.**24**, p.421.

Spinrad, H., and Taylor, B.J. 1971, *Astrophys. J.*, **163**, 303.

Stetson, P.B. 1987, *Pub. Astronom. Soc. Pac.*, **99**, 191.

Stetson, P.B. *DAOPHOT User's Manual*, private communication.

Stetson, P.B., Harris, W.E. 1988, *Astronom. J.*, **96**, 909.

Suntzeff, N.B. 1981, *Astrophys. J. Suppl.*, **47**, 1.

Twarog, B.A. 1978, *Astrophys. J.*, **220**, 890.

Twarog, B.A., and Anthony-Twarog, B.J. 1989, *Astron. J.*, **97**, 759.

VandenBerg, D.A. 1983, *Astrophys. J. Suppl.*, **51**, 29.

VandenBerg, D.A. 1985, *Astrophys. J.*, **58**, 711.

VandenBerg, D.A. 1990, *preprint*: The Status of Stellar Evolution Models.

VandenBerg, D.A., and Poll, H.E. 1989, *Astronom. J.*, **98**, 1451.

Wielen R. 1971, *Astronom. Astrophys.*, **13**, 309.

Wielen R. 1975, in *Dynamics of Stellar Systems*, I.A.U. Symp. No. **69**, ed. by A. Hayli (Reidel, Dordrecht), p.119.

Wildey, R.L., Burbidge, E.M., Sandage, A.R., and Burbidge, G.R. 1962, *Astrophys. J.*, **135**, 94.

Appendix A

Tables of Standard Stars

The following tables contain the details of the standard stars which were used to reduce the photometry of the four clusters. The entries are:

- Column 1: The identification of the star. In tables A.1 to A.4 the "*L*" refers to Landolt (1983) stars, and the "*ES*" to Eggen and Sandage's (1969) photoelectric stars. In tables A.5 to A.8 the stars are E-region standard stars (Graham 1982).
- Columns 2, 3, and 4: The universal time at which the frame of the star was taken, the airmass, and the integration time in seconds.
- Columns 5, 6, and 7: The observed magnitude (B or V), the listed magnitude (B or V) from the papers mentioned in column 1, and the computed magnitude (B or V) which puts the observed magnitude on the same instrumental system as the listed magnitude.
- Columns 8, and 9: The residual $V_{tabulated} - V_{computed}$, and its sigma.

Table A.1. Standard Stars in V, Sept.10/11 1986 (NGC 188 and NGC 6791)

ID	UT	X	Int.	$V_{obs.}$	$V_{tab.}$	$V_{comp.}$	Res.	σ
L110-340	2.950	1.176	3	10.023	14.599	14.592	0.007	0.023
L110-340	2.967	1.177	3	10.023	14.602	14.592	0.010	0.023
L110-450	3.000	1.175	10	11.585	16.153	16.149	0.004	0.024
L110-450	3.017	1.175	10	11.585	16.161	16.149	0.012	0.024
L110-441	3.267	1.182	6	11.120	15.660	15.683	-0.023	0.024
L110-441	3.283	1.183	6	11.120	15.658	15.683	-0.025	0.024
L109-954	3.283	1.183	25	12.440	17.012	16.998	0.014	0.024
L109-959	3.283	1.183	25	12.790	17.359	17.351	0.008	0.024
L109-949	3.283	1.183	25	12.850	17.400	17.412	-0.012	0.024
L109-956	3.283	1.183	25	14.630	19.199	19.188	0.011	0.031
L109-954	3.383	1.284	25	12.440	17.025	17.009	0.016	0.024
L109-959	3.383	1.284	25	12.790	17.358	17.361	-0.003	0.024
L109-949	3.383	1.284	25	12.850	17.406	17.422	-0.016	0.024
L109-956	3.383	1.284	25	14.630	19.222	19.199	0.023	0.031
L112-805	3.583	1.238	15	12.090	16.663	16.659	0.004	0.024
L112-805	3.600	1.236	15	12.090	16.663	16.659	0.004	0.024
L113-488	5.600	1.172	10	10.160	14.701	14.742	-0.041	0.026
L113-493	5.600	1.172	10	11.770	16.332	16.351	-0.019	0.025
L113-492	5.600	1.172	10	12.180	16.731	16.763	-0.032	0.026
L113-495	5.600	1.172	10	12.440	17.006	17.020	-0.014	0.025
L113-488	5.617	1.172	10	10.160	14.707	14.742	-0.035	0.026
L113-493	5.617	1.172	10	11.770	16.338	16.352	-0.014	0.025
L113-492	5.617	1.172	10	12.180	16.746	16.763	-0.017	0.026
L113-495	5.617	1.172	10	12.440	17.011	17.021	-0.010	0.025
L113-488	5.650	1.172	6	10.160	14.717	14.743	-0.026	0.026
L113-493	5.650	1.172	6	11.770	16.332	16.353	-0.020	0.025
L113-492	5.650	1.172	6	12.180	16.746	16.764	-0.018	0.026
L113-495	5.650	1.172	6	12.440	17.043	17.022	0.022	0.026
L113-488	5.650	1.172	6	10.160	14.714	14.743	-0.029	0.026
L113-493	5.650	1.172	6	11.770	16.348	16.353	-0.004	0.025
L113-492	5.650	1.172	6	12.180	16.745	16.764	-0.019	0.026
L113-495	5.650	1.172	6	12.440	17.010	17.022	-0.011	0.026
L109-954	5.750	2.269	25	12.440	17.138	17.148	-0.010	0.024
L109-959	5.750	2.269	25	12.790	17.490	17.500	-0.010	0.024
L109-949	5.750	2.269	25	12.850	17.528	17.561	-0.033	0.024
L109-956	5.750	2.269	25	14.630	19.334	19.338	-0.004	0.032
L109-954	5.767	2.287	25	12.440	17.138	17.150	-0.012	0.024

Table A.1. (cont'd)

ID	UT	X	Int.	$V_{obs.}$	$V_{tab.}$	$V_{comp.}$	Res.	σ
L109-959	5.767	2.287	25	12.790	17.490	17.503	-0.013	0.024
L109-949	5.767	2.287	25	12.850	17.518	17.564	-0.046	0.024
L109-956	5.767	2.287	25	14.630	19.339	19.340	-0.001	0.031
L95-74	12.367	1.187	30	11.529	16.099	16.107	-0.008	0.023
L95-73	12.367	1.187	30	12.310	16.848	16.891	-0.043	0.024
L95-74	12.383	1.187	30	11.529	16.102	16.106	-0.004	0.023
L95-73	12.383	1.187	30	12.310	16.854	16.890	-0.036	0.024
L96-737	12.433	1.184	20	11.718	16.297	16.289	0.007	0.023
L96-736	12.433	1.184	20	11.920	16.483	16.497	-0.015	0.025
L96-737	12.433	1.184	20	11.718	16.290	16.289	0.000	0.023
L96-736	12.433	1.184	20	11.920	16.491	16.497	-0.007	0.025
L98-667	12.600	1.445	3	8.378	12.963	12.974	-0.011	0.024
L98-653	12.600	1.445	3	9.538	14.115	14.134	-0.020	0.023
L98-667	12.617	1.444	3	8.378	12.978	12.973	0.005	0.024
L98-653	12.617	1.444	3	9.538	14.131	14.133	-0.002	0.023
ESI-60	8.633	1.668	500	15.170	19.873	19.887	-0.014	0.027
ESI-61	8.633	1.668	500	14.100	18.806	18.814	-0.008	0.026
ESI-62	8.633	1.668	500	14.810	19.520	19.527	-0.006	0.025
ESI-63	8.633	1.668	500	15.850	20.515	20.567	-0.051	0.031
ESI-65	8.633	1.668	500	15.350	20.068	20.067	0.001	0.027
ESI-66	8.633	1.668	500	14.970	19.662	19.686	-0.023	0.025
ESI-76	8.633	1.668	500	14.940	19.658	19.657	0.001	0.027
ESI-91	8.633	1.668	500	14.840	19.592	19.557	0.035	0.025
ESI-93	8.633	1.668	500	14.530	19.267	19.247	0.020	0.025
ESI-101	8.633	1.668	500	15.000	19.743	19.717	0.026	0.025
ESI-103	8.633	1.668	500	15.140	19.822	19.858	-0.035	0.025
ESI-104	8.633	1.668	500	15.390	20.125	20.107	0.018	0.027
ESI-107	8.633	1.668	500	15.950	20.615	20.663	-0.047	0.031
ESI-109	8.633	1.668	500	16.220	20.921	20.937	-0.015	0.030
ESI-110	8.633	1.668	500	16.860	21.528	21.576	-0.048	0.034
ESI-112	8.633	1.668	500	14.400	19.107	19.117	-0.010	0.024
ESI-60	8.500	1.668	60	15.170	19.889	19.885	0.005	0.028
ESI-61	8.500	1.668	60	14.100	18.821	18.812	0.009	0.034
ESI-62	8.500	1.668	60	14.810	19.533	19.524	0.009	0.033
ESI-63	8.500	1.668	60	15.850	20.529	20.565	-0.035	0.030
ESI-65	8.500	1.668	60	15.350	20.074	20.065	0.010	0.032
ESI-66	8.500	1.668	60	14.970	19.704	19.683	0.021	0.031

Table A.1. (cont'd)

ID	UT	X	Int.	$V_{obs.}$	$V_{tab.}$	$V_{comp.}$	Res.	σ
ESI-69	8.500	1.668	60	12.260	16.942	16.971	-0.028	0.025
ESI-75	8.500	1.668	60	13.870	18.532	18.582	-0.050	0.029
ESI-76	8.500	1.668	60	14.940	19.645	19.655	-0.009	0.028
ESI-91	8.500	1.668	60	14.840	19.597	19.555	0.043	0.028
ESI-93	8.500	1.668	60	14.530	19.279	19.245	0.035	0.028
ESI-101	8.500	1.668	60	15.000	19.749	19.715	0.035	0.025
ESI-103	8.500	1.668	60	15.140	19.836	19.855	-0.019	0.027
ESI-104	8.500	1.668	60	15.390	20.131	20.105	0.027	0.029
ESI-105	8.500	1.668	60	12.300	17.022	17.012	0.011	0.026
ESI-107	8.500	1.668	60	15.950	20.611	20.660	-0.049	0.027
ESI-109	8.500	1.668	60	16.220	20.899	20.934	-0.035	0.027
ESI-110	8.500	1.668	60	16.860	21.514	21.574	-0.060	0.031
ESI-112	8.500	1.668	60	14.400	19.120	19.115	0.006	0.030
ESI-113	8.500	1.668	60	15.970	20.630	20.684	-0.054	0.026
ESI-116	8.500	1.668	60	13.840	18.508	18.553	-0.045	0.028
ESI-4	6.533	1.706	500	16.280	20.942	20.947	-0.005	0.026
ESI-6	6.533	1.706	500	14.850	19.540	19.517	0.024	0.025
ESI-20	6.533	1.706	500	14.200	18.917	18.867	0.051	0.024
ESI-34	6.533	1.706	500	15.830	20.499	20.498	0.001	0.025
ESI-41	6.533	1.706	500	15.230	19.927	19.898	0.029	0.026
ESI-42	6.533	1.706	500	15.060	19.754	19.727	0.028	0.025
ESI-43	6.533	1.706	500	14.930	19.626	19.599	0.028	0.025
ESI-44	6.533	1.706	500	16.360	21.012	21.028	-0.016	0.028
ESI-45	6.533	1.706	500	15.000	19.697	19.668	0.029	0.025
ESI-47	6.533	1.706	500	14.925	19.628	19.593	0.035	0.025
ESI-48	6.533	1.706	500	14.885	19.551	19.553	-0.002	0.025
ESI-49	6.533	1.706	500	15.650	20.324	20.318	0.006	0.025
ESI-56	6.533	1.706	500	16.410	21.063	21.078	-0.014	0.026
ESI-3	6.417	1.710	60	13.960	18.664	18.627	0.037	0.025
ESI-4	6.417	1.710	60	16.280	20.992	20.945	0.048	0.026
ESI-6	6.417	1.710	60	14.850	19.562	19.514	0.049	0.025
ESI-34	6.417	1.710	60	15.830	20.529	20.495	0.034	0.025
ESI-41	6.417	1.710	60	15.230	19.947	19.895	0.052	0.025
ESI-42	6.417	1.710	60	15.060	19.766	19.724	0.043	0.028
ESI-43	6.417	1.710	60	14.930	19.645	19.596	0.049	0.027
ESI-44	6.417	1.710	60	16.360	21.032	21.025	0.007	0.027

Table A.1. (end)

ID	UT	X	Int.	$V_{obs.}$	$V_{tab.}$	$V_{comp.}$	Res.	σ
ESI-45	6.417	1.710	60	15.000	19.714	19.665	0.049	0.026
ESI-48	6.417	1.710	60	14.885	19.566	19.550	0.016	0.028
ESI-49	6.417	1.710	60	15.650	20.345	20.315	0.030	0.029
ESI-50	6.417	1.710	60	13.860	18.528	18.526	0.002	0.026
ESI-56	6.417	1.710	60	16.410	21.101	21.075	0.027	0.025
ESI-59	6.417	1.710	60	13.950	18.618	18.613	0.005	0.025
ESI-4	11.300	1.706	500	16.280	20.932	20.981	-0.048	0.037
ESI-6	11.300	1.706	500	14.850	19.564	19.550	0.014	0.029
ESI-90	11.300	1.706	500	15.690	20.370	20.391	-0.021	0.028
ESI-91	11.300	1.706	500	14.840	19.546	19.542	0.005	0.029
ESI-93	11.300	1.706	500	14.530	19.252	19.232	0.021	0.029
ESII-185	11.300	1.706	500	15.410	20.132	20.112	0.021	0.028
ESIII-49	11.300	1.706	500	15.350	20.045	20.052	-0.006	0.027
ESIII-57	11.300	1.706	500	15.760	20.428	20.462	-0.033	0.026
ESI-4	12.033	1.733	60	16.280	21.003	20.946	0.057	0.030
ESI-6	12.033	1.733	60	14.850	19.563	19.515	0.048	0.029
ESI-90	12.033	1.733	60	15.690	20.391	20.357	0.035	0.025
ESI-91	12.033	1.733	60	14.840	19.562	19.507	0.056	0.030
ESI-93	12.033	1.733	60	14.530	19.249	19.197	0.053	0.030
ESIII-49	12.033	1.733	60	15.350	20.047	20.017	0.030	0.026
ESIII-57	12.033	1.733	60	15.760	20.442	20.427	0.016	0.027

Table A.2. Standard Stars in B, Sept.10/11 1986 (NGC 188 and NGC 6791)

ID	UT	X	Int.	$V_{obs.}$	$V_{tab.}$	$V_{comp.}$	Res.	σ
L110-340	2.917	1.176	2	10.324	14.489	14.508	-0.020	0.021
L110-450	3.033	1.175	20	12.535	16.590	16.565	0.025	0.022
L110-450	3.033	1.176	20	12.535	16.594	16.565	0.028	0.022
L110-441	3.233	1.181	10	11.660	15.772	15.779	-0.007	0.023
L110-441	3.250	1.182	10	11.660	15.770	15.778	-0.008	0.023
L109-954	3.417	1.288	40	13.740	17.710	17.701	0.009	0.022
L109-949	3.417	1.288	40	13.630	17.711	17.711	0.000	0.022
L109-959	3.417	1.288	40	13.710	17.766	17.759	0.007	0.023
L109-956	3.417	1.288	40	15.920	19.863	19.884	-0.021	0.045
L109-949	3.433	1.291	40	13.630	17.717	17.711	0.006	0.022
L109-954	3.433	1.291	40	13.740	17.715	17.702	0.013	0.022
L109-959	3.433	1.291	40	13.710	17.774	17.759	0.015	0.023
L109-956	3.433	1.291	40	15.920	19.889	19.884	0.005	0.046
L112-805	3.533	1.244	12	12.240	16.422	16.453	-0.031	0.021
L112-805	3.550	1.243	12	12.240	16.430	16.453	-0.023	0.021
L113-488	5.583	1.173	10	10.860	14.897	14.918	-0.021	0.024
L113-493	5.583	1.173	10	12.570	16.599	16.605	-0.006	0.024
L113-492	5.583	1.173	10	12.740	16.824	16.830	-0.006	0.024
L113-495	5.583	1.173	10	13.390	17.389	17.390	-0.001	0.023
L113-488	5.583	1.173	10	10.860	14.902	14.918	-0.016	0.024
L113-493	5.583	1.173	10	12.570	16.593	16.605	-0.012	0.024
L113-492	5.583	1.173	10	12.740	16.824	16.830	-0.006	0.024
L113-495	5.583	1.173	10	13.390	17.392	17.390	0.002	0.023
L109-954	5.717	2.230	40	13.740	17.897	17.893	0.004	0.022
L109-949	5.717	2.230	40	13.630	17.915	17.903	0.012	0.022
L109-959	5.717	2.230	40	13.710	17.972	17.951	0.022	0.023
L109-956	5.717	2.230	40	15.920	20.048	20.075	-0.027	0.046
L109-954	5.733	2.247	40	13.740	17.898	17.897	0.001	0.022
L109-949	5.733	2.247	40	13.630	17.904	17.907	-0.003	0.022
L109-959	5.733	2.247	40	13.710	17.951	17.954	-0.003	0.023
L109-956	5.733	2.247	40	15.920	20.041	20.079	-0.038	0.046
L109-954	5.783	2.305	75	13.740	17.897	17.910	-0.014	0.022
L109-949	5.783	2.305	75	13.630	17.905	17.920	-0.015	0.022
L109-959	5.783	2.305	75	13.710	17.959	17.968	-0.009	0.022
L109-956	5.783	2.305	75	15.920	20.065	20.093	-0.028	0.044
L109-954	5.817	2.335	75	13.740	17.890	17.917	-0.028	0.022
L109-949	5.817	2.335	75	13.630	17.903	17.927	-0.024	0.022

Table A.2. (cont'd)

ID	UT	X	Int.	$V_{obs.}$	$V_{tab.}$	$V_{comp.}$	Res.	σ
L109-959	5.817	2.335	75	13.710	17.959	17.975	-0.016	0.022
L109-956	5.817	2.335	75	15.920	20.055	20.099	-0.045	0.044
L95-74	12.333	1.185	40	12.656	16.627	16.629	-0.002	0.021
L95-73	12.333	1.185	40	13.020	17.067	17.089	-0.022	0.023
L95-74	12.350	1.186	40	12.656	16.607	16.628	-0.021	0.021
L95-73	12.350	1.186	40	13.020	17.061	17.088	-0.027	0.023
L96-736	12.467	1.183	40	12.360	16.472	16.484	-0.012	0.024
L96-737	12.467	1.183	40	13.049	16.977	16.968	0.009	0.021
L96-736	12.483	1.182	40	12.360	16.471	16.483	-0.012	0.024
L96-737	12.483	1.182	40	13.049	16.963	16.967	-0.004	0.021
L98-667	12.567	1.452	3	8.406	12.663	12.679	-0.016	0.021
L98-653	12.567	1.452	3	9.534	13.805	13.814	-0.009	0.021
L98-667	12.583	1.450	3	8.406	12.722	12.677	0.045	0.021
L98-653	12.583	1.450	3	9.534	13.806	13.813	-0.007	0.021
ESI-60	9.367	1.669	600	15.840	20.061	20.072	-0.011	0.023
ESI-61	9.367	1.669	600	15.200	19.287	19.333	-0.046	0.023
ESI-62	9.367	1.669	600	15.590	19.770	19.797	-0.026	0.023
ESI-63	9.367	1.669	600	16.570	20.743	20.791	-0.047	0.027
ESI-65	9.367	1.669	600	16.030	20.264	20.260	0.005	0.025
ESI-76	9.367	1.669	600	15.620	19.869	19.850	0.020	0.023
ESI-91	9.367	1.669	600	15.550	19.812	19.773	0.039	0.022
ESI-93	9.367	1.669	600	15.230	19.488	19.455	0.033	0.022
ESI-101	9.367	1.669	600	15.680	19.946	19.910	0.037	0.023
ESI-103	9.367	1.669	600	15.760	20.015	20.004	0.012	0.022
ESI-104	9.367	1.669	600	16.080	20.321	20.308	0.014	0.025
ESI-107	9.367	1.669	600	17.340	21.400	21.406	-0.006	0.029
ESI-109	9.367	1.669	600	16.980	21.175	21.191	-0.016	0.028
ESI-110	9.367	1.669	600	17.660	21.812	21.862	-0.050	0.027
ESI-112	9.367	1.669	600	15.090	19.311	19.318	-0.006	0.022
ESI-60	8.367	1.669	60	15.840	20.058	20.059	-0.001	0.025
ESI-61	8.367	1.669	60	15.200	19.301	19.320	-0.019	0.025
ESI-62	8.367	1.669	60	15.590	19.778	19.784	-0.005	0.024
ESI-63	8.367	1.669	60	16.570	20.744	20.778	-0.033	0.024
ESI-65	8.367	1.669	60	16.030	20.265	20.247	0.019	0.025
ESI-66	8.367	1.669	60	15.850	20.028	20.021	0.008	0.023
ESI-69	8.367	1.669	60	13.560	17.600	17.634	-0.034	0.024
ESI-75	8.367	1.669	60	14.950	19.031	19.075	-0.043	0.025

Table A.2. (cont'd)

ID	UT	X	Int.	$V_{obs.}$	$V_{tab.}$	$V_{comp.}$	Res.	σ
ESI-76	8.367	1.669	60	15.620	19.870	19.837	0.034	0.023
ESI-103	8.367	1.669	60	15.760	20.021	19.991	0.031	0.023
ESI-104	8.367	1.669	60	16.080	20.336	20.294	0.042	0.026
ESI-105	8.367	1.669	60	13.470	17.601	17.574	0.027	0.023
ESI-107	8.367	1.669	60	17.340	21.428	21.393	0.035	0.024
ESI-109	8.367	1.669	60	16.980	21.198	21.178	0.020	0.025
ESI-112	8.367	1.669	60	15.090	19.334	19.304	0.030	0.024
ESI-116	8.367	1.669	60	14.790	18.912	18.945	-0.032	0.025
ESI-6	9.367	1.669	600	15.800	19.968	19.968	0.001	0.022
ESI-15	9.367	1.669	600	15.630	19.854	19.828	0.027	0.022
ESI-17	9.367	1.669	600	15.680	19.938	19.908	0.031	0.022
ESI-20	9.367	1.669	600	15.140	19.295	19.310	-0.015	0.023
ESI-34	9.367	1.669	600	16.560	20.735	20.778	-0.043	0.026
ESI-41	9.367	1.669	600	15.960	20.169	20.178	-0.009	0.023
ESI-42	9.367	1.669	600	16.030	20.182	20.193	-0.011	0.024
ESI-43	9.367	1.669	600	15.550	19.790	19.794	-0.003	0.022
ESI-44	9.367	1.669	600	17.110	21.274	21.324	-0.049	0.029
ESI-45	9.367	1.669	600	15.720	19.916	19.941	-0.024	0.022
ESI-47	9.367	1.669	600	15.645	19.866	19.866	0.001	0.022
ESI-48	9.367	1.669	600	15.635	19.812	19.849	-0.036	0.022
ESI-49	9.367	1.669	600	16.370	20.547	20.591	-0.043	0.023
ESI-3	6.200	1.718	60	14.440	18.718	18.675	0.043	0.023
ESI-4	6.200	1.718	60	17.110	21.260	21.265	-0.004	0.027
ESI-20	6.200	1.718	60	15.140	19.314	19.269	0.045	0.029
ESI-34	6.200	1.718	60	16.560	20.766	20.738	0.029	0.024
ESI-41	6.200	1.718	60	15.960	20.173	20.138	0.036	0.023
ESI-42	6.200	1.718	60	16.030	20.194	20.152	0.042	0.023
ESI-43	6.200	1.718	60	15.550	19.790	19.753	0.037	0.024
ESI-44	6.200	1.718	60	17.110	21.293	21.283	0.010	0.025
ESI-45	6.200	1.718	60	15.720	19.928	19.900	0.028	0.024
ESI-47	6.200	1.718	60	15.645	19.860	19.825	0.035	0.024
ESI-48	6.200	1.718	60	15.635	19.814	19.808	0.006	0.026
ESI-49	6.200	1.718	60	16.370	20.549	20.550	-0.001	0.023
ESI-50	6.200	1.718	60	14.410	18.591	18.629	-0.038	0.024
ESI-56	6.200	1.718	60	17.230	21.386	21.387	-0.001	0.025
ESI-59	6.200	1.718	60	14.960	19.048	19.073	-0.025	0.023
ESI-6	10.317	1.681	600	15.800	19.988	19.973	0.016	0.025

Table A.2. (end)

ID	UT	X	Int.	$V_{obs.}$	$V_{tab.}$	$V_{comp.}$	Res.	σ
ESI-90	10.317	1.681	600	16.440	20.659	20.659	0.001	0.025
ESI-91	10.317	1.681	600	15.550	19.802	19.778	0.024	0.026
ESI-93	10.317	1.681	600	15.230	19.485	19.460	0.025	0.025
ESII-185	10.317	1.681	600	16.110	20.307	20.340	-0.033	0.023
ESIII-49	10.317	1.681	600	16.010	20.248	20.249	-0.001	0.023
ESIII-57	10.317	1.681	600	16.470	20.683	20.698	-0.015	0.025
ESI-4	12.150	1.738	60	17.110	21.244	21.281	-0.037	0.031
ESI-6	12.150	1.738	60	15.800	19.969	19.944	0.026	0.024
ESI-90	12.150	1.738	60	16.440	20.676	20.630	0.047	0.025
ESI-91	12.150	1.738	60	15.550	19.797	19.749	0.048	0.025
ESI-93	12.150	1.738	60	15.230	19.478	19.431	0.047	0.026
ESII-185	12.150	1.738	60	16.110	20.330	20.311	0.019	0.025
ESIII-49	12.150	1.738	60	16.010	20.236	20.221	0.016	0.025
ESIII-57	12.150	1.738	60	16.470	20.668	20.669	-0.001	0.028

Table A.3. Standard Stars in V, Sept. 11/12 1986 (NGC 188)

ID	UT	X	Int.	$V_{obs.}$	$V_{tab.}$	$V_{comp.}$	Res.	σ
L108-475	2.633	1.365	10	11.308	15.899	15.910	-0.011	0.009
L108-551	2.817	1.404	5	10.705	15.298	15.309	-0.010	0.008
L109-71	2.900	1.238	10	11.491	16.077	16.066	0.011	0.009
L109-381	2.967	1.244	12	11.728	16.306	16.306	0.000	0.009
L110-340	3.067	1.180	5	10.023	14.589	14.588	0.002	0.008
L110-450	3.150	1.180	10	11.585	16.145	16.153	-0.008	0.010
L111-775	3.350	1.179	10	10.747	15.320	15.320	0.000	0.009
L109-954	3.483	1.309	40	12.440	17.031	17.035	-0.003	0.010
L93-424	9.833	1.169	25	11.620	16.205	16.201	0.004	0.008
L95-96	9.850	1.372	10	10.014	14.609	14.627	-0.018	0.008
L95-301	9.917	1.346	15	11.219	15.825	15.833	-0.008	0.010
L95-302	9.917	1.346	15	11.680	16.298	16.292	0.006	0.010
L95-74	12.233	1.184	25	11.529	16.116	16.113	0.003	0.008
L95-132	12.317	1.184	20	12.062	16.646	16.642	0.003	0.009
L95-96	12.383	1.189	8	10.014	14.585	14.594	-0.009	0.008
L95-301	12.433	1.185	15	11.219	15.806	15.803	0.003	0.010
L95-302	12.433	1.185	15	11.680	16.284	16.262	0.022	0.010
L96-36	12.517	1.186	7	10.589	15.175	15.168	0.006	0.008
L92-263	12.083	1.721	30	11.784	16.445	16.464	-0.020	0.008
ESI-3	4.033	1.821	500	13.960	18.659	18.645	0.014	0.014
ESI-4	4.033	1.821	500	16.280	20.979	20.967	0.013	0.015
ESI-6	4.033	1.821	500	14.850	19.562	19.537	0.025	0.014
ESI-10	4.033	1.821	500	14.900	19.580	19.586	-0.006	0.012
ESI-11	4.033	1.821	500	16.106	20.805	20.794	0.012	0.011
ESI-14	4.033	1.821	500	15.450	20.159	20.136	0.023	0.014
ESI-122	4.033	1.821	500	17.500	22.172	22.188	-0.015	0.014
ESII-112	4.033	1.821	500	16.120	20.827	20.806	0.021	0.013
ESII-113	4.033	1.821	500	16.450	21.136	21.137	0.000	0.012
ESII-115	4.033	1.821	500	15.850	20.557	20.536	0.021	0.013
ESII-121	4.033	1.821	500	16.260	20.922	20.946	-0.024	0.011
ESI-3	3.900	1.829	60	13.960	18.624	18.646	-0.022	0.031
ESI-6	3.900	1.829	60	14.850	19.554	19.538	0.016	0.029
ESI-10	3.900	1.829	60	14.900	19.567	19.587	-0.020	0.026
ESI-14	3.900	1.829	60	15.450	20.152	20.137	0.015	0.025
ESI-122	3.900	1.829	60	17.500	22.202	22.189	0.014	0.030
ESII-112	3.900	1.829	60	16.120	20.811	20.807	0.004	0.014
ESII-113	3.900	1.829	60	16.450	21.112	21.138	-0.025	0.019

Table A.3. (end)

ID	UT	X	Int.	$V_{obs.}$	$V_{tab.}$	$V_{comp.}$	Res.	σ
ESII-115	3.900	1.829	60	15.850	20.535	20.537	-0.002	0.015
ESII-121	3.900	1.829	60	16.260	20.931	20.947	-0.016	0.029
ESII-177	11.083	1.701	500	16.030	20.697	20.706	-0.008	0.061
ESIII-22	11.083	1.701	500	15.280	19.946	19.956	-0.009	0.026
ESIII-33	11.083	1.701	500	15.530	20.199	20.205	-0.006	0.014
ESII-177	8.500	1.668	60	16.030	20.701	20.699	0.003	0.034
ESII-211	8.500	1.668	60	17.380	22.046	22.050	-0.003	0.042

Table A.4. Standard Stars in B, Sept. 11/12 1986 (NGC 188)

ID	UT	X	Int.	$V_{obs.}$	$V_{tab.}$	$V_{comp.}$	Res.	σ
L108-475	2.583	1.356	15	12.687	16.638	16.652	-0.013	0.011
L108-551	2.833	1.408	5	10.880	15.105	15.109	-0.003	0.010
L109-71	2.867	1.235	15	11.812	15.978	15.971	0.007	0.010
L109-381	3.000	1.247	18	12.429	16.519	16.512	0.007	0.012
L110-340	3.033	1.179	4	10.324	14.467	14.476	-0.009	0.010
L110-506	3.233	1.182	25	11.910	16.001	16.009	-0.008	0.015
L111-775	3.400	1.179	15	12.485	16.346	16.339	0.007	0.011
L109-954	3.433	1.300	40	13.740	17.704	17.713	-0.008	0.013
L92-342	9.550	1.186	30	12.051	16.188	16.186	0.002	0.010
L93-424	9.733	1.169	35	12.704	16.684	16.699	-0.015	0.011
L95-96	9.867	1.366	10	10.161	14.385	14.396	-0.011	0.011
L95-301	9.900	1.351	20	12.504	16.505	16.498	0.006	0.012
L95-302	9.900	1.351	20	12.520	16.620	16.607	0.012	0.012
L92-342	12.133	1.745	30	12.051	16.305	16.304	0.001	0.010
L95-74	12.250	1.185	35	12.656	16.638	16.638	0.001	0.011
L95-132	12.283	1.183	25	12.511	16.653	16.633	0.020	0.011
L95-96	12.400	1.190	8	10.161	14.338	14.347	-0.010	0.011
L95-301	12.417	1.184	15	12.504	16.453	16.452	0.002	0.012
L95-302	12.417	1.184	15	12.520	16.569	16.560	0.009	0.013
L96-36	12.533	1.186	10	10.839	15.007	15.002	0.005	0.010
F11	9.700	1.145	40	11.825	16.092	16.090	0.002	0.010
L92-263	12.100	1.729	40	12.832	16.932	16.954	-0.022	0.011
ESI-6	6.650	1.703	600	15.800	19.949	19.946	0.004	0.016
ESI-31	6.650	1.703	600	17.020	21.213	21.201	0.012	0.032
ESII-112	6.650	1.703	600	16.850	21.058	21.042	0.017	0.022
ESII-113	6.650	1.703	600	17.260	21.435	21.435	0.001	0.022
ESII-115	6.650	1.703	600	16.580	20.780	20.772	0.009	0.017
ESII-121	6.650	1.703	600	16.970	21.143	21.166	-0.022	0.016
ESI-4	3.783	1.836	60	17.110	21.279	21.303	-0.024	0.026
ESI-6	3.783	1.836	60	15.800	20.004	19.968	0.036	0.022
ESI-10	3.783	1.836	60	15.660	19.832	19.868	-0.036	0.019
ESI-14	3.783	1.836	60	16.170	20.394	20.386	0.008	0.024
ESI-31	3.783	1.836	60	17.020	21.255	21.224	0.032	0.021
ESI-122	3.783	1.836	60	18.500	22.662	22.658	0.004	0.037
ESII-112	3.783	1.836	60	16.850	21.076	21.064	0.012	0.018
ESII-115	3.783	1.836	60	16.580	20.810	20.794	0.016	0.018
ESII-121	3.783	1.836	60	16.970	21.227	21.188	0.039	0.040

Table A.4. (end)

ID	UT	X	Int.	$V_{obs.}$	$V_{tab.}$	$V_{comp.}$	Res.	σ
ESII-211	10.200	1.679	600	18.330	22.434	22.468	-0.033	0.028
ESIII-22	10.200	1.679	600	15.970	20.137	20.162	-0.024	0.019
ESIII-33	10.200	1.679	600	16.190	20.408	20.388	0.020	0.023
ESII-211	10.083	1.677	60	18.330	22.456	22.467	-0.011	0.040
ESIII-22	10.083	1.677	60	15.970	20.136	20.162	-0.025	0.032
ESIII-33	10.083	1.677	60	16.190	20.418	20.388	0.030	0.022

Table A.5. Standard Stars in V, Jan. 23/24 1987 (NGC 2204)

ID	UT	X	Int.	$V_{obs.}$	$V_{tab.}$	$V_{comp.}$	Res.	σ
E2 20-S	1.333	1.040	1	9.502	12.583	12.578	0.005	0.009
E2 m	1.450	1.050	30	13.097	16.176	16.176	0.000	0.013
E3 33-T	1.617	1.090	4	10.053	13.134	13.142	-0.008	0.007
E3 55-R	1.700	1.090	3	10.659	13.738	13.741	-0.003	0.009
E3 59-X	1.767	1.080	8	11.345	14.408	14.427	-0.019	0.011
E3 58-W	1.850	1.070	15	11.570	14.651	14.648	0.004	0.010
-2 524	1.933	1.400	5	10.307	13.454	13.450	0.004	0.007
GD 71	2.000	1.440	30	13.027	16.185	16.177	0.008	0.008
95-52	2.083	1.270	1	9.574	12.683	12.695	-0.012	0.009
95-96	2.117	1.280	3	10.014	13.132	13.134	-0.002	0.007
95-74	2.167	1.280	8	11.529	14.648	14.655	-0.008	0.008
95-73	2.167	1.280	8	12.310	15.394	15.434	-0.040	0.017
95-236	2.250	1.290	8	11.492	14.618	14.618	0.000	0.008
96-36	2.317	1.180	6	10.589	13.702	13.689	0.014	0.007
E4 7-K	8.250	1.170	1	9.405	12.500	12.488	0.012	0.009
E4 108	8.283	1.180	2	9.776	12.876	12.873	0.003	0.009
E4 48-T	8.333	1.170	5	10.587	13.670	13.671	0.000	0.008
E4 57-a	8.383	1.180	6	11.343	14.447	14.436	0.012	0.010
E5 32-P	8.450	1.040	1	9.236	12.300	12.301	-0.001	0.023
E5 46-S	8.483	1.030	5	10.586	13.647	13.643	0.004	0.010
E5 56-V	8.533	1.030	7	10.865	13.928	13.925	0.003	0.008
100340	8.600	1.240	3	10.117	13.208	13.211	-0.004	0.008
+5 2468	8.650	1.250	1	9.348	12.437	12.445	-0.008	0.009

Table A.6. Standard Stars in B, Jan. 23/24 1987 (NGC 2204)

ID	UT	X	Int.	$V_{obs.}$	$V_{tab.}$	$V_{comp.}$	Res.	σ
E2 20-S	1.300	1.040	3	10.089	13.193	13.179	0.014	0.011
E2 m	1.417	1.040	45	13.903	16.988	16.964	0.024	0.016
E3 33-T	1.583	1.090	8	11.211	14.232	14.242	-0.010	0.012
E3 55-R	1.683	1.090	6	10.717	13.894	13.896	-0.002	0.012
E3 59-X	1.750	1.080	12	11.754	14.897	14.882	0.015	0.016
E3 58-W	1.817	1.080	15	11.699	14.857	14.865	-0.007	0.015
-2 524	1.900	1.390	5	10.203	13.525	13.525	0.001	0.011
GD 71	1.983	1.440	30	12.772	16.149	16.136	0.013	0.012
95-52	2.050	1.260	3	10.103	13.278	13.282	-0.005	0.011
95-96	2.100	1.280	3	10.161	13.388	13.402	-0.014	0.011
95-74	2.150	1.270	15	12.656	15.773	15.754	0.019	0.012
95-236	2.233	1.290	12	12.227	15.382	15.388	-0.006	0.011
96-36	2.300	1.180	6	10.839	14.017	14.026	-0.009	0.010
E4 7-K	8.233	1.160	2	9.486	12.678	12.675	0.003	0.011
E4 108	8.267	1.180	6	11.683	14.621	14.627	-0.005	0.014
E4 48-T	8.317	1.170	6	10.788	13.953	13.964	-0.011	0.011
E4 57-a	8.367	1.180	12	12.631	15.681	15.660	0.021	0.017
E5 32-P	8.433	1.040	3	10.754	13.680	13.704	-0.024	0.025
E5 46-S	8.467	1.030	8	11.180	14.252	14.249	0.003	0.014
E5 56-V	8.517	1.030	10	11.848	14.858	14.865	-0.007	0.013
100340	8.583	1.240	3	9.875	13.147	13.140	0.006	0.012
+5 2468	8.633	1.250	2	9.232	12.478	12.484	-0.006	0.011

Table A.7. Standard Stars in V, Feb. 09/10 1986 (Mel 66)

ID	UT	X	Int.	$V_{obs.}$	$V_{tab.}$	$V_{comp.}$	Res.	σ
E1 i	0.400	1.397	4	13.759	15.746	15.742	0.005	0.015
E1 49-V	0.400	1.397	4	11.640	13.624	13.615	0.009	0.021
E2 o	0.583	1.063	10	14.090	15.998	16.008	-0.010	0.015
E2 s	0.583	1.063	10	14.596	16.518	16.518	0.000	0.014
E2 I	0.583	1.063	10	15.751	17.661	17.676	-0.015	0.027
E2 t	0.583	1.063	10	15.171	17.114	17.091	0.023	0.016
E3 o	0.900	1.069	13	14.804	16.731	16.716	0.015	0.015
E3 e	0.900	1.069	13	12.867	14.745	14.779	-0.035	0.025
E3 k	0.900	1.069	13	14.078	16.007	15.990	0.016	0.014
E3 v	0.900	1.069	13	16.254	18.183	18.165	0.018	0.030
E3 o	0.917	1.068	11	14.804	16.743	16.715	0.028	0.015
E3 e	0.917	1.068	11	12.867	14.750	14.779	-0.028	0.025
E3 v	0.917	1.068	11	16.254	18.180	18.164	0.016	0.030
E3 k	0.917	1.068	11	14.078	16.012	15.990	0.023	0.014
E3 55-R	0.983	1.065	1	10.659	12.546	12.558	-0.012	0.013
E3 59-X	0.983	1.065	1	11.345	13.241	13.251	-0.010	0.015
E3 58-W	1.100	1.058	3	11.570	13.457	13.467	-0.010	0.014
E4 h	1.200	1.396	15	13.760	15.703	15.718	-0.015	0.017
E4 qM	1.200	1.396	15	16.148	18.108	18.115	-0.006	0.020
E4 rM	1.200	1.396	15	16.756	18.748	18.727	0.021	0.054
E4 57-a	1.683	1.390	3	11.343	13.278	13.305	-0.027	0.014
E4 48-T	1.733	1.284	1	10.587	12.497	12.509	-0.012	0.013
GD108	5.117	1.086	5	13.560	15.401	15.405	-0.003	0.030
E5 c	5.450	1.134	5	13.399	15.272	15.273	-0.001	0.014
E5 59-Y	5.450	1.134	5	12.869	14.727	14.726	0.001	0.013
E5 h	5.500	1.130	10	14.225	16.106	16.106	0.000	0.016
E5 k	5.717	1.107	40	15.376	17.239	17.238	0.002	0.021
E5 o	5.717	1.107	40	16.525	18.418	18.391	0.027	0.021
E5 m	5.717	1.107	40	15.814	17.735	17.678	0.057	0.028
E6 l	9.067	1.061	10	12.336	14.227	14.229	-0.002	0.015
E6 g	9.283	1.053	5	12.177	14.041	14.056	-0.015	0.013
G153-41	9.383	1.215	5	13.410	15.299	15.301	-0.001	0.032

Table A.8. Standard Stars in B, Feb. 09/10 1986 (Mel 66)

ID	UT	X	Int.	$V_{obs.}$	$V_{tab.}$	$V_{comp.}$	Res.	σ
E1 i	0.383	1.392	5	14.675	16.594	16.581	0.014	0.020
E1 49-V	0.383	1.392	5	12.204	14.159	14.136	0.023	0.026
E2 o	0.600	1.065	15	14.660	16.506	16.489	0.018	0.019
E2 s	0.600	1.065	15	15.323	17.139	17.140	-0.001	0.018
E2 I	0.600	1.065	15	16.638	18.436	18.443	-0.007	0.035
E2 t	0.600	1.065	15	15.805	17.650	17.629	0.021	0.021
E3 o	0.867	1.072	16	15.356	17.203	17.182	0.021	0.018
E3 e	0.867	1.072	16	13.452	15.244	15.276	-0.031	0.027
E3 k	0.867	1.072	16	14.662	16.497	16.486	0.012	0.018
E3 v	0.867	1.072	16	16.763	18.617	18.592	0.025	0.034
E3 55-R	1.017	1.063	1	10.717	12.560	12.574	-0.014	0.016
E3 59-X	1.017	1.063	1	11.754	13.580	13.585	-0.005	0.019
E3 58-W	1.100	1.058	3	11.699	13.533	13.548	-0.015	0.019
E4 h	1.233	1.390	20	14.375	16.261	16.284	-0.023	0.022
E4 qM	1.233	1.390	20	17.173	18.987	19.051	-0.064	0.041
E4 rM	1.233	1.390	20	17.984	19.779	19.847	-0.068	0.069
E4 57-a	1.650	1.294	3	12.631	14.462	14.452	0.010	0.019
E4 48-T	1.750	1.281	1	10.788	12.676	12.685	-0.009	0.015
GD108	5.133	1.086	10	13.330	15.197	15.164	0.033	0.040
E5 c	5.433	1.136	5	14.292	16.051	16.056	-0.005	0.021
E5 59-Y	5.433	1.136	5	12.932	14.747	14.758	-0.011	0.016
E5 h	5.517	1.128	15	15.486	17.204	17.220	-0.016	0.022
E5 k	5.700	1.109	40	15.878	17.670	17.663	0.007	0.030
E5 o	5.700	1.109	40	17.229	19.030	18.999	0.031	0.029
E5 m	5.700	1.109	40	16.426	18.285	18.203	0.083	0.033
E6 l	9.017	1.064	3	13.655	15.365	15.386	-0.022	0.022
E6 l	9.050	1.063	10	13.655	15.378	15.387	-0.009	0.022
E6 g	9.267	1.054	5	12.735	14.517	14.524	-0.007	0.019
G153-41	9.367	1.219	5	13.190	15.099	15.089	0.011	0.046

Appendix B

Finding Charts

The following charts represent the regions which were observed in the four clusters. The position of the frames with respect to the center of the cluster are as follows:

- NGC 2204: The reference coordinates are those of the frame NE, centered 19" N and 45" E of the cluster center (see p. 41). Scale: 100 units on the x or y axes (N/S and E/W directions, respectively) correspond to about 53".

- Melotte 66: There is only one region, centered 50" S and 13" E of the cluster center (see p. 35). Scale: 100 units on the x or y axes (N/S and E/W directions, respectively) correspond to about 57".

- NGC 188: The reference coordinates are those of the frame NE, centered 109" N and 268" E of the cluster center (see p. 19). Scale: 100 units on the x or y axes (N/S and E/W directions, respectively) correspond to about 83".

- NGC 6791: There is only one region, centered 4" W and 73" S if the cluster center (see p. 18). Scale: 100 units on the x or y axes (N/S and E/W directions, respectively) correspond to about 83".

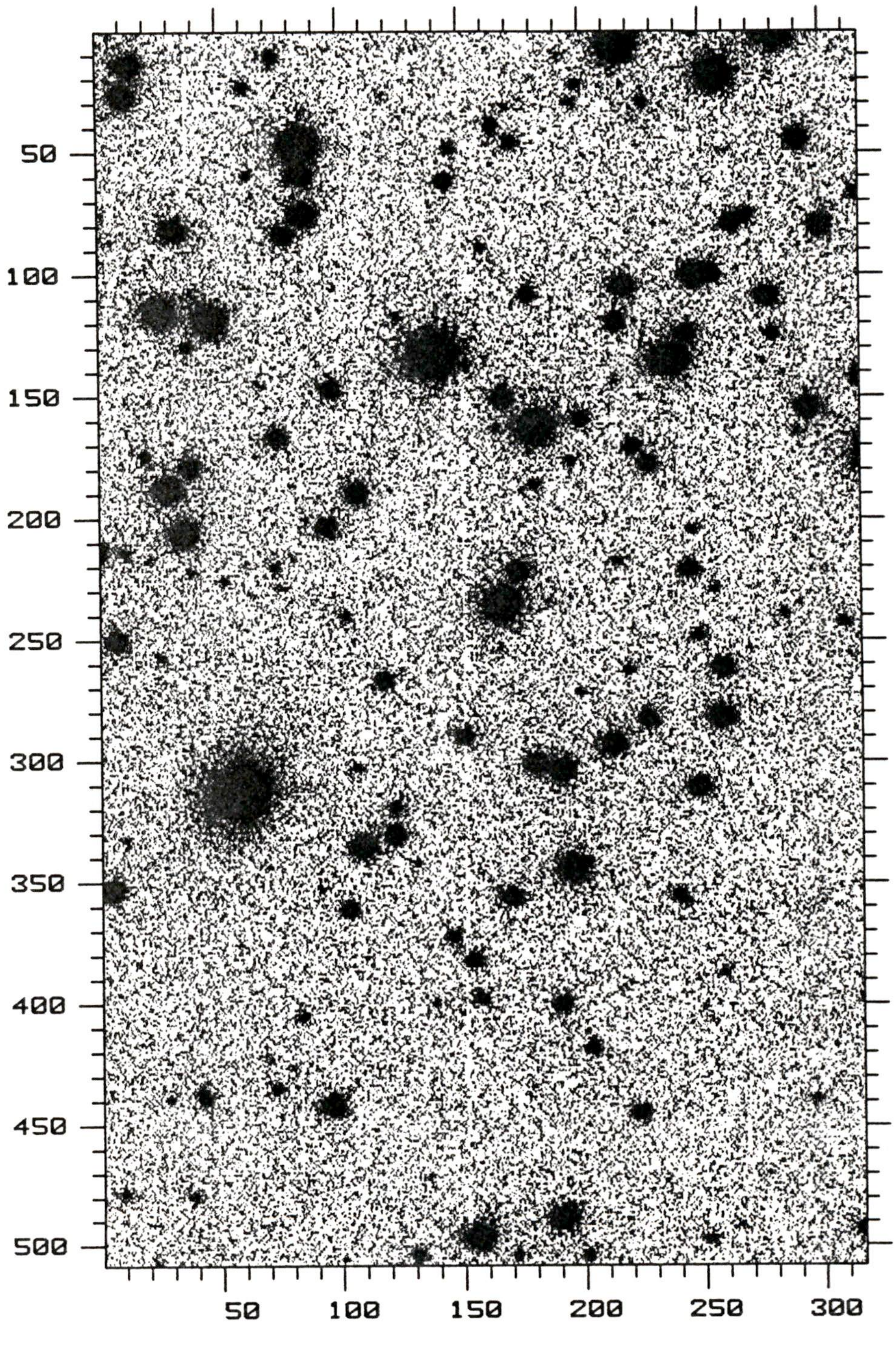

Fig. B.1. Region NE of NGC 2204 (reference frame), centered 19" N and 45" E of the cluster center. The center is at the position (190, 160). Scale: 53"/100 units.

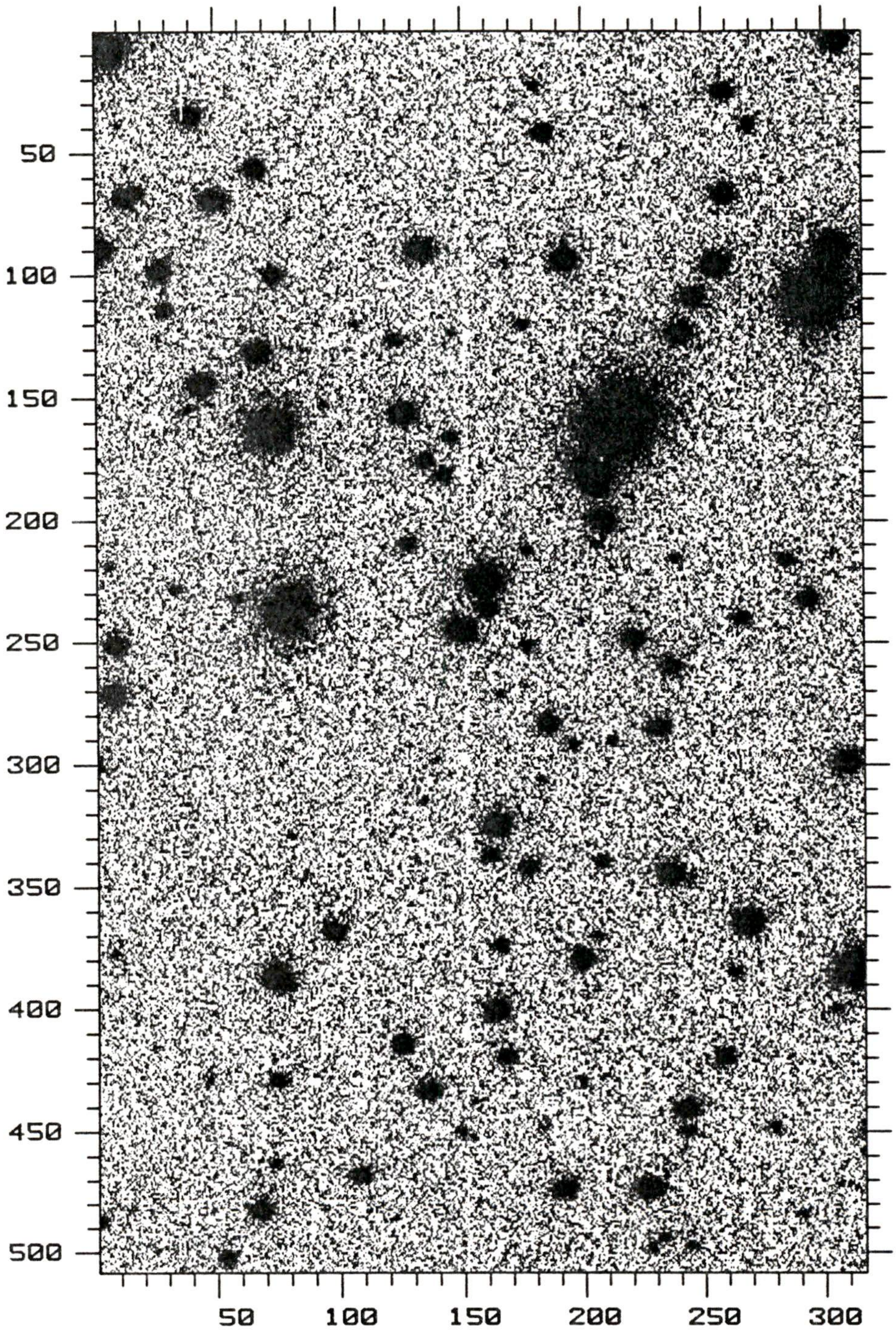

Fig. B.2. Region SE of NGC 2204, centered 103" S and 45" E of the cluster center. The coordinates can be related to those of the reference frame by a shift of: $x(\mathrm{SE}) - x(\mathrm{NE}) = -250$, and $y(\mathrm{SE}) - y(\mathrm{NE}) = -10$. Scale: 53"/100 units.

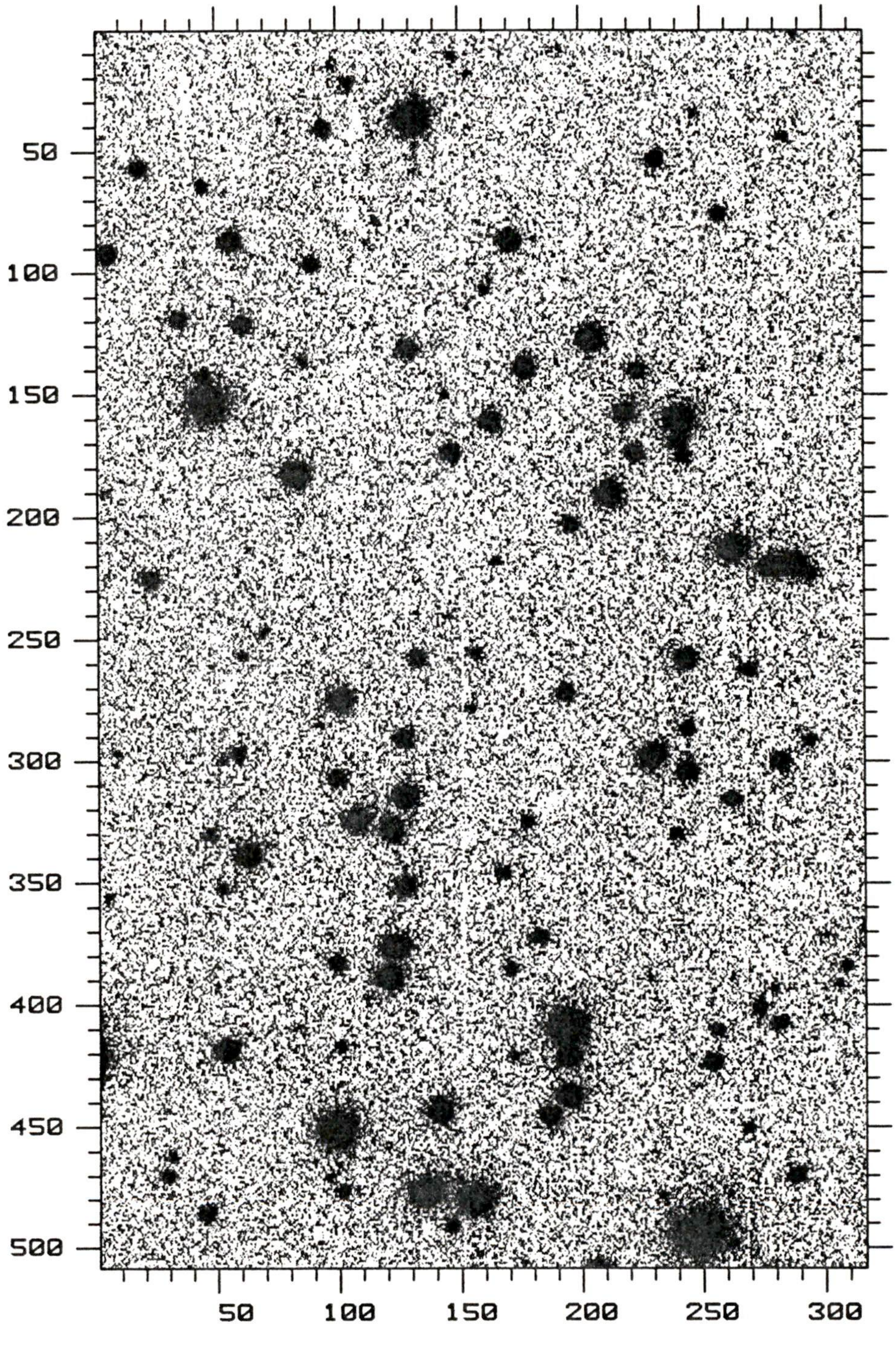

Fig. B.3. Region NW of NGC 2204, centered 90" N and 135" W of the cluster center. The coordinates can be put on the reference scale by a shift of: $x(\mathrm{NW}) - x(\mathrm{NE}) = 110$, and $y(\mathrm{NW}) - y(\mathrm{NE}) = 362$. Scale: 53"/100 units.

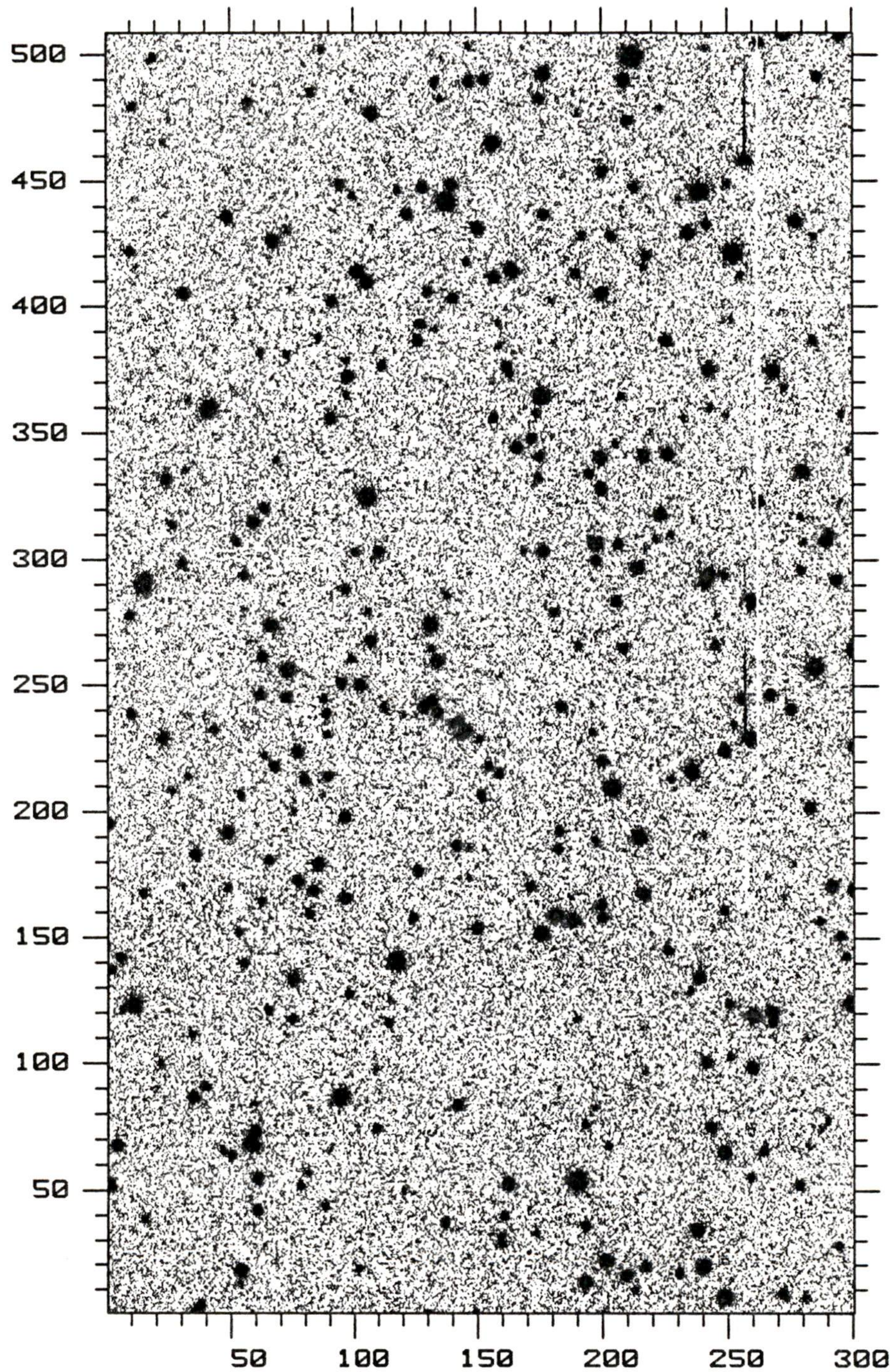

Fig. B.4. Single region of Melotte 66, centered 50" S and 13" E of the cluster center. The center is at the position (240, 240). Scale: 57"/100 units.

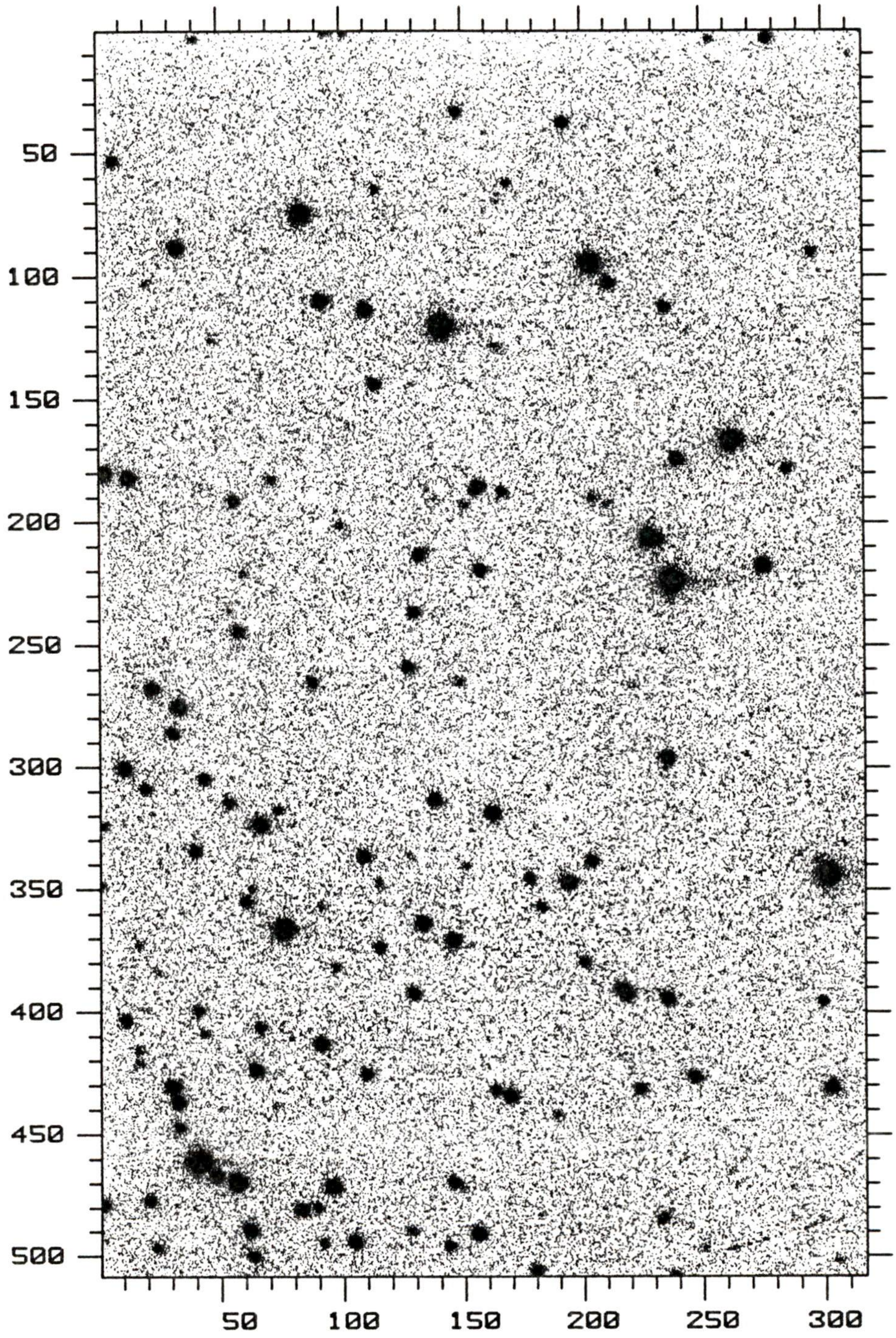

Fig. B.5. Region NE of NGC 188 (reference frame), centered 109" N and 268" E of the cluster center. The center does not appear on this frame. Scale: 83"/100 units.

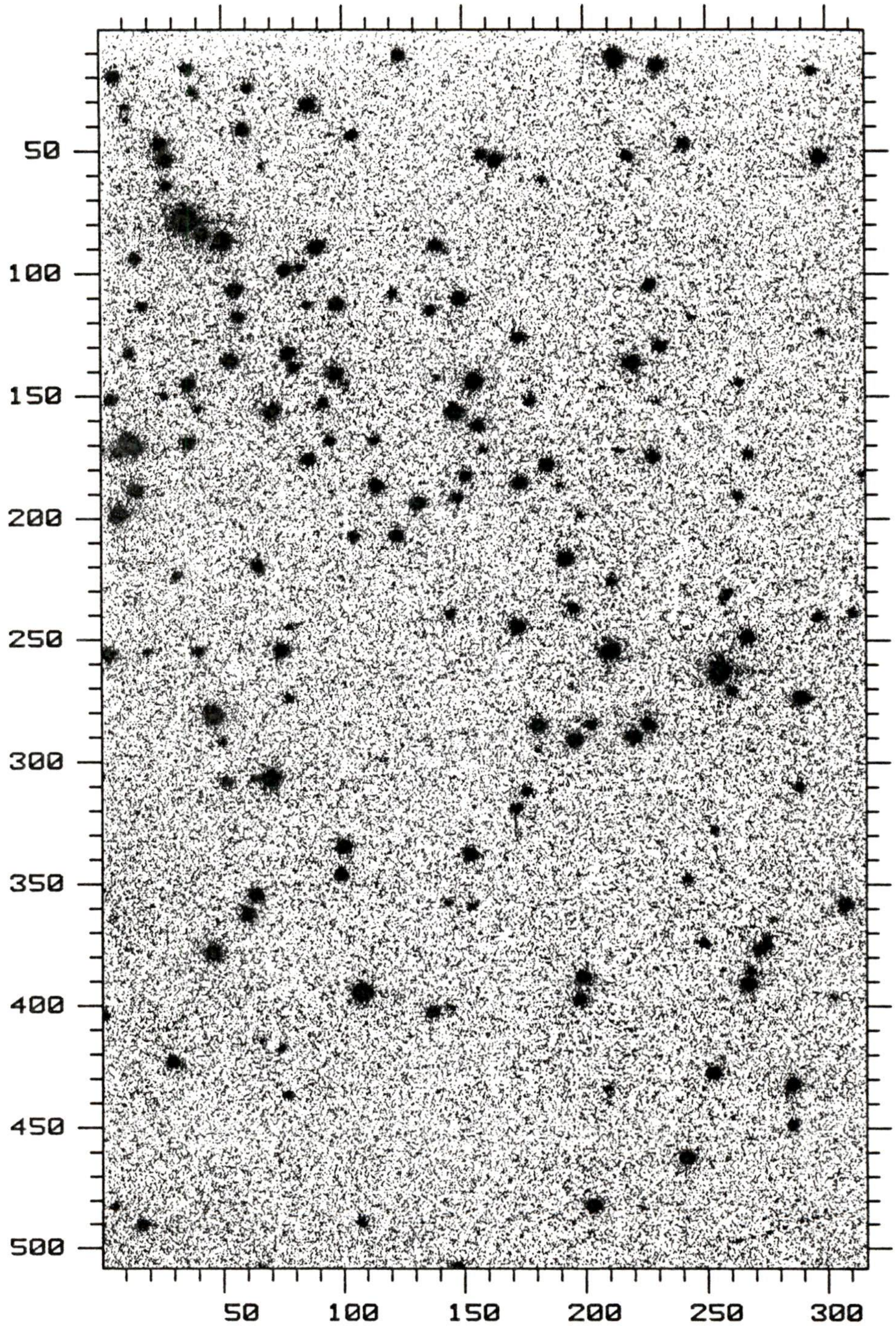

Fig. B.6. Region NW of NGC 188, centered 103" N and 73" E of the cluster center. The coordinates can be related to those of the reference frame by a shift of: $x(\mathrm{NE}) - x(\mathrm{NW}) = 5$, and $y(\mathrm{NE}) - y(\mathrm{NW}) = 383$. Scale: 83"/100 units.

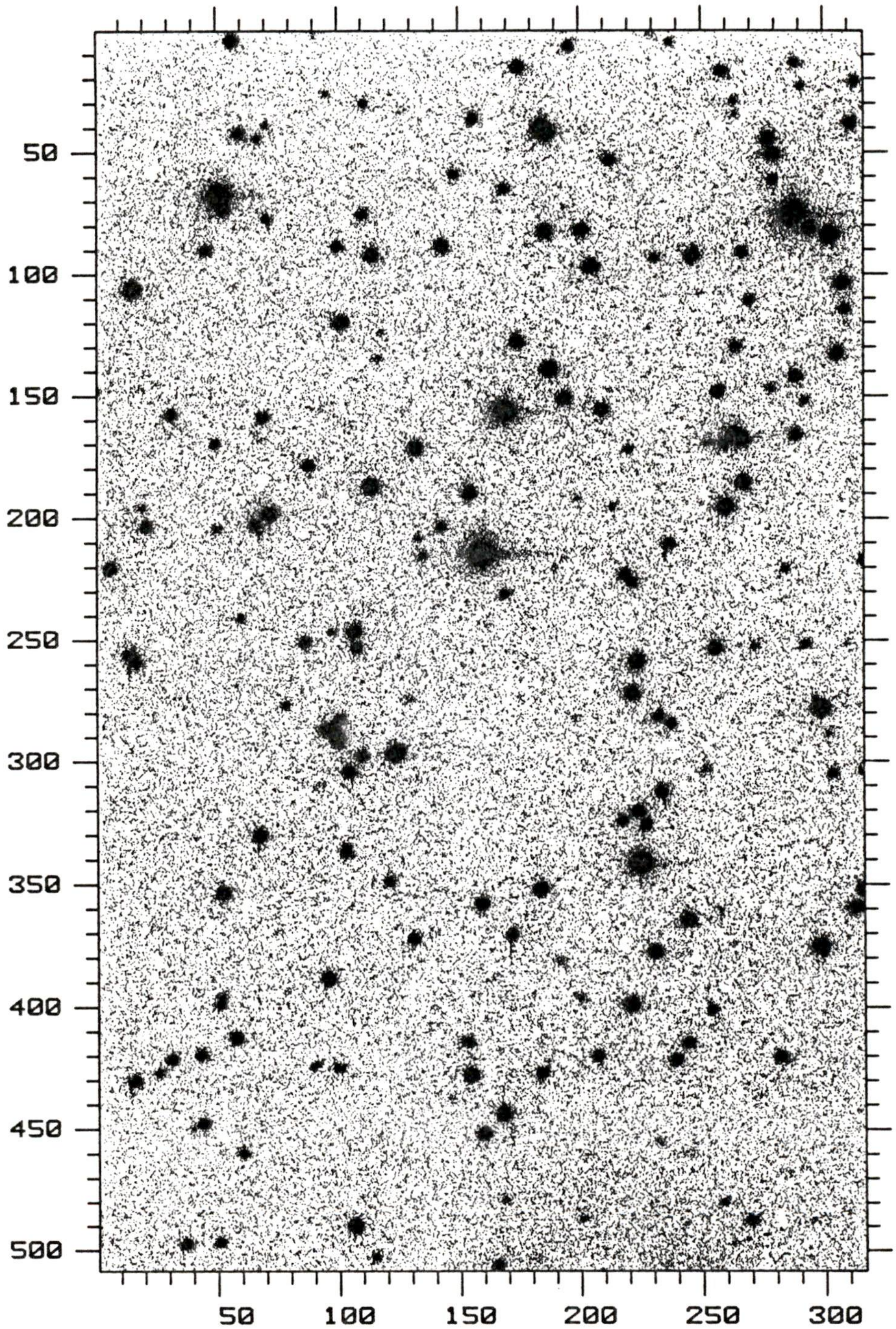

Fig. B.7. Region SW of NGC 188, centered 85" S and 61" E of the cluster center. The coordinates can be related to those of the reference frame by a shift of: $x(\mathrm{NE}) - x(\mathrm{SW}) = -247$, and $y(\mathrm{NE}) - y(\mathrm{SW}) = 385$. Scale: 83"/100 units.

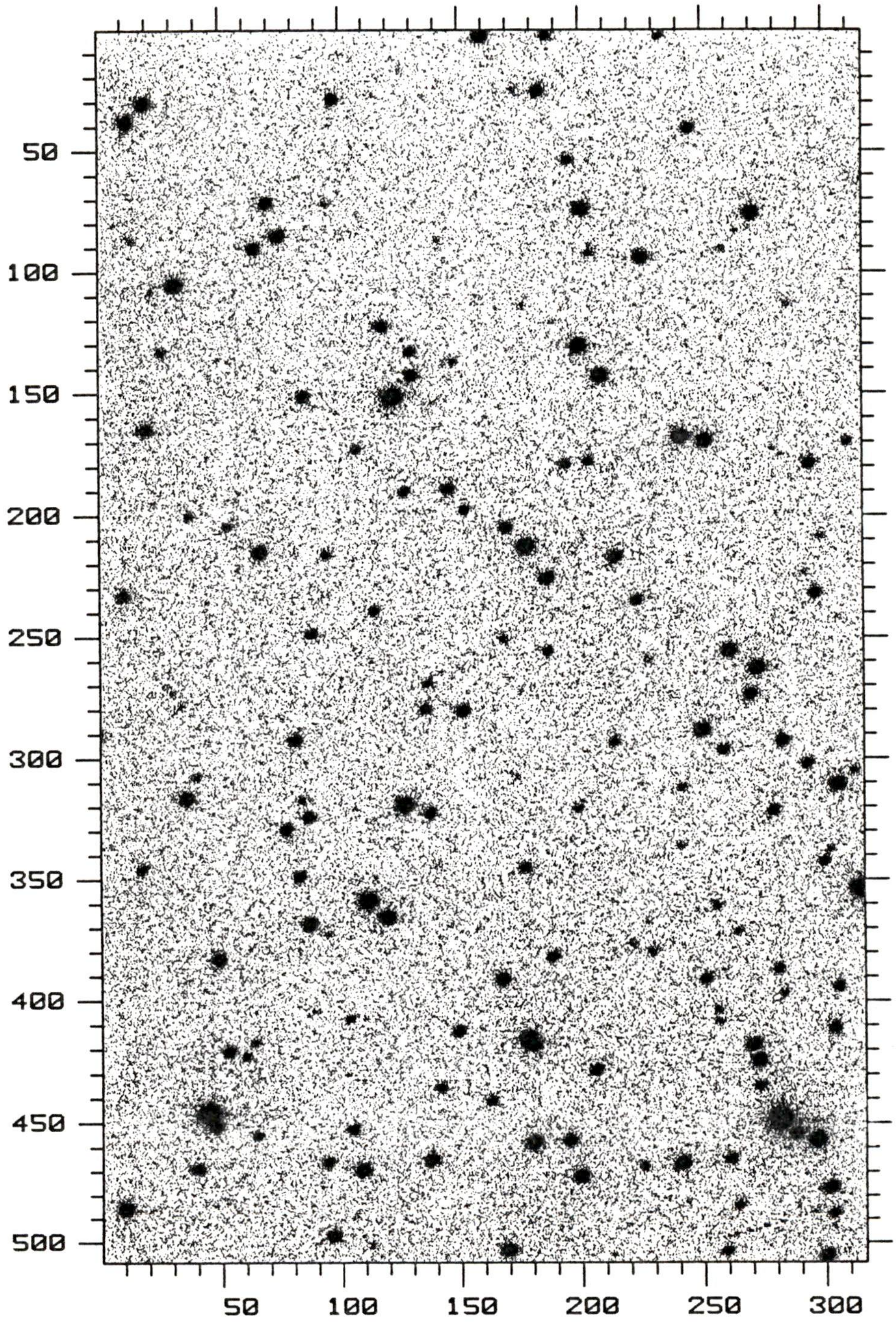

Fig. B.8. Region SE of NGC 188, centered 91" S and 268" E of the cluster center. The coordinates can be related to those of the reference frame by a shift of: $x(\mathrm{NE}) - x(\mathrm{SE}) = -240$, and $y(\mathrm{NE}) - y(\mathrm{SE}) = 11$. Scale: 83"/100 units.

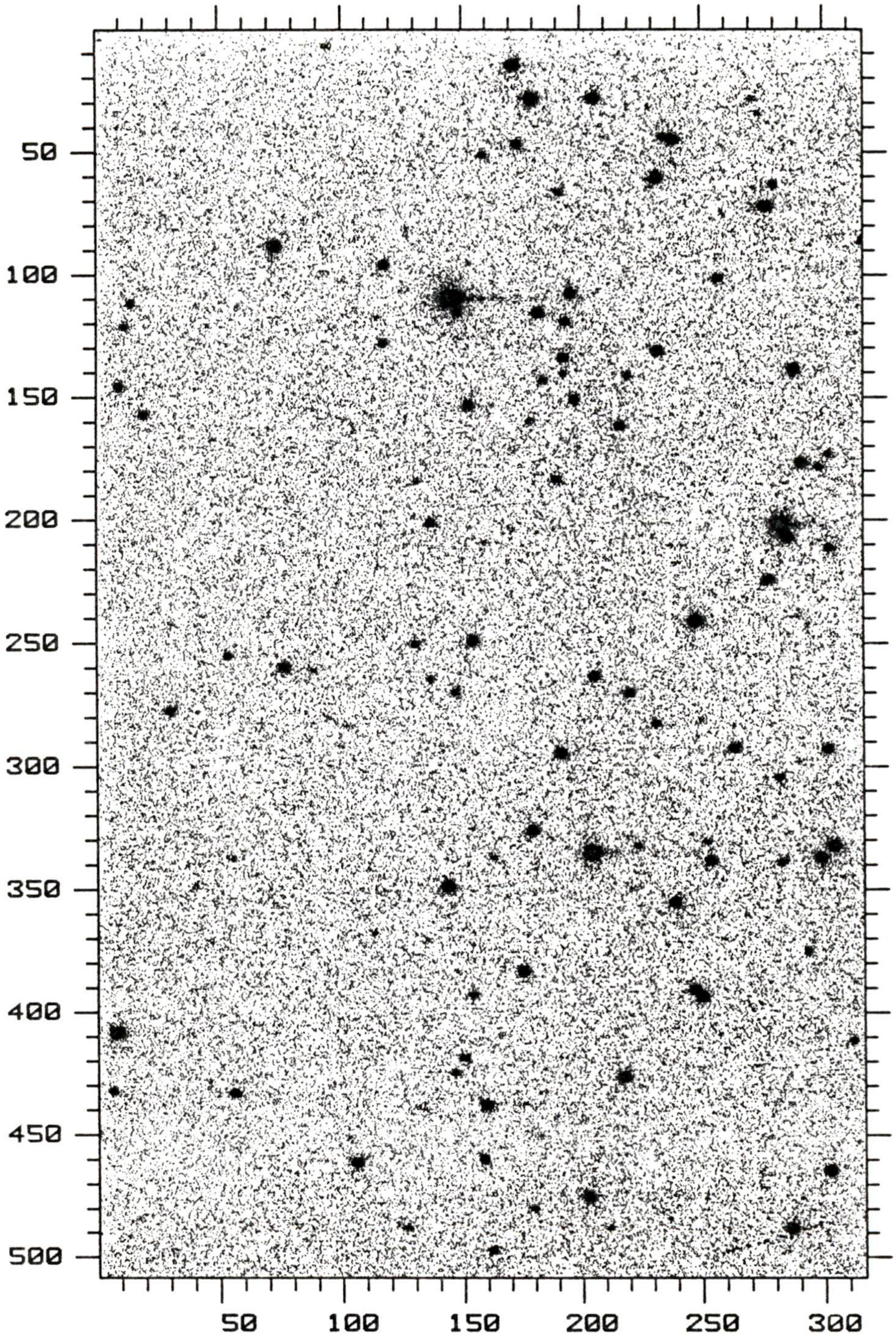

Fig. B.9. Region SS of NGC 188, centered 298" S and 61" E of the cluster center. The coordinates can be related to those of the reference frame by a shift of: $x(\mathrm{NE}) - x(\mathrm{SS}) = -478$, and $y(\mathrm{NE}) - y(\mathrm{SS}) = 251$. Scale: 83"/100 units.

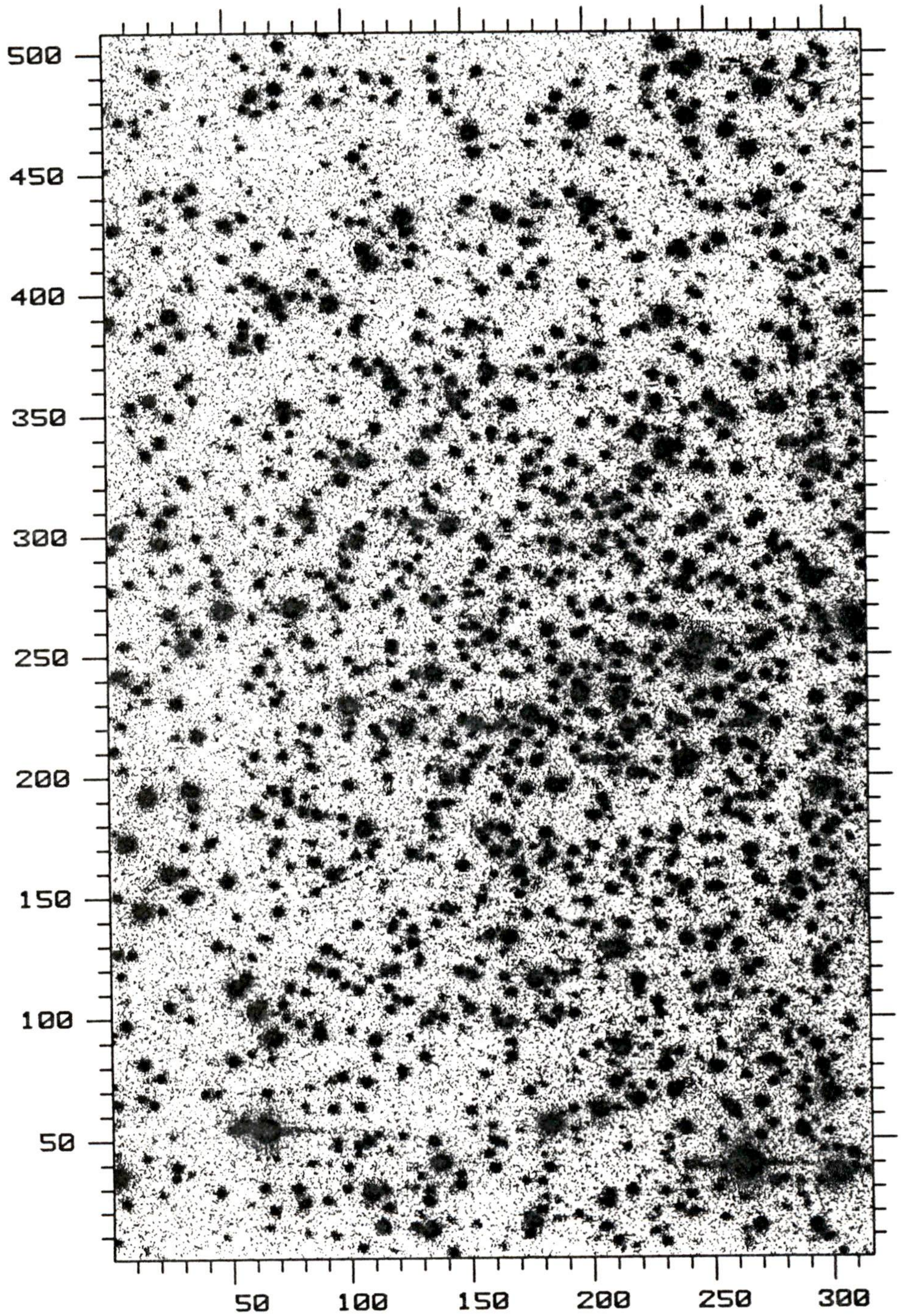

Fig. B.10. Single region of NGC 6791, centered 4" W and 73" S of the cluster center. The center is at the position (240, 250). Scale: 83"/100 units.

Appendix C

Photometry Tables

The following photometry tables list: the identification number of the star, the x and y coordinates (with respect to the chosen frame of reference, indicated in appendix B), the V magnitude and its sigma, the B-V colour and its sigma.

Table C.1. Photometry for NGC 2204

ID	x	y	V	σ_V	B-V	σ_{B-V}
1	322.49	172.85	13.047	0.007	1.038	0.014
2	562.18	394.02	13.161	0.008	0.529	0.016
3	166.81	235.22	13.518	0.008	0.046	0.014
4	328.11	249.53	13.634	0.010	1.131	0.016
5	-10.86	88.98	13.672	0.007	1.082	0.014
6	83.55	46.85	13.770	0.012	0.968	0.018
7	454.10	188.83	13.780	0.009	1.017	0.016
8	408.02	235.01	13.864	0.007	0.515	0.014
9	237.15	134.59	13.866	0.008	0.974	0.015
10	-62.80	-208.68	13.881	0.010	0.946	0.019
11	180.67	162.87	13.887	0.007	0.544	0.014
12	215.57	6.30	13.897	0.012	1.010	0.018
13	255.76	18.08	14.084	0.013	1.039	0.020
14	45.97	118.28	14.191	0.014	0.039	0.021
15	331.06	243.17	14.361	0.008	0.538	0.016
16	25.45	114.95	14.401	0.014	0.621	0.020
17	35.20	206.22	14.767	0.015	0.638	0.021
18	553,49	99.35	14.850	0.010	0.473	0.017
19	195.45	344.27	14.866	0.008	0.114	0.015
20	399.15	254.89	14.887	0.008	0.499	0.015
21	131.31	-202.37	14.898	0.016	0.378	0.022
22	323.50	397.17	14.981	0.009	0.545	0.016
23	155.54	496.55	14.989	0.011	0.581	0.017
24	152.49	-149.69	15.027	0.012	0.362	0.018
25	517.42	374.77	15.044	0.013	0.584	0.021
26	28.47	187.90	15.081	0.019	0.504	0.025
27	413.19	334.59	15.172	0.008	0.524	0.015
28	10.94	26.19	15.284	0.014	0.415	0.021
29	13.68	13.77	15.321	0.013	0.449	0.021
30	190.55	488.53	15.335	0.010	0.458	0.017
31	558.15	308.98	15.339	0.009	0.450	0.017
32	257.01	281.59	15.443	0.009	0.422	0.017
33	31.48	81.15	15.444	0.014	0.246	0.021
34	102.01	-172.31	15.445	0.011	0.658	0.018
35	554.89	14.38	15.471	0.014	0.501	0.022
36	109.52	335.06	15.475	0.015	0.470	0.022
37	190.81	303.56	15.485	0.009	0.431	0.017

Table C.1. (cont.)

ID	x	y	V	σ_V	B-V	σ_{B-V}
38	504.94	106.01	15.494	0.013	0.730	0.019
39	-2.12	-38.22	15.528	0.008	0.457	0.016
40	85.30	75.00	15.546	0.010	0.393	0.017
41	177.54	-143.09	15.549	0.010	0.367	0.018
42	94.73	-235.82	15.560	0.013	0.399	0.021
43	96.16	441.65	15.598	0.019	0.387	0.025
44	-47.33	-23.82	15.600	0.008	0.413	0.015
45	485.66	354.20	15.612	0.012	0.427	0.019
46	-9.15	-87.82	15.624	0.009	0.405	0.018
47	442.57	104.00	15.630	0.011	0.433	0.018
48	457.86	209.69	15.635	0.010	0.412	0.018
49	212.36	292.63	15.638	0.009	0.358	0.017
50	294.20	154.51	15.644	0.009	0.441	0.017
51	375.69	166.15	15.675	0.017	0.430	0.026
52	167.98	-142.09	15.695	0.011	0.385	0.018
53	454.95	195.32	15.720	0.012	0.634	0.020
54	-26.92	-180.64	15.725	0.008	0.642	0.017
55	5.30	352.96	15.741	0.016	0.669	0.023
56	383.23	99.88	15.756	0.008	0.459	0.017
57	412.59	410.27	15.756	0.011	0.444	0.018
58	317.44	141.43	15.776	0.009	0.477	0.016
59	107.44	189.57	15.803	0.011	0.455	0.018
60	-56.43	55.77	15.838	0.009	0.587	0.017
61	490.12	133.49	15.910	0.011	0.405	0.018
62	84.54	58.44	15.913	0.011	0.365	0.020
63	17.56	-48.12	15.919	0.013	0.342	0.022
64	476.42	483.21	15.980	0.025	0.422	0.045
65	217.39	104.72	15.987	0.009	0.384	0.018
66	6.96	250.15	15.996	0.017	0.419	0.024
67	299.61	79.50	15.997	0.013	0.421	0.021
68	180.72	300.94	16.061	0.011	0.380	0.019
69	317.24	492.28	16.063	0.013	0.456	0.020
70	12.02	-35.38	16.075	0.009	0.392	0.017
71	289.93	44.46	16.107	0.010	0.435	0.020
72	277.10	108.44	16.116	0.012	0.486	0.021
73	347.22	377.76	16.137	0.012	0.493	0.020
74	491.74	450.60	16.143	0.013	0.473	0.020

Table C.1. (cont.)

ID	x	y	V	σ_V	B-V	σ_{B-V}
75	253.14	99.67	16.156	0.012	0.419	0.021
76	448.97	389.20	16.194	0.011	0.423	0.019
77	67.11	-223.79	16.243	0.013	0.399	0.021
78	508.36	77.02	16.243	0.015	0.412	0.026
79	470.65	258.34	16.247	0.014	0.412	0.022
80	440.65	483.14	16.247	0.013	0.536	0.023
81	480.03	294.63	16.264	0.013	0.436	0.020
82	60.91	-276.06	16.267	0.013	0.643	0.020
83	95.02	203.20	16.274	0.011	0.443	0.020
84	167.16	150.23	16.278	0.013	0.456	0.022
85	257.83	261.09	16.280	0.013	0.718	0.022
86	434.64	293.19	16.282	0.012	0.490	0.021
87	121.91	330.44	16.299	0.012	0.458	0.021
88	120.69	-65.74	16.301	0.018	0.449	0.029
89	245.48	99.23	16.319	0.010	0.734	0.020
90	173.52	221.50	16.330	0.013	0.444	0.020
91	77.05	83.06	16.341	0.012	0.581	0.020
92	495.45	119.03	16.379	0.015	0.830	0.023
93	118.98	-63.54	16.391	0.019	0.494	0.032
94	37.90	179.00	16.406	0.016	0.452	0.024
95	542.48	241.80	16.408	0.013	0.448	0.022
96	248.15	310.27	16.413	0.011	0.431	0.019
97	262.46	78.47	16.454	0.012	0.444	0.022
98	384.88	443.32	16.464	0.014	0.461	0.023
99	133.64	-104.60	16.473	0.011	0.420	0.020
100	52.93	-201.86	16.512	0.012	0.446	0.020
101	-53.10	-276.02	16.558	0.015	0.408	0.024
102	134.09	-58.56	16.565	0.012	0.463	0.020
103	409.57	245.94	16.610	0.014	0.533	0.025
104	108.97	-205.39	16.637	0.013	0.444	0.022
105	74.55	166.64	16.651	0.015	0.497	0.024
106	507.84	429.37	16.656	0.018	0.688	0.027
107	317.02	66.35	16.668	0.094	1.084	0.136
108	96.43	146.26	16.674	0.021	0.417	0.031
109	17.36	-11.30	16.679	0.013	0.486	0.024
110	-105.67	-270.37	16.698	0.014	0.514	0.027
111	485.55	269.73	16.744	0.013	0.802	0.024

Table C.1. (cont.)

ID	x	y	V	σ_V	B-V	σ_{B-V}
112	507.96	34.72	16.746	0.015	0.472	0.025
113	357.73	477.95	16.787	0.014	0.604	0.029
114	170.12	355.50	16.793	0.020	0.440	0.029
115	227.09	282.49	16.832	0.015	0.501	0.027
116	374.62	425.08	16.850	0.018	0.519	0.041
117	36.83	-188.92	16.853	0.016	0.460	0.026
118	243.94	220.60	16.873	0.014	0.455	0.026
119	324.03	110.01	16.876	0.014	0.532	0.025
120	191.07	399.64	16.885	0.013	0.789	0.030
121	243.63	123.72	16.922	0.016	0.499	0.026
122	214.86	119.78	16.929	0.014	0.485	0.027
123	433.92	51.67	16.949	0.017	0.511	0.027
124	17.34	-72.24	16.969	0.014	0.485	0.024
125	150.94	289.42	16.976	0.015	0.536	0.027
126	426.44	351.60	16.984	0.019	0.665	0.032
127	227.50	177.15	16.990	0.016	0.579	0.028
128	154.02	381.58	17.039	0.016	0.533	0.029
129	118.42	266.55	17.040	0.020	0.549	0.032
130	42.74	437.42	17.045	0.031	0.527	0.044
131	19.33	-231.62	17.058	0.015	0.535	0.026
132	417.49	429.26	17.095	0.019	0.538	0.032
133	171.97	-62.56	17.109	0.015	0.539	0.027
134	553.91	105.86	17.113	0.033	0.668	0.048
135	-10.43	-55.83	17.152	0.017	0.505	0.029
136	-48.34	-241.70	17.161	0.015	0.769	0.027
137	83.54	-90.96	17.173	0.013	0.494	0.028
138	144.03	61.17	17.191	0.014	0.619	0.030
139	103.62	361.15	17.200	0.019	0.548	0.033
140	384.80	185.50	17.205	0.017	0.832	0.032
141	222.64	444.82	17.249	0.016	0.563	0.032
142	221.61	170.33	17.253	0.016	0.676	0.028
143	114.41	-222.92	17.300	0.021	0.488	0.033
144	-87.46	-137.47	17.333	0.018	0.527	0.032
145	-64.72	123.54	17.359	0.023	0.588	0.039
146	178.09	107.36	17.364	0.019	0.583	0.034
147	324.29	439.04	17.393	0.026	0.694	0.044
148	113.10	-188.81	17.400	0.016	0.489	0.028

Table C.1. (cont.)

ID	x	y	V	σ_V	B-V	σ_{B-V}
149	303.55	512.49	17.433	0.027	0.841	0.042
150	-10.73	19.96	17.503	0.018	0.556	0.030
151	130.68	-193.83	17.518	0.026	0.513	0.040
152	410.77	347.02	17.519	0.023	0.666	0.040
153	199.48	159.34	17.541	0.022	0.507	0.044
154	151.95	-47.18	17.561	0.018	0.560	0.035
155	391.96	191.01	17.564	0.019	0.682	0.034
156	377.59	219.32	17.567	0.026	0.633	0.044
157	86.06	-159.68	17.577	0.026	0.688	0.047
158	22.76	-105.17	17.621	0.021	0.509	0.034
159	279.28	123.89	17.631	0.028	0.654	0.048
160	-75.22	-243.99	17.647	0.021	0.567	0.044
161	414.50	383.76	17.693	0.029	0.735	0.048
162	515.20	249.83	17.697	0.024	0.615	0.041
163	73.18	9.83	17.768	0.026	0.544	0.045
164	171.28	45.29	17.799	0.030	0.557	0.051
165	-19.90	-266.61	17.804	0.026	0.549	0.042
166	203.49	417.85	17.827	0.027	0.759	0.048
167	533.95	225.63	17.828	0.031	0.549	0.046
168	268.23	75.99	17.832	0.042	0.759	0.068
169	157.19	397.17	17.882	0.021	0.599	0.047
170	183.66	-139.97	17.913	0.033	0.703	0.052
171	372.70	135.86	17.922	0.034	0.703	0.065
172	247.58	102.84	17.930	0.029	1.167	0.067
173	492.37	459.49	17.938	0.027	0.654	0.051
174	134.09	-76.40	17.960	0.027	0.553	0.056
175	-81.04	107.38	17.972	0.023	0.621	0.047
176	374.43	422.78	17.990	0.091	0.874	0.163
177	-51.22	-65.55	18.008	0.028	0.655	0.046
178	122.59	318.69	18.050	0.032	0.636	0.055
179	-65.11	-220.06	18.069	0.028	0.556	0.050
180	130.41	503.87	18.074	0.034	0.844	0.067
181	158.80	-100.47	18.088	0.044	0.618	0.083
182	-62.75	-32.25	18.112	0.038	0.603	0.062
183	57.55	-17.06	18.138	0.039	0.617	0.062
184	519.44	47.94	18.162	0.047	1.067	0.097
185	147.55	-286.82	18.180	0.036	1.277	0.075

Table C.1. (cont.)

ID	x	y	V	σ_V	B-V	σ_{B-V}
186	67.71	-37.99	18.181	0.033	0.720	0.059
187	239.04	354.67	18.215	0.050	0.688	0.083
188	146.53	47.72	18.251	0.039	0.672	0.068
189	132.85	-187.63	18.263	0.041	0.684	0.065
190	60.92	22.56	18.267	0.036	0.714	0.065
191	474.84	484.52	18.280	0.199	0.867	0.446
192	12.78	-31.10	18.295	0.036	0.748	0.071
193	424.96	129.97	18.305	0.048	1.166	0.093
194	19.44	174.17	18.329	0.044	0.788	0.079
195	394.53	175.40	18.358	0.045	0.969	0.087
196	-25.76	-177.17	18.392	0.049	0.850	0.085
197	200.99	504.28	18.401	0.044	0.584	0.071
198	-8.47	113.46	18.422	0.033	0.761	0.066
199	72.35	434.73	18.424	0.037	0.699	0.071
200	183.91	-71.25	18.437	0.044	1.564	0.098
201	145.88	372.26	18.453	0.046	0.725	0.082
202	129.70	-32.78	18.501	0.040	0.660	0.068
203	247.88	247.74	18.577	0.050	0.690	0.099
204	163.76	37.65	18.594	0.056	0.504	0.098
205	36.43	128.63	18.596	0.048	0.618	0.086
206	-65.38	-299.05	18.608	0.056	1.268	0.115
207	456.81	348.89	18.615	0.074	0.725	0.139
208	251.23	497.14	18.658	0.072	0.583	0.117
209	308.93	241.95	18.675	0.062	0.750	0.113
210	83.38	404.85	18.680	0.058	0.689	0.120
211	9.37	477.44	18.683	0.065	0.884	0.133
212	198.82	21.20	18.728	0.043	0.776	0.091
213	-9.40	54.39	18.744	0.037	0.464	0.065
214	528.48	458.02	18.750	0.064	0.774	0.124
215	426.48	261.63	18.777	0.071	0.754	0.128
216	46.55	-107.18	18.782	0.055	0.574	0.098
217	323.19	472.95	18.800	0.076	0.943	0.122
218	445.12	301.94	18.848	0.081	1.052	0.146
219	219.42	262.26	18.858	0.062	0.720	0.114
220	242.16	356.96	18.889	0.084	0.549	0.138
221	426.02	221.80	18.895	0.074	0.975	0.153
222	180.38	185.56	18.901	0.068	0.774	0.131

Table C.1. (cont.)

ID	x	y	V	σ_V	B-V	σ_{B-V}
223	399.32	460.03	18.917	0.094	0.679	0.139
224	487.46	225.32	18.923	0.090	0.813	0.137
225	195.92	175.72	18.978	0.055	1.284	0.187
226	214.97	217.38	18.979	0.079	0.517	0.132
227	152.03	136.45	18.986	0.094	0.886	0.163
228	107.09	302.56	18.989	0.086	0.818	0.146
229	257.70	386.85	18.989	0.092	0.806	0.171
230	158.92	87.96	18.992	0.073	0.700	0.130
231	-57.61	-10.56	18.996	0.042	0.546	0.093
232	554.27	409.79	19.042	0.086	0.810	0.147
233	296.55	438.73	19.064	0.102	0.761	0.177
234	283.76	237.93	19,065	0.093	0.781	0.163
235	171.43	503.56	19.068	0.087	0.798	0.178
236	62.44	58.47	19.121	0.066	0.811	0.136
237	-48.88	-105.86	19.197	0.080	0.618	0.121
238	55.24	-144.36	19.203	0.082	1.061	0.141
239	461.41	300.30	19.218	0.096	0.860	0.166
240	25.27	256.67	19.230	0.086	1.214	0.210
241	52.14	225.24	19.241	0.090	0.884	0.167
242	494.56	507.16	19.251	0.102	0.981	0.191
243	477.93	508.59	19.253	0.104	0.740	0.197
244	429.93	32.36	19.260	0.103	0.392	0.174
245	163.74	40.97	19.267	0.100	0.558	0.174
246	147.44	124.67	19.335	0.255	1.045	0.368
247	196.18	28.91	19.336	0.083	1.108	0.214
248	454.30	219.09	19.354	0.131	0.337	0.193
249	50.63	-255.88	19.392	0.097	1.420	0.183
250	255.26	228.71	19.424	0.095	1.141	0.238
251	-105.64	-6.40	19.458	0.132	0.611	0.185
252	343.95	161.97	19.469	0.096	0.950	0.273
253	10.56	332.37	19.492	0.145	0.902	0.269
254	123.94	115.94	19.494	0.115	0.741	0.209
255	-40.05	-115.85	19.505	0.103	0.693	0.179
256	329.78	400.69	19.520	0.115	0.424	0.193
257	38.32	479.11	19.535	0.090	0.712	0.215
258	319.32	242.63	19.557	0.130	0.944	0.263
259	289.64	164.31	19.560	0.127	0.859	0.254

Table C.1. (end)

ID	x	y	V	σ_V	B-V	σ_{B-V}
260	44.04	-84.34	19.568	0.118	0.857	0.191
261	414.87	281.16	19.591	0.161	0.784	0.259
262	556.01	481.11	19.626	0.153	1.211	0.301
263	6.43	-284.15	19.650	0.116	0.905	0.208
264	169.52	30.90	19.706	0.138	1.232	0.318
265	-57.33	-63.48	19.725	0.121	0.673	0.192
266	131.12	341.88	19.740	0.145	1.396	0.388
267	395.75	133.18	19.740	0.132	0.969	0.274
268	330.60	338.66	19.778	0.122	0.746	0.268
269	417.73	104.93	19.824	0.147	1.378	0.446
270	431.61	457.70	19.849	0.181	1.038	0.402
271	75.08	228.27	19.875	0.215	0.731	0.328
272	66.21	144.08	19.879	0.155	1.168	0.343
273	553.52	387.40	19.885	0.249	0.647	0.369
274	190.88	9.11	19.917	0.180	0.685	0.271
275	259.84	48.68	19.997	0.193	1.073	0.428
276	264.36	491.69	20.059	0.238	0.843	0.396
277	432.05	316.42	20.100	0.127	1.185	0.481
278	419.37	230.36	20.462	0.283	0.619	0.464
279	50.92	107.32	21.796	0.628	-1.434	0.777

Table C.2. Photometry for Mel 66

ID	x	y	V	σ_V	B-V	σ_{B-V}
1	138.35	442.41	14.099	0.015	1.236	0.028
2	212.27	499.46	14.314	0.018	0.499	0.029
3	252.94	421.46	14.436	0.019	1.074	0.032
4	239.46	446.11	14.451	0.017	1.036	0.032
5	190.23	54.22	14.463	0.016	0.638	0.029
6	117.57	140.88	14.498	0.020	1.064	0.031
7	106.04	325.53	14.653	0.022	1.075	0.032
8	285.26	257.70	14.677	0.021	1.099	0.035
9	94.73	87.35	14.912	0.016	0.958	0.027
10	58.52	68.73	15.086	0.016	0.706	0.030
11	236.35	216.42	15.111	0.014	1.078	0.026
12	15.32	289.75	15.228	0.018	1.086	0.030
13	11.23	123.48	15.301	0.016	0.640	0.027
14	248.98	7.31	15.443	0.018	0.740	0.034
15	176.23	364.77	15.472	0.019	0.630	0.029
16	204.62	209.86	15.480	0.017	0.214	0.029
17	260.53	119.45	15.520	0.015	1.021	0.026
18	198.02	306.78	15.543	0.020	1.036	0.031
19	42.06	360.14	15.551	0.019	0.389	0.030
20	215.10	190.51	15.717	0.018	0.776	0.028
21	201.77	21.88	15.788	0.020	0.906	0.034
22	258.75	229.47	15.792	0.020	0.812	0.098
23	177.10	492.65	15.888	0.021	0.994	0.030
24	188.62	157.57	15.913	0.016	0.980	0.031
25	67.80	426.68	15.972	0.025	0.980	0.043
26	156.96	465.48	16.062	0.019	0.590	0.031
27	248.96	65.30	16.071	0.018	0.977	0.031
28	131.68	274.54	16.100	0.016	0.253	0.029
29	259.85	283.54	16.101	0.018	0.555	0.032
30	240.85	19.79	16.102	0.034	1.000	0.047
31	73.24	256.43	16.172	0.016	0.497	0.026
32	134.63	260.33	16.248	0.014	0.875	0.027
33	214.73	297.14	16.250	0.017	0.538	0.032
34	175.76	152.21	16.269	0.016	0.505	0.027
35	267.74	120.66	16.355	0.027	0.584	0.053
36	243.21	294.61	16.374	0.018	0.558	0.029
37	280.49	335.47	16.374	0.016	0.576	0.028

Table C.2. (cont.)

ID	x	y	V	σ_V	B-V	σ_{B-V}
38	268.78	374.84	16.384	0.022	0.314	0.036
39	234.98	429.59	16.391	0.021	0.990	0.034
40	106.37	409.88	16.407	0.018	0.794	0.029
41	102.24	414.07	16.413	0.017	0.582	0.030
42	200.85	405.24	16.425	0.017	0.569	0.029
43	238.26	34.65	16.428	0.018	0.659	0.032
44	164.56	414.51	16.443	0.016	0.608	0.028
45	277.52	434.52	16.498	0.017	0.601	0.031
46	59.67	315.46	16.516	0.017	0.591	0.029
47	163.01	53.07	16.544	0.019	0.654	0.032
48	107.87	477.33	16.545	0.016	0.621	0.029
49	292.18	171.09	16.563	0.019	0.630	0.031
50	181.47	159.24	16.584	0.018	0.695	0.030
51	216.65	167.89	16.598	0.021	0.575	0.034
52	289.82	308.23	16.610	0.022	0.613	0.036
53	129.04	241.81	16.617	0.021	0.616	0.032
54	102.80	250.73	16.634	0.018	0.582	0.030
55	209.26	490.42	16.663	0.018	0.598	0.027
56	85.59	179.64	16.692	0.016	0.539	0.027
57	4.83	68.00	16.700	0.019	0.816	0.034
58	60.35	73.46	16.707	0.017	0.571	0.029
59	54.44	18.03	16.722	0.018	0.597	0.037
60	199.86	340.55	16.772	0.020	0.378	0.033
61	145.68	232.60	16.786	0.016	0.616	0.030
62	193.51	13.21	16.803	0.016	0.814	0.036
63	241.34	291.30	16.817	0.018	0.539	0.032
64	98.07	372.71	16.875	0.018	0.600	0.033
65	66.61	274.39	16.889	0.016	0.624	0.028
66	49.26	192.12	16.894	0.020	0.579	0.031
67	61.19	55.06	16.905	0.020	0.584	0.032
68	177.13	303.86	16.921	0.019	0.610	0.030
69	243.00	375.53	16.931	0.019	0.573	0.031
70	77.44	224.21	16.996	0.015	0.582	0.026
71	257.53	458.59	16.998	0.019	0.615	0.033
72	96.48	198.38	17.010	0.015	0.567	0.025
73	223.98	318.47	17.032	0.018	0.565	0.033
74	157.55	412.11	17.046	0.015	0.615	0.027

Table C.2. (cont.)

ID	x	y	V	σ_V	B-V	σ_{B-V}
75	68.15	218.19	17.053	0.016	1.362	0.027
76	15.91	292.43	17.064	0.032	0.644	0.044
77	239.19	134.54	17.075	0.024	0.583	0.036
78	23.25	229.40	17.098	0.018	0.602	0.027
79	24.52	332.46	17.147	0.016	0.613	0.026
80	217.50	341.68	17.157	0.018	0.581	0.031
81	293.97	292.30	17.164	0.019	0.611	0.033
82	49.41	436.10	17.179	0.018	0.597	0.030
83	75.65	133.66	17.186	0.019	0.566	0.030
84	226.79	341.88	17.195	0.019	0.595	0.034
85	209.96	16.15	17.201	0.019	0.578	0.036
86	107.18	268.12	17.223	0.017	0.569	0.032
87	259.90	98.93	17.228	0.019	0.601	0.031
88	129.15	447.96	17.231	0.021	0.606	0.030
89	150.95	431.79	17.247	0.020	0.583	0.032
90	283.11	202.32	17.293	0.017	0.573	0.029
91	166.51	344.94	17.298	0.022	0.606	0.034
92	31.95	405.61	17.300	0.020	0.643	0.033
93	141.05	403.35	17.307	0.021	0.613	0.031
94	268.22	116.93	17.315	0.029	1.129	0.057
95	201.12	454.38	17.331	0.023	0.580	0.034
96	200.31	328.57	17.339	0.018	0.598	0.027
97	122.89	437.36	17.344	0.017	0.617	0.030
98	243.82	75.38	17.348	0.017	0.585	0.030
99	255.87	245.21	17.350	0.105	0.584	0.120
100	249.15	224.39	17.350	0.017	0.563	0.032
101	134.58	239.58	17.354	0.016	0.595	0.032
102	128.32	393.38	17.359	0.018	0.918	0.029
103	132.52	244.40	17.366	0.016	0.586	0.030
104	150.32	154.26	17.400	0.019	0.559	0.028
105	63.21	261.85	17.411	0.021	0.585	0.034
106	91.74	402.31	17.413	0.016	0.622	0.029
107	153.42	490.60	17.418	0.016	0.580	0.027
108	206.17	283.90	17.425	0.020	0.570	0.032
109	183.55	159.19	17.444	0.024	0.981	0.038
110	200.15	220.58	17.444	0.020	0.586	0.032
111	140.57	449.08	17.455	0.020	0.583	0.034

Table C.2. (cont.)

ID	x	y	V	σ_V	B-V	σ_{B-V}
112	147.36	489.71	17.464	0.021	0.621	0.033
113	96.92	165.86	17.473	0.022	0.556	0.037
114	241.68	100.91	17.497	0.018	0.647	0.034
115	142.18	187.27	17.497	0.020	0.619	0.031
116	72.75	245.56	17.502	0.021	0.579	0.034
117	275.78	241.13	17.506	0.021	0.572	0.038
118	209.03	265.21	17.509	0.017	0.553	0.033
119	62.26	246.70	17.523	0.020	0.631	0.032
120	91.30	356.21	17.530	0.019	0.595	0.034
121	217.76	19.55	17.533	0.018	0.582	0.037
122	267.49	246.79	17.539	0.019	0.552	0.032
123	80.35	212.92	17.540	0.018	0.567	0.028
124	226.35	386.57	17.554	0.022	0.629	0.032
125	83.97	169.07	17.558	0.021	0.561	0.032
126	184.26	241.94	17.565	0.021	0.574	0.038
127	110.76	303.59	17.570	0.029	0.622	0.039
128	177.72	436.95	17.574	0.021	0.575	0.036
129	126.81	386.90	17.595	0.021	0.584	0.034
130	272.26	8.80	17.613	0.021	0.587	0.036
131	95.29	251.00	17.621	0.020	0.576	0.031
132	61.16	42.35	17.649	0.019	0.579	0.036
133	5.99	142.38	17.654	0.019	0.560	0.034
134	64.27	320.96	17.682	0.023	0.591	0.035
135	172.46	348.25	17.682	0.018	0.662	0.033
136	142.49	84.10	17.684	0.020	0.754	0.036
137	198.12	299.92	17.707	0.024	0.593	0.038
138	36.24	183.43	17.741	0.025	0.576	0.038
139	38.40	4.02	17.758	0.021	0.780	0.037
140	77.68	172.89	17.769	0.021	0.597	0.032
141	200.63	158.44	17.776	0.018	0.661	0.033
142	126.38	177.18	17.790	0.020	0.595	0.038
143	89.76	214.70	17.808	0.022	0.741	0.037
144	35.43	87.15	17.810	0.016	0.613	0.032
145	98.19	128.00	17.831	0.022	1.304	0.033
146	263.48	323.37	17.846	0.021	0.659	0.075
147	175.56	483.03	17.861	0.022	0.600	0.035
148	210.66	474.39	17.870	0.021	0.588	0.037

Table C.2. (cont.)

ID	x	y	V	σ_V	B-V	σ_{B-V}
149	263.11	505.14	17.876	0.259	0.613	0.296
150	207.01	306.42	17.890	0.019	0.615	0.034
151	291.22	310.41	17.890	0.031	0.700	0.051
152	286.48	491.61	17.894	0.025	0.595	0.037
153	152.08	206.76	17.948	0.023	0.607	0.034
154	10.21	277.95	17.958	0.021	1.040	0.034
155	137.38	37.75	17.971	0.022	0.684	0.041
156	162.99	376.69	17.980	0.024	0.576	0.038
157	204.72	428.15	17.996	0.026	0.598	0.046
158	97.14	288.58	18.024	0.022	0.769	0.040
159	171.57	170.87	18.034	0.021	0.587	0.037
160	157.28	356.62	18.037	0.020	0.598	0.032
161	218.65	420.37	18.074	0.019	0.634	0.035
162	140.30	235.25	18.081	0.018	1.081	0.036
163	95.00	449.10	18.083	0.021	0.636	0.046
164	89.01	239.43	18.103	0.019	0.648	0.036
165	175.74	341.31	18.119	0.019	0.619	0.039
166	182.84	185.83	18.123	0.025	0.697	0.038
167	143.43	236.45	18.133	0.019	0.667	0.036
168	195.37	334.61	18.137	0.020	0.627	0.035
169	82.19	159.85	18.139	0.024	0.685	0.036
170	226.63	145.32	18.144	0.020	0.619	0.032
171	163.69	374.17	18.144	0.024	0.616	0.040
172	200.07	163.46	18.159	0.029	0.622	0.071
173	213.74	447.78	18.168	0.021	0.725	0.043
174	40.33	91.23	18.177	0.019	0.713	0.038
175	249.07	161.15	18.196	0.022	0.622	0.036
176	183.34	192.80	18.203	0.022	0.671	0.042
177	56.05	139.94	18.247	0.027	0.792	0.047
178	242.63	433.12	18.276	0.020	0.737	0.036
179	264.92	66.00	18.291	0.023	0.632	0.038
180	10.34	422.40	18.297	0.026	0.660	0.041
181	10.69	238.67	18.312	0.021	0.665	0.042
182	131.12	406.06	18.337	0.033	0.644	0.048
183	295.57	151.24	18.354	0.020	0.643	0.037
184	133.90	489.53	18.377	0.026	0.635	0.040
185	52.95	307.43	18.380	0.021	0.703	0.067

Table C.2. (cont.)

ID	x	y	V	σ_V	B-V	σ_{B-V}
186	19.48	499.18	18.380	0.020	0.726	0.032
187	56.07	294.29	18.388	0.027	0.671	0.043
188	57.85	481.90	18.394	0.029	0.766	0.050
189	284.77	387.11	18.403	0.023	0.651	0.045
190	75.51	117.69	18.410	0.033	1.007	0.111
191	278.90	52.44	18.425	0.019	0.631	0.038
192	279.82	296.13	18.425	0.021	0.673	0.038
193	88.58	44.01	18.439	0.023	0.672	0.047
194	31.34	298.80	18.443	0.026	0.663	0.041
195	75.99	118.29	18.445	0.108	1.101	0.220
196	54.26	207.15	18.461	0.029	0.685	0.052
197	159.36	215.83	18.464	0.025	0.646	0.047
198	43.68	233.00	18.466	0.021	0.773	0.036
199	294.43	27.89	18.472	0.243	0.955	0.294
200	295.10	28.50	18.473	0.024	0.920	0.047
201	245.52	266.32	18.493	0.025	0.642	0.040
202	109.75	75.11	18.494	0.022	1.088	0.043
203	65.65	181.47	18.499	0.022	0.718	0.054
204	251.13	124.24	18.499	0.021	0.674	0.037
205	231.07	17.28	18.515	0.024	0.678	0.044
206	249.18	293.95	18.526	0.026	0.649	0.045
207	160.51	28.95	18.532	0.025	0.807	0.053
208	193.67	36.35	18.550	0.025	0.807	0.043
209	112.27	376.98	18.559	0.027	0.711	0.043
210	193.16	428.55	18.565	0.023	0.787	0.041
211	47.28	66.13	18.566	0.024	0.709	0.049
212	11.28	479.86	18.568	0.034	0.896	0.050
213	202.80	68.02	18.568	0.022	0.801	0.055
214	190.65	413.42	18.578	0.024	0.666	0.048
215	62.46	164.73	18.586	0.024	0.779	0.043
216	155.14	218.43	18.589	0.022	0.682	0.036
217	181.18	279.45	18.602	0.026	0.736	0.045
218	161.15	40.14	18.627	0.020	0.762	0.038
219	124.67	158.55	18.633	0.022	0.627	0.042
220	2.69	137.48	18.640	0.022	0.777	0.045
221	113.07	241.74	18.660	0.068	0.869	0.094
222	99.58	260.93	18.664	0.026	0.698	0.047

Table C.2. (cont.)

ID	x	y	V	σ_V	B-V	σ_{B-V}
223	297.77	143.15	18.678	0.022	0.766	0.047
224	50.74	64.46	18.678	0.024	0.661	0.060
225	14.99	168.22	18.688	0.020	0.706	0.038
226	49.09	169.91	18.747	0.027	0.692	0.049
227	65.75	121.36	18.758	0.024	0.689	0.044
228	273.14	7.87	18.785	0.027	0.688	0.078
229	27.00	314.42	18.807	0.024	0.733	0.046
230	78.48	52.35	18.816	0.026	0.731	0.049
231	138.24	286.29	18.830	0.026	0.727	0.049
232	22.22	100.35	18.837	0.037	1.339	0.079
233	114.88	116.45	18.842	0.036	0.866	0.068
234	16.13	38.98	18.844	0.030	0.856	0.068
235	196.80	231.92	18.845	0.027	0.715	0.046
236	193.69	76.76	18.854	0.024	0.928	0.045
237	53.90	152.56	18.860	0.034	1.066	0.064
238	101.29	303.43	18.915	0.031	0.735	0.045
239	34.83	111.60	18.917	0.023	0.605	0.052
240	102.01	18.63	18.919	0.028	0.834	0.054
241	259.61	55.44	18.924	0.030	0.777	0.055
242	239.06	19.09	18.948	0.088	1.305	0.269
243	221.84	309.12	18.950	0.027	0.832	0.054
244	208.45	364.94	18.958	0.022	0.545	0.063
245	83.09	485.64	18.962	0.024	0.812	0.043
246	88.26	245.16	18.966	0.027	0.888	0.049
247	252.68	234.90	18.967	0.031	0.993	0.060
248	159.82	32.01	18.975	0.039	0.777	0.066
249	86.37	387.68	18.985	0.027	0.735	0.061
250	281.51	7.30	18.990	0.039	0.754	0.065
251	272.99	368.39	18.997	0.030	0.768	0.064
252	250.59	449.23	19.000	0.026	0.827	0.055
253	151.27	229.41	19.017	0.024	0.750	0.045
254	143.12	230.37	19.017	0.031	0.760	0.061
255	64.17	222.78	19.019	0.029	0.757	0.062
256	89.22	230.79	19.021	0.026	0.831	0.051
257	228.13	213.16	19.053	0.027	0.727	0.065
258	132.38	264.96	19.079	0.036	0.882	0.057
259	32.64	336.04	19.116	0.028	0.898	0.056

Table C.2. (cont.)

ID	x	y	V	σ_V	B-V	σ_{B-V}
260	191.34	266.34	19.147	0.022	0.750	0.047
261	33.35	214.18	19.152	0.028	0.811	0.052
262	255.70	412.59	19.152	0.056	0.868	0.094
263	279.69	317.53	19.162	0.024	0.881	0.066
264	62.83	382.26	19.215	0.030	0.815	0.052
265	100.23	444.91	19.216	0.033	0.909	0.065
266	175.65	333.15	19.234	0.025	0.771	0.065
267	287.37	157.07	19.235	0.031	0.764	0.061
268	296.24	358.02	19.239	0.038	0.769	0.072
269	213.84	10.38	19.244	0.042	0.821	0.072
270	280.99	307.30	19.255	0.049	0.800	0.086
271	135.85	483.14	19.260	0.032	0.779	0.060
272	26.93	208.81	19.264	0.030	0.807	0.060
273	81.53	57.44	19.274	0.024	0.941	0.050
274	197.99	189.16	19.275	0.031	0.794	0.052
275	173.95	358.51	19.292	0.029	0.791	0.049
276	87.48	502.44	19.294	0.069	0.972	0.116
277	35.53	1.99	19.299	0.036	0.761	0.084
278	105.91	279.82	19.300	0.024	0.783	0.063
279	200.48	164.38	19.322	0.040	0.607	0.113
280	159.04	393.78	19.345	0.037	0.782	0.076
281	290.54	78.02	19.346	0.032	0.799	0.060
282	73.10	381.26	19.367	0.036	0.893	0.068
283	146.56	417.73	19.375	0.034	0.783	0.056
284	147.43	503.68	19.387	0.037	0.789	0.065
285	246.07	278.43	19.391	0.034	1.513	0.104
286	206.33	346.64	19.394	0.043	0.789	0.068
287	69.24	339.88	19.405	0.057	0.817	0.080
288	118.96	447.03	19.419	0.045	0.816	0.070
289	243.70	359.98	19.421	0.036	0.934	0.072
290	169.14	304.04	19.433	0.029	0.838	0.058
291	251.01	103.18	19.452	0.038	0.787	0.072
292	97.72	365.38	19.457	0.041	0.912	0.077
293	228.13	310.37	19.468	0.054	0.822	0.076
294	75.63	200.49	19.473	0.038	0.932	0.087
295	224.02	479.35	19.492	0.043	0.933	0.105
296	217.37	415.75	19.493	0.040	0.844	0.072

Table C.2. (cont.)

ID	x	y	V	σ_V	B-V	σ_{B-V}
297	73.51	430.76	19.539	0.036	0.797	0.058
298	6.82	122.03	19.539	0.043	0.826	0.084
299	235.63	129.10	19.545	0.036	0.812	0.079
300	285.24	428.21	19.567	0.036	0.919	0.079
301	190.40	117.75	19.575	0.039	0.997	0.081
302	174.30	33.15	19.592	0.041	0.868	0.086
303	241.83	503.15	19.619	0.030	0.837	0.097
304	33.68	363.72	19.644	0.046	0.878	0.075
305	197.49	83.27	19.670	0.041	0.846	0.067
306	54.32	12.78	19.678	0.040	0.886	0.066
307	160.16	254.90	19.691	0.058	1.265	0.114
308	233.60	356.57	19.701	0.047	0.861	0.100
309	97.24	378.92	19.709	0.045	1.133	0.096
310	219.01	350.62	19.768	0.170	1.539	0.251
311	282.68	67.85	19.773	0.046	0.887	0.104
312	180.68	402.69	19.774	0.053	0.881	0.095
313	23.38	465.69	19.792	0.063	0.928	0.112
314	121.14	50.71	19.803	0.044	0.859	0.100
315	241.14	191.52	19.846	0.073	0.933	0.104
316	192.91	52.97	19.867	0.277	1.232	0.425
317	298.98	343.23	19.892	0.044	0.995	0.092
318	287.82	74.91	19.895	0.047	1.021	0.094
319	59.90	84.37	19.903	0.036	0.948	0.130
320	134.07	391.43	19.924	0.044	0.909	0.093
321	31.27	170.70	19.926	0.077	0.949	0.141
322	190.85	477.24	19.959	0.067	0.906	0.103
323	257.29	334.63	19.962	0.050	0.881	0.093
324	109.45	97.88	19.975	0.036	1.033	0.106
325	159.46	384.50	19.984	0.064	0.918	0.119
326	115.12	125.64	19.986	0.052	0.771	0.097
327	196.93	242.66	20.008	0.038	1.140	0.151
328	251.99	395.35	20.010	0.046	0.917	0.109
329	249.64	357.54	20.025	0.046	0.934	0.108
330	147.57	186.65	20.031	0.064	1.014	0.124
331	90.61	66.06	20.043	0.059	0.952	0.126
332	277.13	179.81	20.070	0.051	0.989	0.126
333	217.99	304.67	20.078	0.057	0.911	0.117

Table C.2. (cont.)

ID	x	y	V	σ_V	B-V	σ_{B-V}
334	173.52	330.88	20.080	0.045	1.113	0.120
335	219.73	350.62	20.087	0.047	0.945	0.134
336	276.74	66.94	20.094	0.042	0.957	0.140
337	19.78	382.27	20.164	0.050	1.039	0.202
338	214.48	244.73	20.172	0.060	0.977	0.141
339	108.39	431.90	20.187	0.065	0.979	0.162
340	198.34	270.95	20.189	0.063	1.406	0.166
341	146.45	174.37	20.194	0.064	0.926	0.103
342	272.13	166.55	20.196	0.055	0.964	0.130
343	121.15	238.76	20.222	0.058	0.996	0.107
344	217.12	97.18	20.241	0.060	0.980	0.103
345	87.33	206.82	20.245	0.064	1.352	0.162
346	230.98	443.61	20.285	0.083	1.091	0.120
347	136.77	498.60	20.286	0.098	0.829	0.160
348	171.81	440.73	20.294	0.079	1.306	0.174
349	25.75	475.15	20.350	0.058	1.024	0.149
350	150.93	335.61	20.363	0.076	1.022	0.178
351	187.47	166.47	20.367	0.060	0.968	0.147
352	177.11	76.18	20.367	0.138	1.481	0.253
353	9.92	372.20	20.388	0.076	1.632	0.131
354	138.68	368.99	20.397	0.063	1.163	0.128
355	273.90	6.89	20.404	0.168	0.649	0.226
356	282.16	110.68	20.410	0.076	1.019	0.151
357	182.88	482.87	20.426	0.064	1.025	0.139
358	241.43	210.79	20.428	0.066	1.223	0.152
359	20.49	355.42	20.436	0.065	1.005	0.173
360	198.18	396.49	20.447	0.076	1.241	0.193
361	178.05	235.21	20.449	0.073	1.111	0.141
362	74.51	407.24	20.468	0.069	1.047	0.190
363	121.14	58.80	20.473	0.069	0.985	0.167
364	49.19	454.63	20.483	0.065	1.005	0.113
365	224.85	252.17	20.485	0.067	1.371	0.152
366	194.26	49.01	20.485	0.128	1.623	0.255
367	222.32	220.59	20.518	0.095	0.874	0.350
368	55.76	280.96	20.523	0.069	0.976	0.163
369	125.90	128.94	20.531	0.112	1.218	0.266
370	91.05	391.23	20.540	0.060	0.992	0.193

Table C.2. (cont.)

ID	x	y	V	σ_V	B-V	σ_{B-V}
371	232.21	344.71	20.541	0.108	1.085	0.190
372	233.87	277.84	20.548	0.090	1.136	0.161
373	236.73	394.08	20.552	0.058	1.191	0.280
374	237.00	315.72	20.577	0.106	1.515	0.354
375	169.71	10.89	20.595	0.075	1.598	0.275
376	10.22	136.27	20.603	0.132	1.642	0.325
377	39.36	83.33	20.603	0.069	1.306	0.147
378	107.94	300.57	20.616	0.065	0.783	0.363
379	242.63	482.42	20.620	0.100	1.652	0.423
380	249.64	157.57	20.621	0.119	1.041	0.243
381	68.77	272.58	20.634	0.090	1.043	0.231
382	190.79	334.54	20.636	0.078	1.072	0.142
383	183.32	90.83	20.670	0.065	1.069	0.161
384	181.60	385.86	20.673	0.118	0.787	0.189
385	213.99	183.87	20.673	0.076	0.912	0.228
386	115.19	458.36	20.678	0.096	1.001	0.377
387	104.22	390.50	20.722	0.130	1.112	0.213
388	295.94	323.45	20.729	0.048	0.646	0.142
389	196.91	161.84	20.736	0.107	0.689	0.276
390	150.03	410.49	20.770	0.056	1.097	0.250
391	67.82	372.57	20.770	0.068	0.993	0.254
392	139.43	207.97	20.780	0.115	1.083	0.215
393	200.81	165.05	20.787	0.328	0.326	0.393
394	70.69	426.55	20.808	0.288	0.800	0.602
395	248.91	394.10	20.815	0.100	0.950	0.178
396	75.09	343.41	20.875	0.032	1.009	0.070
397	61.70	235.00	20.876	0.104	1.156	0.252
398	18.62	194.35	20.885	0.084	1.169	0.252
399	293.57	115.69	20.888	0.082	0.987	0.225
400	272.59	337.04	20.889	0.154	1.342	0.287
401	245.73	136.98	20.903	0.104	1.419	0.248
402	285.28	346.67	20.905	0.049	0.963	0.083
403	287.29	250.43	20.923	0.257	1.387	0.394
404	20.39	90.42	20.926	0.119	0.958	0.267
405	217.64	115.86	20.935	0.091	1.179	0.226
406	177.68	282.89	20.942	0.191	1.129	0.282
407	50.63	128.31	20.988	0.115	1.571	0.268

Table C.2. (cont.)

ID	x	y	V	σ_V	B-V	σ_{B-V}
408	289.83	385.57	21.008	0.117	1.039	0.223
409	255.44	298.24	21.025	0.105	1.017	0.253
410	244.07	484.77	21.041	0.141	1.623	0.423
411	126.14	269.63	21.044	0.141	1.144	0.284
412	194.82	416.27	21.063	0.089	1.253	0.170
413	53.16	395.30	21.072	0.088	1.038	0.209
414	17.75	396.15	21.087	0.099	0.802	0.191
415	170.16	458.45	21.094	0.193	1.194	0.274
416	20.35	96.51	21.113	0.083	1.195	0.314
417	236.33	168.01	21.116	0.142	1.157	0.312
418	242.01	67.18	21.118	0.122	1.251	0.293
419	262.55	88.82	21.125	0.160	1.241	0.413
420	114.83	459.18	21.127	0.277	0.668	0.609
421	284.18	482.83	21.139	0.122	1.319	0.256
422	272.67	113.67	21.143	0.137	1.080	0.318
423	184.54	275.87	21.149	0.134	1.383	0.331
424	97.90	481.34	21.151	0.165	1.626	0.255
425	257.00	498.68	21.155	0.324	1.418	0.422
426	70.26	145.31	21.171	0.050	1.207	0.084
427	160.56	234.53	21.176	0.065	1.130	0.114
428	117.75	367.48	21.183	0.250	0.938	0.381
429	196.93	129.49	21.204	0.161	1.111	0.371
430	21.20	103.03	21.216	0.043	1.380	0.117
431	191.67	271.70	21.217	0.306	0.594	0.372
432	271.92	349.20	21.222	0.121	1.124	1.520
433	167.22	371.55	21.259	0.143	0.998	0.456
434	246.44	477.36	21.259	0.191	1.346	0.302
435	222.98	369.57	21.261	0.070	1.692	0.141
436	150.32	42.53	21.288	0.048	1.139	0.085
437	287.33	483.44	21.305	0.214	0.958	0.366
438	56.90	61.08	21.349	0.164	0.540	0.310
439	13.22	415.65	21.370	0.140	0.663	0.213
440	137.00	131.45	21.394	0.047	1.264	0.096
441	186.65	278.20	21.402	0.054	1.576	0.127
442	125.82	126.35	21.410	0.218	1.113	0.312
443	292.57	496.53	21.413	0.424	1.005	0.710
444	226.01	168.98	21.418	0.045	1.211	0.100

Table C.2. (cont.)

ID	x	y	V	σ_V	B-V	σ_{B-V}
445	188.50	401.72	21.420	0.048	0.827	0.087
446	273.32	114.22	21.421	0.183	1.030	0.333
447	80.13	149.48	21.430	0.041	1.304	0.106
448	261.47	204.82	21.442	0.103	0.613	0.139
449	93.83	284.83	21.445	0.174	1.327	2.178
450	180.01	230.31	21.470	0.050	1.167	0.065
451	125.44	131.83	21.478	0.138	1.373	0.203
452	197.90	57.73	21.479	0.434	1.959	0.645
453	118.76	203.84	21.480	0.082	0.536	0.125
454	165.39	480.83	21.488	0.046	1.680	0.131
455	289.69	94.03	21.490	0.047	1.452	0.109
456	197.55	90.64	21.490	0.123	1.204	0.364
457	259.19	436.74	21.508	0.057	0.909	0.090
458	91.27	29.92	21.508	0.125	1.618	0.611
459	44.22	383.99	21.514	0.181	1.067	0.349
460	93.73	186.31	21.528	0.189	1.496	0.455
461	238.67	139.83	21.561	0.176	1.204	0.268
462	24.98	478.38	21.567	0.042	1.629	0.136
463	99.08	53.19	21.571	0.058	1.291	0.166
464	145.73	420.69	21.576	0.049	1.533	0.154
465	209.99	36.08	21.600	0.137	0.907	0.251
466	249.54	40.08	21.608	0.130	1.142	0.292
467	241.16	301.33	21.629	0.032	1.518	0.137
468	165.43	76.33	21.634	0.220	1.271	0.325
469	134.37	192.98	21.645	0.238	1.397	0.903
470	35.69	329.59	21.651	0.115	0.788	0.428
471	192.14	143.56	21.671	0.301	1.403	0.473
472	265.15	259.27	21.690	0.530	1.153	0.661
473	106.66	19.23	21.696	0.073	0.533	0.091
474	225.93	188.00	21.716	0.161	1.218	0.261
475	137.59	200.93	21.734	0.197	1.324	0.331
476	152.63	308.20	21.740	0.182	1.464	0.418
477	52.53	256.58	21.743	0.080	1.290	0.126
478	208.76	140.58	21.757	0.039	1.365	0.152
479	284.51	113.40	21.770	0.059	0.693	0.105
480	24.90	195.55	21.812	0.161	1.500	0.490
481	155.40	452.88	21.826	0.274	1.633	0.643

Table C.2. (cont.)

ID	x	y	V	σ_V	B-V	σ_{B-V}
482	219.24	344.20	21.846	0.208	1.252	0.504
483	170.70	391.87	21.850	0.073	1.806	0.225
484	279.16	91.23	21.886	0.076	1.961	0.187
485	151.04	505.66	21.896	0.063	1.556	0.166
486	252.67	494.06	21.910	0.090	1.306	0.161
487	75.11	59.09	21.919	0.064	1.515	0.214
488	84.31	80.36	21.946	0.078	1.776	0.138
489	76.88	481.64	21.947	0.079	1.564	0.188
490	134.54	466.79	21.958	0.082	1.678	0.217
491	227.55	231.33	21.958	0.086	1.160	0.143
492	152.68	214.77	21.968	0.066	1.515	0.159
493	219.76	62.64	21.968	0.230	1.591	0.438
494	199.10	78.60	21.992	0.132	1.375	0.333
495	143.45	340.09	21.995	0.083	1.138	0.131
496	169.14	438.98	22.013	0.069	1.097	0.150
497	165.78	115.66	22.019	0.088	1.406	0.193
498	264.65	458.93	22.030	0.267	1.329	0.703
499	295.28	143.21	22.055	0.108	1.081	0.182
500	298.06	14.88	22.064	0.082	1.513	0.174
501	213.12	78.86	22.087	0.080	1.584	0.215
502	152.41	89.82	22.098	0.070	1.453	0.209
503	223.28	210.88	22.158	0.099	2.103	0.334
504	114.39	244.16	22.159	0.296	1.242	0.453
505	253.56	267.40	22.178	0.246	1.221	0.449
506	296.51	31.25	22.189	0.163	1.119	0.257
507	159.07	182.92	22.198	0.252	1.077	1.659
508	149.46	325.17	22.232	0.104	1.290	0.249
509	117.07	298.95	22.250	0.063	0.811	0.128
510	178.92	49.70	22.258	0.097	0.826	0.139
511	243.52	33.20	22.265	0.376	0.510	0.490
512	46.17	495.94	22.294	0.100	1.485	0.167
513	126.67	234.43	22.309	0.056	1.377	0.200
514	76.40	457.09	22.338	0.103	1.185	0.175
515	221.35	26.28	22.351	0.072	1.474	0.200
516	227.05	37.86	22.358	0.081	1.518	0.394
517	73.98	11.46	22.360	0.092	0.815	0.183
518	35.64	247.56	22.369	0.091	1.221	0.268

Table C.2. (cont.)

ID	x	y	V	σ_V	B-V	σ_{B-V}
519	137.09	493.48	22.369	0.152	1.730	0.283
520	224.00	405.75	22.382	0.349	1.822	0.673
521	143.42	180.81	22.384	0.119	1.857	0.361
522	21.20	142.98	22.398	0.081	2.187	0.524
523	86.63	397.41	22.411	0.123	0.973	0.279
524	297.77	386.82	22.412	0.162	3.005	1.420
525	153.40	33.38	22.444	0.122	1.497	0.243
526	122.55	475.53	22.459	0.092	1.747	0.266
527	225.25	384.39	22.471	0.318	0.738	0.429
528	78.54	355.67	22.489	0.090	0.686	0.141
529	244.76	37.42	22.502	0.138	1.654	0.302
530	40.60	277.34	22.516	0.111	1.747	0.388
531	201.19	394.70	22.530	0.096	2.442	0.497
532	75.36	299.12	22.531	0.114	1.191	0.230
533	95.48	113.01	22.549	0.083	1.286	0.286
534	208.01	229.14	22.550	0.115	1.754	0.286
535	298.61	216.02	22.588	0.103	1.981	0.350
536	256.17	407.09	22.618	0.122	1.385	0.389
537	247.99	196.71	22.642	0.134	0.992	0.237
538	194.17	196.42	22.651	0.128	1.279	0.233
539	38.11	406.53	22.653	0.157	1.218	0.301
540	31.27	422.30	22.661	0.108	1.366	0.220
541	255.95	403.03	22.668	0.130	1.727	0.755
542	19.14	474.35	22.682	0.107	1.747	0.484
543	117.06	350.93	22.682	0.152	1.610	0.301
544	210.61	190.32	22.688	0.192	1.861	0.568
545	209.95	302.70	22.708	0.161	1.250	0.316
546	245.97	339.79	22.720	0.120	1.603	0.414
547	194.76	253.68	22.748	0.129	1.407	0.314
548	3.10	163.49	22.757	0.409	0.996	0.894
549	62.77	78.66	22.764	0.234	0.573	0.531
550	140.52	192.17	22.773	0.153	1.745	0.397
551	47.39	470.30	22.817	0.141	0.792	0.292
552	289.95	70.85	22.823	0.174	1.848	0.569
553	203.30	263.48	22.849	0.198	2.165	0.773
554	163.69	179.44	22.856	0.152	2.373	0.957
555	77.28	467.27	22.862	0.226	1.103	0.384

Table C.2. (end)

ID	x	y	V	σ_V	B-V	σ_{B-V}
556	31.72	184.49	22.892	0.232	0.696	0.541
557	129.93	420.07	22.898	0.163	1.176	0.292
558	90.83	368.24	22.992	0.199	2.031	0.761
559	155.06	502.15	23.034	0.184	0.938	0.318
560	98.30	418.62	23.055	0.159	0.839	0.288
561	82.92	489.78	23.064	0.161	1.997	0.819
562	240.29	41.16	23.124	0.218	1.271	0.575
563	288.16	57.64	23.179	0.249	-0.060	0.290
564	225.50	193.85	23.292	0.220	-0.211	0.267

Table C.3. Photometry for NGC 188

ID	x	y	V	σ_V	B-V	σ_{B-V}
1	41.35	460.08	11.945	0.026	1.131	0.046
2	-21.05	725.66	12.228	0.024	1.254	0.043
3	-76.76	540.61	12.307	0.025	1.152	0.043
4	261.57	644.37	12.417	0.027	1.261	0.047
5	301.38	342.67	12.492	0.012	0.789	0.023
6	141.34	119.05	12.535	0.011	0.895	0.019
7	203.50	93.55	13.052	0.009	0.968	0.021
8	262.28	165.74	13.154	0.010	0.828	0.019
9	-116.80	162.93	13.342	0.027	1.109	0.052
10	114.06	775.99	13.387	0.025	0.659	0.043
11	75.72	364.98	13.411	0.018	0.513	0.036
12	228.39	204.92	13.454	0.011	0.730	0.021
13	-128.08	370.31	13.586	0.027	1.087	0.046
14	52.62	662.13	13.603	0.029	1.094	0.050
15	83.61	73.54	13.605	0.016	0.642	0.027
16	-112.39	330.82	13.647	0.028	1.211	0.049
17	-122.15	681.06	13.791	0.027	0.927	0.046
18	76.12	687.87	13.832	0.025	0.501	0.044
19	13.90	579.60	13.837	0.027	1.060	0.046
20	52.52	759.62	13.938	0.032	0.969	0.057
21	56.24	468.13	13.977	0.029	0.519	0.049
22	-174.75	582.33	13.997	0.028	1.036	0.047
23	-229.31	496.99	14.009	0.027	1.052	0.047
24	-230.71	490.57	14.022	0.025	1.031	0.043
25	-61.48	427.09	14.081	0.029	0.286	0.051
26	-61.47	424.40	14.083	0.026	0.278	0.045
27	-22.41	643.12	14.106	0.030	1.027	0.048
28	216.79	635.84	14.111	0.027	0.510	0.047
29	66.25	322.14	14.243	0.026	1.029	0.045
30	76.50	537.24	14.256	0.027	0.888	0.047
31	-61.39	223.98	14.266	0.030	0.601	0.051
32	17.52	550.49	14.304	0.027	0.468	0.045
33	33.27	274.12	14.353	0.025	1.070	0.042
34	-58.23	523.40	14.398	0.026	0.598	0.045
35	-132.20	571.64	14.404	0.027	0.676	0.045
36	-91.65	812.09	14.419	0.027	1.083	0.046
37	-207.15	116.79	14.438	0.026	1.003	0.045

Table C.3. (cont.)

ID	x	y	V	σ_V	B-V	σ_{B-V}
38	-39.26	141.85	14.449	0.028	1.003	0.049
39	160.61	525.06	14.485	0.025	0.626	0.043
40	2.43	179.20	14.547	0.030	0.742	0.049
41	-60.00	466.55	14.563	0.026	0.700	0.043
42	-77.75	828.16	14.578	0.028	0.482	0.047
43	-59.10	469.18	14.584	0.029	0.702	0.049
44	0.91	477.15	14.618	0.028	1.018	0.049
45	152.96	537.67	14.619	0.047	0.777	0.080
46	-119.81	376.76	14.641	0.027	0.528	0.047
47	-24.68	783.21	14.672	0.028	0.630	0.047
48	-139.06	630.82	14.789	0.027	0.674	0.045
49	275.36	216.54	14.794	0.021	0.715	0.032
50	-172.25	226.15	14.814	0.028	0.709	0.046
51	-1.53	748.82	14.814	0.026	0.719	0.044
52	-24.27	656.09	14.817	0.029	0.727	0.047
53	48.28	465.64	14.826	0.027	0.713	0.049
54	-79.33	14.09	14.844	0.029	0.709	0.047
55	193.77	346.05	14.855	0.015	0.747	0.026
56	30.95	429.03	14.871	0.026	0.956	0.043
57	10.69	299.53	14.872	0.020	0.757	0.036
58	209.79	863.13	14.875	0.025	0.780	0.044
59	-131.65	476.28	14.879	0.026	0.713	0.044
60	80.50	635.48	14.882	0.026	0.736	0.045
61	91.61	412.18	14.882	0.022	0.730	0.037
62	226.21	670.60	14.882	0.026	0.720	0.044
63	247.83	843.28	14.883	0.027	0.738	0.046
64	-41.00	481.05	14.885	0.026	0.697	0.044
65	-39.80	483.26	14.887	0.029	0.721	0.049
66	-130.53	480.47	14.889	0.026	0.720	0.046
67	20.50	552.22	14.891	0.027	0.715	0.047
68	-152.54	379.54	14.896	0.027	0.701	0.046
69	61.76	487.95	14.897	0.027	0.782	0.046
70	91.60	108.71	14.911	0.013	0.836	0.024
71	291.30	813.28	14.911	0.027	0.706	0.047
72	-102.93	472.61	14.922	0.025	0.930	0.042
73	106.43	715.75	14.922	0.027	0.706	0.045
74	-219.69	41.62	14.923	0.026	0.726	0.045

Table C.3. (cont.)

ID	x	y	V	σ_V	B-V	σ_{B-V}
75	235.39	294.92	14.926	0.018	0.758	0.029
76	225.94	517.46	14.929	0.026	0.710	0.045
77	-139.44	873.96	14.934	0.027	0.661	0.047
78	32.88	435.27	14.936	0.025	0.712	0.042
79	103.14	522.07	14.940	0.026	0.696	0.044
80	-101.90	476.16	14.941	0.029	0.944	0.049
81	161.81	317.60	14.943	0.014	0.648	0.026
82	66.61	743.51	14.943	0.027	0.779	0.045
83	-203.06	327.65	14.953	0.026	0.655	0.046
84	-232.00	640.39	14.956	0.027	0.949	0.048
85	198.45	597.83	14.958	0.026	0.608	0.044
86	20.94	569.89	14.969	0.026	0.689	0.044
87	-22.02	704.95	14.972	0.027	0.857	0.045
88	186.84	666.12	14.972	0.025	0.684	0.044
89	-30.18	154.15	14.976	0.030	0.697	0.049
90	295.01	654.97	14.981	0.026	0.696	0.045
91	273.21	772.17	14.981	0.026	0.686	0.044
92	-177.84	714.47	14.984	0.027	0.636	0.049
93	-37.85	85.35	14.985	0.029	0.696	0.047
94	-14.97	761.82	14.986	0.026	0.700	0.044
95	-62.26	736.02	14.989	0.027	0.670	0.045
96	-86.12	836.09	14.992	0.027	0.897	0.045
97	-180.02	586.90	14.995	0.027	0.676	0.045
98	302.90	429.47	14.997	0.016	0.856	0.030
99	-147.65	670.16	14.998	0.026	0.668	0.044
100	303.38	433.71	15.000	0.027	0.815	0.045
101	-71.88	402.39	15.001	0.026	0.897	0.046
102	-71.37	399.49	15.006	0.025	0.885	0.042
103	144.98	369.56	15.007	0.012	0.728	0.025
104	-227.10	49.24	15.007	0.027	0.676	0.046
105	178.47	625.83	15.028	0.025	0.687	0.043
106	-146.24	674.46	15.029	0.027	0.654	0.047
107	272.73	629.88	15.031	0.026	0.681	0.044
108	12.52	180.75	15.032	0.023	0.700	0.040
109	69.92	735.86	15.034	0.025	0.697	0.043
110	-71.86	511.86	15.036	0.025	0.671	0.042
111	-187.98	796.72	15.036	0.026	0.988	0.045

Table C.3. (cont.)

ID	x	y	V	σ_V	B-V	σ_{B-V}
112	-59.29	429.45	15.047	0.030	0.639	0.054
113	-59.31	426.78	15.049	0.027	0.663	0.050
114	-70.01	514.82	15.063	0.027	0.675	0.048
115	59.65	516.72	15.065	0.029	0.663	0.052
116	-192.07	462.59	15.081	0.080	0.900	0.132
117	190.99	559.23	15.086	0.026	0.960	0.044
118	-91.55	574.10	15.086	0.026	0.708	0.045
119	132.74	362.43	15.095	0.015	0.706	0.027
120	155.26	490.62	15.102	0.021	0.817	0.037
121	232.21	665.72	15.105	0.026	0.698	0.044
122	-52.11	535.43	15.119	0.025	0.651	0.043
123	240.21	173.37	15.121	0.019	0.937	0.030
124	-150.12	772.61	15.125	0.026	0.530	0.045
125	219.59	394.20	15.132	0.027	0.667	0.046
126	218.24	391.89	15.134	0.026	0.734	0.044
127	216.84	389.64	15.136	0.025	0.792	0.043
128	-113.77	555.79	15.139	0.025	0.675	0.043
129	313.66	739.58	15.143	0.026	0.678	0.045
130	-192.76	457.03	15.145	0.073	0.771	0.116
131	-144.87	504.12	15.162	0.026	0.701	0.044
132	-143.16	508.60	15.170	0.028	0.667	0.054
133	211.71	101.49	15.170	0.015	1.441	0.027
134	9.69	637.54	15.179	0.026	0.647	0.045
135	109.97	112.19	15.206	0.014	0.712	0.026
136	-193.61	737.99	15.216	0.025	0.662	0.043
137	108.67	335.38	15.222	0.014	1.324	0.026
138	137.76	574.74	15.224	0.025	0.714	0.043
139	-52.68	236.95	15.226	0.029	0.660	0.049
140	202.09	672.13	15.238	0.025	0.682	0.044
141	169.57	433.94	15.242	0.020	0.726	0.034
142	95.50	470.26	15.242	0.068	0.673	0.127
143	-169.18	82.70	15.244	0.026	1.253	0.045
144	120.25	567.72	15.250	0.025	0.696	0.043
145	-141.28	688.63	15.252	0.027	0.670	0.045
146	179.62	566.60	15.259	0.025	0.711	0.043
147	32.42	87.01	15.276	0.038	0.704	0.068
148	156.40	184.42	15.292	0.012	0.730	0.023

Table C.3. (cont.)

ID	x	y	V	σ_V	B-V	σ_{B-V}
149	259.08	808.69	15.292	0.026	0.708	0.044
150	95.84	469.94	15.302	0.027	0.663	0.064
151	128.67	588.39	15.312	0.025	0.716	0.044
152	205.27	769.46	15.319	0.025	0.677	0.044
153	-164.46	96.27	15.325	0.027	0.652	0.047
154	104.22	493.33	15.338	0.022	0.674	0.039
155	158.74	719.12	15.341	0.025	0.684	0.043
156	21.97	267.01	15.354	0.023	0.585	0.039
157	-229.11	643.29	15.354	0.026	0.645	0.047
158	-11.95	696.79	15.362	0.029	0.657	0.048
159	-219.10	175.87	15.378	0.026	0.657	0.045
160	-24.64	228.49	15.388	0.029	0.603	0.047
161	32.41	87.71	15.408	0.103	0.668	0.232
162	-80.63	890.23	15.409	0.027	0.892	0.047
163	-240.04	604.61	15.416	0.025	0.704	0.044
164	-36.61	539.98	15.418	0.027	0.666	0.047
165	32.50	87.43	15.445	0.053	0.737	0.090
166	-44.97	466.10	15.448	0.025	0.677	0.043
167	-44.08	468.42	15.451	0.027	0.676	0.047
168	82.46	479.55	15.458	0.022	0.673	0.039
169	-189.47	388.35	15.461	0.027	0.690	0.046
170	235.25	393.06	15.467	0.014	0.692	0.026
171	42.34	526.22	15.470	0.025	0.680	0.045
172	-190.32	393.87	15.474	0.027	0.631	0.046
173	64.79	422.39	15.475	0.024	0.801	0.041
174	-13.23	105.45	15.488	0.030	0.701	0.049
175	137.71	312.12	15.493	0.014	0.705	0.025
176	-142.70	720.62	15.496	0.026	0.680	0.045
177	236.40	396.08	15.526	0.025	0.660	0.044
178	-55.80	36.74	15.526	0.026	0.696	0.047
179	-6.51	805.73	15.529	0.027	0.715	0.046
180	-86.78	742.22	15.553	0.026	0.580	0.045
181	277.76	757.82	15.583	0.027	0.713	0.047
182	-87.98	291.56	15.596	0.026	0.667	0.046
183	-158.36	303.67	15.598	0.025	0.678	0.044
184	-9.20	594.70	15.626	0.036	0.748	0.057
185	-61.70	811.13	15.633	0.025	0.700	0.046

Table C.3. (cont.)

ID	x	y	V	σ_V	B-V	σ_{B-V}
186	-201.78	832.26	15.637	0.024	0.657	0.042
187	-174.02	101.42	15.655	0.025	0.678	0.045
188	70.79	601.04	15.664	0.025	0.685	0.043
189	13.58	554.04	15.664	0.026	0.742	0.045
190	-1.55	798.96	15.665	0.028	0.710	0.049
191	-230.33	814.67	15.680	0.024	0.579	0.048
192	234.53	555.78	15.687	0.026	0.710	0.046
193	131.71	212.32	15.690	0.009	1.273	0.021
194	-137.97	637.53	15.702	0.025	0.669	0.044
195	-33.34	438.54	15.725	0.027	0.764	0.047
196	143.35	783.76	15.728	0.027	0.702	0.046
197	105.15	727.14	15.748	0.026	0.757	0.046
198	-150.97	671.39	15.754	0.026	0.682	0.045
199	204.20	778.53	15.758	0.029	0.702	0.049
200	-228.60	244.02	15.763	0.030	0.601	0.050
201	-153.81	162.56	15.777	0.025	0.722	0.045
202	42.30	550.32	15.778	0.026	0.679	0.047
203	-202.54	804.04	15.783	0.025	0.696	0.045
204	91.94	557.07	15.784	0.026	0.675	0.045
205	11.73	401.65	15.800	0.025	0.838	0.043
206	35.85	804.37	15.811	0.025	0.715	0.045
207	-199.29	479.88	15.812	0.027	0.754	0.048
208	-13.46	665.99	15.814	0.030	0.702	0.052
209	-186.32	431.78	15.818	0.027	0.675	0.045
210	-200.47	474.44	15.822	0.024	0.767	0.043
211	-27.12	607.27	15.828	0.028	0.714	0.047
212	-186.52	426.64	15.828	0.024	0.700	0.043
213	43.63	303.78	15.837	0.020	0.820	0.035
214	162.28	543.27	15.839	0.025	0.702	0.046
215	157.18	218.00	15.851	0.012	0.755	0.025
216	30.63	284.97	15.857	0.022	0.720	0.038
217	-214.76	805.63	15.861	0.024	0.661	0.046
218	-152.64	335.20	15.885	0.030	0.675	0.050
219	-135.65	682.15	15.909	0.027	0.706	0.048
220	10.63	532.69	15.910	0.027	0.741	0.048
221	-158.16	562.99	15.915	0.026	0.766	0.048
222	-18.90	710.16	15.915	0.030	0.693	0.052

Table C.3. (cont.)

ID	x	y	V	σ_V	B-V	σ_{B-V}
223	-76.39	615.07	15.918	0.030	1.420	0.054
224	280.50	756.19	15.920	0.034	1.354	0.058
225	-224.89	587.99	15.936	0.024	0.521	0.043
226	-108.39	153.83	15.949	0.029	0.737	0.049
227	246.59	425.32	15.950	0.012	0.739	0.027
228	23.46	871.68	15.953	0.029	0.703	0.050
229	145.32	468.91	15.954	0.018	0.710	0.034
230	203.58	337.17	15.973	0.012	0.800	0.025
231	-141.28	39.77	15.984	0.028	0.746	0.047
232	-162.03	340.61	15.990	0.027	0.705	0.048
233	-156.46	359.73	15.991	0.027	0.695	0.047
234	247.03	428.50	15.993	0.029	0.715	0.049
235	-208.95	881.41	16.001	0.025	0.681	0.048
236	55.60	190.14	16.003	0.021	0.729	0.038
237	192.46	36.31	16.003	0.014	0.810	0.028
238	-90.07	420.36	16.009	0.025	0.723	0.044
239	-90.01	423.53	16.011	0.027	0.727	0.048
240	-69.16	216.39	16.011	0.028	0.795	0.049
241	-214.89	542.31	16.014	0.029	0.726	0.051
242	-38.56	804.16	16.016	0.029	0.740	0.051
243	-103.34	290.91	16.018	0.030	0.701	0.051
244	-28.14	708.64	16.022	0.031	0.717	0.052
245	235.15	111.34	16.025	0.017	0.780	0.029
246	63.17	498.70	16.026	0.026	0.819	0.046
247	129.72	391.60	16.038	0.018	0.742	0.036
248	-176.59	543.09	16.039	0.026	0.715	0.050
249	110.98	588.72	16.058	0.029	0.711	0.048
250	-93.52	200.13	16.065	0.033	0.772	0.053
251	-114.76	756.52	16.071	0.027	0.737	0.047
252	83.00	514.05	16.094	0.035	0.683	0.064
253	110.10	424.38	16.096	0.018	0.956	0.034
254	-159.36	635.33	16.104	0.027	0.713	0.048
255	237.45	510.65	16.113	0.028	0.815	0.052
256	127.16	257.78	16.121	0.012	0.766	0.030
257	113.79	142.51	16.136	0.010	0.762	0.023
258	20.95	475.54	16.157	0.026	0.773	0.047
259	-120.56	133.73	16.177	0.027	0.758	0.045

Table C.3. (cont.)

ID	x	y	V	σ_V	B-V	σ_{B-V}
260	-145.10	477.17	16.178	0.033	0.761	0.058
261	57.69	243.32	16.185	0.023	0.269	0.039
262	85.86	519.33	16.201	0.027	0.912	0.048
263	6.59	51.94	16.203	0.021	0.759	0.038
264	178.01	699.79	16.205	0.032	0.746	0.054
265	-73.76	754.64	16.206	0.029	0.731	0.052
266	156.97	563.86	16.213	0.027	0.895	0.047
267	39.76	332.96	16.216	0.022	0.752	0.040
268	-146.25	472.87	16.218	0.028	0.731	0.051
269	-103.38	587.66	16.220	0.030	0.736	0.052
270	-24.12	610.45	16.244	0.031	1.335	0.053
271	-101.50	333.59	16.246	0.029	0.741	0.049
272	163.84	431.85	16.262	0.019	0.760	0.038
273	-50.86	392.96	16.267	0.033	0.888	0.060
274	95.21	470.58	16.270	0.068	0.773	0.131
275	-151.22	259.84	16.270	0.030	0.855	0.052
276	-145.60	676.74	16.271	0.029	0.720	0.053
277	179.70	506.13	16.272	0.020	0.760	0.046
278	33.40	445.68	16.273	0.028	0.759	0.052
279	-194.89	782.98	16.275	0.030	0.762	0.049
280	-8.27	668.58	16.290	0.032	0.845	0.056
281	115.22	372.26	16.297	0.013	0.786	0.031
282	-15.83	245.91	16.304	0.038	0.782	0.061
283	-134.46	463.73	16.304	0.029	0.737	0.049
284	-61.89	356.47	16.308	0.030	0.745	0.051
285	-135.36	459.66	16.313	0.029	0.739	0.050
286	-76.46	452.09	16.324	0.030	0.773	0.053
287	-50.34	390.62	16.325	0.027	0.815	0.048
288	84.43	513.37	16.328	0.039	0.822	0.059
289	-92.83	798.71	16.328	0.028	0.642	0.050
290	291.78	829.97	16.335	0.038	0.500	0.062
291	153.63	888.99	16.349	0.027	0.671	0.049
292	201.71	618.38	16.352	0.027	0.735	0.050
293	-77.15	449.22	16.359	0.030	0.764	0.053
294	-52.04	13.60	16.385	0.026	0.638	0.047
295	-194.88	880.87	16.390	0.026	0.713	0.053
296	266.41	652.18	16.401	0.047	0.786	0.085

Table C.3. (cont.)

ID	x	y	V	σ_V	B-V	σ_{B-V}
297	177.44	344.20	16.401	0.024	0.614	0.050
298	57.71	689.18	16.417	0.031	0.774	0.054
299	19.34	307.72	16.421	0.023	0.711	0.042
300	129.71	235.29	16.430	0.011	0.852	0.030
301	147.96	31.99	16.432	0.012	0.814	0.029
302	182.48	692.94	16.442	0.028	0.863	0.052
303	53.94	313.48	16.443	0.023	0.880	0.042
304	-124.71	733.01	16.450	0.029	0.790	0.049
305	224.12	430.27	16.456	0.013	0.749	0.037
306	66.60	405.31	16.462	0.028	0.773	0.051
307	153.82	572.59	16.464	0.026	0.650	0.049
308	224.52	433.06	16.466	0.027	0.750	0.050
309	87.77	263.77	16.493	0.011	0.630	0.027
310	-144.87	666.34	16.501	0.028	0.767	0.048
311	254.66	755.41	16.506	0.032	0.804	0.058
312	-124.27	250.02	16.515	0.032	0.733	0.056
313	143.38	495.44	16.535	0.022	1.066	0.043
314	60.64	353.54	16.550	0.023	0.778	0.041
315	-97.92	443.19	16.552	0.028	0.815	0.049
316	-97.40	446.50	16.561	0.027	0.791	0.049
317	-43.16	64.75	16.576	0.028	0.896	0.049
318	-174.31	466.10	16.590	0.034	0.788	0.061
319	150.72	620.80	16.595	0.031	0.889	0.054
320	-145.97	809.11	16.617	0.030	0.909	0.051
321	208.53	665.75	16.618	0.033	0.721	0.060
322	-175.19	461.24	16.624	0.028	0.775	0.049
323	204.44	188.87	16.639	0.014	1.594	0.033
324	166.40	186.28	16.645	0.013	0.985	0.033
325	-44.50	190.02	16.646	0.035	0.806	0.059
326	100.94	549.31	16.664	0.029	0.788	0.052
327	-24.83	304.37	16.670	0.030	0.763	0.055
328	-111.71	201.18	16.699	0.036	0.821	0.060
329	200.62	378.10	16.709	0.013	0.844	0.035
330	98.16	533.88	16.709	0.030	0.806	0.053
331	273.70	554.88	16.726	0.032	0.981	0.055
332	41.77	397.87	16.730	0.026	0.796	0.047
333	94.80	471.01	16.738	0.078	0.792	0.142

Table C.3. (cont.)

ID	x	y	V	σ_V	B-V	σ_{B-V}
334	24.11	494.97	16.754	0.026	0.827	0.047
335	-86.36	208.74	16.764	0.027	0.817	0.048
336	7.93	785.28	16.765	0.033	0.726	0.058
337	295.52	88.96	16.767	0.016	0.904	0.042
338	19.05	514.43	16.780	0.032	0.798	0.055
339	-221.40	356.77	16.783	0.026	0.764	0.045
340	46.49	635.81	16.793	0.031	0.663	0.053
341	-35.21	188.74	16.816	0.030	0.815	0.055
342	-52.03	266.96	16.820	0.037	0.964	0.060
343	-110.81	599.43	16.827	0.034	0.775	0.056
344	-108.87	144.31	16.834	0.032	0.964	0.054
345	-185.07	843.86	16.835	0.029	0.820	0.050
346	294.32	691.07	16.870	0.035	0.844	0.062
347	299.36	394.25	16.872	0.020	0.857	0.043
348	248.19	729.00	16.875	0.034	0.819	0.059
349	285.20	176.78	16.886	0.016	0.956	0.041
350	-135.30	418.39	16.886	0.029	1.317	0.049
351	-135.27	414.29	16.887	0.027	1.305	0.047
352	88.85	478.66	16.891	0.022	0.848	0.042
353	300.32	398.41	16.894	0.032	0.835	0.055
354	-196.48	554.25	16.899	0.026	0.827	0.046
355	217.38	606.91	16.925	0.035	0.855	0.058
356	-131.74	183.55	16.926	0.028	0.630	0.049
357	274.32	767.03	16.927	0.035	0.662	0.059
358	114.22	870.56	16.935	0.031	0.844	0.052
359	182.62	355.76	16.950	0.014	0.931	0.037
360	-219.56	811.32	16.958	0.025	0.915	0.045
361	83.78	655.39	16.967	0.029	0.868	0.052
362	37.80	604.71	16.982	0.030	0.994	0.050
363	-195.94	588.66	16.982	0.026	0.865	0.045
364	-9.55	389.98	16.997	0.031	0.972	0.051
365	-179.02	433.46	16.999	0.029	0.846	0.052
366	-190.41	453.96	17.006	0.096	1.341	0.330
367	-130.72	887.18	17.012	0.035	0.820	0.056
368	269.19	571.78	17.017	0.034	0.842	0.057
369	-144.61	226.86	17.030	0.034	0.865	0.054
370	73.66	316.07	17.034	0.026	0.919	0.047

Table C.3. (cont.)

ID	x	y	V	σ_V	B-V	σ_{B-V}
371	-14.35	478.25	17.038	0.033	0.579	0.058
372	-25.92	556.39	17.046	0.030	0.835	0.051
373	127.63	488.90	17.051	0.023	0.871	0.044
374	184.20	533.29	17.054	0.032	0.900	0.057
375	-5.72	13.75	17.067	0.029	0.821	0.050
376	232.32	486.63	17.095	0.035	0.832	0.061
377	119.48	549.35	17.098	0.031	0.842	0.056
378	-167.39	661.29	17.107	0.028	0.888	0.048
379	-194.18	780.44	17.108	0.038	1.334	0.073
380	302.50	621.75	17.110	0.039	0.523	0.067
381	69.63	688.17	17.110	0.053	0.744	0.098
382	-212.41	144.12	17.129	0.030	0.718	0.051
383	2.39	323.19	17.133	0.035	0.942	0.057
384	71.30	181.21	17.152	0.028	0.923	0.052
385	83.06	817.92	17.159	0.029	0.894	0.050
386	-39.69	331.73	17.161	0.030	0.923	0.050
387	233.46	484.25	17.176	0.032	0.896	0.060
388	-198.97	318.55	17.208	0.025	0.892	0.044
389	-211.44	407.16	17.239	0.124	0.532	0.165
390	265.38	611.42	17.264	0.038	0.922	0.061
391	-102.19	280.02	17.265	0.034	0.910	0.054
392	55.93	672.97	17.268	0.033	1.393	0.055
393	92.03	493.70	17.276	0.023	0.892	0.046
394	46.26	536.10	17.296	0.028	1.031	0.048
395	25.62	636.49	17.301	0.029	0.953	0.048
396	-185.67	625.20	17.301	0.027	0.882	0.046
397	-70.42	261.73	17.312	0.030	0.933	0.049
398	169.06	60.87	17.336	0.014	0.807	0.034
399	-34.34	103.42	17.416	0.035	0.806	0.059
400	-155.13	328.18	17.423	0.033	0.789	0.054
401	259.22	708.92	17.435	0.033	1.088	0.054
402	32.50	531.13	17.450	0.027	0.941	0.047
403	44.20	407.48	17.476	0.025	0.945	0.043
404	-226.65	580.30	17.485	0.028	0.968	0.046
405	148.70	263.62	17.493	0.024	1.003	0.053
406	97.26	380.40	17.496	0.014	0.966	0.032
407	215.68	815.09	17.497	0.030	0.961	0.052

Table C.3. (cont.)

ID	x	y	V	σ_V	B-V	σ_{B-V}
408	-201.24	211.04	17.505	0.035	0.587	0.053
409	-10.90	270.56	17.514	0.056	1.697	0.085
410	71.78	889.35	17.522	0.029	0.926	0.054
411	-155.89	808.62	17.525	0.028	0.605	0.048
412	316.94	619.96	17.527	0.031	0.586	0.056
413	269.42	525.36	17.533	0.030	1.021	0.051
414	-17.76	387.72	17.563	0.030	1.457	0.050
415	-185.45	215.90	17.567	0.028	0.992	0.047
416	234.61	481.89	17.572	0.019	0.865	0.055
417	-148.09	631.12	17.589	0.027	0.918	0.047
418	165.08	553.07	17.598	0.028	0.972	0.047
419	-90.91	147.95	17.602	0.032	1.095	0.051
420	6.76	553.52	17.608	0.034	1.072	0.056
421	-32.20	579.90	17.610	0.028	0.969	0.048
422	-45.59	780.72	17.611	0.029	1.040	0.049
423	114.68	63.41	17.613	0.014	0.701	0.031
424	-175.29	428.09	17.617	0.032	0.960	0.052
425	-175.40	423.19	17.622	0.026	0.958	0.045
426	150.72	782.17	17.631	0.028	1.090	0.049
427	189.46	440.80	17.635	0.017	0.988	0.037
428	189.66	442.99	17.635	0.028	0.958	0.048
429	150.66	191.55	17.641	0.015	0.917	0.039
430	16.65	371.82	17.641	0.022	1.001	0.041
431	5.79	687.53	17.645	0.030	1.026	0.049
432	16.85	413.87	17.648	0.026	0.964	0.045
433	17.39	419.07	17.649	0.025	1.188	0.043
434	59.83	219.61	17.686	0.029	1.187	0.056
435	305.45	500.66	17.698	0.022	1.118	0.043
436	12.14	863.92	17.698	0.030	0.532	0.051
437	159.45	740.21	17.704	0.029	0.999	0.048
438	145.59	523.74	17.721	0.029	1.095	0.049
439	-54.07	765.68	17.725	0.028	0.961	0.046
440	263.53	613.62	17.727	0.039	1.133	0.063
441	304.51	504.91	17.727	0.047	1.103	0.069
442	63.37	348.60	17.733	0.022	1.161	0.038
443	321.44	562.94	17.737	0.029	0.965	0.048
444	-112.82	592.81	17.759	0.029	0.976	0.050

Table C.3. (cont.)

ID	x	y	V	σ_V	B-V	σ_{B-V}
445	210.65	191.40	17.760	0.015	1.360	0.029
446	204.67	579.73	17.768	0.029	1.124	0.048
447	1.82	347.32	17.772	0.028	0.989	0.048
448	150.58	339.39	17.778	0.017	1.004	0.034
449	-45.21	871.11	17.814	0.029	0.973	0.050
450	45.88	455.31	17.821	0.105	1.813	0.305
451	80.71	798.57	17.830	0.030	0.708	0.052
452	-224.67	97.82	17.841	0.026	0.999	0.045
453	99.46	200.21	17.843	0.014	0.738	0.032
454	280.61	753.21	17.843	0.046	0.953	0.076
455	72.26	795.77	17.864	0.029	1.028	0.047
456	115.14	345.81	17.865	0.014	1.059	0.028
457	91.55	355.54	17.870	0.014	1.026	0.029
458	196.35	567.57	17.892	0.029	1.029	0.049
459	-62.21	124.73	17.925	0.026	1.023	0.046
460	-77.24	863.05	17.937	0.026	1.025	0.047
461	-13.20	839.16	17.944	0.031	1.028	0.051
462	84.52	625.68	17.951	0.027	1.032	0.046
463	187.61	676.33	17.954	0.029	1.199	0.048
464	-216.27	118.72	17.959	0.026	0.878	0.045
465	24.66	382.44	17.969	0.022	1.206	0.041
466	107.52	526.32	17.971	0.029	1.024	0.049
467	20.14	101.30	17.977	0.023	1.053	0.040
468	249.78	498.69	18.021	0.028	1.195	0.049
469	-144.46	383.19	18.023	0.030	1.061	0.053
470	135.34	209.60	18.028	0.014	1.092	0.031
471	250.57	495.43	18.042	0.016	1.168	0.034
472	220.55	553.59	18.048	0.028	1.186	0.047
473	-150.87	410.15	18.056	0.039	1.080	0.058
474	-150.98	414.58	18.064	0.026	1.035	0.045
475	-208.69	283.54	18.082	0.025	1.049	0.045
476	163.34	126.64	18.099	0.015	0.697	0.031
477	233.49	250.73	18.100	0.016	1.123	0.031
478	47.27	124.63	18.135	0.020	1.088	0.037
479	149.54	738.74	18.136	0.029	0.613	0.048
480	-205.57	289.79	18.136	0.027	1.110	0.048
481	-47.01	576.15	18.140	0.026	1.269	0.047

Table C.3. (cont.)

ID	x	y	V	σ_V	B-V	σ_{B-V}
482	127.61	335.41	18.151	0.017	1.188	0.032
483	-205.30	833.69	18.185	0.031	0.995	0.058
484	-143.83	82.65	18.190	0.027	1.092	0.047
485	11.93	744.85	18.197	0.030	1.094	0.049
486	-65.13	35.99	18.216	0.049	1.265	0.083
487	149.59	471.21	18.222	0.028	1.160	0.049
488	283.43	745.91	18.231	0.030	1.101	0.052
489	-116.55	658.65	18.256	0.027	1.073	0.047
490	-47.52	666.06	18.257	0.028	1.215	0.049
491	-56.00	604.56	18.268	0.027	1.086	0.045
492	-99.62	820.81	18.347	0.027	1.146	0.049
493	309.13	777.21	18.360	0.029	0.849	0.049
494	-123.34	132.35	18.361	0.038	1.484	0.083
495	260.79	463.62	18.377	0.082	1.747	0.192
496	-157.84	225.88	18.378	0.029	1.296	0.049
497	311.52	8.57	18.409	0.024	1.182	0.037
498	-198.39	451.86	18.420	0.198	1.068	0.299
499	274.32	835.49	18.435	0.029	0.992	0.050
500	236.07	532.89	18.454	0.027	1.276	0.047
501	-97.68	354.60	18.456	0.024	1.152	0.045
502	72.82	437.31	18.475	0.026	0.875	0.047
503	166.66	128.68	18.480	0.020	1.222	0.036
504	233.16	56.61	18.487	0.017	1.265	0.032
505	63.83	634.27	18.494	0.030	1.185	0.050
506	-156.70	391.14	18.509	0.031	1.162	0.058
507	221.77	265.43	18.517	0.021	1.041	0.034
508	201.13	650.32	18.529	0.030	0.814	0.048
509	260.54	467.09	18.529	0.134	1.428	0.224
510	53.86	234.40	18.529	0.021	0.723	0.039
511	35.61	457.15	18.549	0.234	-0.161	0.330
512	-126.42	512.32	18.562	0.030	0.808	0.057
513	-179.70	428.58	18.562	0.415	-1.186	0.540
514	-128.30	508.35	18.565	0.027	0.830	0.045
515	164.55	66.40	18.576	0.024	1.611	0.045
516	-51.02	459.41	18.584	0.026	1.474	0.051
517	283.14	111.72	18.593	0.019	1.265	0.037
518	-51.81	457.04	18.593	0.025	1.473	0.050

Table C.3. (cont.)

ID	x	y	V	σ_V	B-V	σ_{B-V}
519	296.23	336.93	18.600	0.165	1.559	0.373
520	17.49	757.87	18.624	0.027	1.498	0.053
521	-19.23	667.80	18.626	0.028	1.156	0.055
522	-97.42	97.56	18.640	0.026	0.776	0.046
523	101.46	569.85	18.644	0.026	1.200	0.045
524	-129.50	518.97	18.646	0.026	0.183	0.046
525	40.08	806.93	18.650	0.033	1.203	0.075
526	-58.44	806.37	18.660	0.030	1.247	0.062
527	-50.11	131.76	18.666	0.028	1.351	0.056
528	-120.24	417.62	18.670	0.027	1.294	0.056
529	-120.26	421.37	18.690	0.026	1.196	0.052
530	122.92	680.02	18.704	0.027	0.827	0.047
531	89.53	258.91	18.707	0.017	1.213	0.031
532	243.55	121.21	18.725	0.020	1.315	0.041
533	312.51	797.72	18.764	0.028	1.298	0.057
534	41.17	183.57	18.771	0.025	1.246	0.048
535	-64.46	887.89	18.779	0.059	0.719	0.094
536	27.06	820.42	18.787	0.027	1.220	0.052
537	-228.37	530.53	18.791	0.031	1.344	0.059
538	3.29	492.87	18.819	0.030	1.263	0.055
539	106.52	690.01	18.822	0.031	1.283	0.054
540	-234.27	459.38	18.839	0.026	1.608	0.064
541	30.64	427.03	18.842	0.196	1.672	0.389
542	214.50	527.62	18.851	0.028	0.661	0.047
543	242.18	669.13	18.881	0.032	1.355	0.064
544	-149.61	240.07	18.882	0.034	1.566	0.060
545	-233.36	465.54	18.887	0.032	1.452	0.079
546	-82.21	772.87	18.891	0.028	1.308	0.054
547	-0.56	842.36	18.895	0.031	1.309	0.056
548	289.87	334.08	18.946	0.031	0.783	0.064
549	14.95	447.04	18.951	0.027	1.290	0.058
550	-83.04	33.62	18.981	0.030	1.304	0.065
551	78.43	322.72	18.983	0.034	1.369	0.062
552	150.23	887.66	18.989	0.053	0.780	0.093
553	188.88	848.47	18.990	0.028	1.315	0.052
554	-128.42	838.05	18.992	0.030	1.238	0.053
555	208.42	875.16	19.001	0.030	1.006	0.052

Table C.3. (cont.)

ID	x	y	V	σ_V	B-V	σ_{B-V}
556	-203.50	56.01	19.013	0.030	1.535	0.061
557	-43.56	537.18	19.025	0.034	1.390	0.059
558	-7.80	352.03	19.025	0.037	1.375	0.060
559	-205.37	715.78	19.029	0.029	1.533	0.063
560	215.91	416.67	19.031	0.035	1.039	0.053
561	-81.26	141.76	19.045	0.028	1.487	0.060
562	23.11	462.80	19.055	0.040	1.369	0.081
563	-65.22	318.34	19.063	0.029	0.543	0.061
564	-224.36	779.98	19.072	0.030	1.352	0.064
565	216.55	419.30	19.073	0.029	0.944	0.055
566	36.04	337.48	19.075	0.030	1.272	0.054
567	-38.57	617.57	19.088	0.030	1.625	0.065
568	19.45	397.65	19.090	0.032	1.063	0.058
569	-42.09	355.33	19.097	0.032	1.397	0.061
570	138.04	189.31	19.114	0.055	0.646	0.092
571	128.35	776.87	19.116	0.076	1.164	0.162
572	155.33	554.59	19.121	0.029	1.507	0.071
573	-196.23	421.68	19.128	0.031	1.365	0.070
574	-12.12	378.63	19.137	0.027	0.927	0.056
575	-44.98	487.83	19.139	0.027	1.460	0.060
576	-25.70	191.53	19.147	0.030	1.438	0.065
577	-113.16	27.94	19.150	0.028	1.357	0.063
578	63.47	504.25	19.163	0.044	0.614	0.073
579	-196.22	416.28	19.166	0.032	1.304	0.061
580	-31.83	683.22	19.170	0.027	1.566	0.074
581	-43.64	490.05	19.171	0.034	1.457	0.072
582	180.00	858.94	19.192	0.030	1.337	0.051
583	194.72	699.85	19.221	0.030	1.193	0.055
584	-40.99	226.44	19.239	0.042	1.510	0.083
585	-153.32	693.84	19.241	0.035	0.540	0.057
586	8.94	767.16	19.245	0.034	1.433	0.074
587	-171.40	754.20	19.250	0.033	1.388	0.080
588	91.54	173.74	19.250	0.288	-2.986	0.366
589	166.18	515.44	19.251	0.027	1.224	0.053
590	-92.90	618.43	19.276	0.030	1.312	0.063
591	-113.59	367.55	19.285	0.048	1.277	0.095
592	-182.35	456.46	19.320	0.244	0.484	0.388

Table C.3. (cont.)

ID	x	y	V	σ_V	B-V	σ_{B-V}
593	40.90	252.35	19.339	0.035	1.407	0.073
594	-188.25	489.16	19.376	0.032	0.602	0.064
595	25.66	337.03	19.385	0.034	1.215	0.064
596	-185.88	493.30	19.386	0.033	0.639	0.073
597	-183.39	497.58	19.407	0.033	0.894	0.063
598	10.42	286.12	19.409	0.033	1.417	0.079
599	-10.11	244.41	19.457	0.032	1.530	0.085
600	23.79	246.53	19.468	0.034	1.368	0.066
601	-188.00	453.11	19.477	0.269	0.793	0.612
602	267.72	185.33	19.492	0.075	1.915	0.182
603	169.64	750.16	19.500	0.035	0.969	0.075
604	-177.22	388.78	19.525	0.034	1.504	0.087
605	223.33	363.44	19.525	0.054	1.395	0.080
606	-160.21	345.61	19.548	0.036	0.724	0.063
607	133.64	878.02	19.557	0.040	1.063	0.085
608	15.10	416.05	19.575	0.056	1.802	0.112
609	-173.29	85.32	19.589	0.038	1.222	0.093
610	11.19	144.95	19.596	0.058	1.580	0.130
611	60.83	656.87	19.605	0.063	1.847	0.135
612	27.87	341.66	19.634	0.039	1.434	0.072
613	38.90	37.43	19.635	0.045	1.460	0.090
614	63.12	569.33	19.641	0.038	1.470	0.084
615	118.51	680.08	19.646	0.035	1.216	0.069
616	147.60	254.94	19.693	0.033	1.059	0.057
617	-6.85	510.15	19.716	0.033	1.376	0.076
618	-62.32	791.38	19.721	0.038	1.214	0.088
619	-50.71	697.24	19.729	0.066	0.572	0.108
620	-6.83	751.10	19.735	0.035	1.380	0.077
621	255.91	698.17	19.738	0.033	1.553	0.083
622	46.29	574.76	19.739	0.036	1.400	0.087
623	-74.65	786.36	19.741	0.041	1.401	0.075
624	-106.69	392.71	19.746	0.038	1.550	0.110
625	126.81	117.08	19.752	0.060	0.715	0.111
626	-34.84	651.00	19.755	0.041	1.505	0.083
627	-123.46	38.94	19.762	0.056	1.030	0.104
628	-107.22	396.23	19.763	0.048	1.609	0.098
629	151.74	450.59	19.772	0.057	1.352	0.124

Table C.3. (cont.)

ID	x	y	V	σ_V	B-V	σ_{B-V}
630	25.15	578.78	19.773	0.181	1.440	0.289
631	-137.34	600.58	19.810	0.034	1.416	0.077
632	-52.73	669.80	19.811	0.032	1.483	0.097
633	183.41	667.03	19.812	0.077	1.615	0.177
634	-159.14	140.64	19.825	0.046	1.600	0.102
635	-94.86	148.38	19.834	0.072	0.614	0.106
636	-196.41	527.29	19.843	0.040	0.440	0.068
637	-1.62	645.35	19.852	0.074	1.399	0.138
638	-39.93	581.22	19.879	0.047	1.581	0.116
639	77.62	343.50	19.887	0.052	1.570	0.085
640	18.16	29.11	19.889	0.049	1.584	0.102
641	-37.64	115.09	19.890	0.042	1.522	0.083
642	232.55	20.66	19.912	0.045	0.844	0.072
643	15.77	764.63	19.920	0.046	1.602	0.113
644	114.37	32.26	19.925	0.041	1.371	0.074
645	-92.99	20.79	19.953	0.046	1.217	0.094
646	39.47	717.25	19.953	0.058	1.426	0.134
647	24.37	202.99	19.955	0.048	0.534	0.079
648	-87.56	886.02	19.959	0.060	0.203	0.110
649	36.72	471.50	19.964	0.314	0.950	0.520
650	-72.15	50.13	19.974	0.035	1.325	0.095
651	278.27	329.91	19.974	0.054	1.591	0.098
652	-89.90	44.14	19.988	0.036	1.598	0.134
653	143.94	373.85	19.989	0.076	1.275	0.131
654	-105.31	115.37	19.996	0.042	0.523	0.072
655	66.03	468.14	19.996	0.133	0.163	0.234
656	247.83	318.99	20.034	0.068	0.965	0.104
657	-49.81	767.19	20.039	0.067	1.383	0.120
658	14.78	463.37	20.043	0.059	0.647	0.098
659	78.08	138.70	20.045	0.062	1.529	0.106
660	223.82	524.81	20.048	0.043	1.059	0.077
661	-237.38	254.71	20.055	0.064	1.224	0.118
662	286.08	482.52	20.055	0.075	1.338	0.206
663	164.91	148.98	20.071	0.062	0.782	0.094
664	29.37	456.71	20.074	0.313	0.687	0.574
665	299.27	686.09	20.075	0.039	1.516	0.117
666	-47.06	691.95	20.077	0.098	1.906	0.202

Table C.3. (cont.)

ID	x	y	V	σ_V	B-V	σ_{B-V}
667	151.66	573.57	20.084	0.076	0.211	0.400
668	-122.44	696.26	20.097	0.051	1.332	0.131
669	268.27	95.59	20.105	0.057	1.527	0.106
670	-76.58	776.94	20.111	0.044	1.560	0.146
671	285.66	486.38	20.117	0.129	1.188	0.241
672	37.54	197.85	20.119	0.060	1.557	0.116
673	-11.98	322.07	20.123	0.063	0.709	0.116
674	37.45	765.78	20.139	0.047	1.473	0.121
675	262.75	725.68	20.148	0.052	0.558	0.093
676	180.92	844.42	20.160	0.042	1.410	0.113
677	16.64	165.47	20.160	0.044	1.524	0.102
678	-218.61	90.87	20.165	0.049	0.968	0.094
679	91.32	212.31	20.178	0.112	1.658	0.243
680	263.49	519.36	20.185	0.060	1.162	0.114
681	206.72	379.12	20.188	0.081	0.905	0.122
682	30.76	471.46	20.192	0.206	1.138	0.394
683	280.07	503.14	20.213	0.057	1.038	0.136
684	164.36	622.77	20.223	0.096	1.081	0.178
685	242.97	150.15	20.230	0.069	1.657	0.155
686	95.35	721.54	20.230	0.054	0.940	0.106
687	-118.37	767.54	20.230	0.051	1.402	0.119
688	138.91	620.52	20.231	0.045	1.283	0.114
689	-12.74	198.30	20.255	0.061	1.947	0.149
690	24.91	30.10	20.284	0.051	0.938	0.103
691	278.96	506.96	20.287	0.048	1.051	0.108
692	-17.56	755.76	20.289	0.048	1.635	0.141
693	59.67	473.00	20.289	0.463	0.577	0.810
694	89.29	430.94	20.295	0.086	1.557	0.148
695	64.68	427.20	20.303	0.093	1.215	0.170
696	29.04	143.55	20.305	0.052	1.667	0.132
697	223.44	444.68	20.309	0.055	1.588	0.143
698	291.97	408.69	20.320	0.102	1.460	0.169
699	-76.00	370.09	20.325	0.087	0.788	0.163
700	-178.08	304.01	20.333	0.049	1.665	0.167
701	-153.09	368.53	20.336	0.052	1.463	0.143
702	90.48	130.43	20.339	0.063	1.334	0.120
703	139.91	140.62	20.352	0.092	1.846	0.154

Table C.3. (cont.)

ID	x	y	V	σ_V	B-V	σ_{B-V}
704	65.97	139.26	20.359	0.080	0.918	0.141
705	-27.70	618.67	20.365	0.042	1.546	0.122
706	292.53	412.79	20.367	0.057	1.517	0.149
707	223.15	441.79	20.369	0.109	1.620	0.168
708	209.21	291.93	20.370	0.038	1.050	0.077
709	-175.69	290.87	20.372	0.057	1.417	0.147
710	311.76	86.82	20.376	0.080	0.664	0.128
711	-4.49	182.87	20.378	0.044	1.521	0.143
712	-10.72	880.20	20.379	0.150	0.753	0.284
713	-161.71	169.73	20.386	0.045	1.487	0.121
714	316.05	835.68	20.404	0.098	1.121	0.188
715	-172.34	558.13	20.409	0.054	0.565	0.106
716	58.49	476.62	20.410	0.234	0.567	0.509
717	242.38	30.74	20.427	0.107	1.659	0.170
718	187.39	803.65	20.432	0.086	1.225	0.211
719	236.45	69.58	20.433	0.080	1.257	0.141
720	-144.20	73.88	20.433	0.072	0.593	0.116
721	253.65	747.65	20.440	0.126	1.845	0.242
722	-16.31	42.27	20.443	0.046	1.727	0.141
723	-228.60	118.54	20.470	0.114	0.705	0.216
724	269.64	676.89	20.471	0.065	1.403	0.149
725	-227.70	120.84	20.474	0.093	0.791	0.205
726	234.20	277.39	20.484	0.065	1.620	0.154
727	80.03	44.97	20.502	0.073	1.643	0.188
728	-127.26	185.62	20.505	0.101	0.941	0.170
729	235.56	490.23	20.515	0.088	2.103	0.221
730	33.77	626.63	20.530	0.068	1.573	0.155
731	91.99	601.68	20.558	0.096	1.431	0.177
732	-176.76	669.35	20.575	0.067	1.339	0.167
733	-180.65	304.71	20.575	0.058	0.780	0.143
734	176.11	103.22	20.577	0.098	1.533	0.147
735	262.71	425.26	20.581	0.066	1.632	0.155
736	188.41	80.42	20.588	0.091	1.465	0.149
737	-80.94	491.53	20.589	0.067	1.461	0.171
738	11.04	204.59	20.589	0.130	1.282	0.209
739	81.62	127.97	20.590	0.075	0.679	0.127
740	-217.08	574.23	20.596	0.082	1.464	0.239

Table C.3. (cont.)

ID	x	y	V	σ_V	B-V	σ_{B-V}
741	152.41	439.83	20.608	0.072	0.655	0.125
742	180.89	264.05	20.610	0.099	1.705	0.180
743	28.97	579.87	20.616	0.112	1.125	0.242
744	245.47	761.16	20.630	0.080	1.517	0.213
745	-6.21	365.12	20.631	0.106	0.674	0.201
746	-13.29	602.84	20.651	0.063	1.223	0.153
747	65.39	775.23	20.654	0.112	1.502	0.289
748	214.55	376.52	20.656	0.109	1.587	0.192
749	-92.75	523.74	20.660	0.078	0.623	0.149
750	-126.00	337.78	20.678	0.081	0.553	0.136
751	273.77	343.10	20.686	0.088	1.526	0.166
752	-203.44	450.52	20.700	0.288	0.399	0.525
753	126.18	873.87	20.704	0.081	1.041	0.158
754	234.94	493.24	20.706	0.080	2.118	0.211
755	-81.05	794.28	20.717	0.098	1.866	0.265
756	-105.73	711.28	20.728	0.067	1.621	0.266
757	-98.87	102.65	20.748	0.050	1.625	0.186
758	-182.08	92.19	20.751	0.066	0.779	0.128
759	-115.96	171.25	20.754	0.268	0.463	0.527
760	172.83	474.45	20.758	0.072	1.370	0.142
761	262.94	428.93	20.769	0.153	1.309	0.261
762	24.16	711.32	20.774	0.097	2.106	0.331
763	301.50	776.08	20.806	0.054	1.347	0.183
764	29.56	385.93	20.828	0.108	1.783	0.252
765	-57.74	448.25	20.831	0.096	1.186	0.172
766	207.44	123.50	20.834	0.183	1.432	0.268
767	4.98	209.68	20.840	0.090	0.624	0.150
768	139.86	181.91	20.846	0.146	1.086	0.207
769	161.07	163.29	20.870	0.074	1.521	0.197
770	-167.75	675.06	20.871	0.070	0.263	0.116
771	294.88	794.30	20.876	0.083	1.332	0.211
772	168.11	298.95	20.884	0.091	1.514	0.174
773	-218.13	831.58	20.909	0.274	1.486	0.495
774	-222.67	876.90	20.918	0.156	2.005	0.369
775	-222.31	123.66	20.939	0.139	1.372	0.239
776	81.32	158.44	20.952	0.126	1.086	0.202
777	22.98	622.64	20.954	0.098	1.341	0.256

Table C.3. (cont.)

ID	x	y	V	σ_V	B-V	σ_{B-V}
778	281.80	45.31	21.011	0.103	1.304	0.205
779	276.39	865.12	21.013	0.118	0.167	0.175
780	229.13	363.62	21.025	0.198	1.134	0.355
781	46.18	25.69	21.040	0.110	0.907	0.192
782	-0.13	281.48	21.048	0.127	1.151	0.246
783	209.55	234.57	21.081	0.164	1.569	0.251
784	53.70	718.16	21.105	0.105	1.856	0.307
785	53.87	248.89	21.107	0.086	1.851	0.257
786	161.30	760.05	21.119	0.119	0.783	0.202
787	-167.79	586.51	21.127	0.113	0.903	0.267
788	55.37	207.24	21.144	0.119	1.493	0.274
789	238.54	830.84	21.149	0.091	0.614	0.150
790	81.68	322.45	21.164	0.098	1.421	0.216
791	135.56	841.98	21.166	0.094	0.546	0.198
792	-15.73	420.39	21.184	0.117	0.864	0.241
793	-136.01	291.08	21.200	0.130	1.879	0.475
794	53.47	424.40	21.202	0.111	1.817	0.381
795	40.61	845.79	21.215	0.119	1.175	0.324
796	34.09	579.53	21.215	0.210	1.028	0.386
797	9.54	850.96	21.216	0.245	1.358	0.414
798	-58.42	326.09	21.269	0.095	0.567	0.234
799	18.33	435.99	21.278	0.164	1.156	0.477
800	-190.05	672.00	21.286	0.111	0.589	0.189
801	44.15	435.50	21.296	0.170	0.848	0.269
802	-83.02	750.90	21.317	0.128	1.754	0.480
803	-115.03	468.28	21.337	0.074	1.640	0.383
804	-208.95	277.87	21.345	0.146	0.697	0.306
805	296.82	481.35	21.382	0.133	1.221	0.252
806	237.58	885.33	21.409	0.141	0.344	0.243
807	17.25	435.54	21.410	0.194	1.421	0.502
808	227.26	745.27	21.421	0.145	2.083	0.571
809	258.77	867.82	21.430	0.149	1.561	0.405
810	47.06	360.32	21.452	0.079	0.326	0.141
811	130.83	460.54	21.572	0.233	1.654	0.520
812	-194.83	477.26	21.584	0.181	1.336	0.515
813	-31.73	468.34	21.586	0.160	0.244	0.325
814	73.65	487.94	21.587	0.203	1.046	0.442

Table C.3. (end)

ID	x	y	V	σ_V	B-V	σ_{B-V}
815	297.57	477.23	21.590	0.225	1.041	0.399
816	301.74	150.89	21.602	0.345	0.541	0.477
817	-209.64	275.02	21.615	0.158	0.627	0.386
818	17.12	561.06	21.676	0.208	0.910	0.404
819	-199.62	381.16	21.682	0.138	1.314	0.374
820	-182.94	287.05	21.687	0.133	0.565	0.242
821	24.12	612.07	21.726	0.183	0.178	0.284
822	115.63	469.14	21.756	0.249	0.836	0.398
823	21.19	274.28	21.905	0.152	1.151	0.377
824	12.84	256.74	21.952	0.227	1.174	0.522
825	-39.19	466.98	22.003	0.216	0.887	0.503
826	-225.31	494.67	22.014	0.288	0.704	0.581
827	257.46	789.46	22.015	0.226	1.461	0.602
828	-62.17	412.13	22.034	0.244	-0.100	0.388
829	-47.20	477.21	22.039	0.239	1.863	0.717
830	76.82	329.71	22.067	0.648	1.977	1.077
831	-168.46	427.04	22.100	0.218	0.585	0.412
832	13.68	826.15	22.119	0.161	1.568	0.587
833	-2.20	488.40	22.133	0.223	1.528	0.687
834	-9.32	483.13	22.166	0.330	0.122	0.499
835	-166.97	443.04	22.203	0.277	0.538	0.478
836	-12.22	467.91	22.304	0.307	0.590	0.554
837	33.73	255.30	22.341	0.631	1.185	0.915
838	-61.80	382.03	22.378	0.362	1.465	0.879
839	78.16	412.90	22.422	0.393	1.617	0.669
840	-160.59	664.75	22.538	0.468	0.861	0.987

Table C.4. Photometry for NGC 6791

ID	x	y	V	σ_V	B-V	σ_{B-V}
1	310.12	265.41	12.978	0.023	1.156	0.037
2	246.40	255.20	13.459	0.016	1.030	0.029
3	296.24	195.70	13.869	0.022	1.651	0.035
4	299.05	69.62	13.926	0.022	1.586	0.038
5	302.43	36.46	14.048	0.034	0.771	0.050
6	48.13	269.86	14.055	0.023	1.627	0.034
7	182.63	57.05	14.058	0.017	0.685	0.029
8	232.66	336.81	14.123	0.016	1.602	0.027
9	100.95	230.31	14.143	0.013	1.623	0.023
10	243.09	247.11	14.227	0.021	1.317	0.034
11	137.51	41.58	14.511	0.013	1.312	0.024
12	125.31	432.91	14.521	0.018	1.349	0.029
13	242.51	474.51	14.560	0.013	1.376	0.026
14	176.41	226.35	14.565	0.013	1.319	0.025
15	177.26	116.44	14.568	0.010	1.396	0.021
16	77.24	270.74	14.568	0.026	1.355	0.038
17	240.78	208.41	14.572	0.015	1.531	0.031
18	16.19	192.94	14.576	0.015	1.487	0.025
19	232.84	392.04	14.577	0.023	1.325	0.038
20	201.72	372.32	14.615	0.012	1.373	0.026
21	203.20	63.13	14.616	0.014	1.345	0.024
22	298.20	330.30	14.620	0.014	1.364	0.029
23	202.46	437.42	14.623	0.012	1.073	0.023
24	253.68	116.49	14.627	0.014	1.364	0.026
25	13.63	145.55	14.638	0.011	1.368	0.023
26	107.07	179.30	14.659	0.013	1.367	0.024
27	108.57	29.20	14.668	0.015	1.242	0.025
28	7.11	173.52	14.687	0.014	1.348	0.026
29	212.09	88.44	14.714	0.012	1.385	0.023
30	279.62	354.61	14.743	0.019	1.436	0.031
31	233.59	504.71	14.821	0.016	1.424	0.030
32	291.66	283.44	14.842	0.015	1.397	0.025
33	111.66	414.45	14.844	0.012	1.349	0.022
34	274.58	486.35	14.851	0.058	0.793	0.083
35	268.40	225.23	14.856	0.016	0.865	0.029
36	107.72	332.51	14.913	0.012	1.398	0.022
37	67.63	93.21	14.926	0.014	0.706	0.024

Table C.4. (cont.)

ID	x	y	V	σ_V	B-V	σ_{B-V}
38	256.11	353.02	15.008	0.025	1.436	0.038
39	211.43	129.08	15.038	0.022	0.460	0.032
40	131.07	333.43	15.050	0.013	1.142	0.023
41	198.83	472.91	15.050	0.022	0.549	0.033
42	311.06	369.38	15.054	0.018	1.085	0.032
43	268.28	460.77	15.062	0.024	1.424	0.039
44	136.32	243.41	15.067	0.014	0.765	0.026
45	32.46	254.71	15.098	0.014	1.376	0.024
46	299.23	216.68	15.130	0.024	1.391	0.043
47	60.67	103.47	15.142	0.011	0.773	0.021
48	143.12	305.00	15.189	0.022	1.135	0.033
49	213.84	234.87	15.213	0.023	1.199	0.035
50	52.00	113.67	15.267	0.013	0.859	0.023
51	167.10	433.54	15.289	0.016	1.369	0.027
52	212.71	231.51	15.299	0.019	1.350	0.030
53	24.67	160.88	15.307	0.016	0.822	0.026
54	255.14	246.18	15.329	0.025	1.312	0.040
55	54.89	57.25	15.372	0.015	0.705	0.030
56	185.61	197.24	15.394	0.019	1.359	0.031
57	124.15	220.80	15.426	0.020	0.735	0.032
58	196.76	233.64	15.437	0.022	1.346	0.039
59	175.30	16.57	15.451	0.013	1.341	0.024
60	71.49	397.27	15.509	0.015	0.802	0.025
61	166.35	134.18	15.524	0.020	0.816	0.032
62	94.38	397.28	15.530	0.022	0.710	0.034
63	285.17	157.91	15.544	0.032	1.341	0.048
64	27.27	392.49	15.552	0.013	1.187	0.024
65	277.74	143.94	15.558	0.025	0.844	0.039
66	219.09	67.47	15.579	0.015	1.286	0.027
67	196.25	234.47	15.595	0.051	1.305	0.083
68	153.42	468.18	15.647	0.023	0.601	0.036
69	171.23	161.26	15.647	0.017	0.903	0.032
70	274.93	440.94	15.665	0.036	1.119	0.053
71	246.18	497.11	15.677	0.027	0.670	0.043
72	233.98	70.82	15.687	0.023	1.302	0.035
73	296.06	122.31	15.703	0.016	1.327	0.030
74	295.06	232.49	15.708	0.026	1.305	0.043

Table C.4. (cont.)

ID	x	y	V	σ_V	B-V	σ_{B-V}
75	269.74	65.66	15.710	0.021	1.314	0.034
76	74.86	353.90	15.735	0.024	1.300	0.036
77	108.61	419.78	15.783	0.019	1.277	0.032
78	159.91	258.90	15.811	0.026	0.889	0.038
79	83.16	310.86	15.828	0.023	1.281	0.036
80	251.32	80.53	15.850	0.021	1.300	0.034
81	34.84	195.49	15.856	0.014	0.916	0.027
82	120.28	364.71	15.884	0.021	0.700	0.033
83	295.30	123.24	15.926	0.037	1.305	0.069
84	239.47	494.59	15.937	0.025	1.035	0.042
85	98.80	324.83	15.978	0.026	1.150	0.041
86	22.92	298.05	15.994	0.016	0.954	0.027
87	209.97	74.33	16.003	0.018	1.073	0.031
88	32.60	151.20	16.008	0.015	1.306	0.026
89	310.22	393.59	16.040	0.029	1.286	0.045
90	191.70	245.23	16.042	0.022	1.200	0.041
91	237.43	206.60	16.048	0.023	0.701	0.038
92	132.17	12.37	16.079	0.015	1.293	0.027
93	131.68	13.24	16.079	0.448	1.296	0.590
94	293.51	89.32	16.111	0.024	1.253	0.044
95	234.07	263.36	16.114	0.019	0.682	0.032
96	239.82	133.00	16.122	0.026	0.536	0.041
97	37.17	218.10	16.123	0.016	1.250	0.029
98	21.45	491.94	16.125	0.020	1.215	0.032
99	197.54	370.46	16.127	0.020	1.269	0.044
100	71.91	486.43	16.127	0.021	1.211	0.038
101	295.86	81.12	16.145	0.025	1.241	0.039
102	232.57	389.95	16.179	0.052	1.344	0.084
103	141.95	199.78	16.188	0.023	0.902	0.036
104	270.88	254.74	16.204	0.029	0.758	0.044
105	259.17	468.71	16.206	0.028	0.638	0.045
106	268.21	367.33	16.214	0.023	0.636	0.040
107	222.76	344.61	16.243	0.020	1.387	0.034
108	312.60	232.07	16.262	0.031	1.005	0.046
109	105.21	299.02	16.307	0.023	0.867	0.038
110	247.30	307.03	16.307	0.039	1.024	0.055
111	230.66	81.80	16.344	0.023	0.880	0.035

Table C.4. (cont.)

ID	x	y	V	σ_V	B-V	σ_{B-V}
112	61.46	406.47	16.345	0.022	1.146	0.035
113	197.81	236.07	16.361	0.028	0.759	0.046
114	87.33	94.76	16.365	0.026	0.610	0.038
115	286.73	151.65	16.367	0.024	0.700	0.041
116	294.97	283.27	16.384	0.021	1.209	0.038
117	282.75	383.46	16.388	0.049	1.274	0.102
118	316.60	258.14	16.397	0.065	1.142	0.402
119	36.64	435.66	16.398	0.015	1.197	0.027
120	255.59	423.37	16.403	0.021	0.764	0.038
121	18.45	357.29	16.410	0.019	1.229	0.030
122	26.08	268.29	16.424	0.015	1.220	0.027
123	260.29	42.84	16.468	0.170	1.244	0.354
124	263.48	241.13	16.469	0.024	1.214	0.042
125	4.46	302.78	16.478	0.017	0.782	0.029
126	113.19	14.89	16.481	0.022	0.875	0.036
127	287.85	53.65	16.495	0.036	1.230	0.067
128	244.94	463.63	16.500	0.036	1.266	0.057
129	5.33	301.87	16.503	0.103	0.780	0.169
130	295.99	164.27	16.514	0.022	1.238	0.049
131	262.83	328.42	16.517	0.022	0.804	0.038
132	104.93	298.02	16.520	0.047	0.815	0.077
133	161.69	169.88	16.525	0.028	0.711	0.043
134	153.87	222.51	16.527	0.020	0.790	0.032
135	28.55	231.59	16.540	0.021	1.147	0.035
136	183.71	261.14	16.547	0.024	0.753	0.040
137	219.41	116.73	16.560	0.025	0.814	0.038
138	49.14	157.86	16.567	0.020	0.732	0.031
139	85.93	165.63	16.578	0.022	1.207	0.037
140	126.83	131.96	16.581	0.022	1.162	0.036
141	37.44	260.69	16.600	0.016	1.217	0.028
142	93.64	160.31	16.601	0.022	0.781	0.038
143	287.14	54.23	16.623	0.053	1.106	0.089
144	110.83	92.12	16.639	0.024	0.973	0.038
145	35.48	189.16	16.641	0.016	0.653	0.028
146	190.90	244.63	16.645	0.023	1.139	0.059
147	218.82	202.12	16.649	0.020	0.932	0.038
148	62.34	185.70	16.660	0.029	0.695	0.045

Table C.4. (cont.)

ID	x	y	V	σ_V	B-V	σ_{B-V}
149	174.33	195.76	16.666	0.028	0.785	0.044
150	156.88	299.69	16.668	0.023	1.205	0.039
151	225.40	248.54	16.673	0.027	1.238	0.041
152	4.20	428.05	16.703	0.016	0.929	0.032
153	4.43	243.09	16.720	0.015	0.772	0.026
154	250.29	226.03	16.721	0.027	0.847	0.044
155	264.46	213.93	16.731	0.032	1.147	0.049
156	161.03	369.20	16.743	0.019	0.911	0.033
157	302.89	197.06	16.747	0.024	1.182	0.043
158	259.24	281.25	16.748	0.047	1.062	0.081
159	22.77	306.65	16.754	0.015	0.752	0.027
160	239.82	281.72	16.763	0.026	1.201	0.041
161	236.99	223.78	16.766	0.031	0.874	0.052
162	63.20	245.23	16.773	0.019	1.178	0.032
163	148.64	224.46	16.781	0.019	1.173	0.035
164	50.91	83.71	16.781	0.020	0.839	0.031
165	222.51	327.21	16.801	0.020	0.673	0.036
166	281.42	427.51	16.802	0.024	0.892	0.038
167	252.06	134.68	16.809	0.098	0.950	0.164
168	289.91	182.92	16.810	0.056	0.936	0.120
169	140.82	146.46	16.831	0.019	1.214	0.031
170	149.84	104.75	16.834	0.023	1.189	0.036
171	254.07	235.40	16.843	0.025	1.226	0.045
172	308.80	44.66	16.846	0.026	0.915	0.046
173	151.21	118.51	16.862	0.083	1.115	0.128
174	152.37	439.55	16.868	0.022	0.887	0.035
175	159.38	296.42	16.873	0.023	1.206	0.040
176	223.31	266.18	16.875	0.020	0.853	0.039
177	250.84	328.61	16.876	0.015	0.804	0.027
178	150.66	118.87	16.883	0.184	1.141	0.321
179	87.28	121.70	16.884	0.018	1.184	0.030
180	208.97	153.71	16.892	0.023	1.189	0.038
181	56.59	117.92	16.905	0.019	0.828	0.031
182	265.19	119.96	16.915	0.025	0.876	0.039
183	183.98	169.10	16.922	0.017	1.012	0.030
184	229.09	356.43	16.923	0.021	0.790	0.039
185	234.55	291.33	16.932	0.025	0.917	0.039

Table C.4. (cont.)

ID	x	y	V	σ_V	B-V	σ_{B-V}
186	244.03	112.51	16.939	0.021	1.241	0.038
187	223.48	224.01	16.940	0.031	1.161	0.045
188	290.24	182.37	16.940	0.064	0.861	0.188
189	89.96	481.74	16.945	0.025	0.673	0.038
190	287.75	70.45	16.951	0.022	1.298	0.038
191	147.63	163.68	16.969	0.022	1.162	0.035
192	228.95	253.82	16.974	0.027	1.555	0.042
193	242.75	285.90	16.977	0.105	0.828	0.169
194	216.71	425.14	16.979	0.025	0.847	0.042
195	268.27	13.52	17.000	0.030	1.162	0.054
196	304.29	191.73	17.007	0.029	0.728	0.047
197	214.30	139.07	17.012	0.021	1.183	0.036
198	107.39	50.64	17.016	0.021	0.780	0.035
199	269.44	52.14	17.028	0.026	0.903	0.059
200	284.83	397.02	17.034	0.030	1.194	0.056
201	194.47	331.32	17.047	0.018	0.939	0.030
202	187.65	297.73	17.051	0.040	0.771	0.069
203	32.83	196.23	17.055	0.028	0.859	0.050
204	36.76	445.08	17.058	0.020	0.920	0.033
205	193.66	169.64	17.060	0.027	0.871	0.041
206	213.97	252.68	17.064	0.020	1.178	0.036
207	267.27	168.66	17.069	0.026	0.798	0.049
208	275.58	386.40	17.072	0.026	1.168	0.042
209	268.41	212.43	17.075	0.027	1.035	0.042
210	139.65	482.72	17.075	0.026	0.853	0.042
211	126.94	169.04	17.080	0.016	0.900	0.028
212	74.22	503.90	17.083	0.023	1.052	0.042
213	83.93	256.71	17.098	0.017	0.686	0.029
214	66.67	403.99	17.108	0.024	1.020	0.037
215	65.03	382.72	17.109	0.016	0.912	0.029
216	159.51	50.58	17.111	0.021	1.186	0.034
217	132.13	25.76	17.111	0.023	0.882	0.040
218	215.65	220.62	17.113	0.032	0.854	0.049
219	268.93	15.64	17.118	0.033	0.892	0.052
220	6.65	98.23	17.127	0.017	0.894	0.034
221	62.03	483.00	17.135	0.034	0.754	0.059
222	258.46	63.07	17.141	0.047	0.924	0.084

Table C.4. (cont.)

ID	x	y	V	σ_V	B-V	σ_{B-V}
223	271.49	192.32	17.141	0.022	1.212	0.036
224	256.10	211.23	17.146	0.044	1.174	0.079
225	86.76	493.38	17.146	0.025	1.143	0.040
226	256.68	213.20	17.147	0.045	0.727	0.080
227	256.38	212.22	17.147	0.036	0.850	0.072
228	249.37	129.85	17.154	0.024	0.930	0.038
229	287.87	94.44	17.155	0.025	1.039	0.039
230	126.54	168.78	17.156	0.068	0.875	0.112
231	250.86	295.20	17.157	0.020	1.217	0.038
232	174.18	143.58	17.159	0.023	1.051	0.038
233	297.77	265.23	17.160	0.032	0.916	0.052
234	32.13	441.54	17.162	0.019	1.419	0.034
235	77.71	31.16	17.169	0.020	1.139	0.038
236	74.54	194.91	17.174	0.022	1.134	0.036
237	283.52	383.13	17.183	0.052	0.877	0.095
238	295.77	163.28	17.184	0.026	1.212	0.099
239	293.77	172.65	17.187	0.031	0.800	0.046
240	186.40	103.47	17.193	0.021	0.999	0.038
241	253.79	232.90	17.196	0.025	1.223	0.044
242	261.27	131.24	17.203	0.021	0.921	0.041
243	234.69	157.48	17.205	0.027	1.018	0.042
244	70.26	232.13	17.211	0.015	1.187	0.029
245	220.68	319.82	17.226	0.025	1.180	0.038
246	23.17	379.40	17.227	0.019	0.755	0.034
247	208.32	207.68	17.229	0.021	1.163	0.039
248	106.01	372.77	17.243	0.021	0.774	0.036
249	274.83	33.20	17.253	0.024	0.904	0.044
250	145.23	32.60	17.254	0.031	0.876	0.049
251	238.88	280.85	17.256	0.028	1.048	0.044
252	126.40	426.66	17.258	0.019	1.097	0.033
253	299.77	177.71	17.261	0.237	1.019	0.359
254	266.46	169.23	17.262	0.032	0.819	0.064
255	276.44	103.60	17.268	0.022	1.212	0.038
256	62.56	483.74	17.273	0.054	0.784	0.083
257	228.40	367.43	17.287	0.020	1.197	0.035
258	165.88	268.80	17.303	0.021	0.906	0.034
259	201.62	316.15	17.305	0.018	1.146	0.034

Table C.4. (cont.)

ID	x	y	V	σ_V	B-V	σ_{B-V}
260	185.75	281.13	17.306	0.028	0.935	0.046
261	274.19	56.98	17.307	0.026	1.176	0.043
262	275.72	507.45	17.309	0.028	1.173	0.046
263	156.77	289.05	17.309	0.038	1.142	0.062
264	245.51	226.51	17.309	0.025	0.873	0.040
265	215.71	464.30	17.311	0.022	0.982	0.038
266	209.77	213.49	17.313	0.021	0.933	0.036
267	210.99	240.99	17.319	0.027	0.866	0.042
268	57.75	383.74	17.319	0.020	0.924	0.034
269	284.10	382.87	17.320	0.131	1.086	0.257
270	254.10	39.68	17.321	0.043	1.003	0.088
271	239.55	40.07	17.326	0.020	0.971	0.035
272	127.46	14.20	17.330	0.016	0.886	0.029
273	311.16	260.75	17.333	0.229	1.708	0.374
274	170.82	341.40	17.338	0.020	0.987	0.036
275	195.69	235.30	17.339	0.091	0.908	0.146
276	258.29	62.35	17.340	0.040	1.018	0.098
277	2.65	211.85	17.343	0.025	1.149	0.050
278	90.48	129.52	17.343	0.023	0.918	0.037
279	161.51	344.05	17.345	0.016	0.913	0.031
280	139.85	370.08	17.346	0.018	1.164	0.034
281	164.34	179.18	17.347	0.024	0.897	0.049
282	255.70	436.32	17.350	0.017	1.009	0.031
283	206.01	294.36	17.350	0.024	0.906	0.041
284	256.00	214.10	17.351	0.049	0.716	0.139
285	168.46	410.30	17.354	0.023	1.151	0.042
286	3.45	127.98	17.355	0.019	0.724	0.032
287	189.18	384.81	17.357	0.028	0.924	0.043
288	99.74	339.19	17.360	0.020	0.906	0.034
289	141.83	214.67	17.360	0.023	0.938	0.040
290	26.93	40.10	17.361	0.019	0.917	0.031
291	96.51	76.82	17.361	0.026	0.894	0.040
292	177.96	206.94	17.365	0.024	0.904	0.041
293	238.35	56.34	17.366	0.041	1.046	0.077
294	117.83	276.27	17.367	0.019	1.154	0.033
295	206.79	24.57	17.367	0.019	0.903	0.034
296	99.25	272.26	17.368	0.018	0.910	0.032

Table C.4. (cont.)

ID	x	y	V	σ_V	B-V	σ_{B-V}
297	293.39	12.65	17.373	0.026	0.874	0.044
298	78.04	400.60	17.373	0.128	0.783	0.196
299	132.31	99.62	17.373	0.024	0.925	0.041
300	226.89	490.80	17.374	0.027	0.950	0.044
301	294.49	280.79	17.376	0.036	1.001	0.057
302	77.49	400.60	17.376	0.206	0.802	0.431
303	118.93	369.85	17.376	0.020	0.878	0.036
304	189.52	482.62	17.377	0.023	0.883	0.038
305	304.96	213.99	17.383	0.028	0.901	0.044
306	70.27	145.13	17.385	0.017	0.963	0.032
307	271.26	271.48	17.386	0.021	0.917	0.034
308	133.29	15.02	17.386	0.022	0.860	0.038
309	162.17	191.93	17.388	0.021	0.906	0.037
310	113.29	345.95	17.390	0.021	0.798	0.036
311	134.53	50.19	17.391	0.019	0.863	0.036
312	238.60	55.51	17.392	0.038	1.089	0.073
313	308.97	232.43	17.394	0.034	0.896	0.051
314	256.08	299.32	17.394	0.018	0.921	0.032
315	175.61	218.99	17.394	0.038	0.885	0.061
316	121.21	238.50	17.400	0.046	0.790	0.074
317	165.24	178.68	17.400	0.031	0.929	0.057
318	196.08	259.75	17.400	0.021	0.906	0.036
319	206.88	28.39	17.401	0.018	1.160	0.034
320	209.99	8.30	17.404	0.017	1.010	0.030
321	170.34	214.43	17.404	0.020	0.937	0.034
322	57.94	433.05	17.407	0.021	0.860	0.036
323	81.90	186.75	17.412	0.019	0.649	0.032
324	12.46	237.68	17.414	0.015	0.879	0.028
325	44.69	131.07	17.420	0.016	1.018	0.032
326	216.80	223.04	17.423	0.025	0.881	0.041
327	271.61	202.68	17.424	0.026	0.988	0.041
328	219.88	112.60	17.424	0.024	0.977	0.041
329	302.82	181.10	17.425	0.023	0.940	0.055
330	174.19	70.99	17.425	0.022	0.892	0.038
331	145.13	365.17	17.426	0.022	1.044	0.037
332	295.10	269.36	17.426	0.020	0.999	0.039
333	131.60	383.50	17.427	0.021	0.880	0.035

Table C.4. (cont.)

ID	x	y	V	σ_V	B-V	σ_{B-V}
334	244.86	104.19	17.427	0.017	1.198	0.032
335	255.65	65.07	17.427	0.020	0.911	0.037
336	186.63	255.17	17.428	0.022	0.979	0.037
337	149.18	202.49	17.428	0.019	0.953	0.035
338	159.31	135.41	17.428	0.030	0.887	0.065
339	119.51	489.77	17.431	0.026	1.036	0.041
340	308.14	303.59	17.432	0.034	0.913	0.058
341	185.34	248.90	17.434	0.020	0.876	0.034
342	294.86	33.42	17.435	0.019	0.892	0.034
343	292.24	137.46	17.436	0.019	0.919	0.040
344	175.43	325.03	17.438	0.017	0.866	0.035
345	192.81	102.66	17.440	0.022	0.923	0.035
346	74.76	350.05	17.441	0.028	0.995	0.045
347	84.95	400.37	17.444	0.021	1.088	0.038
348	288.14	291.14	17.445	0.020	1.175	0.035
349	292.62	15.15	17.445	0.027	0.822	0.046
350	207.15	300.93	17.445	0.027	0.885	0.043
351	169.77	255.26	17.446	0.020	0.873	0.037
352	237.35	483.29	17.447	0.019	1.145	0.036
353	179.38	473.70	17.447	0.025	0.857	0.041
354	291.78	321.64	17.447	0.025	0.916	0.038
355	167.65	198.29	17.451	0.017	1.021	0.034
356	239.44	378.49	17.451	0.025	0.940	0.040
357	169.76	172.24	17.453	0.021	1.039	0.037
358	311.32	249.13	17.453	0.031	0.967	0.049
359	314.65	319.96	17.455	0.029	0.935	0.049
360	182.94	176.69	17.456	0.098	0.904	0.179
361	87.60	409.77	17.459	0.022	0.835	0.036
362	58.15	388.57	17.459	0.021	0.848	0.039
363	269.14	122.89	17.460	0.023	0.670	0.038
364	155.31	150.03	17.460	0.026	1.048	0.042
365	70.43	173.34	17.462	0.024	0.911	0.042
366	158.11	402.75	17.464	0.018	0.892	0.034
367	218.94	290.91	17.466	0.051	0.875	0.121
368	32.14	324.38	17.466	0.016	1.070	0.034
369	273.73	242.53	17.467	0.044	0.968	0.081
370	87.49	220.32	17.470	0.019	0.906	0.032

Table C.4. (cont.)

ID	x	y	V	σ_V	B-V	σ_{B-V}
371	242.09	286.08	17.470	0.194	0.494	0.323
372	145.84	120.25	17.471	0.015	0.886	0.031
373	195.03	442.99	17.472	0.019	1.060	0.031
374	71.25	182.21	17.473	0.022	0.870	0.038
375	196.55	309.22	17.473	0.020	0.898	0.035
376	124.38	107.92	17.474	0.020	1.105	0.042
377	297.72	283.52	17.474	0.044	1.018	0.073
378	282.40	338.67	17.476	0.019	1.119	0.035
379	137.77	121.67	17.477	0.035	0.782	0.057
380	205.18	14.34	17.478	0.016	1.103	0.031
381	198.94	347.62	17.480	0.021	1.091	0.036
382	148.74	199.51	17.480	0.019	0.882	0.035
383	227.65	107.25	17.481	0.016	0.911	0.031
384	92.85	63.99	17.483	0.025	1.115	0.042
385	222.79	201.68	17.489	0.025	1.044	0.046
386	238.89	54.64	17.490	0.023	1.068	0.058
387	159.49	179.66	17.490	0.018	0.891	0.031
388	293.70	374.73	17.490	0.029	1.128	0.045
389	271.21	277.75	17.494	0.023	0.913	0.039
390	16.98	335.07	17.495	0.022	1.021	0.038
391	166.09	178.15	17.497	0.033	0.845	0.061
392	257.78	342.47	17.497	0.020	0.932	0.034
393	193.99	463.22	17.497	0.020	0.859	0.035
394	74.97	190.82	17.499	0.024	0.837	0.038
395	156.94	174.70	17.499	0.019	1.034	0.032
396	252.96	154.54	17.500	0.021	0.893	0.036
397	158.90	134.80	17.500	0.093	0.972	0.190
398	174.02	312.87	17.500	0.023	0.928	0.040
399	79.79	24.51	17.500	0.027	1.017	0.047
400	14.16	82.44	17.502	0.030	1.059	0.067
401	138.88	345.44	17.504	0.016	0.839	0.030
402	182.60	119.72	17.504	0.017	0.919	0.033
403	307.61	218.21	17.504	0.025	1.037	0.043
404	205.86	191.40	17.504	0.018	0.898	0.034
405	229.83	138.57	17.513	0.020	0.931	0.034
406	210.98	206.76	17.514	0.028	0.946	0.043
407	193.71	157.62	17.514	0.024	0.880	0.043

Table C.4. (cont.)

ID	x	y	V	σ_V	B-V	σ_{B-V}
408	71.74	479.99	17.516	0.025	1.057	0.043
409	113.65	30.47	17.519	0.022	0.850	0.041
410	188.45	195.97	17.519	0.044	0.952	0.068
411	136.14	188.85	17.519	0.021	0.899	0.035
412	68.38	195.02	17.520	0.022	0.853	0.037
413	297.60	250.54	17.523	0.024	1.118	0.043
414	180.59	165.02	17.524	0.020	0.882	0.035
415	186.79	238.52	17.524	0.026	0.864	0.038
416	17.45	65.94	17.529	0.020	1.071	0.038
417	202.85	138.30	17.530	0.017	0.884	0.032
418	166.90	111.58	17.532	0.022	0.825	0.036
419	167.70	168.78	17.533	0.024	0.894	0.039
420	146.92	354.65	17.536	0.023	0.887	0.040
421	217.49	312.43	17.538	0.021	1.120	0.036
422	186.16	221.85	17.539	0.019	0.882	0.035
423	251.09	358.34	17.540	0.026	1.136	0.042
424	110.82	369.35	17.540	0.021	0.886	0.035
425	119.24	121.02	17.541	0.017	0.856	0.032
426	190.11	244.03	17.542	0.065	0.895	0.108
427	149.99	359.64	17.544	0.021	0.848	0.036
428	181.96	39.66	17.548	0.024	0.894	0.037
429	286.87	373.42	17.549	0.022	0.869	0.049
430	246.18	233.37	17.550	0.025	0.838	0.045
431	274.42	257.67	17.550	0.025	0.862	0.045
432	183.60	144.37	17.550	0.018	0.906	0.034
433	307.49	416.37	17.552	0.026	0.888	0.045
434	295.23	357.86	17.552	0.027	0.902	0.042
435	105.02	458.39	17.555	0.037	0.836	0.071
436	242.46	288.53	17.555	0.026	1.140	0.050
437	18.76	442.64	17.556	0.019	0.694	0.034
438	258.17	61.60	17.556	0.061	0.839	0.120
439	156.36	288.30	17.556	0.070	1.103	0.110
440	313.88	263.89	17.557	0.179	0.523	0.278
441	240.27	28.13	17.559	0.021	0.805	0.043
442	301.92	300.95	17.563	0.021	0.890	0.036
443	157.01	493.44	17.564	0.021	0.829	0.036
444	265.43	222.17	17.567	0.025	0.866	0.047

Table C.4. (cont.)

ID	x	y	V	σ_V	B-V	σ_{B-V}
445	299.07	177.53	17.568	0.317	0.985	0.481
446	128.04	414.08	17.569	0.022	0.904	0.038
447	100.24	289.26	17.572	0.019	0.888	0.036
448	79.22	98.75	17.574	0.019	0.854	0.034
449	167.11	100.04	17.575	0.026	0.880	0.043
450	94.10	279.96	17.580	0.020	0.923	0.044
451	314.80	307.85	17.581	0.031	1.079	0.050
452	272.42	438.56	17.581	0.040	0.884	0.063
453	78.08	272.82	17.581	0.302	1.001	0.403
454	133.73	274.96	17.586	0.024	0.726	0.038
455	209.28	315.13	17.586	0.022	0.881	0.036
456	235.69	177.76	17.587	0.032	0.860	0.056
457	153.69	388.46	17.588	0.019	0.860	0.038
458	140.21	274.33	17.590	0.016	0.851	0.031
459	122.10	357.09	17.590	0.024	1.104	0.042
460	115.03	373.10	17.590	0.023	0.841	0.035
461	307.21	185.57	17.596	0.032	0.876	0.059
462	167.46	354.97	17.600	0.027	0.865	0.049
463	142.00	3.62	17.600	0.020	0.888	0.036
464	5.89	25.29	17.600	0.020	0.916	0.039
465	261.77	110.08	17.601	0.020	0.874	0.040
466	146.04	238.89	17.602	0.028	0.938	0.046
467	105.83	458.26	17.604	0.093	0.838	0.208
468	245.49	329.51	17.605	0.020	0.934	0.040
469	281.40	451.93	17.605	0.025	0.861	0.043
470	212.12	309.52	17.606	0.049	0.837	0.095
471	131.53	85.29	17.608	0.019	0.773	0.035
472	239.03	302.18	17.608	0.044	0.890	0.076
473	95.79	358.02	17.608	0.018	0.843	0.034
474	291.52	495.94	17.608	0.024	0.863	0.039
475	100.81	197.60	17.611	0.020	0.856	0.038
476	241.27	417.45	17.612	0.018	0.878	0.034
477	279.61	416.19	17.615	0.018	0.855	0.035
478	146.39	335.80	17.616	0.022	0.882	0.038
479	235.90	364.65	17.618	0.019	0.906	0.034
480	63.03	106.90	17.619	0.017	0.823	0.031
481	313.59	256.24	17.621	0.047	0.889	0.078

Table C.4. (cont.)

ID	x	y	V	σ_V	B-V	σ_{B-V}
482	162.60	98.86	17.621	0.028	0.837	0.047
483	167.29	85.21	17.622	0.016	0.871	0.032
484	169.78	354.07	17.622	0.024	0.885	0.045
485	196.19	239.44	17.623	0.024	0.877	0.043
486	13.26	82.47	17.623	0.068	1.018	0.140
487	249.68	386.30	17.624	0.019	0.877	0.034
488	256.71	186.01	17.624	0.024	0.858	0.040
489	134.49	183.35	17.625	0.098	1.001	0.194
490	55.30	349.48	17.626	0.015	0.847	0.032
491	239.43	223.12	17.627	0.045	0.941	0.090
492	283.44	295.63	17.629	0.024	0.826	0.040
493	294.55	118.95	17.630	0.024	0.966	0.044
494	191.04	315.76	17.633	0.040	0.898	0.073
495	176.54	422.63	17.636	0.019	0.898	0.034
496	167.35	305.91	17.639	0.023	0.884	0.038
497	278.85	357.09	17.639	0.051	0.974	0.086
498	138.57	490.88	17.640	0.017	0.909	0.034
499	26.39	350.61	17.641	0.018	0.891	0.034
500	286.88	372.46	17.643	0.053	0.858	0.141
501	72.93	209.63	17.645	0.021	0.891	0.042
502	14.97	311.17	17.647	0.024	0.816	0.050
503	9.21	127.58	17.648	0.016	0.870	0.032
504	307.67	184.80	17.649	0.102	0.869	0.233
505	24.43	105.92	17.649	0.024	0.827	0.039
506	6.72	402.75	17.649	0.022	0.877	0.039
507	276.44	297.01	17.653	0.026	0.926	0.047
508	216.07	29.80	17.653	0.022	0.857	0.040
509	268.35	305.82	17.654	0.026	0.875	0.042
510	277.41	222.46	17.656	0.041	0.807	0.079
511	265.65	169.84	17.657	0.042	0.935	0.070
512	80.36	25.35	17.661	0.043	1.003	0.074
513	182.56	177.20	17.665	0.113	0.980	0.210
514	263.99	275.46	17.667	0.020	0.848	0.035
515	180.76	223.52	17.668	0.020	0.963	0.036
516	202.96	184.57	17.668	0.038	0.867	0.079
517	280.65	246.10	17.671	0.020	0.874	0.036
518	51.00	430.70	17.672	0.036	0.878	0.074

Table C.4. (cont.)

ID	x	y	V	σ_V	B-V	σ_{B-V}
519	284.16	145.09	17.673	0.020	0.859	0.036
520	273.76	353.58	17.676	0.022	0.857	0.040
521	94.26	119.42	17.680	0.051	1.379	0.171
522	194.90	211.92	17.681	0.025	0.865	0.042
523	180.59	284.49	17.684	0.018	0.879	0.032
524	164.57	117.70	17.685	0.021	0.865	0.035
525	237.94	279.95	17.688	0.032	0.889	0.048
526	187.53	294.65	17.689	0.063	0.846	0.094
527	288.30	444.39	17.689	0.021	0.772	0.038
528	106.68	390.83	17.693	0.017	0.873	0.030
529	178.42	21.81	17.695	0.031	0.835	0.049
530	203.73	226.27	17.697	0.021	0.905	0.036
531	223.95	176.75	17.700	0.022	0.873	0.038
532	42.11	173.78	17.701	0.023	0.914	0.045
533	260.27	351.45	17.702	0.029	0.750	0.049
534	50.87	55.78	17.704	0.044	0.704	0.071
535	311.46	69.51	17.704	0.034	0.892	0.056
536	159.41	39.17	17.707	0.020	0.726	0.035
537	191.56	163.24	17.707	0.022	0.858	0.040
538	14.26	468.18	17.707	0.038	1.519	0.095
539	286.33	407.58	17.709	0.022	0.883	0.038
540	314.36	432.98	17.710	0.041	0.846	0.075
541	313.83	357.29	17.711	0.044	0.862	0.083
542	240.04	420.87	17.716	0.020	0.892	0.036
543	74.35	392.42	17.718	0.021	0.849	0.038
544	204.57	216.40	17.719	0.027	0.931	0.042
545	277.63	495.62	17.723	0.021	0.875	0.043
546	201.94	184.63	17.723	0.039	0.868	0.082
547	275.10	258.63	17.723	0.033	0.890	0.060
548	192.09	63.49	17.724	0.019	0.893	0.036
549	104.68	244.94	17.725	0.038	0.861	0.055
550	304.38	357.14	17.726	0.033	0.852	0.059
551	218.15	274.59	17.729	0.026	0.921	0.044
552	219.32	343.15	17.729	0.031	0.873	0.049
553	77.32	426.28	17.730	0.020	0.983	0.038
554	190.50	316.40	17.733	0.043	0.867	0.077
555	84.96	303.99	17.734	0.033	0.877	0.051

Table C.4. (cont.)

ID	x	y	V	σ_V	B-V	σ_{B-V}
556	200.97	184.66	17.736	0.044	0.888	0.106
557	222.41	415.45	17.738	0.029	0.873	0.056
558	237.39	201.97	17.744	0.024	0.877	0.054
559	67.37	21.88	17.746	0.021	0.696	0.037
560	168.23	355.65	17.748	0.030	0.886	0.056
561	149.81	62.87	17.759	0.020	0.803	0.035
562	64.10	281.27	17.759	0.016	0.839	0.032
563	155.40	459.49	17.759	0.038	0.785	0.088
564	174.37	272.00	17.762	0.020	0.807	0.036
565	96.66	331.95	17.762	0.018	0.866	0.034
566	291.62	387.10	17.765	0.026	0.914	0.060
567	106.78	304.32	17.766	0.018	1.040	0.043
568	190.01	317.07	17.767	0.046	0.881	0.087
569	264.66	229.36	17.768	0.019	0.840	0.043
570	103.31	48.80	17.769	0.022	0.710	0.037
571	294.39	340.97	17.769	0.024	0.850	0.044
572	49.83	416.02	17.771	0.033	0.889	0.061
573	107.44	74.88	17.771	0.027	0.839	0.052
574	217.06	216.54	17.772	0.036	0.869	0.057
575	224.81	387.08	17.772	0.017	0.887	0.034
576	103.65	139.62	17.773	0.022	0.909	0.035
577	81.35	272.30	17.774	0.073	0.947	0.101
578	298.56	177.38	17.774	0.433	0.618	1.025
579	270.19	157.65	17.775	0.026	0.901	0.043
580	10.90	355.26	17.777	0.018	0.872	0.033
581	3.11	65.87	17.777	0.037	0.611	0.076
582	239.76	302.78	17.779	0.080	0.904	0.145
583	178.97	207.53	17.783	0.023	0.907	0.044
584	198.40	207.68	17.784	0.024	0.865	0.042
585	312.58	332.41	17.787	0.021	0.860	0.041
586	294.95	330.52	17.790	0.027	0.798	0.080
587	219.86	358.13	17.792	0.022	0.874	0.038
588	203.37	207.34	17.792	0.014	0.911	0.032
589	279.64	107.13	17.793	0.024	0.899	0.041
590	30.93	161.68	17.796	0.018	0.905	0.034
591	303.74	357.69	17.799	0.083	0.848	0.282
592	144.77	359.07	17.799	0.025	0.865	0.043

Table C.4. (cont.)

ID	x	y	V	σ_V	B-V	σ_{B-V}
593	249.83	193.76	17.801	0.020	0.871	0.038
594	64.58	70.59	17.803	0.020	0.871	0.039
595	240.82	155.48	17.803	0.024	0.887	0.041
596	173.70	11.69	17.806	0.024	0.837	0.039
597	267.85	260.89	17.807	0.025	0.864	0.042
598	153.15	387.47	17.807	0.021	0.854	0.044
599	174.01	368.18	17.808	0.020	0.889	0.034
600	253.28	310.93	17.809	0.045	0.934	0.077
601	270.26	372.24	17.810	0.020	0.894	0.035
602	174.70	218.82	17.810	0.050	0.845	0.086
603	262.02	482.34	17.813	0.036	0.942	0.063
604	228.35	263.43	17.813	0.020	0.820	0.036
605	115.41	23.01	17.815	0.022	0.818	0.037
606	31.87	384.66	17.819	0.024	0.859	0.063
607	182.30	177.68	17.821	0.149	0.885	0.280
608	286.67	55.63	17.823	0.056	0.790	0.122
609	104.03	64.95	17.829	0.023	0.848	0.037
610	203.83	295.75	17.835	0.031	0.887	0.049
611	136.71	311.86	17.837	0.022	0.953	0.038
612	158.70	370.48	17.839	0.030	0.897	0.056
613	212.03	463.97	17.839	0.028	0.919	0.050
614	54.53	378.51	17.839	0.021	0.880	0.038
615	215.10	296.87	17.843	0.024	0.876	0.039
616	119.45	254.74	17.845	0.044	0.929	0.071
617	236.71	418.43	17.845	0.019	0.836	0.036
618	121.79	79.85	17.846	0.022	0.874	0.039
619	164.95	283.46	17.851	0.019	0.890	0.035
620	202.02	171.43	17.851	0.045	0.954	0.076
621	237.33	56.04	17.851	0.031	1.007	0.069
622	203.99	271.19	17.853	0.022	0.897	0.041
623	119.64	255.67	17.854	0.026	0.818	0.052
624	98.28	31.09	17.854	0.022	0.889	0.038
625	185.21	222.74	17.854	0.023	0.798	0.042
626	44.85	29.53	17.855	0.016	0.862	0.035
627	234.65	225.06	17.856	0.039	0.877	0.077
628	169.58	221.31	17.857	0.019	0.873	0.040
629	249.79	437.48	17.858	0.023	0.885	0.044

Table C.4. (cont.)

ID	x	y	V	σ_V	B-V	σ_{B-V}
630	51.43	312.02	17.861	0.074	1.005	0.109
631	270.67	308.72	17.863	0.026	0.870	0.049
632	274.95	74.22	17.866	0.026	0.943	0.047
633	301.08	247.93	17.867	0.029	0.913	0.055
634	246.70	234.26	17.869	0.025	0.889	0.048
635	247.13	373.24	17.870	0.022	0.939	0.043
636	297.61	346.88	17.873	0.027	0.833	0.047
637	119.25	253.84	17.873	0.045	0.937	0.069
638	56.23	115.35	17.876	0.020	0.869	0.038
639	128.84	243.05	17.882	0.015	0.823	0.034
640	156.13	459.97	17.882	0.065	1.029	0.149
641	292.50	316.30	17.887	0.019	0.890	0.036
642	197.06	139.79	17.887	0.038	0.932	0.076
643	103.99	112.60	17.888	0.023	0.937	0.041
644	154.70	209.39	17.889	0.017	0.872	0.034
645	218.18	291.14	17.892	0.037	0.903	0.090
646	116.13	210.70	17.897	0.016	0.853	0.033
647	61.32	209.63	17.899	0.022	0.847	0.039
648	254.24	174.70	17.903	0.024	0.934	0.041
649	296.56	223.29	17.904	0.018	0.867	0.037
650	200.16	404.88	17.906	0.019	0.887	0.033
651	50.16	430.36	17.908	0.043	0.963	0.091
652	276.83	223.01	17.909	0.061	0.909	0.149
653	139.14	101.04	17.910	0.032	0.867	0.052
654	180.25	213.84	17.910	0.022	0.860	0.038
655	22.77	340.83	17.911	0.033	1.016	0.067
656	205.98	308.93	17.911	0.024	0.896	0.039
657	298.39	259.95	17.911	0.042	0.962	0.076
658	293.98	330.03	17.914	0.032	0.837	0.075
659	36.39	357.58	17.915	0.015	1.013	0.032
660	159.34	220.97	17.917	0.023	0.860	0.045
661	101.93	223.04	17.917	0.018	0.867	0.034
662	59.00	238.65	17.920	0.021	0.863	0.037
663	307.67	98.30	17.920	0.024	0.888	0.042
664	63.86	421.32	17.920	0.018	0.831	0.036
665	309.43	39.24	17.926	0.028	0.941	0.052
666	291.91	392.71	17.929	0.026	1.425	0.055

Table C.4. (cont.)

ID	x	y	V	σ_V	B-V	σ_{B-V}
667	93.46	119.51	17.931	0.068	1.049	0.182
668	141.07	189.86	17.935	0.041	0.908	0.068
669	212.68	310.05	17.936	0.042	0.817	0.109
670	87.17	184.71	17.936	0.026	0.883	0.046
671	179.28	408.24	17.938	0.020	0.874	0.036
672	131.22	305.87	17.942	0.021	0.834	0.042
673	63.54	31.48	17.943	0.016	0.891	0.034
674	68.17	342.99	17.944	0.022	0.848	0.040
675	277.31	296.23	17.944	0.034	0.929	0.064
676	276.87	82.22	17.949	0.019	-0.113	0.034
677	96.19	275.14	17.950	0.021	0.861	0.040
678	300.66	260.86	17.952	0.043	0.895	0.112
679	2.56	295.86	17.952	0.023	0.799	0.038
680	223.26	415.92	17.955	0.043	0.895	0.087
681	239.18	251.26	17.960	0.028	0.910	0.057
682	89.99	26.03	17.961	0.029	0.860	0.054
683	295.79	145.76	17.963	0.021	0.978	0.041
684	217.48	291.36	17.964	0.093	0.875	0.226
685	265.42	182.00	17.966	0.047	0.871	0.106
686	136.06	254.37	17.967	0.018	0.932	0.034
687	208.74	333.82	17.969	0.026	0.939	0.043
688	275.08	290.01	17.970	0.024	0.863	0.046
689	287.15	377.17	17.970	0.021	0.963	0.043
690	34.81	367.01	17.973	0.021	0.835	0.036
691	143.85	360.06	17.975	0.060	0.898	0.119
692	136.60	180.73	17.975	0.021	0.910	0.039
693	215.33	164.08	17.978	0.027	0.938	0.043
694	92.78	119.64	17.980	0.105	0.657	0.200
695	67.40	252.44	17.980	0.024	0.916	0.043
696	168.98	356.32	17.985	0.036	0.719	0.068
697	164.13	436.47	17.986	0.024	0.887	0.045
698	311.98	338.81	17.986	0.019	0.820	0.033
699	294.21	154.10	17.986	0.027	0.917	0.049
700	310.16	159.17	17.987	0.020	0.915	0.050
701	210.66	348.42	17.989	0.022	0.907	0.036
702	115.26	119.78	17.992	0.023	0.851	0.043
703	105.01	387.51	17.992	0.019	0.892	0.033

Table C.4. (cont.)

ID	x	y	V	σ_V	B-V	σ_{B-V}
704	151.14	280.95	17.993	0.026	0.858	0.042
705	316.13	270.84	17.993	0.066	0.812	0.098
706	218.86	266.21	17.994	0.021	0.883	0.043
707	118.71	310.71	17.995	0.020	0.885	0.038
708	183.51	414.00	17.999	0.021	0.872	0.039
709	258.51	43.58	17.999	0.454	0.231	0.612
710	247.37	174.37	18.000	0.033	0.822	0.066
711	279.22	34.17	18.001	0.030	0.917	0.067
712	235.51	22.37	18.003	0.015	0.869	0.027
713	25.50	311.47	18.004	0.018	0.913	0.038
714	154.01	263.10	18.004	0.015	0.902	0.036
715	117.23	104.51	18.006	0.016	0.857	0.034
716	154.35	246.00	18.008	0.024	0.927	0.045
717	201.12	172.04	18.010	0.085	0.918	0.146
718	222.39	297.79	18.014	0.024	0.869	0.042
719	3.69	151.36	18.015	0.018	0.887	0.037
720	147.89	255.76	18.015	0.020	0.945	0.037
721	214.67	172.79	18.016	0.015	0.892	0.029
722	21.69	145.71	18.017	0.019	0.749	0.034
723	196.13	139.54	18.017	0.043	0.901	0.077
724	180.78	100.53	18.018	0.020	0.882	0.041
725	238.63	152.23	18.021	0.027	0.818	0.046
726	298.47	54.08	18.026	0.023	0.939	0.039
727	291.86	338.97	18.027	0.027	0.918	0.055
728	160.93	103.39	18.031	0.018	0.796	0.034
729	292.49	386.60	18.037	0.037	0.896	0.094
730	242.73	40.64	18.038	0.026	0.877	0.048
731	129.89	420.35	18.041	0.020	0.891	0.032
732	98.07	184.26	18.043	0.013	0.899	0.039
733	39.29	70.10	18.045	0.022	0.954	0.035
734	22.44	419.91	18.047	0.018	0.862	0.033
735	253.81	88.89	18.048	0.022	0.882	0.036
736	56.23	499.83	18.049	0.019	0.898	0.036
737	184.81	327.66	18.054	0.024	0.940	0.040
738	165.10	98.04	18.054	0.033	0.905	0.062
739	81.58	111.80	18.054	0.023	0.842	0.037
740	43.08	174.29	18.055	0.036	0.918	0.069

Table C.4. (cont.)

ID	x	y	V	σ_V	B-V	σ_{B-V}
741	279.01	293.57	18.056	0.034	0.883	0.051
742	186.26	369.99	18.056	0.019	0.838	0.033
743	226.11	327.38	18.061	0.028	0.967	0.052
744	228.50	102.26	18.061	0.022	0.831	0.043
745	270.97	96.26	18.062	0.016	0.943	0.036
746	121.15	481.37	18.064	0.027	1.567	0.046
747	279.75	200.86	18.064	0.019	0.931	0.037
748	155.43	177.88	18.070	0.032	1.002	0.047
749	199.15	246.16	18.071	0.015	0.845	0.030
750	292.08	459.54	18.073	0.024	0.876	0.041
751	310.57	427.56	18.074	0.030	0.927	0.046
752	251.49	355.89	18.075	0.032	0.917	0.051
753	261.30	297.91	18.075	0.019	0.889	0.033
754	300.53	500.02	18.077	0.031	0.632	0.077
755	281.84	90.09	18.078	0.015	0.863	0.035
756	233.61	246.78	18.078	0.036	0.779	0.061
757	67.94	328.20	18.080	0.019	1.163	0.034
758	31.11	364.11	18.082	0.013	0.856	0.028
759	284.38	169.04	18.083	0.016	0.878	0.032
760	311.26	302.43	18.085	0.067	0.832	0.113
761	146.24	357.03	18.087	0.032	0.858	0.052
762	111.65	172.86	18.089	0.017	0.914	0.029
763	81.61	221.58	18.091	0.014	0.873	0.029
764	251.89	30.43	18.092	0.038	0.820	0.061
765	247.81	135.67	18.093	0.022	0.941	0.067
766	236.72	177.74	18.094	0.036	0.932	0.073
767	296.43	9.51	18.097	0.016	0.845	0.035
768	227.59	478.83	18.101	0.028	0.917	0.046
769	309.29	228.08	18.102	0.019	0.883	0.050
770	126.94	287.48	18.104	0.022	0.935	0.038
771	230.01	8.09	18.105	0.016	0.858	0.031
772	111.81	221.15	18.105	0.020	0.983	0.035
773	31.08	385.29	18.106	0.044	0.966	0.104
774	167.73	210.72	18.107	0.019	0.882	0.042
775	287.32	338.71	18.108	0.024	0.920	0.043
776	290.52	477.60	18.108	0.027	0.862	0.041
777	259.88	142.63	18.108	0.021	0.922	0.038

Table C.4. (cont.)

ID	x	y	V	σ_V	B-V	σ_{B-V}
778	177.20	332.02	18.108	0.018	0.909	0.035
779	132.75	30.31	18.109	0.016	0.666	0.034
780	196.86	267.99	18.110	0.019	1.030	0.033
781	163.73	221.66	18.114	0.019	0.859	0.039
782	119.86	108.58	18.117	0.019	0.895	0.035
783	22.70	339.89	18.117	0.043	1.063	0.089
784	122.72	144.08	18.119	0.019	0.894	0.037
785	7.16	472.82	18.122	0.029	0.867	0.048
786	282.55	273.45	18.123	0.034	0.814	0.054
787	259.70	236.25	18.124	0.021	0.929	0.038
788	289.97	260.78	18.124	0.022	0.908	0.036
789	235.21	213.46	18.125	0.027	0.931	0.056
790	272.34	156.39	18.125	0.029	0.882	0.049
791	312.30	296.59	18.127	0.182	1.851	0.433
792	173.51	156.62	18.128	0.018	0.909	0.031
793	298.41	38.51	18.133	0.034	0.885	0.064
794	272.66	232.74	18.138	0.025	0.885	0.039
795	136.29	227.88	18.138	0.015	0.950	0.038
796	90.43	334.92	18.139	0.032	0.903	0.052
797	254.15	311.09	18.141	0.068	0.902	0.124
798	178.83	366.26	18.144	0.019	0.710	0.032
799	193.78	119.78	18.147	0.019	0.865	0.033
800	272.78	207.95	18.149	0.019	0.891	0.033
801	125.02	360.68	18.156	0.019	0.898	0.033
802	293.69	409.35	18.160	0.019	0.882	0.034
803	84.55	205.31	18.164	0.015	1.023	0.136
804	175.98	430.34	18.166	0.023	0.868	0.042
805	289.15	66.45	18.167	0.036	0.992	0.054
806	241.52	20.73	18.173	0.049	0.914	0.098
807	186.20	232.58	18.173	0.018	0.855	0.030
808	157.02	45.31	18.173	0.019	0.858	0.036
809	118.39	138.03	18.174	0.024	0.940	0.046
810	166.39	200.46	18.174	0.017	0.966	0.038
811	20.37	77.06	18.176	0.017	0.804	0.035
812	302.80	129.15	18.177	0.028	0.970	0.054
813	103.67	168.11	18.178	0.020	0.865	0.034
814	252.86	213.89	18.179	0.055	0.907	0.081

Table C.4. (cont.)

ID	x	y	V	σ_V	B-V	σ_{B-V}
815	205.99	273.21	18.180	0.021	0.890	0.039
816	234.47	173.60	18.181	0.021	0.892	0.034
817	45.88	281.51	18.181	0.021	0.894	0.037
818	229.82	493.79	18.187	0.028	0.887	0.049
819	127.27	137.76	18.188	0.053	0.850	0.088
820	181.24	377.28	18.188	0.019	0.918	0.033
821	116.52	113.40	18.189	0.017	0.845	0.033
822	243.45	306.06	18.189	0.038	0.894	0.063
823	84.12	122.17	18.190	0.029	0.929	0.048
824	247.43	457.99	18.193	0.021	0.901	0.041
825	290.84	492.64	18.197	0.028	0.902	0.045
826	295.94	46.70	18.205	0.031	1.285	0.056
827	221.99	288.35	18.210	0.017	0.898	0.034
828	274.70	182.54	18.211	0.020	0.912	0.036
829	313.15	186.46	18.213	0.021	0.882	0.053
830	173.15	19.14	18.215	0.022	0.894	0.048
831	181.59	335.06	18.215	0.026	1.034	0.048
832	185.37	438.24	18.216	0.019	1.163	0.037
833	215.84	240.66	18.216	0.020	0.778	0.033
834	154.49	460.26	18.216	0.032	0.886	0.083
835	175.01	251.97	18.218	0.023	0.895	0.037
836	227.85	148.18	18.219	0.018	0.882	0.034
837	188.93	285.27	18.221	0.019	0.898	0.034
838	249.35	258.00	18.222	0.055	0.903	0.106
839	167.70	274.43	18.223	0.019	0.887	0.033
840	272.16	426.31	18.223	0.022	0.864	0.038
841	89.86	284.87	18.224	0.020	0.883	0.034
842	207.26	187.36	18.225	0.027	0.905	0.047
843	202.90	89.38	18.227	0.016	0.898	0.029
844	171.42	151.97	18.228	0.023	0.935	0.043
845	98.95	39.79	18.228	0.016	0.876	0.028
846	312.60	384.63	18.229	0.020	0.994	0.037
847	117.24	200.38	18.230	0.025	0.927	0.044
848	163.70	230.15	18.236	0.015	0.936	0.030
849	197.98	488.31	18.236	0.020	0.900	0.036
850	265.53	241.51	18.237	0.077	0.909	0.110
851	268.52	492.46	18.237	0.077	0.867	0.145

Table C.4. (cont.)

ID	x	y	V	σ_V	B-V	σ_{B-V}
852	194.25	272.30	18.243	0.019	0.994	0.036
853	31.15	172.02	18.245	0.019	0.894	0.036
854	267.53	436.41	18.245	0.018	1.245	0.039
855	157.35	211.95	18.247	0.021	0.916	0.042
856	158.42	365.11	18.248	0.050	1.050	0.109
857	233.38	164.90	18.248	0.029	0.900	0.049
858	176.49	245.37	18.249	0.019	0.887	0.035
859	152.27	327.98	18.250	0.019	0.880	0.034
860	58.93	477.98	18.250	0.020	0.905	0.038
861	145.36	36.92	18.251	0.015	0.878	0.057
862	184.49	306.67	18.253	0.017	0.881	0.037
863	253.80	51.07	18.253	0.048	0.967	0.102
864	257.70	190.06	18.256	0.022	0.873	0.038
865	285.84	33.02	18.256	0.022	0.922	0.038
866	115.44	442.56	18.258	0.019	0.997	0.034
867	41.88	291.97	18.259	0.016	0.769	0.029
868	249.95	154.20	18.264	0.022	0.898	0.046
869	212.86	254.80	18.267	0.033	0.912	0.056
870	256.98	137.46	18.268	0.021	0.940	0.034
871	99.82	296.73	18.268	0.016	0.851	0.035
872	293.74	415.03	18.273	0.020	0.860	0.033
873	261.80	222.36	18.275	0.035	0.853	0.068
874	134.95	183.79	18.278	0.074	0.916	0.241
875	155.69	277.02	18.278	0.023	0.905	0.040
876	45.72	285.98	18.279	0.019	0.925	0.035
877	6.89	255.32	18.280	0.016	0.806	0.034
878	311.62	469.99	18.282	0.035	0.885	0.061
879	36.70	403.86	18.283	0.015	1.533	0.038
880	301.30	46.74	18.286	0.023	0.868	0.043
881	217.50	218.57	18.286	0.049	1.066	0.083
882	305.43	325.12	18.286	0.024	0.917	0.044
883	264.66	191.65	18.292	0.048	0.914	0.085
884	120.51	129.25	18.292	0.023	0.891	0.041
885	254.27	283.52	18.295	0.023	0.903	0.042
886	135.07	342.60	18.297	0.023	0.863	0.040
887	148.03	375.61	18.299	0.022	0.972	0.039
888	217.49	384.61	18.301	0.019	0.952	0.036

Table C.4. (cont.)

ID	x	y	V	σ_V	B-V	σ_{B-V}
889	111.13	85.08	18.301	0.017	0.892	0.033
890	212.50	247.09	18.303	0.045	1.033	0.078
891	309.21	329.30	18.306	0.028	0.932	0.051
892	133.30	393.02	18.308	0.019	0.787	0.033
893	136.77	139.92	18.308	0.019	0.905	0.031
894	239.90	117.87	18.312	0.021	0.978	0.038
895	267.03	164.06	18.313	0.115	0.768	0.225
896	263.95	76.85	18.314	0.020	0.902	0.035
897	229.60	29.20	18.315	0.018	0.854	0.036
898	68.58	156.00	18.316	0.021	0.725	0.038
899	71.86	106.88	18.317	0.033	0.860	0.053
900	129.72	126.47	18.321	0.014	1.453	0.037
901	236.04	86.35	18.322	0.016	0.904	0.049
902	109.28	430.84	18.324	0.017	0.905	0.033
903	299.91	261.83	18.325	0.108	0.995	0.332
904	178.81	33.57	18.326	0.020	0.896	0.035
905	230.21	320.83	18.328	0.022	0.944	0.043
906	72.96	235.26	18.330	0.017	1.006	0.039
907	164.91	332.34	18.334	0.017	0.871	0.032
908	271.92	82.06	18.335	0.034	0.963	0.071
909	71.06	400.41	18.336	0.025	0.895	0.043
910	72.77	302.52	18.338	0.019	0.917	0.037
911	199.70	147.53	18.339	0.015	0.920	0.031
912	251.13	316.67	18.341	0.019	0.886	0.033
913	304.09	206.62	18.342	0.021	0.943	0.045
914	137.49	272.45	18.343	0.020	0.867	0.044
915	89.76	246.26	18.343	0.029	0.863	0.056
916	209.22	269.74	18.345	0.015	0.945	0.033
917	138.73	321.25	18.346	0.015	0.895	0.031
918	165.70	224.18	18.346	0.024	0.920	0.053
919	223.83	72.97	18.346	0.030	0.831	0.046
920	180.84	437.87	18.348	0.021	0.903	0.036
921	220.55	230.33	18.350	0.018	0.887	0.036
922	4.61	118.83	18.350	0.022	0.880	0.042
923	246.88	113.65	18.351	0.038	0.962	0.071
924	235.86	167.76	18.353	0.021	0.908	0.035
925	98.52	283.48	18.353	0.046	1.109	0.126

Table C.4. (cont.)

ID	x	y	V	σ_V	B-V	σ_{B-V}
926	99.93	217.75	18.354	0.022	0.990	0.045
927	208.29	90.89	18.354	0.021	0.894	0.039
928	47.78	259.02	18.355	0.019	0.957	0.034
929	240.74	352.29	18.355	0.019	0.840	0.035
930	98.10	114.63	18.359	0.024	0.912	0.038
931	278.08	299.76	18.359	0.025	0.996	0.044
932	205.09	129.82	18.361	0.041	0.851	0.074
933	159.58	366.25	18.366	0.027	0.738	0.048
934	298.54	111.13	18.369	0.054	0.916	0.100
935	236.13	330.77	18.369	0.019	0.907	0.037
936	264.58	182.42	18.369	0.067	1.026	0.153
937	37.44	300.38	18.372	0.016	0.831	0.033
938	104.24	5.97	18.374	0.017	0.859	0.035
939	9.76	281.51	18.375	0.018	0.908	0.035
940	204.72	245.39	18.382	0.019	0.972	0.035
941	100.86	249.16	18.384	0.020	0.896	0.035
942	134.79	102.54	18.387	0.029	0.676	0.047
943	214.93	207.75	18.394	0.025	0.944	0.043
944	151.61	276.28	18.394	0.019	0.936	0.037
945	213.21	317.73	18.396	0.029	0.780	0.047
946	203.62	25.01	18.400	0.023	0.874	0.045
947	74.86	114.29	18.401	0.025	0.908	0.044
948	252.18	347.27	18.401	0.014	0.887	0.030
949	101.33	333.91	18.402	0.035	0.833	0.069
950	263.44	371.22	18.402	0.021	0.935	0.038
951	121.64	52.73	18.403	0.018	0.952	0.035
952	166.92	286.37	18.403	0.020	0.889	0.039
953	197.55	216.60	18.403	0.040	1.065	0.073
954	181.72	298.57	18.406	0.019	0.885	0.036
955	247.27	399.97	18.409	0.025	0.941	0.042
956	313.73	155.90	18.413	0.025	0.918	0.051
957	5.99	222.28	18.415	0.025	0.904	0.050
958	154.68	255.73	18.420	0.019	0.921	0.037
959	86.09	153.33	18.420	0.043	0.881	0.069
960	28.10	312.35	18.421	0.021	0.923	0.048
961	297.31	483.48	18.422	0.075	0.901	0.143
962	245.35	353.93	18.425	0.017	0.922	0.033

Table C.4. (cont.)

ID	x	y	V	σ_V	B-V	σ_{B-V}
963	259.75	221.61	18.429	0.038	0.943	0.079
964	221.02	99.55	18.430	0.014	1.006	0.033
965	214.90	159.73	18.431	0.019	0.949	0.035
966	43.99	70.32	18.434	0.013	1.190	0.031
967	35.37	181.23	18.434	0.020	0.899	0.035
968	94.71	50.41	18.434	0.020	0.905	0.038
969	26.31	35.54	18.437	0.017	0.868	0.033
970	298.08	341.92	18.438	0.101	0.789	0.145
971	192.31	219.77	18.438	0.016	0.880	0.035
972	74.17	326.41	18.440	0.019	0.949	0.031
973	274.58	110.35	18.443	0.019	0.971	0.035
974	300.82	327.35	18.444	0.069	1.048	0.130
975	210.13	63.82	18.446	0.024	0.926	0.040
976	216.28	72.45	18.447	0.022	0.911	0.046
977	183.93	98.62	18.449	0.024	0.993	0.053
978	150.72	350.61	18.450	0.021	0.889	0.038
979	262.19	197.71	18.455	0.025	0.898	0.048
980	205.58	380.20	18.458	0.019	0.916	0.033
981	290.92	178.97	18.458	0.043	0.889	0.064
982	206.82	252.01	18.464	0.023	0.916	0.040
983	132.30	369.82	18.472	0.026	0.940	0.044
984	258.30	201.58	18.473	0.022	0.868	0.042
985	61.00	58.63	18.476	0.132	-0.451	0.270
986	310.25	216.79	18.478	0.042	0.972	0.066
987	86.69	186.70	18.478	0.032	1.010	0.056
988	111.32	490.53	18.480	0.021	0.877	0.041
989	254.07	18.12	18.483	0.018	0.880	0.036
990	149.39	262.78	18.484	0.038	1.054	0.062
991	224.79	308.04	18.486	0.032	0.994	0.055
992	113.31	218.31	18.492	0.024	1.037	0.043
993	241.99	277.88	18.492	0.019	0.911	0.044
994	266.18	207.41	18.495	0.023	0.959	0.056
995	210.82	253.15	18.495	0.032	0.913	0.055
996	149.38	250.42	18.500	0.019	0.978	0.038
997	261.07	184.27	18.500	0.027	0.913	0.055
998	217.98	157.54	18.500	0.019	0.976	0.037
999	183.19	319.81	18.505	0.021	0.917	0.039

Table C.4. (cont.)

ID	x	y	V	σ_V	B-V	σ_{B-V}
1000	192.85	54.96	18.508	0.031	0.856	0.050
1001	200.89	431.38	18.509	0.015	0.849	0.036
1002	250.71	271.67	18.510	0.026	0.927	0.047
1003	199.38	381.80	18.513	0.021	0.902	0.038
1004	243.79	492.02	18.519	0.025	0.966	0.040
1005	246.93	479.31	18.521	0.026	0.914	0.048
1006	73.46	101.38	18.522	0.021	0.952	0.040
1007	192.78	226.85	18.522	0.018	0.987	0.033
1008	238.11	338.99	18.523	0.020	0.965	0.038
1009	167.20	90.98	18.524	0.021	0.912	0.039
1010	144.78	214.05	18.528	0.041	1.025	0.072
1011	86.31	307.95	18.529	0.034	0.956	0.061
1012	205.40	255.64	18.529	0.024	0.840	0.043
1013	188.71	134.56	18.531	0.020	0.922	0.038
1014	237.40	154.66	18.533	0.036	0.890	0.058
1015	171.53	206.58	18.536	0.019	0.892	0.034
1016	157.71	386.25	18.538	0.023	1.099	0.043
1017	231.27	41.69	18.546	0.020	0.967	0.039
1018	166.49	243.13	18.551	0.020	0.966	0.035
1019	123.11	269.20	18.551	0.019	1.023	0.039
1020	132.59	216.33	18.558	0.022	0.947	0.042
1021	301.05	159.10	18.559	0.027	0.895	0.071
1022	135.16	12.82	18.559	0.050	1.070	0.081
1023	59.03	126.73	18.562	0.030	0.874	0.060
1024	288.74	74.95	18.565	0.033	1.017	0.071
1025	201.03	327.52	18.568	0.025	0.779	0.046
1026	138.82	498.67	18.568	0.016	0.929	0.033
1027	250.58	419.25	18.571	0.022	0.956	0.038
1028	35.38	407.60	18.572	0.019	1.311	0.040
1029	288.70	208.23	18.572	0.020	1.008	0.038
1030	190.08	198.10	18.574	0.039	1.012	0.073
1031	222.33	340.29	18.576	0.043	0.948	0.077
1032	300.81	163.68	18.578	0.038	0.996	0.077
1033	204.83	397.13	18.581	0.026	0.945	0.050
1034	111.64	53.05	18.583	0.025	0.858	0.043
1035	134.99	313.91	18.583	0.028	0.704	0.045
1036	284.00	261.66	18.583	0.021	0.974	0.037

Table C.4. (cont.)

ID	x	y	V	σ_V	B-V	σ_{B-V}
1037	203.95	313.51	18.585	0.026	0.917	0.049
1038	217.18	252.09	18.586	0.032	0.801	0.053
1039	296.05	503.08	18.586	0.039	0.918	0.092
1040	12.69	68.33	18.591	0.030	0.872	0.054
1041	296.57	76.79	18.593	0.059	1.118	0.087
1042	121.22	289.36	18.600	0.024	0.925	0.039
1043	119.27	140.24	18.602	0.034	0.883	0.061
1044	145.05	476.45	18.604	0.030	0.912	0.048
1045	152.21	218.24	18.606	0.019	0.918	0.046
1046	220.86	166.83	18.614	0.050	0.896	0.073
1047	309.63	210.79	18.616	0.028	0.944	0.047
1048	200.17	291.74	18.617	0.027	0.987	0.048
1049	245.40	375.36	18.617	0.030	0.962	0.058
1050	270.06	287.65	18.618	0.025	0.931	0.049
1051	206.99	130.50	18.619	0.031	0.978	0.051
1052	164.81	384.83	18.629	0.019	1.003	0.038
1053	253.59	194.29	18.631	0.027	1.015	0.048
1054	304.27	312.92	18.632	0.030	0.801	0.050
1055	132.30	234.04	18.637	0.019	1.010	0.036
1056	214.11	47.77	18.642	0.024	0.930	0.048
1057	59.18	378.48	18.646	0.027	0.832	0.051
1058	279.73	240.22	18.646	0.035	0.904	0.084
1059	95.22	127.14	18.650	0.024	0.855	0.040
1060	220.86	285.22	18.652	0.020	0.940	0.043
1061	278.45	77.37	18.653	0.029	0.944	0.059
1062	192.95	371.27	18.656	0.035	0.891	0.067
1063	200.13	227.17	18.656	0.038	0.949	0.063
1064	134.66	344.72	18.657	0.019	0.938	0.038
1065	75.66	163.91	18.658	0.024	0.941	0.044
1066	138.82	109.61	18.661	0.015	1.592	0.047
1067	198.88	361.68	18.662	0.026	0.966	0.044
1068	154.54	341.93	18.665	0.020	0.948	0.037
1069	32.78	101.15	18.665	0.017	0.877	0.053
1070	281.34	93.46	18.669	0.020	0.911	0.046
1071	248.56	334.47	18.675	0.023	0.997	0.047
1072	225.62	12.10	18.676	0.030	0.917	0.048
1073	262.01	191.86	18.676	0.031	1.006	0.057

Table C.4. (cont.)

ID	x	y	V	σ_V	B-V	σ_{B-V}
1074	240.16	19.73	18.678	0.074	1.047	0.159
1075	267.91	111.06	18.678	0.024	0.997	0.041
1076	53.12	403.64	18.679	0.017	0.922	0.036
1077	158.56	419.02	18.679	0.026	0.774	0.050
1078	160.72	159.94	18.680	0.025	0.930	0.042
1079	194.64	295.69	18.683	0.026	0.956	0.053
1080	199.14	149.80	18.685	0.022	0.935	0.040
1081	178.49	325.91	18.685	0.027	0.921	0.055
1082	68.20	169.41	18.686	0.023	0.898	0.046
1083	64.86	307.75	18.686	0.023	0.927	0.042
1084	127.65	224.27	18.687	0.022	0.922	0.043
1085	150.64	420.79	18.687	0.024	0.972	0.041
1086	134.91	167.45	18.687	0.014	0.911	0.037
1087	4.55	407.27	18.690	0.023	0.938	0.051
1088	185.04	339.80	18.691	0.077	0.903	0.145
1089	130.56	291.64	18.695	0.019	1.078	0.040
1090	230.07	333.38	18.698	0.047	0.947	0.082
1091	224.09	169.38	18.702	0.024	1.020	0.051
1092	260.32	199.37	18.703	0.018	0.984	0.045
1093	282.21	140.05	18.703	0.028	0.983	0.073
1094	297.81	485.38	18.704	0.108	0.740	0.211
1095	123.30	238.20	18.707	0.141	1.158	0.219
1096	278.49	101.21	18.707	0.034	0.935	0.063
1097	249.41	174.63	18.709	0.017	1.108	0.083
1098	204.21	117.44	18.712	0.017	1.030	0.037
1099	285.89	63.30	18.721	0.032	0.952	0.057
1100	262.16	496.69	18.723	0.663	0.503	0.973
1101	135.84	175.58	18.725	0.019	1.005	0.041
1102	281.02	264.51	18.726	0.024	1.105	0.042
1103	303.25	253.54	18.727	0.035	0.976	0.058
1104	14.18	385.06	18.729	0.022	0.917	0.047
1105	190.01	118.82	18.730	0.025	0.994	0.048
1106	36.51	153.33	18.730	0.030	0.983	0.056
1107	207.09	420.28	18.732	0.022	0.962	0.047
1108	273.68	84.25	18.732	0.026	0.921	0.055
1109	287.17	480.53	18.733	0.018	0.909	0.040
1110	248.99	163.40	18.739	0.019	1.032	0.048

Table C.4. (cont.)

ID	x	y	V	σ_V	B-V	σ_{B-V}
1111	243.58	441.91	18.742	0.013	0.837	0.040
1112	91.50	229.79	18.742	0.022	0.909	0.040
1113	222.07	458.76	18.742	0.014	0.918	0.034
1114	172.59	34.05	18.745	0.017	0.871	0.039
1115	299.31	126.64	18.746	0.039	1.006	0.127
1116	185.83	118.50	18.751	0.031	1.037	0.056
1117	248.99	447.23	18.751	0.025	0.775	0.043
1118	162.84	49.38	18.753	0.035	0.917	0.055
1119	176.91	171.57	18.757	0.027	1.066	0.056
1120	241.02	389.10	18.760	0.023	0.874	0.046
1121	51.94	337.94	18.762	0.018	0.715	0.035
1122	213.05	431.43	18.766	0.038	0.953	0.071
1123	83.57	213.57	18.766	0.022	0.989	0.053
1124	207.34	125.94	18.769	0.027	0.761	0.046
1125	237.96	236.68	18.774	0.029	0.871	0.053
1126	130.54	299.56	18.775	0.047	0.859	0.091
1127	211.90	139.98	18.777	0.059	1.025	0.090
1128	255.46	104.81	18.778	0.080	0.996	0.121
1129	310.17	190.25	18.783	0.043	1.029	0.080
1130	83.67	41.67	18.785	0.019	0.948	0.044
1131	7.96	240.00	18.788	0.025	0.984	0.052
1132	13.52	473.06	18.793	0.024	0.887	0.054
1133	124.98	311.27	18.794	0.022	0.993	0.049
1134	300.53	494.75	18.797	0.052	0.926	0.111
1135	195.08	148.70	18.798	0.019	0.948	0.037
1136	259.92	127.72	18.798	0.039	0.916	0.081
1137	244.27	401.37	18.799	0.027	0.981	0.048
1138	280.74	155.03	18.800	0.032	1.405	0.063
1139	76.88	495.97	18.801	0.032	0.908	0.058
1140	194.15	19.51	18.802	0.049	0.911	0.070
1141	60.67	188.40	18.805	0.054	0.926	0.104
1142	28.69	217.73	18.806	0.019	0.929	0.040
1143	109.76	492.68	18.808	0.025	1.434	0.060
1144	109.07	116.87	18.810	0.029	0.876	0.047
1145	196.73	86.02	18.811	0.026	0.958	0.050
1146	293.68	107.14	18.811	0.024	0.965	0.042
1147	170.83	189.29	18.811	0.021	0.994	0.053

Table C.4. (cont.)

ID	x	y	V	σ_V	B-V	σ_{B-V}
1148	205.22	390.60	18.816	0.026	1.029	0.045
1149	94.30	47.82	18.819	0.026	0.980	0.049
1150	303.86	3.12	18.821	0.026	0.909	0.054
1151	98.28	177.66	18.822	0.027	0.967	0.045
1152	70.16	270.38	18.823	0.027	0.974	0.052
1153	236.07	73.62	18.825	0.045	1.023	0.091
1154	249.41	105.35	18.828	0.019	0.949	0.046
1155	158.95	56.59	18.830	0.026	0.892	0.042
1156	24.02	428.95	18.831	0.025	0.795	0.041
1157	70.62	56.06	18.832	0.266	-0.604	0.454
1158	53.44	380.69	18.837	0.033	1.011	0.064
1159	37.36	280.30	18.843	0.030	0.935	0.050
1160	152.63	205.33	18.846	0.022	0.907	0.048
1161	19.81	388.50	18.850	0.019	0.996	0.045
1162	258.17	37.13	18.852	0.263	-0.221	0.428
1163	60.74	267.07	18.854	0.023	0.959	0.044
1164	93.14	11.17	18.857	0.035	0.929	0.064
1165	135.01	362.31	18.858	0.026	0.789	0.048
1166	177.78	463.59	18.860	0.018	0.994	0.042
1167	16.10	232.49	18.863	0.019	0.940	0.042
1168	270.80	411.39	18.865	0.025	0.963	0.052
1169	220.79	221.22	18.869	0.041	0.959	0.070
1170	195.90	158.29	18.869	0.056	1.017	0.083
1171	199.54	261.76	18.870	0.032	1.010	0.055
1172	289.99	285.88	18.876	0.080	0.965	0.131
1173	97.10	494.02	18.877	0.022	1.016	0.050
1174	145.33	146.04	18.881	0.020	1.002	0.051
1175	312.77	239.33	18.881	0.053	1.020	0.106
1176	199.43	64.92	18.881	0.031	0.877	0.055
1177	176.57	369.68	18.884	0.040	1.015	0.064
1178	228.49	243.42	18.884	0.019	1.029	0.040
1179	232.97	281.50	18.885	0.018	1.096	0.036
1180	24.20	257.14	18.887	0.019	1.005	0.038
1181	133.49	318.18	18.887	0.022	0.930	0.042
1182	113.82	482.62	18.888	0.027	0.874	0.045
1183	227.86	308.30	18.893	0.036	1.037	0.071
1184	43.99	387.96	18.894	0.020	1.008	0.051

Table C.4. (cont.)

ID	x	y	V	σ_V	B-V	σ_{B-V}
1185	300.28	410.88	18.895	0.068	0.900	0.122
1186	277.65	370.00	18.895	0.038	1.065	0.065
1187	80.51	352.11	18.896	0.015	0.999	0.041
1188	86.73	98.54	18.897	0.042	0.917	0.078
1189	230.50	344.30	18.898	0.021	1.012	0.047
1190	295.43	71.75	18.906	0.191	4.485	0.439
1191	184.79	218.38	18.906	0.097	0.996	0.181
1192	6.78	204.31	18.907	0.020	0.916	0.039
1193	297.78	192.27	18.909	0.125	1.127	0.213
1194	293.07	209.38	18.909	0.028	0.948	0.052
1195	92.76	406.06	18.913	0.030	1.132	0.060
1196	14.53	43.95	18.917	0.019	0.777	0.036
1197	260.74	34.65	18.918	0.160	0.488	0.236
1198	214.24	77.62	18.920	0.040	1.024	0.064
1199	182.49	111.07	18.920	0.034	0.938	0.095
1200	174.31	404.01	18.924	0.040	0.981	0.083
1201	118.84	223.64	18.928	0.026	1.003	0.051
1202	290.53	288.64	18.931	0.046	1.060	0.084
1203	113.05	272.89	18.932	0.021	1.003	0.049
1204	85.32	285.04	18.932	0.017	0.962	0.037
1205	251.70	282.51	18.933	0.034	1.035	0.058
1206	16.56	240.34	18.935	0.031	1.026	0.047
1207	161.60	341.24	18.939	0.036	0.985	0.062
1208	225.93	21.46	18.942	0.018	1.119	0.043
1209	65.32	14.59	18.943	0.019	1.001	0.046
1210	265.86	164.72	18.948	0.203	1.303	0.271
1211	227.05	273.68	18.953	0.038	0.923	0.072
1212	97.39	162.40	18.954	0.049	0.988	0.099
1213	306.02	392.71	18.956	0.047	0.712	0.087
1214	80.53	65.19	18.956	0.049	1.006	0.081
1215	238.28	34.24	18.959	0.022	0.999	0.046
1216	65.40	379.13	18.960	0.029	1.034	0.059
1217	100.67	96.01	18.961	0.020	1.014	0.039
1218	247.57	330.45	18.962	0.025	1.136	0.080
1219	129.09	36.20	18.963	0.038	0.963	0.059
1220	308.83	174.55	18.965	0.027	1.007	0.088
1221	194.70	123.66	18.965	0.028	0.994	0.058

Table C.4. (cont.)

ID	x	y	V	σ_V	B-V	σ_{B-V}
1222	42.10	473.85	18.967	0.019	0.996	0.048
1223	126.06	136.75	18.969	0.100	1.314	0.196
1224	82.43	192.95	18.970	0.023	0.735	0.052
1225	101.56	219.17	18.973	0.034	0.985	0.071
1226	241.66	201.86	18.973	0.037	0.667	0.057
1227	105.15	75.57	18.974	0.052	1.030	0.092
1228	292.28	156.91	18.974	0.033	0.914	0.070
1229	255.57	220.92	18.981	0.022	0.853	0.052
1230	116.27	216.41	18.990	0.028	0.911	0.051
1231	227.08	199.69	18.994	0.038	1.118	0.080
1232	215.47	67.81	18.994	0.039	0.954	0.077
1233	96.70	434.37	18.994	0.022	0.965	0.045
1234	184.14	166.44	18.996	0.038	1.016	0.079
1235	151.39	384.42	18.996	0.033	0.950	0.070
1236	121.76	77.42	18.999	0.035	0.959	0.070
1237	68.71	238.92	18.999	0.028	0.898	0.048
1238	134.92	204.58	19.001	0.027	0.985	0.059
1239	65.10	476.77	19.001	0.059	0.653	0.120
1240	183.60	340.07	19.001	0.101	1.245	0.220
1241	314.89	38.38	19.003	0.080	0.932	0.165
1242	53.01	143.18	19.008	0.019	0.636	0.039
1243	141.67	351.63	19.011	0.020	0.993	0.048
1244	30.56	261.35	19.013	0.025	1.019	0.069
1245	264.49	437.43	19.014	0.025	1.032	0.057
1246	109.61	462.84	19.016	0.022	1.141	0.050
1247	218.85	303.08	19.020	0.042	1.070	0.099
1248	274.92	433.65	19.023	0.021	1.029	0.042
1249	109.14	169.17	19.028	0.025	1.087	0.053
1250	103.22	431.30	19.028	0.029	0.890	0.061
1251	84.46	210.48	19.030	0.026	0.962	0.060
1252	144.73	386.29	19.030	0.015	0.984	0.058
1253	170.20	242.36	19.031	0.026	0.993	0.044
1254	272.05	138.17	19.031	0.030	1.128	0.068
1255	149.55	435.68	19.034	0.024	1.024	0.058
1256	126.03	309.10	19.038	0.019	1.075	0.048
1257	129.19	123.71	19.039	0.020	0.832	0.047
1258	301.10	433.96	19.039	0.046	0.945	0.087

Table C.4. (cont.)

ID	x	y	V	σ_V	B-V	σ_{B-V}
1259	65.82	134.48	19.040	0.028	1.044	0.055
1260	8.34	243.98	19.042	0.027	0.902	0.062
1261	286.02	27.62	19.045	0.038	1.059	0.062
1262	84.94	173.50	19.048	0.021	0.725	0.043
1263	158.27	375.27	19.049	0.021	1.028	0.046
1264	253.83	33.37	19.050	0.073	0.775	0.127
1265	190.52	375.09	19.059	0.043	0.894	0.069
1266	25.32	443.95	19.062	0.029	0.779	0.051
1267	97.94	385.19	19.066	0.031	1.050	0.051
1268	289.86	406.80	19.069	0.042	0.957	0.074
1269	270.06	82.99	19.072	0.056	0.730	0.112
1270	151.23	209.57	19.074	0.029	1.119	0.061
1271	187.52	61.41	19.074	0.024	0.631	0.054
1272	129.51	427.53	19.075	0.041	1.057	0.078
1273	301.01	84.34	19.081	0.034	1.140	0.057
1274	185.73	17.78	19.081	0.020	0.945	0.045
1275	128.55	302.92	19.082	0.019	1.014	0.049
1276	102.91	214.48	19.082	0.037	0.886	0.064
1277	7.29	305.40	19.083	0.067	1.198	0.119
1278	194.25	284.01	19.086	0.056	1.069	0.158
1279	231.62	86.48	19.087	0.056	1.265	0.235
1280	187.38	141.15	19.087	0.041	1.038	0.067
1281	227.45	93.90	19.087	0.047	1.199	0.080
1282	210.02	201.97	19.095	0.036	1.157	0.166
1283	173.42	98.02	19.095	0.028	0.999	0.052
1284	146.79	108.62	19.095	0.025	0.892	0.042
1285	121.71	420.85	19.100	0.028	0.947	0.067
1286	179.86	403.73	19.102	0.061	0.953	0.140
1287	102.99	332.89	19.104	0.060	1.077	0.136
1288	231.35	51.45	19.105	0.028	0.576	0.052
1289	310.98	364.09	19.106	0.040	1.082	0.075
1290	57.84	462.43	19.106	0.034	1.021	0.054
1291	49.98	130.40	19.106	0.016	1.003	0.046
1292	239.58	344.49	19.106	0.022	0.926	0.050
1293	227.73	206.78	19.108	0.024	0.717	0.053
1294	20.68	28.75	19.110	0.025	1.043	0.051
1295	249.16	38.64	19.110	0.042	0.900	0.079

Table C.4. (cont.)

ID	x	y	V	σ_V	B-V	σ_{B-V}
1296	46.12	225.62	19.112	0.034	0.993	0.057
1297	86.86	375.40	19.116	0.020	1.020	0.052
1298	164.61	265.10	19.117	0.037	1.017	0.068
1299	185.33	115.19	19.128	0.035	0.726	0.060
1300	186.17	219.06	19.130	0.116	1.297	0.248
1301	188.84	477.08	19.132	0.046	0.737	0.079
1302	123.86	484.11	19.132	0.047	1.096	0.083
1303	96.70	261.02	19.133	0.030	0.997	0.058
1304	138.06	279.23	19.135	0.023	1.030	0.054
1305	63.37	476.05	19.135	0.066	0.809	0.143
1306	112.74	207.92	19.140	0.028	1.005	0.056
1307	54.42	111.49	19.141	0.068	1.014	0.101
1308	245.31	424.42	19.141	0.022	0.961	0.058
1309	284.69	166.71	19.142	0.028	0.769	0.059
1310	272.86	307.58	19.143	0.038	0.914	0.088
1311	264.11	33.82	19.145	0.117	-0.320	0.193
1312	118.49	247.92	19.146	0.035	1.026	0.066
1313	155.77	77.52	19.150	0.029	1.063	0.069
1314	261.14	347.90	19.150	0.040	1.130	0.091
1315	267.12	253.78	19.150	0.061	0.981	0.136
1316	143.98	190.34	19.151	0.076	0.938	0.126
1317	275.59	197.44	19.152	0.038	1.077	0.086
1318	177.57	342.56	19.152	0.018	1.230	0.054
1319	304.59	366.02	19.156	0.038	0.886	0.074
1320	29.90	264.60	19.158	0.025	1.412	0.063
1321	165.29	205.35	19.160	0.024	1.097	0.057
1322	180.73	26.78	19.165	0.032	1.029	0.069
1323	186.64	477.28	19.168	0.047	0.891	0.085
1324	285.59	360.11	19.170	0.044	1.020	0.102
1325	301.78	170.65	19.173	0.038	1.028	0.076
1326	59.99	495.39	19.173	0.028	0.998	0.055
1327	187.83	362.98	19.177	0.033	0.886	0.068
1328	143.89	219.13	19.180	0.034	0.945	0.058
1329	30.19	112.94	19.180	0.030	1.047	0.063
1330	96.66	370.89	19.184	0.033	1.001	0.059
1331	109.64	454.40	19.187	0.068	1.026	0.097
1332	241.72	231.53	19.187	0.025	1.010	0.051

Table C.4. (cont.)

ID	x	y	V	σ_V	B-V	σ_{B-V}
1333	220.74	163.47	19.190	0.026	1.068	0.048
1334	151.31	55.72	19.192	0.022	1.097	0.051
1335	18.78	286.26	19.192	0.026	1.166	0.059
1336	128.76	22.04	19.199	1.052	-1.046	1.420
1337	186.74	101.41	19.202	0.087	1.091	0.184
1338	77.58	343.63	19.203	0.018	0.916	0.047
1339	117.90	195.03	19.206	0.020	1.034	0.051
1340	24.82	246.12	19.208	0.019	0.778	0.041
1341	262.57	54.01	19.212	0.069	0.988	0.154
1342	123.57	306.52	19.213	0.025	1.015	0.054
1343	138.39	266.13	19.216	0.035	0.931	0.059
1344	175.60	286.73	19.217	0.034	1.139	0.061
1345	26.66	479.63	19.221	0.058	1.020	0.134
1346	251.83	235.08	19.226	0.038	1.065	0.110
1347	305.89	91.30	19.226	0.032	1.043	0.076
1348	68.16	44.42	19.227	0.040	0.746	0.143
1349	253.62	164.51	19.229	0.020	0.673	0.039
1350	81.13	299.15	19.231	0.024	1.034	0.056
1351	314.82	361.63	19.234	0.039	1.039	0.103
1352	260.09	86.64	19.234	0.038	0.885	0.079
1353	275.87	40.32	19.236	0.150	0.733	0.231
1354	154.24	133.71	19.237	0.057	0.918	0.111
1355	229.67	79.44	19.238	0.043	0.835	0.093
1356	259.15	493.56	19.238	0.153	1.023	0.205
1357	2.49	45.74	19.240	0.041	0.743	0.074
1358	140.11	406.51	19.241	0.027	1.039	0.046
1359	89.02	319.07	19.242	0.027	1.034	0.066
1360	214.94	93.51	19.245	0.036	1.141	0.081
1361	58.83	321.63	19.245	0.027	0.994	0.050
1362	301.95	361.72	19.246	0.043	1.091	0.080
1363	9.71	230.84	19.249	0.041	1.198	0.091
1364	140.86	17.50	19.250	0.031	0.720	0.058
1365	34.54	321.51	19.251	0.032	1.249	0.074
1366	229.14	274.57	19.252	0.048	1.355	0.087
1367	209.15	283.91	19.255	0.020	0.998	0.045
1368	71.02	218.67	19.261	0.025	0.771	0.054
1369	260.75	59.53	19.264	0.057	0.926	0.110

Table C.4. (cont.)

ID	x	y	V	σ_V	B-V	σ_{B-V}
1370	313.35	452.96	19.268	0.027	1.068	0.069
1371	11.44	345.37	19.271	0.029	1.095	0.051
1372	91.04	185.12	19.274	0.035	1.028	0.063
1373	170.28	54.85	19.275	0.023	0.984	0.055
1374	61.23	443.94	19.275	0.025	1.196	0.061
1375	58.36	86.27	19.277	0.028	1.026	0.048
1376	288.55	23.22	19.277	0.030	0.904	0.065
1377	244.22	84.09	19.279	0.031	0.998	0.061
1378	307.31	132.34	19.282	0.053	1.057	0.086
1379	183.16	172.54	19.282	0.039	1.014	0.080
1380	128.90	19.86	19.287	0.046	1.059	0.078
1381	217.02	5.89	19.289	0.033	1.075	0.060
1382	301.49	284.66	19.294	0.063	0.626	0.112
1383	298.30	116.73	19.294	0.060	0.974	0.111
1384	262.90	12.50	19.296	0.024	0.738	0.049
1385	285.57	85.37	19.296	0.038	0.978	0.076
1386	314.18	368.05	19.296	0.184	1.691	0.300
1387	296.46	380.20	19.300	0.048	1.052	0.093
1388	151.54	15.92	19.300	0.030	1.124	0.049
1389	132.13	284.19	19.305	0.026	1.172	0.069
1390	193.94	50.25	19.306	0.042	1.029	0.083
1391	222.58	88.70	19.310	0.043	1.038	0.076
1392	19.02	431.20	19.311	0.029	1.025	0.064
1393	299.92	9.89	19.312	0.028	1.258	0.078
1394	117.63	322.85	19.313	0.052	1.274	0.226
1395	268.03	316.05	19.314	0.034	1.056	0.058
1396	160.29	204.05	19.316	0.043	1.048	0.070
1397	228.44	457.82	19.317	0.029	1.135	0.077
1398	275.08	195.56	19.320	0.040	1.083	0.093
1399	272.02	242.26	19.320	0.203	0.918	0.384
1400	116.41	47.02	19.323	0.025	0.971	0.055
1401	98.20	481.54	19.323	0.032	1.003	0.064
1402	247.17	281.27	19.324	0.033	1.177	0.069
1403	271.71	331.62	19.326	0.030	1.334	0.062
1404	156.60	154.26	19.335	0.043	1.072	0.083
1405	250.07	184.53	19.337	0.032	1.055	0.056
1406	123.03	282.24	19.340	0.019	1.145	0.051

Table C.4. (cont.)

ID	x	y	V	σ_V	B-V	σ_{B-V}
1407	128.99	306.08	19.343	0.041	0.962	0.105
1408	45.99	385.21	19.343	0.027	1.137	0.076
1409	66.81	84.88	19.344	0.025	1.059	0.066
1410	157.81	317.08	19.346	0.029	1.104	0.063
1411	179.59	73.53	19.350	0.037	1.042	0.059
1412	261.78	250.95	19.351	0.034	1.075	0.083
1413	306.03	350.85	19.352	0.068	0.970	0.123
1414	233.06	220.03	19.352	0.028	1.066	0.067
1415	293.23	69.47	19.353	0.151	2.720	0.236
1416	222.77	406.30	19.353	0.028	1.641	0.076
1417	163.83	127.59	19.359	0.030	1.043	0.060
1418	280.84	77.55	19.361	0.049	1.136	0.093
1419	294.01	211.79	19.362	0.046	0.994	0.097
1420	30.96	404.01	19.364	0.038	1.092	0.073
1421	213.38	170.18	19.366	0.022	1.144	0.060
1422	267.69	170.92	19.366	0.034	1.050	0.179
1423	153.94	124.86	19.366	0.089	1.153	0.158
1424	299.78	413.79	19.366	0.074	0.976	0.150
1425	309.86	205.70	19.367	0.055	1.073	0.138
1426	63.26	134.46	19.371	0.036	0.871	0.071
1427	309.71	140.65	19.372	0.041	1.251	0.085
1428	264.10	8.50	19.375	0.025	0.711	0.052
1429	180.29	422.94	19.375	0.041	1.182	0.079
1430	87.40	426.27	19.376	0.022	1.136	0.042
1431	200.36	165.38	19.384	0.033	0.911	0.057
1432	84.91	244.76	19.385	0.045	0.742	0.074
1433	228.04	159.36	19.388	0.047	1.066	0.100
1434	283.02	97.79	19.390	0.041	1.050	0.106
1435	101.90	486.18	19.390	0.037	1.059	0.084
1436	25.04	52.60	19.391	0.031	1.082	0.063
1437	102.83	282.71	19.392	0.038	1.015	0.088
1438	149.04	267.77	19.393	0.025	1.131	0.061
1439	258.98	252.73	19.394	0.039	0.999	0.089
1440	313.71	346.68	19.396	0.043	1.054	0.083
1441	278.73	424.64	19.404	0.064	0.990	0.130
1442	103.32	45.16	19.405	0.036	0.735	0.082
1443	310.61	463.01	19.407	0.041	1.090	0.078

Table C.4. (cont.)

ID	x	y	V	σ_V	B-V	σ_{B-V}
1444	49.43	278.28	19.407	0.047	1.074	0.083
1445	193.26	79.34	19.409	0.029	1.039	0.057
1446	301.35	255.80	19.409	0.055	1.149	0.109
1447	169.34	229.91	19.409	0.042	1.117	0.090
1448	178.48	429.92	19.410	0.042	1.230	0.099
1449	2.58	58.55	19.414	0.091	1.149	0.165
1450	252.45	50.31	19.414	0.133	0.751	0.263
1451	265.22	278.82	19.418	0.056	1.166	0.096
1452	137.52	493.80	19.419	0.049	1.239	0.085
1453	285.44	324.88	19.424	0.035	0.970	0.082
1454	54.15	290.34	19.429	0.033	1.139	0.062
1455	230.64	473.91	19.429	0.035	1.127	0.090
1456	17.22	196.48	19.429	0.062	0.916	0.104
1457	239.26	336.17	19.432	0.030	0.877	0.064
1458	269.21	147.95	19.432	0.034	1.065	0.068
1459	26.46	205.43	19.433	0.028	1.015	0.075
1460	213.02	300.77	19.434	0.045	1.207	0.079
1461	109.42	439.34	19.435	0.027	1.142	0.070
1462	293.77	184.97	19.439	0.039	1.195	0.107
1463	30.73	286.76	19.443	0.036	1.072	0.090
1464	125.00	93.38	19.443	0.034	0.983	0.061
1465	279.89	21.95	19.445	0.033	0.972	0.064
1466	242.66	256.02	19.445	0.195	1.172	0.312
1467	19.66	298.06	19.450	0.063	1.236	0.117
1468	302.78	187.96	19.451	0.083	1.097	0.142
1469	263.46	47.24	19.460	0.228	-0.919	0.349
1470	167.04	143.59	19.464	0.030	1.073	0.068
1471	291.21	49.51	19.469	0.099	0.722	0.141
1472	270.78	102.25	19.470	0.037	1.025	0.070
1473	305.09	209.55	19.472	0.039	1.075	0.102
1474	127.32	31.35	19.474	0.026	1.061	0.077
1475	298.87	32.13	19.476	0.048	0.878	0.086
1476	255.32	278.25	19.476	0.030	1.200	0.072
1477	47.03	11.06	19.478	0.036	0.832	0.061
1478	298.19	132.61	19.478	0.060	1.035	0.137
1479	209.12	183.09	19.479	0.027	1.047	0.080
1480	166.90	219.98	19.481	0.047	1.095	0.109

Table C.4. (cont.)

ID	x	y	V	σ_V	B-V	σ_{B-V}
1481	212.90	486.23	19.482	0.027	1.052	0.078
1482	193.25	273.71	19.483	0.086	0.570	0.158
1483	292.41	58.35	19.483	0.038	1.207	0.097
1484	227.78	104.25	19.484	0.044	1.285	0.139
1485	77.49	259.20	19.484	0.027	1.091	0.060
1486	286.55	358.36	19.486	0.058	1.043	0.103
1487	130.42	166.92	19.487	0.047	1.139	0.094
1488	80.13	215.32	19.487	0.035	0.999	0.124
1489	276.06	269.30	19.489	0.024	1.068	0.073
1490	52.44	428.09	19.490	0.037	1.131	0.097
1491	288.50	490.17	19.491	0.054	0.824	0.090
1492	271.45	359.67	19.492	0.030	1.321	0.101
1493	194.18	109.77	19.493	0.038	0.958	0.080
1494	203.84	123.46	19.494	0.037	0.916	0.078
1495	317.08	373.15	19.494	1.902	0.743	2.494
1496	314.19	500.47	19.495	0.067	1.101	0.130
1497	230.09	174.19	19.498	0.027	1.052	0.059
1498	219.22	109.47	19.499	0.042	1.033	0.115
1499	29.04	288.11	19.502	0.038	0.816	0.088
1500	92.16	75.65	19.502	0.037	0.600	0.074
1501	278.76	276.45	19.502	0.038	1.160	0.083
1502	292.31	213.28	19.505	0.049	1.475	0.131
1503	93.38	455.31	19.510	0.030	0.936	0.060
1504	179.95	442.44	19.510	0.044	1.050	0.069
1505	302.55	140.59	19.511	0.044	1.035	0.094
1506	248.93	407.97	19.511	0.030	1.117	0.078
1507	136.36	381.09	19.513	0.031	1.108	0.069
1508	72.65	305.49	19.514	0.038	1.142	0.084
1509	252.46	97.04	19.514	0.055	1.157	0.108
1510	41.71	327.41	19.516	0.033	1.075	0.086
1511	80.11	309.93	19.518	0.069	0.873	0.129
1512	93.98	342.30	19.520	0.029	1.051	0.067
1513	237.05	451.08	19.520	0.038	0.855	0.065
1514	200.73	133.66	19.520	0.033	0.926	0.075
1515	200.46	241.68	19.521	0.021	0.935	0.064
1516	236.14	250.44	19.523	0.052	1.039	0.179
1517	270.98	140.59	19.528	0.041	1.387	0.125

Table C.4. (cont.)

ID	x	y	V	σ_V	B-V	σ_{B-V}
1518	208.39	82.15	19.532	0.039	0.747	0.081
1519	223.80	17.61	19.534	0.033	1.225	0.074
1520	151.42	224.49	19.534	0.117	1.519	0.216
1521	84.30	315.63	19.534	0.034	1.042	0.073
1522	294.75	127.46	19.536	0.039	1.110	0.127
1523	68.20	48.99	19.537	0.252	0.487	0.431
1524	165.67	350.30	19.538	0.032	1.180	0.075
1525	287.56	110.79	19.539	0.033	1.095	0.078
1526	87.93	245.58	19.544	0.074	1.300	0.176
1527	230.32	353.16	19.546	0.078	1.123	0.151
1528	175.25	296.55	19.546	0.045	1.120	0.076
1529	82.93	72.88	19.548	0.038	0.777	0.067
1530	161.38	68.37	19.554	0.039	0.953	0.069
1531	261.95	474.10	19.555	0.043	0.704	0.083
1532	265.55	51.49	19.557	0.142	0.828	0.250
1533	141.22	29.53	19.559	0.038	1.117	0.092
1534	112.92	318.90	19.559	0.038	1.114	0.073
1535	154.78	123.41	19.559	0.043	1.160	0.140
1536	244.40	144.91	19.562	0.035	1.199	0.078
1537	121.64	232.43	19.563	0.344	-2.700	0.449
1538	225.40	221.03	19.564	0.080	1.091	0.131
1539	71.71	245.19	19.564	0.031	1.167	0.072
1540	18.85	368.84	19.564	0.033	1.493	0.087
1541	123.74	31.62	19.567	0.028	1.319	0.106
1542	314.35	36.80	19.567	0.059	1.160	0.258
1543	2.64	178.17	19.568	0.052	1.148	0.104
1544	240.62	147.53	19.569	0.028	1.087	0.071
1545	293.80	355.11	19.570	0.045	0.538	0.074
1546	75.92	264.14	19.570	0.065	1.199	0.110
1547	162.14	251.78	19.573	0.041	1.037	0.084
1548	237.52	446.28	19.575	0.038	1.041	0.082
1549	146.53	308.02	19.576	0.048	1.229	0.105
1550	229.84	44.89	19.577	0.039	1.060	0.082
1551	56.46	206.42	19.579	0.036	1.450	0.076
1552	67.65	60.21	19.582	0.226	0.038	0.340
1553	114.26	448.23	19.582	0.049	1.097	0.090
1554	146.72	96.03	19.586	0.042	0.959	0.080

Table C.4. (cont.)

ID	x	y	V	σ_V	B-V	σ_{B-V}
1555	131.35	171.22	19.588	0.029	1.298	0.090
1556	278.10	219.14	19.588	0.038	1.087	0.105
1557	223.03	263.84	19.589	0.112	1.173	0.200
1558	172.27	166.35	19.590	0.034	1.016	0.077
1559	175.15	321.28	19.592	0.041	1.190	0.101
1560	132.20	225.63	19.593	0.040	1.217	0.120
1561	76.20	199.99	19.593	0.038	1.155	0.082
1562	86.27	196.27	19.596	0.036	1.209	0.075
1563	75.35	112.16	19.611	0.060	1.123	0.115
1564	214.31	315.44	19.616	0.067	1.150	0.117
1565	217.18	304.46	19.616	0.034	1.406	0.176
1566	230.48	426.88	19.619	0.045	1.155	0.153
1567	225.61	352.50	19.624	0.033	1.251	0.130
1568	264.96	26.64	19.632	0.129	1.010	0.274
1569	110.42	167.29	19.633	0.036	1.283	0.092
1570	95.89	266.29	19.633	0.028	1.135	0.062
1571	194.79	322.52	19.635	0.048	1.092	0.101
1572	179.46	45.00	19.637	0.031	1.190	0.090
1573	40.44	461.89	19.641	0.038	0.963	0.067
1574	245.48	39.22	19.644	0.070	0.989	0.132
1575	198.37	17.39	19.645	0.042	1.154	0.081
1576	252.77	91.28	19.649	0.060	1.168	0.105
1577	281.75	240.45	19.650	0.045	1.090	0.204
1578	224.01	131.17	19.650	0.043	1.046	0.086
1579	60.08	201.98	19.650	0.024	1.061	0.065
1580	229.35	216.39	19.653	0.037	1.203	0.105
1581	179.45	157.43	19.654	0.047	1.066	0.101
1582	112.11	247.73	19.656	0.034	1.039	0.094
1583	180.46	110.98	19.656	0.061	1.101	0.123
1584	171.67	122.57	19.656	0.034	1.066	0.078
1585	291.77	336.69	19.657	0.054	1.077	0.176
1586	223.72	323.97	19.658	0.047	1.224	0.162
1587	199.02	458.94	19.660	0.041	1.048	0.110
1588	209.36	162.76	19.663	0.037	1.182	0.092
1589	210.98	452.17	19.663	0.029	1.320	0.075
1590	211.73	201.43	19.663	0.135	0.917	0.189
1591	135.74	418.14	19.663	0.047	1.270	0.115

Table C.4. (cont.)

ID	x	y	V	σ_V	B-V	σ_{B-V}
1592	105.61	431.06	19.668	0.047	1.419	0.132
1593	16.44	494.67	19.669	0.124	0.976	0.187
1594	193.04	320.97	19.677	0.049	1.298	0.094
1595	177.85	154.28	19.680	0.060	1.016	0.127
1596	101.80	65.81	19.681	0.050	1.560	0.134
1597	266.43	191.50	19.683	0.165	1.401	0.389
1598	114.58	154.32	19.684	0.041	1.163	0.099
1599	81.31	12.15	19.685	0.051	0.690	0.093
1600	62.59	296.61	19.686	0.037	1.075	0.075
1601	76.91	336.17	19.688	0.044	0.815	0.073
1602	163.31	462.34	19.688	0.029	1.240	0.094
1603	18.95	503.11	19.689	0.051	1.292	0.114
1604	147.77	484.88	19.691	0.043	0.859	0.088
1605	281.81	175.94	19.691	0.054	0.979	0.101
1606	279.06	167.86	19.694	0.038	1.311	0.093
1607	186.07	25.55	19.696	0.045	1.176	0.103
1608	222.55	193.11	19.697	0.029	1.068	0.069
1609	286.61	466.54	19.697	0.034	1.391	0.095
1610	152.68	409.60	19.699	0.043	1.046	0.087
1611	134.90	145.70	19.700	0.021	1.090	0.056
1612	263.24	339.32	19.701	0.026	1.171	0.067
1613	282.04	224.74	19.701	0.106	1.033	0.199
1614	32.34	109.68	19.702	0.043	1.077	0.095
1615	208.07	99.24	19.703	0.029	1.104	0.086
1616	272.90	197.36	19.707	0.047	1.051	0.100
1617	262.87	84.08	19.707	0.054	1.044	0.128
1618	67.94	285.55	19.708	0.056	1.316	0.140
1619	304.82	430.26	19.708	0.089	0.970	0.167
1620	30.97	259.40	19.712	0.026	1.010	0.115
1621	133.63	356.77	19.715	0.038	1.119	0.088
1622	84.81	419.83	19.719	0.034	1.100	0.069
1623	25.60	319.82	19.720	0.040	0.765	0.085
1624	106.49	384.59	19.721	0.029	1.265	0.088
1625	232.17	47.40	19.725	0.044	1.093	0.093
1626	109.09	245.38	19.733	0.036	1.003	0.104
1627	268.88	46.29	19.734	0.263	0.417	0.489
1628	301.18	463.66	19.736	0.051	1.034	0.099

Table C.4. (cont.)

ID	x	y	V	σ_V	B-V	σ_{B-V}
1629	303.88	434.28	19.740	0.081	1.600	0.226
1630	86.09	205.06	19.741	0.160	0.650	0.221
1631	229.93	86.24	19.747	0.100	0.630	0.291
1632	160.57	354.85	19.750	0.036	0.908	0.065
1633	57.70	24.51	19.755	0.042	1.034	0.103
1634	82.80	248.04	19.755	0.056	0.918	0.093
1635	32.55	37.33	19.757	0.038	0.711	0.071
1636	227.38	140.84	19.758	0.063	1.122	0.123
1637	233.92	151.66	19.759	0.053	1.037	0.117
1638	220.03	151.11	19.762	0.081	1.461	0.150
1639	245.09	21.01	19.763	0.058	1.020	0.125
1640	71.23	294.11	19.764	0.045	1.154	0.118
1641	309.68	445.16	19.764	0.037	1.065	0.111
1642	111.58	311.08	19.766	0.038	1.247	0.076
1643	282.89	413.39	19.772	0.032	1.093	0.093
1644	189.87	123.84	19.773	0.045	1.124	0.097
1645	152.61	180.80	19.774	0.058	1.055	0.103
1646	22.15	352.25	19.774	0.038	1.283	0.101
1647	122.59	354.89	19.776	0.080	1.922	0.233
1648	102.01	302.66	19.782	0.074	1.072	0.136
1649	270.51	33.33	19.784	0.294	0.485	0.447
1650	238.34	213.93	19.785	0.116	0.701	0.186
1651	135.63	297.71	19.785	0.042	1.212	0.090
1652	265.85	495.82	19.785	0.282	0.608	0.654
1653	310.50	95.45	19.791	0.056	0.743	0.113
1654	202.82	197.76	19.793	0.035	1.059	0.087
1655	253.15	67.39	19.796	0.070	1.117	0.149
1656	64.14	162.66	19.799	0.029	1.096	0.087
1657	289.26	188.89	19.800	0.070	1.195	0.130
1658	134.15	439.86	19.801	0.044	1.158	0.101
1659	76.96	286.82	19.802	0.044	1.151	0.124
1660	62.83	48.26	19.805	0.265	0.947	0.436
1661	19.25	476.95	19.806	0.063	0.835	0.101
1662	186.77	318.17	19.807	0.050	0.836	0.094
1663	226.00	277.53	19.809	0.053	1.160	0.115
1664	265.06	91.04	19.814	0.091	0.878	0.187
1665	229.79	13.45	19.815	0.073	1.182	0.120

Table C.4. (cont.)

ID	x	y	V	σ_V	B-V	σ_{B-V}
1666	187.20	174.77	19.817	0.047	1.251	0.124
1667	282.16	275.13	19.819	0.136	2.071	0.338
1668	67.02	273.49	19.820	0.042	0.926	0.094
1669	139.09	203.95	19.823	0.048	0.621	0.094
1670	11.79	351.54	19.825	0.049	1.247	0.097
1671	23.99	436.69	19.828	0.039	1.193	0.124
1672	285.98	122.76	19.830	0.059	1.260	0.122
1673	229.22	319.10	19.830	0.066	1.198	0.183
1674	104.62	122.90	19.835	0.046	0.822	0.087
1675	115.35	157.32	19.835	0.070	1.052	0.150
1676	304.55	480.36	19.840	0.038	1.084	0.098
1677	162.81	6.80	19.851	0.077	0.749	0.120
1678	112.22	229.93	19.851	0.086	1.902	0.253
1679	38.56	247.06	19.852	0.033	1.208	0.092
1680	54.91	184.02	19.853	0.039	1.303	0.087
1681	204.62	112.36	19.854	0.060	1.032	0.108
1682	148.37	139.40	19.855	0.038	1.282	0.081
1683	210.72	165.81	19.857	0.056	1.279	0.135
1684	270.80	161.11	19.858	0.061	1.111	0.124
1685	89.54	53.25	19.864	0.176	0.491	0.254
1686	76.47	55.27	19.865	0.164	0.304	0.272
1687	13.80	5.75	19.870	0.058	0.802	0.102
1688	261.76	26.27	19.870	0.793	0.317	1.042
1689	182.75	431.85	19.871	0.040	1.354	0.116
1690	165.88	461.84	19.873	0.040	1.029	0.103
1691	15.12	76.24	19.874	0.058	1.157	0.113
1692	240.78	73.90	19.874	0.153	1.030	0.276
1693	98.95	292.44	19.879	0.066	0.847	0.127
1694	133.08	202.40	19.882	0.051	1.100	0.125
1695	145.55	428.93	19.884	0.056	1.252	0.149
1696	117.49	425.38	19.885	0.046	1.017	0.095
1697	291.55	394.88	19.887	0.056	1.383	0.164
1698	276.68	131.94	19.887	0.038	1.100	0.092
1699	271.93	355.97	19.888	0.042	1.248	0.163
1700	81.81	145.03	19.901	0.042	1.184	0.083
1701	220.55	387.25	19.907	0.047	1.208	0.126
1702	116.18	427.51	19.908	0.059	0.351	0.095

Table C.4. (cont.)

ID	x	y	V	σ_V	B-V	σ_{B-V}
1703	287.19	413.86	19.916	0.051	1.019	0.111
1704	153.25	285.39	19.917	0.061	1.289	0.111
1705	90.51	41.44	19.920	0.040	1.199	0.122
1706	227.05	485.11	19.923	0.161	1.155	0.282
1707	143.80	143.21	19.924	0.046	1.565	0.109
1708	257.78	269.25	19.926	0.059	1.184	0.099
1709	312.17	42.86	19.926	0.076	1.153	0.212
1710	111.05	235.27	19.930	0.052	0.604	0.099
1711	164.40	173.80	19.935	0.050	1.257	0.125
1712	138.79	208.15	19.936	0.052	1.153	0.126
1713	242.03	446.38	19.939	0.036	1.154	0.082
1714	177.83	440.43	19.940	0.061	1.419	0.105
1715	304.57	168.77	19.950	0.066	1.171	0.141
1716	145.30	377.46	19.951	0.054	0.814	0.102
1717	290.75	8.38	19.952	0.049	0.934	0.125
1718	112.93	210.52	19.953	0.044	1.042	0.110
1719	201.01	9.24	19.953	0.062	1.171	0.122
1720	311.16	413.22	19.962	0.066	0.926	0.170
1721	191.90	140.11	19.968	0.059	1.315	0.122
1722	180.48	306.87	19.973	0.056	1.106	0.141
1723	271.93	260.65	19.974	0.091	1.025	0.144
1724	83.50	102.88	19.975	0.074	1.015	0.121
1725	274.77	325.95	19.978	0.052	1.320	0.122
1726	238.09	357.34	19.978	0.038	1.349	0.150
1727	178.30	104.16	19.989	0.198	0.328	0.281
1728	238.26	95.68	19.989	0.060	1.252	0.130
1729	285.33	71.63	19.996	0.122	0.712	0.194
1730	24.05	279.96	19.997	0.043	1.249	0.113
1731	8.50	352.15	20.001	0.057	1.256	0.113
1732	287.89	76.68	20.004	0.100	1.276	0.268
1733	139.68	174.86	20.005	0.045	1.182	0.115
1734	157.63	63.82	20.011	0.048	1.185	0.143
1735	221.32	36.91	20.014	0.054	1.332	0.148
1736	273.69	247.22	20.019	0.084	1.115	0.204
1737	153.95	406.41	20.019	0.056	1.422	0.134
1738	48.14	16.12	20.020	0.071	1.269	0.157
1739	165.24	356.86	20.023	0.069	1.256	0.164

Table C.4. (cont.)

ID	x	y	V	σ_V	B-V	σ_{B-V}
1740	68.38	103.13	20.024	0.043	0.947	0.086
1741	245.23	303.18	20.025	0.108	1.099	0.225
1742	288.23	249.52	20.027	0.066	1.176	0.133
1743	252.59	53.67	20.033	0.055	1.140	0.123
1744	292.56	28.51	20.038	0.060	1.186	0.136
1745	263.31	5.26	20.040	0.039	1.185	0.107
1746	67.71	333.85	20.040	0.056	0.862	0.099
1747	129.67	190.71	20.041	0.037	1.443	0.160
1748	258.30	304.36	20.042	0.069	1.358	0.195
1749	243.56	327.24	20.043	0.065	1.284	0.144
1750	235.06	124.84	20.051	0.054	1.589	0.148
1751	263.26	122.84	20.051	0.100	0.810	0.172
1752	309.04	382.25	20.051	0.066	1.373	0.208
1753	208.46	424.85	20.052	0.061	1.385	0.176
1754	125.35	217.38	20.053	0.101	0.838	0.166
1755	57.77	303.60	20.057	0.075	1.316	0.184
1756	278.27	247.80	20.058	0.088	1.242	0.181
1757	225.35	66.67	20.062	0.065	1.669	0.161
1758	166.53	128.80	20.065	0.052	1.061	0.108
1759	30.36	88.39	20.065	0.042	1.086	0.105
1760	112.77	343.83	20.067	0.102	0.998	0.206
1761	296.31	403.16	20.071	0.038	1.119	0.121
1762	82.09	394.66	20.071	0.055	1.175	0.109
1763	212.98	204.10	20.075	0.081	1.503	0.183
1764	291.20	216.42	20.076	0.061	1.019	0.119
1765	116.63	233.16	20.084	0.049	1.413	0.131
1766	48.15	63.55	20.090	0.049	1.324	0.131
1767	159.95	379.53	20.093	0.062	1.739	0.172
1768	250.84	451.67	20.093	0.066	1.106	0.169
1769	127.59	39.19	20.094	0.108	0.784	0.171
1770	214.29	134.00	20.098	0.075	1.211	0.185
1771	45.74	301.79	20.099	0.058	1.111	0.133
1772	233.89	266.76	20.100	0.109	1.189	0.225
1773	236.67	408.87	20.102	0.057	1.261	0.131
1774	116.67	321.93	20.102	0.104	1.055	0.404
1775	208.55	321.87	20.103	0.047	1.283	0.128
1776	160.76	390.51	20.104	0.052	0.653	0.083

Table C.4. (cont.)

ID	x	y	V	σ_V	B-V	σ_{B-V}
1777	174.03	230.52	20.106	0.045	1.361	0.159
1778	255.39	149.72	20.112	0.068	0.909	0.129
1779	46.51	135.96	20.114	0.146	0.679	0.205
1780	250.30	59.86	20.115	0.058	1.136	0.129
1781	307.19	453.21	20.117	0.061	1.269	0.164
1782	182.97	134.99	20.122	0.045	0.979	0.114
1783	295.30	290.44	20.123	0.086	1.023	0.161
1784	117.73	4.49	20.123	0.063	0.963	0.132
1785	222.36	167.92	20.123	0.172	1.196	0.263
1786	286.97	313.29	20.124	0.038	1.807	0.181
1787	166.22	300.32	20.126	0.053	1.270	0.138
1788	46.02	235.11	20.126	0.047	1.153	0.114
1789	35.72	278.21	20.127	0.076	0.503	0.118
1790	15.68	155.00	20.128	0.048	0.824	0.098
1791	44.36	274.54	20.136	0.262	3.072	0.563
1792	315.50	212.82	20.136	0.077	0.998	0.181
1793	126.90	227.60	20.139	0.055	1.252	0.140
1794	211.14	197.14	20.140	0.087	1.360	0.174
1795	115.22	284.73	20.141	0.069	1.230	0.158
1796	13.46	419.68	20.144	0.063	1.181	0.135
1797	263.08	185.42	20.151	0.077	1.579	0.162
1798	302.25	341.57	20.158	0.099	1.501	0.253
1799	218.52	356.10	20.159	0.083	1.446	0.155
1800	312.07	180.98	20.161	0.087	1.453	0.241
1801	65.09	62.63	20.164	0.304	0.072	0.446
1802	168.64	88.96	20.168	0.069	1.207	0.177
1803	296.15	183.80	20.171	0.070	1.672	0.302
1804	3.46	440.02	20.178	0.051	1.292	0.162
1805	123.38	414.34	20.182	0.089	1.539	0.206
1806	39.30	170.93	20.183	0.057	1.390	0.126
1807	46.62	339.64	20.185	0.089	1.194	0.189
1808	87.23	470.42	20.188	0.047	1.012	0.120
1809	264.13	88.62	20.189	0.122	1.126	0.217
1810	51.28	123.28	20.190	0.049	0.899	0.124
1811	306.46	464.35	20.194	0.075	1.332	0.192
1812	166.67	209.12	20.198	0.091	1.493	0.331
1813	296.75	295.16	20.200	0.061	0.980	0.120

Table C.4. (cont.)

ID	x	y	V	σ_V	B-V	σ_{B-V}
1814	313.82	496.06	20.205	0.090	2.137	0.377
1815	222.57	347.81	20.215	0.103	1.173	0.273
1816	201.27	494.70	20.217	0.054	0.443	0.090
1817	164.59	82.36	20.220	0.061	0.902	0.129
1818	288.38	335.34	20.221	0.084	1.231	0.202
1819	291.08	129.78	20.221	0.073	1.284	0.234
1820	76.40	311.99	20.222	0.086	0.824	0.172
1821	134.95	134.21	20.225	0.041	1.070	0.165
1822	260.39	48.99	20.225	0.375	0.268	0.552
1823	272.63	217.44	20.228	0.061	1.066	0.171
1824	303.36	172.54	20.229	0.074	1.135	0.176
1825	306.39	269.87	20.233	0.383	-0.394	0.638
1826	283.85	40.40	20.237	0.154	0.514	0.277
1827	248.60	191.44	20.238	0.061	1.266	0.192
1828	91.01	242.15	20.239	0.054	1.614	0.160
1829	305.29	97.50	20.239	0.122	1.936	0.300
1830	299.07	343.54	20.241	0.200	1.623	0.544
1831	258.84	32.36	20.245	0.307	-0.166	0.440
1832	63.27	394.63	20.247	0.083	1.823	0.656
1833	178.33	79.09	20.251	0.058	1.260	0.169
1834	207.42	361.97	20.252	0.063	1.846	0.226
1835	211.98	337.33	20.254	0.057	1.573	0.192
1836	285.81	402.01	20.258	0.108	1.271	0.284
1837	59.72	49.78	20.264	0.350	0.442	0.503
1838	159.94	212.83	20.268	0.084	1.838	0.321
1839	52.58	308.93	20.272	0.191	1.081	0.372
1840	303.61	466.57	20.273	0.097	1.405	0.204
1841	301.85	116.46	20.274	0.130	1.459	0.304
1842	110.56	505.22	20.282	0.147	1.345	0.352
1843	270.56	87.54	20.282	0.065	1.495	0.211
1844	206.75	385.42	20.283	0.074	1.312	0.151
1845	300.09	266.87	20.285	0.180	0.777	0.333
1846	307.68	292.34	20.285	0.096	1.070	0.159
1847	290.56	411.28	20.289	0.100	1.157	0.253
1848	222.65	400.09	20.290	0.048	1.327	0.140
1849	118.98	298.43	20.293	0.057	1.088	0.158
1850	195.36	285.18	20.294	0.163	1.093	0.249

Table C.4. (cont.)

ID	x	y	V	σ_V	B-V	σ_{B-V}
1851	19.65	203.53	20.294	0.051	1.064	0.157
1852	226.50	33.07	20.296	0.062	1.376	0.167
1853	191.49	75.58	20.301	0.083	1.252	0.151
1854	122.37	337.49	20.302	0.082	0.845	0.149
1855	189.09	88.59	20.303	0.094	1.448	0.219
1856	225.81	483.35	20.307	0.225	0.618	0.317
1857	57.54	53.21	20.309	0.405	0.166	0.757
1858	89.73	102.14	20.310	0.081	1.265	0.167
1859	185.57	161.41	20.311	0.057	1.257	0.153
1860	121.43	301.43	20.311	0.061	1.233	0.134
1861	56.94	377.12	20.312	0.117	0.592	0.169
1862	262.53	230.11	20.314	0.065	1.059	0.323
1863	6.90	108.39	20.316	0.069	0.782	0.139
1864	11.36	406.05	20.318	0.085	1.627	0.265
1865	43.22	149.54	20.323	0.065	1.512	0.168
1866	207.42	66.58	20.327	0.083	1.625	0.187
1867	151.38	504.71	20.327	0.110	1.175	0.213
1868	181.50	463.66	20.328	0.046	1.810	0.210
1869	170.72	201.20	20.330	0.050	1.263	0.109
1870	289.91	40.18	20.334	0.106	0.671	0.198
1871	197.56	358.32	20.335	0.093	1.321	0.168
1872	132.34	63.88	20.335	0.044	1.601	0.193
1873	102.44	255.04	20.336	0.071	1.186	0.176
1874	56.72	448.46	20.342	0.092	1.302	0.208
1875	97.11	223.39	20.343	0.065	0.981	0.131
1876	216.44	334.45	20.348	0.061	1.345	0.200
1877	225.60	240.10	20.355	0.067	1.586	0.157
1878	298.89	502.20	20.356	0.189	0.102	0.413
1879	55.93	187.15	20.357	0.054	0.777	0.094
1880	106.81	23.47	20.361	0.046	1.101	0.136
1881	141.52	318.68	20.364	0.086	1.645	0.208
1882	144.77	111.70	20.371	0.178	0.717	0.249
1883	125.73	279.35	20.380	0.040	1.300	0.130
1884	10.13	36.49	20.382	0.223	0.261	0.507
1885	175.39	63.09	20.383	0.061	1.128	0.149
1886	148.92	275.42	20.385	0.080	1.275	0.188
1887	239.84	308.23	20.385	0.092	1.135	0.241

Table C.4. (cont.)

ID	x	y	V	σ_V	B-V	σ_{B-V}
1888	6.62	411.19	20.386	0.084	1.588	0.216
1889	259.24	255.18	20.391	0.095	0.874	0.216
1890	284.83	104.23	20.399	0.100	1.349	0.256
1891	171.95	117.62	20.400	0.070	1.686	0.258
1892	65.88	88.42	20.401	0.066	1.243	0.165
1893	91.10	73.62	20.402	0.068	1.452	0.238
1894	78.13	20.51	20.403	0.067	1.516	0.232
1895	63.83	269.45	20.407	0.089	1.967	0.251
1896	206.72	388.15	20.410	0.097	1.282	0.184
1897	8.39	437.90	20.412	0.102	1.636	0.241
1898	8.40	103.83	20.412	0.104	1.302	0.245
1899	264.62	348.35	20.414	0.107	1.153	0.263
1900	122.81	175.22	20.418	0.101	1.229	0.223
1901	116.83	297.67	20.419	0.103	1.211	0.216
1902	70.26	439.86	20.420	0.081	1.204	0.237
1903	125.00	39.80	20.421	0.150	1.771	0.321
1904	62.52	286.45	20.422	0.057	1.189	0.148
1905	222.10	305.89	20.425	0.123	1.330	0.262
1906	2.32	486.32	20.428	0.151	1.601	0.410
1907	219.22	34.91	20.430	0.077	1.413	0.227
1908	236.20	171.29	20.430	0.101	1.668	0.218
1909	93.30	322.92	20.431	0.092	1.119	0.204
1910	154.30	311.50	20.433	0.093	0.816	0.152
1911	38.25	428.71	20.433	0.108	0.836	0.203
1912	97.08	282.54	20.434	0.127	0.695	0.562
1913	122.30	411.18	20.435	0.089	1.284	0.212
1914	114.06	145.97	20.437	0.071	1.287	0.162
1915	193.18	199.34	20.438	0.108	2.014	0.408
1916	7.99	168.33	20.439	0.310	-2.808	0.404
1917	11.32	457.84	20.440	0.134	0.725	0.283
1918	179.39	50.36	20.441	0.105	1.007	0.224
1919	181.50	403.43	20.442	0.204	1.553	0.657
1920	308.30	318.51	20.442	0.084	1.511	0.225
1921	20.51	94.00	20.442	0.098	1.124	0.199
1922	297.97	386.76	20.445	0.183	1.302	0.480
1923	191.52	308.41	20.446	0.082	1.033	0.179
1924	47.09	106.25	20.447	0.068	1.016	0.151

Table C.4. (cont.)

ID	x	y	V	σ_V	B-V	σ_{B-V}
1925	301.63	75.74	20.447	0.419	3.152	0.798
1926	141.96	365.18	20.447	0.131	1.097	0.249
1927	176.88	376.04	20.451	0.108	1.524	0.207
1928	253.41	238.52	20.455	0.117	1.502	0.316
1929	309.23	146.87	20.459	0.186	0.719	0.348
1930	281.68	282.31	20.460	0.069	1.155	0.170
1931	90.57	270.94	20.461	0.198	0.228	0.269
1932	225.63	230.80	20.463	0.108	1.404	0.274
1933	307.40	349.42	20.463	0.112	1.542	0.379
1934	143.59	425.30	20.465	0.093	1.109	0.216
1935	177.40	48.75	20.466	0.106	1.057	0.232
1936	56.74	211.59	20.466	0.068	1.285	0.128
1937	252.49	189.64	20.470	0.101	1.315	0.218
1938	16.52	440.32	20.471	0.096	1.466	0.230
1939	80.68	468.98	20.474	0.063	0.981	0.117
1940	140.35	131.05	20.474	0.066	1.870	0.251
1941	118.67	456.95	20.475	0.081	1.207	0.209
1942	56.07	466.90	20.475	0.077	0.793	0.149
1943	260.92	29.86	20.476	0.288	0.247	0.419
1944	285.75	399.07	20.476	0.192	1.015	0.447
1945	19.15	3.32	20.477	0.085	1.587	0.314
1946	271.90	37.01	20.483	0.531	-0.465	0.801
1947	159.14	84.52	20.485	0.081	0.851	0.166
1948	210.79	431.38	20.490	0.097	1.252	0.161
1949	242.37	7.42	20.495	0.075	0.735	0.146
1950	265.92	93.27	20.495	0.142	0.716	0.276
1951	214.53	227.08	20.499	0.102	0.988	0.221
1952	152.03	184.26	20.503	0.101	1.507	0.221
1953	131.65	300.68	20.504	0.223	1.556	0.594
1954	268.87	404.86	20.505	0.059	1.320	0.166
1955	105.90	439.17	20.509	0.065	1.382	0.201
1956	68.24	133.14	20.516	0.078	2.062	0.335
1957	299.15	205.19	20.519	0.134	1.044	0.235
1958	307.87	192.73	20.520	0.149	2.008	0.758
1959	90.30	11.27	20.520	0.179	-2.834	0.234
1960	144.46	204.41	20.523	0.086	1.054	0.170
1961	74.10	137.63	20.526	0.082	1.629	0.204

Table C.4. (cont.)

ID	x	y	V	σ_V	B-V	σ_{B-V}
1962	26.38	56.18	20.536	0.100	2.057	0.272
1963	292.88	265.62	20.537	0.113	1.498	0.333
1964	171.64	430.09	20.540	0.110	1.694	0.287
1965	188.55	448.20	20.544	0.063	1.419	0.203
1966	152.58	266.08	20.545	0.072	1.549	0.217
1967	76.56	253.37	20.546	0.066	1.301	0.172
1968	22.60	368.71	20.546	0.074	1.153	0.172
1969	75.46	256.31	20.549	0.067	1.003	0.150
1970	195.01	44.40	20.549	0.088	1.198	0.187
1971	115.43	261.29	20.550	0.080	1.195	0.215
1972	198.87	330.24	20.558	0.135	1.319	0.293
1973	41.22	83.76	20.558	0.090	0.874	0.208
1974	108.71	185.30	20.559	0.079	1.567	0.188
1975	71.19	65.93	20.563	0.119	0.867	0.201
1976	234.04	194.88	20.580	0.120	1.220	0.213
1977	309.35	56.65	20.585	0.096	1.936	0.303
1978	17.82	157.67	20.590	0.083	1.108	0.215
1979	36.66	430.41	20.596	0.124	1.477	0.306
1980	124.63	178.56	20.599	0.118	1.707	0.392
1981	162.40	479.34	20.601	0.112	1.113	0.285
1982	143.39	89.92	20.603	0.066	1.141	0.153
1983	115.13	94.25	20.607	0.129	1.323	0.264
1984	159.79	424.77	20.607	0.079	1.754	0.297
1985	63.63	231.61	20.610	0.084	1.367	0.252
1986	218.21	468.34	20.617	0.058	1.973	0.263
1987	171.53	446.94	20.620	0.127	1.503	0.289
1988	92.87	208.53	20.621	0.052	1.311	0.176
1989	74.66	285.86	20.628	0.091	1.149	0.258
1990	308.11	129.05	20.629	0.275	2.217	0.516
1991	53.07	457.93	20.630	0.090	1.182	0.168
1992	57.75	60.86	20.631	0.377	0.815	0.548
1993	164.68	164.04	20.638	0.077	1.301	0.229
1994	297.95	465.34	20.639	0.109	1.421	0.253
1995	306.53	442.75	20.641	0.075	1.556	0.296
1996	23.52	198.07	20.641	0.057	1.562	0.299
1997	86.57	320.92	20.642	0.054	1.432	0.224
1998	118.72	306.77	20.643	0.128	0.940	0.217

Table C.4. (cont.)

ID	x	y	V	σ_V	B-V	σ_{B-V}
1999	201.46	306.10	20.643	0.113	1.625	0.380
2000	238.03	234.55	20.644	0.132	1.142	0.277
2001	157.07	182.89	20.645	0.071	1.940	0.381
2002	267.11	29.64	20.645	0.318	0.407	0.539
2003	295.04	58.70	20.648	0.115	1.902	0.416
2004	255.92	292.32	20.651	0.117	0.809	0.191
2005	236.70	211.45	20.652	0.246	1.202	0.748
2006	75.47	366.14	20.655	0.108	1.441	0.224
2007	275.35	149.17	20.657	0.131	1.601	0.341
2008	261.89	376.33	20.666	0.097	0.563	0.144
2009	295.89	40.31	20.668	0.145	0.427	0.264
2010	179.94	329.48	20.670	0.077	0.770	0.187
2011	191.31	51.20	20.675	0.120	1.400	0.284
2012	40.95	20.53	20.677	0.108	1.531	0.248
2013	168.89	183.47	20.681	0.075	1.471	0.305
2014	64.37	205.11	20.691	0.098	1.908	0.319
2015	256.84	47.36	20.698	0.615	-0.143	0.841
2016	280.95	104.40	20.699	0.205	1.515	0.559
2017	76.42	431.54	20.701	0.081	1.332	0.208
2018	206.92	351.28	20.705	0.076	1.602	0.270
2019	199.16	392.57	20.712	0.090	1.142	0.168
2020	244.25	87.44	20.715	0.119	1.160	0.211
2021	73.68	43.71	20.715	0.088	1.363	0.232
2022	217.67	323.76	20.718	0.105	1.753	0.360
2023	83.50	245.96	20.720	0.076	1.382	0.567
2024	60.22	160.30	20.722	0.111	1.139	0.232
2025	150.03	40.86	20.722	0.080	1.239	0.202
2026	283.53	95.83	20.722	0.129	1.391	0.419
2027	145.44	153.95	20.728	0.085	1.252	0.234
2028	68.00	498.30	20.731	0.071	1.812	0.278
2029	180.89	295.35	20.734	0.098	1.730	0.318
2030	215.36	27.56	20.734	0.201	1.879	0.503
2031	282.42	335.30	20.735	0.140	1.083	0.286
2032	291.34	221.84	20.740	0.250	0.238	0.338
2033	197.30	187.22	20.740	0.118	1.996	0.426
2034	8.55	502.69	20.742	0.161	1.593	0.536
2035	16.69	7.62	20.743	0.122	1.182	0.269

Table C.4. (cont.)

ID	x	y	V	σ_V	B-V	σ_{B-V}
2036	258.26	302.11	20.752	0.128	1.236	0.347
2037	174.27	416.96	20.752	0.075	1.716	0.235
2038	21.91	302.90	20.755	0.121	1.638	0.354
2039	81.00	319.08	20.755	0.051	1.164	0.162
2040	275.47	213.55	20.757	0.106	1.262	0.328
2041	74.39	70.93	20.759	0.091	1.038	0.177
2042	195.11	57.09	20.762	0.153	0.625	0.273
2043	283.53	436.95	20.763	0.081	0.707	0.187
2044	295.03	100.79	20.766	0.127	1.181	0.324
2045	186.96	127.88	20.769	0.134	0.748	0.220
2046	112.31	46.54	20.770	0.078	1.458	0.232
2047	196.50	316.91	20.772	0.127	1.743	0.342
2048	277.20	30.29	20.774	0.188	1.520	0.741
2049	305.19	138.60	20.775	0.135	1.381	0.357
2050	299.08	338.72	20.776	0.232	1.261	0.449
2051	244.52	11.98	20.781	0.098	1.805	0.373
2052	57.10	305.44	20.782	0.142	1.826	0.287
2053	60.12	269.92	20.787	0.144	1.808	0.345
2054	179.52	173.15	20.795	0.136	1.310	0.339
2055	91.30	84.97	20.796	0.298	-4.016	0.387
2056	289.83	271.93	20.800	0.095	1.467	0.299
2057	133.90	156.11	20.809	0.081	1.454	0.202
2058	199.42	145.22	20.819	0.091	1.696	0.310
2059	70.64	147.91	20.820	0.120	1.566	0.325
2060	22.79	459.28	20.824	0.096	1.716	0.313
2061	164.52	14.05	20.825	0.098	1.043	0.165
2062	221.15	335.44	20.827	0.105	1.719	0.305
2063	158.54	421.08	20.831	0.140	1.493	0.425
2064	54.30	372.66	20.833	0.093	2.401	0.686
2065	175.47	121.07	20.833	0.123	1.292	0.279
2066	224.56	481.41	20.835	0.329	0.872	0.494
2067	306.44	383.94	20.835	0.128	0.775	0.262
2068	311.13	277.42	20.839	0.117	1.883	0.408
2069	211.21	119.17	20.840	0.120	2.145	0.979
2070	276.45	216.64	20.848	0.106	1.713	0.451
2071	254.00	44.57	20.850	0.801	0.323	1.093
2072	168.85	487.13	20.850	0.174	1.736	0.453

Table C.4. (cont.)

ID	x	y	V	σ_V	B-V	σ_{B-V}
2073	191.10	377.05	20.853	0.200	2.465	0.626
2074	178.57	356.57	20.858	0.135	1.275	0.295
2075	303.37	236.95	20.860	0.082	1.682	0.266
2076	265.82	130.50	20.861	0.239	1.642	0.403
2077	138.22	224.63	20.863	0.087	1.064	0.462
2078	201.04	157.05	20.865	0.113	1.095	0.228
2079	256.90	370.91	20.867	0.094	1.687	0.328
2080	164.95	502.97	20.868	0.095	1.659	0.362
2081	291.10	198.03	20.869	0.129	1.025	0.279
2082	297.18	93.47	20.870	0.121	1.579	0.451
2083	254.63	336.15	20.877	0.119	0.457	0.195
2084	283.38	289.71	20.877	0.090	1.681	0.184
2085	181.61	84.75	20.881	0.092	1.291	0.341
2086	283.32	461.73	20.883	0.115	1.395	0.316
2087	298.25	317.19	20.889	0.145	1.144	0.287
2088	55.65	336.23	20.894	0.091	1.616	0.307
2089	232.26	235.61	20.894	0.146	1.901	0.413
2090	238.75	320.67	20.895	0.148	1.799	0.692
2091	53.10	223.61	20.898	0.110	1.024	0.258
2092	26.01	125.90	20.902	0.106	2.489	0.587
2093	61.18	368.51	20.907	0.144	1.216	0.285
2094	96.94	10.72	20.911	0.329	-1.829	0.429
2095	138.88	160.60	20.916	0.120	1.606	0.293
2096	94.03	148.03	20.925	0.128	1.122	0.281
2097	132.86	365.72	20.926	0.147	0.782	0.278
2098	148.33	59.31	20.926	0.093	1.577	0.279
2099	161.70	267.30	20.926	0.154	1.467	0.376
2100	125.37	61.57	20.931	0.154	1.990	0.502
2101	63.66	191.28	20.932	0.192	1.363	0.529
2102	279.99	468.83	20.933	0.107	0.628	0.211
2103	161.24	194.21	20.933	0.204	1.591	0.830
2104	310.08	137.90	20.934	0.153	1.588	0.288
2105	58.73	447.72	20.935	0.156	1.498	0.658
2106	287.59	308.20	20.943	0.147	1.312	0.266
2107	93.63	306.15	20.945	0.170	1.333	0.337
2108	245.12	392.05	20.946	0.184	1.347	0.321
2109	157.40	267.35	20.948	0.141	0.542	0.252

Table C.4. (cont.)

ID	x	y	V	σ_V	B-V	σ_{B-V}
2110	266.50	95.38	20.967	0.217	0.344	0.366
2111	166.37	394.53	20.977	0.120	1.878	0.460
2112	274.66	22.88	20.977	0.105	0.698	0.234
2113	205.22	484.01	20.978	0.147	0.983	0.281
2114	235.61	328.32	20.987	0.112	1.093	0.280
2115	256.56	154.50	21.000	0.169	1.562	0.493
2116	168.43	282.19	21.001	0.155	1.638	0.512
2117	185.42	398.41	21.010	0.107	1.687	0.268
2118	227.57	116.20	21.011	0.116	1.275	0.299
2119	143.74	129.67	21.016	0.179	0.278	0.265
2120	165.31	33.53	21.018	0.133	1.977	0.428
2121	245.43	337.05	21.018	0.133	1.319	0.358
2122	84.91	253.37	21.022	0.117	0.865	0.329
2123	246.70	312.50	21.023	0.064	2.074	0.365
2124	121.23	160.17	21.023	0.137	0.791	0.250
2125	138.64	83.39	21.023	0.123	1.990	0.329
2126	27.18	286.26	21.024	0.102	1.239	0.278
2127	249.67	488.98	21.024	0.214	1.859	0.552
2128	309.04	195.79	21.031	0.226	1.283	0.537
2129	157.90	381.61	21.033	0.140	1.213	0.306
2130	87.98	10.53	21.036	0.184	1.855	0.524
2131	137.93	53.24	21.039	0.124	2.138	0.423
2132	44.51	187.28	21.040	0.144	2.393	0.490
2133	217.24	328.70	21.049	0.150	2.261	0.671
2134	124.44	266.29	21.062	0.119	1.066	0.277
2135	161.58	427.72	21.065	0.099	1.142	0.305
2136	101.73	492.66	21.076	0.145	2.070	0.574
2137	67.76	494.04	21.077	0.096	1.367	0.292
2138	309.20	503.80	21.083	0.263	1.401	0.485
2139	185.01	276.20	21.083	0.136	1.996	0.347
2140	181.07	255.57	21.087	0.114	1.620	0.230
2141	260.06	244.34	21.089	0.227	0.881	0.352
2142	105.02	9.12	21.090	0.117	1.443	0.420
2143	219.90	212.27	21.092	0.169	1.200	0.292
2144	130.78	345.76	21.093	0.112	1.176	0.347
2145	104.84	401.50	21.096	0.091	1.333	0.258
2146	287.81	486.55	21.097	0.195	0.873	0.345

Table C.4. (cont.)

ID	x	y	V	σ_V	B-V	σ_{B-V}
2147	264.37	208.44	21.099	0.188	0.488	0.418
2148	207.68	265.04	21.103	0.087	1.628	0.304
2149	277.03	283.13	21.104	0.102	2.000	0.297
2150	267.53	233.95	21.113	0.159	1.401	0.376
2151	205.31	319.95	21.116	0.109	1.399	0.394
2152	8.82	310.85	21.118	0.120	1.604	0.417
2153	210.02	469.16	21.119	0.166	0.889	0.327
2154	93.81	442.78	21.121	0.160	1.480	0.404
2155	89.00	369.64	21.126	0.131	0.935	0.237
2156	76.24	452.58	21.128	0.124	1.520	0.325
2157	223.83	82.45	21.129	0.165	1.716	0.474
2158	267.02	353.45	21.130	0.219	1.391	0.422
2159	196.40	270.54	21.135	0.181	0.699	0.319
2160	279.68	180.56	21.138	0.150	1.289	0.383
2161	278.58	203.12	21.139	0.173	1.968	0.578
2162	203.19	426.98	21.143	0.229	-1.792	0.301
2163	148.54	179.60	21.150	0.162	1.829	0.448
2164	306.68	166.52	21.153	0.180	3.759	2.457
2165	309.78	118.66	21.155	0.203	1.744	0.383
2166	257.55	317.89	21.160	0.102	2.036	0.453
2167	186.91	451.46	21.163	0.108	1.355	0.342
2168	17.44	222.82	21.165	0.152	1.159	0.381
2169	159.62	8.25	21.173	0.196	1.763	0.502
2170	196.43	38.81	21.175	0.166	2.210	0.598
2171	138.95	104.80	21.179	0.242	0.558	0.359
2172	110.51	270.35	21.184	0.125	2.075	0.600
2173	64.74	395.70	21.184	0.195	0.997	0.893
2174	162.18	149.12	21.186	0.135	1.844	0.518
2175	288.21	462.75	21.187	0.148	1.215	0.312
2176	92.11	444.55	21.189	0.181	1.417	0.403
2177	273.67	170.33	21.190	0.154	1.683	0.350
2178	58.92	47.02	21.191	0.171	0.376	0.289
2179	127.97	206.43	21.193	0.168	1.821	0.449
2180	299.11	129.03	21.193	0.402	-0.094	0.694
2181	269.57	387.10	21.195	0.249	1.850	0.534
2182	116.01	493.30	21.196	0.108	1.321	0.311
2183	41.41	498.07	21.199	0.492	1.178	0.740

Table C.4. (cont.)

ID	x	y	V	σ_V	B-V	σ_{B-V}
2184	228.75	277.94	21.203	0.180	1.367	0.515
2185	118.48	188.62	21.207	0.185	2.803	1.159
2186	167.68	147.39	21.213	0.129	1.406	0.355
2187	16.66	401.35	21.215	0.125	0.783	0.246
2188	119.08	44.53	21.216	0.115	1.352	0.328
2189	71.00	237.17	21.217	0.177	1.385	0.373
2190	180.39	161.17	21.224	0.195	1.846	0.628
2191	73.13	444.63	21.228	0.176	0.501	0.317
2192	186.81	405.78	21.231	0.138	1.692	0.456
2193	128.71	462.62	21.236	0.143	0.295	0.260
2194	95.86	286.57	21.238	0.201	1.622	0.722
2195	153.05	100.16	21.239	0.144	1.428	0.411
2196	293.45	115.40	21.240	0.230	1.113	0.539
2197	57.91	252.89	21.241	0.142	1.558	0.478
2198	167.62	476.67	21.247	0.227	1.642	0.632
2199	12.50	316.29	21.248	0.131	1.005	0.341
2200	152.44	142.40	21.249	0.167	2.387	0.539
2201	239.71	326.69	21.258	0.164	1.466	0.409
2202	246.64	158.97	21.259	0.123	1.701	0.380
2203	123.15	454.58	21.263	0.192	2.031	0.838
2204	309.24	485.37	21.264	0.127	1.472	0.490
2205	149.62	76.25	21.265	0.185	1.454	0.340
2206	7.01	134.06	21.267	0.166	0.657	0.307
2207	240.96	104.48	21.270	0.164	1.552	0.402
2208	118.15	469.00	21.282	0.135	0.777	0.258
2209	79.24	297.85	21.291	0.137	0.594	0.277
2210	215.70	196.33	21.292	0.168	2.563	0.874
2211	256.55	259.22	21.295	0.250	2.584	1.068
2212	233.70	130.06	21.309	0.174	0.929	0.349
2213	265.20	286.64	21.312	0.117	1.453	0.271
2214	80.18	327.80	21.313	0.162	1.792	0.440
2215	127.45	52.39	21.314	0.155	1.379	0.427
2216	84.28	444.81	21.314	0.207	1.640	0.690
2217	57.64	69.17	21.323	0.149	1.020	0.347
2218	122.68	446.44	21.328	0.177	0.987	0.306
2219	140.56	116.29	21.330	0.205	2.385	0.763
2220	217.28	25.10	21.330	0.214	2.128	0.839

Table C.4. (cont.)

ID	x	y	V	σ_V	B-V	σ_{B-V}
2221	168.93	330.83	21.330	0.153	2.347	0.618
2222	74.19	228.62	21.332	0.153	1.637	0.483
2223	27.15	239.48	21.336	0.118	1.674	0.447
2224	133.09	88.98	21.338	0.132	1.139	0.387
2225	207.82	249.28	21.341	0.196	2.080	0.631
2226	167.51	122.62	21.347	0.223	1.203	0.423
2227	113.28	464.82	21.347	0.183	3.370	1.427
2228	206.13	106.09	21.347	0.174	1.140	0.348
2229	188.13	70.37	21.349	0.154	1.061	0.408
2230	210.31	339.93	21.352	0.168	1.981	0.675
2231	84.04	290.86	21.354	0.125	1.482	0.418
2232	137.76	432.52	21.355	0.179	1.248	0.407
2233	215.70	63.11	21.358	0.319	0.693	0.539
2234	50.80	282.95	21.362	0.183	2.758	1.176
2235	283.36	123.56	21.362	0.182	1.249	0.551
2236	270.32	237.48	21.367	0.144	3.663	2.226
2237	299.28	289.86	21.367	0.210	1.583	0.594
2238	309.62	203.20	21.375	0.291	1.288	0.902
2239	65.31	325.93	21.375	0.258	1.618	0.463
2240	92.87	413.61	21.377	0.171	1.714	0.390
2241	213.62	270.29	21.377	0.113	1.958	0.829
2242	233.75	302.14	21.393	0.228	0.720	0.385
2243	21.26	13.20	21.393	0.160	0.497	0.335
2244	229.59	373.10	21.395	0.137	1.345	0.325
2245	117.62	360.58	21.398	0.194	2.434	0.934
2246	304.35	493.49	21.398	0.223	1.082	0.725
2247	17.34	24.62	21.400	0.163	1.154	0.353
2248	160.05	451.41	21.403	0.156	2.094	0.685
2249	256.52	53.92	21.425	0.124	0.436	0.291
2250	135.47	395.73	21.425	0.168	1.796	0.573
2251	153.18	41.60	21.426	0.150	1.229	0.322
2252	55.02	479.40	21.429	0.168	0.836	0.380
2253	81.53	237.51	21.435	0.132	1.003	0.326
2254	212.79	354.93	21.437	0.227	1.269	0.537
2255	191.54	190.81	21.439	0.154	1.538	0.588
2256	192.45	401.96	21.449	0.230	1.421	0.499
2257	121.77	29.32	21.454	0.127	1.266	0.554

Table C.4. (cont.)

ID	x	y	V	σ_V	B-V	σ_{B-V}
2258	29.34	487.86	21.456	0.250	1.544	0.646
2259	108.88	443.48	21.459	0.211	2.150	0.762
2260	278.14	396.52	21.459	0.253	0.819	0.430
2261	242.07	260.91	21.471	0.327	0.831	0.577
2262	171.34	191.53	21.475	0.168	2.152	0.833
2263	234.18	25.42	21.476	0.165	0.970	0.311
2264	132.96	322.69	21.477	0.171	1.495	0.467
2265	189.79	17.96	21.480	0.143	1.875	0.558
2266	86.18	293.80	21.483	0.141	1.659	0.496
2267	69.83	227.60	21.494	0.189	1.209	0.444
2268	242.32	316.40	21.495	0.149	1.600	0.652
2269	212.51	412.62	21.498	0.153	1.973	0.615
2270	226.54	499.20	21.499	0.263	0.735	0.393
2271	12.82	394.34	21.500	0.236	1.772	0.784
2272	260.17	367.55	21.507	0.206	2.284	0.800
2273	143.93	280.97	21.508	0.295	0.831	0.530
2274	254.67	475.16	21.511	0.211	1.463	0.546
2275	16.35	273.35	21.513	0.254	2.145	0.886
2276	105.00	444.45	21.518	0.205	1.406	0.463
2277	169.85	367.27	21.520	0.177	1.226	0.408
2278	41.11	161.23	21.522	0.178	1.462	0.566
2279	139.01	157.38	21.527	0.209	1.043	0.433
2280	116.10	178.97	21.533	0.172	1.623	0.558
2281	86.25	49.32	21.533	0.280	1.881	0.793
2282	130.20	453.95	21.534	0.189	2.580	0.927
2283	275.68	92.26	21.539	0.174	1.446	0.610
2284	79.93	331.22	21.540	0.170	1.351	0.394
2285	134.03	432.21	21.542	0.287	1.430	0.655
2286	162.13	90.59	21.548	0.221	1.837	0.714
2287	29.20	373.73	21.551	0.149	1.473	0.470
2288	207.31	56.57	21.552	0.197	0.500	0.370
2289	271.91	324.67	21.557	0.207	1.833	0.657
2290	92.72	171.17	21.560	0.169	1.449	0.491
2291	101.80	488.55	21.563	0.231	1.659	0.792
2292	113.53	438.40	21.566	0.160	0.670	0.348
2293	29.77	18.22	21.566	0.207	1.981	0.914
2294	8.34	381.46	21.574	0.134	2.360	1.148

Table C.4. (cont.)

ID	x	y	V	σ_V	B-V	σ_{B-V}
2295	142.80	422.71	21.581	0.249	1.629	0.656
2296	26.21	145.43	21.582	0.234	1.611	0.731
2297	281.60	254.86	21.584	0.128	1.184	0.425
2298	42.99	245.64	21.598	0.130	1.470	0.703
2299	33.72	413.15	21.599	0.193	1.663	0.622
2300	138.39	437.62	21.600	0.147	2.173	0.851
2301	259.00	407.05	21.601	0.332	1.529	0.633
2302	91.17	374.62	21.619	0.275	0.746	0.549
2303	6.72	201.16	21.624	0.159	1.184	0.389
2304	89.01	503.85	21.627	0.295	0.670	0.473
2305	238.07	448.55	21.629	0.244	0.859	0.476
2306	51.27	298.67	21.630	0.235	1.969	0.741
2307	75.76	245.40	21.633	0.178	3.720	2.886
2308	54.33	125.81	21.634	0.172	1.229	0.434
2309	98.46	413.52	21.639	0.175	1.343	0.369
2310	273.43	220.68	21.643	0.189	0.909	0.531
2311	218.73	47.32	21.644	0.178	1.230	0.590
2312	100.87	404.95	21.645	0.167	1.551	0.625
2313	63.67	236.85	21.654	0.168	1.655	0.509
2314	177.40	451.88	21.665	0.254	1.272	0.549
2315	225.63	449.63	21.666	0.208	1.301	0.491
2316	142.35	263.48	21.669	0.128	1.391	0.466
2317	101.34	124.75	21.669	0.340	0.327	0.499
2318	49.76	295.64	21.691	0.274	1.927	0.734
2319	174.29	394.07	21.697	0.199	1.540	0.615
2320	25.14	478.56	21.700	0.522	0.483	0.991
2321	96.44	479.24	21.702	0.270	1.471	0.679
2322	105.14	278.87	21.716	0.196	1.625	0.853
2323	59.74	138.88	21.724	0.214	1.361	0.512
2324	187.61	79.53	21.727	0.166	1.888	0.547
2325	134.32	55.61	21.730	0.230	0.858	0.479
2326	203.84	356.83	21.732	0.209	1.574	0.690
2327	55.08	145.45	21.740	0.182	1.977	0.740
2328	304.07	488.94	21.740	0.280	0.943	0.509
2329	54.65	80.25	21.760	0.182	0.158	0.360
2330	21.70	245.72	21.766	0.114	1.028	0.361
2331	189.12	226.25	21.777	0.202	1.267	0.556

Table C.4. (cont.)

ID	x	y	V	σ_V	B-V	σ_{B-V}
2332	45.07	254.51	21.781	0.240	3.464	2.809
2333	233.35	59.11	21.790	0.354	1.399	0.764
2334	37.59	160.93	21.794	0.237	0.898	0.506
2335	42.55	392.72	21.806	0.169	2.290	1.251
2336	14.22	388.97	21.824	0.321	1.537	0.877
2337	57.37	357.88	21.831	0.217	1.615	0.907
2338	9.04	140.77	21.837	0.283	1.168	0.621
2339	164.37	311.66	21.839	0.138	1.676	0.664
2340	157.65	441.73	21.848	0.212	0.922	0.597
2341	183.61	314.80	21.852	0.206	1.260	0.530
2342	198.32	197.48	21.854	0.232	0.871	0.548
2343	280.59	460.92	21.856	0.279	1.388	0.796
2344	211.21	472.82	21.862	0.303	0.385	0.514
2345	122.65	246.91	21.878	0.215	0.944	0.575
2346	211.34	442.69	21.881	0.233	0.829	0.628
2347	91.04	198.77	21.883	0.149	0.431	0.309
2348	69.22	36.63	21.886	0.195	0.878	0.515
2349	164.71	89.27	21.886	0.307	1.193	0.740
2350	308.40	343.04	21.889	0.366	2.456	1.968
2351	162.78	302.03	21.890	0.233	0.655	0.540
2352	194.15	485.73	21.917	0.281	1.520	0.738
2353	200.24	72.02	21.922	0.257	0.956	0.604
2354	208.69	19.48	21.926	0.226	1.430	0.535
2355	227.38	68.60	21.939	0.347	0.993	0.650
2356	292.00	427.76	21.960	0.314	0.873	0.648
2357	68.18	32.57	21.962	0.305	1.857	0.946
2358	96.68	187.15	21.993	0.259	3.982	5.367
2359	44.12	60.67	22.016	0.203	1.517	0.794
2360	285.18	195.43	22.025	0.238	2.530	1.260
2361	5.29	77.64	22.031	0.269	0.581	0.646
2362	234.37	371.05	22.097	0.252	1.003	0.501
2363	289.54	349.25	22.184	0.452	0.537	0.675
2364	221.31	62.63	22.219	0.431	0.339	0.689
2365	253.42	471.30	22.254	0.345	2.750	1.982
2366	18.16	188.13	22.286	0.345	4.968	12.816
2367	243.74	264.55	22.328	0.720	1.200	1.328
2368	64.08	113.41	22.694	0.780	-0.602	1.037

Table C.4. (end)

ID	x	y	V	σ_V	B-V	σ_{B-V}
2369	177.04	59.87	22.764	0.581	-0.796	0.797

Vita

Surname: **Monteith** Given Names: **Anne-Marie**

Place of Birth: **Montreal, Quebec**

Date of Birth: **March 13, 1968**

Educational Institutions Attended:

University of Ottawa, Ottawa **1985 to 1988**

University of Victoria, Victoria **1988 to 1990**

Degrees Awarded:

B.Sc. (Honours) in Physics, Magna cum Laude, 1988

University of Ottawa

Honours and Awards:

Admission Scholarhip, U. of Ottawa 1985/86

McDonald Scholarship, U. of Ottawa 1986/87

NSERC Undergraduate Research Award 1987

NSERC Postgraduate Scholarship 1988/89

President's Award, U. of Victoria 1988/89

R. M. Petrie Award, U. of Victoria 1989/90

NSERC Postgraduate Scholarship 1989/90

President's Award, U. of Victoria 1989/90